

## ABSTRACT

The main objective of the present research is to investigate structure property of a series of carbazole-thiophene. Electronic properties were evaluated by UV-Vis, cyclic voltammogram and theoretical calculations. Particularly, the effects of conjugation connectivity on photophysical and electrochemical properties, as well as the correlation between carbazole-thiophene were linked at the N-9 position for different core groups via biphenyl, dimethylbiphenyl and phenyl were studied. Literature review on the carbazole-thiophene moieties and their derivatives and methods for the synthesis of carbazole-thiophene have been described. The literature search on the various potential application of carbazole-thiophene were also studied. A brief introduction on the background of this study was provided which gave an insight of the key step involved in the synthesis of carbazole-thiophenes via Suzuki Miyaura and Ullmann coupling reaction. Results of the physical properties on the electronic absorption spectroscopy via UV-visible and fluorescence were discussed. We noted a maximum absorption wavelength at a higher absorbance, indicating that the attachment of thiophene groups at the 3- and 6-positions of the carbazole significantly enhances the optical properties. The absorption bands of all of the compounds were gradually red shifted, when the thiophene group was connected to the carbazole at the 3- and 6-positions and the extent of  $\pi$ -conjugation in the compounds increased, as expected. After the functionalization of the carbazole groups, the fluorescence maxima ( $\lambda_{em}$ ) gradually red shifted upon the addition of thiophene group, resulting a significant red shift in the emission spectrum.  $E_{pa}$  values for **2.38 (P1)**, **2.39 (P2)**, **2.40 (P3)**, **2.41 (P4)**, **2.42 (P5)**, **2.43 (P6)**, **2.44 (P7)**, **2.45 (P8)**, **2.46 (P9)** and **2.47 (P10)** are cathodically shifted compared to those for **1.4 (CBP)**, **2.36 (CDBP)**, **2.37 (BCP)** by the subsequent addition of thiophene molecules, demonstrating that the connection with thiophene at

the 3- and 6-positions on carbazole of **1.4 (CBP)**, **2.36 (CDBP)** and **2.37 (BCP)** gives rise to high electrochemical stability and effectively enhances donor ability. Carbazole substituted with thiophene groups at the 3- and 6-positions leads to greater stabilization of HOMO and LUMO energy levels where the band gap ( $\Delta E$ ) of all the compounds is significantly reduced and such unit can be introduced into the backbone of **1.4 (CBP)**, **2.36 (CDBP)** and **2.37 (BCP)**  $\pi$ -conjugated small molecules to develop new materials with low band gap that may have potential application in optoelectronic fields. A brief introduction of theoretical calculation was provided. A brief theoretical calculation on the carbazole-thiophenes compounds by geometrical optimization and frontier molecular orbital calculations were also discussed. All computation were performed using GAUSSION 09W software package employing the Density Functional Theory (DFT) method with correlation functional B3LYP and 6-31G as functional basis set.

## ABSTRAK

Objektif utama penyelidikan ini adalah untuk menyelidiki struktur satu siri carbazol-thiophen. Sifat elektronik dinilai melalui UV-Vis, cyclic voltammogram dan pengiraan teori. Terutamanya, kesan konjugasi keatas fotofizikal dan elektrokimia, dan juga hubungan diantara carbazol-thiophen pada kedudukan N-9 dengan kedudukan kumpulan teras berbeza melalui bifenal, dimetalbifenal dan fenal telah dikaji. Kajian literatur mengenai sebatian carbazol-thiophen dan terbitannya dan beberapa kaedah untuk sintesis beberapa carbazol-thiophen telah diterangkan. Pencarian maklumat bagi carbazol-thiophen dalam aplikasi yang berpotensi juga dinyatakan. Satu pengenalan ringkas mengenai latar belakang kajian ini telah disediakan. Pengenalan ringkas mengenai kaedah utama dalam sintesis carbazol-thiophen melalui gandingan Suzuki Miyaura dan Ullmann tindak balas. Keputusan sifat-sifat fizikal pada penyerapan spektroskopi elektronik melalui UV-visible dan Floresence dibincangkan. Kita perhatikan penyerapan maksimum panjang gelombang adalah pada penyerapan yang lebih tinggi. Menunjukkan bahawa penyambungan kumpulan thiophen pada kedudukan 3- dan 6- carbazol meningkatkan sifat-sifat optik dengan ketara. Jalur penyerapan semua sebatian secara beransur-ansur beralih 'red shift', apabila kumpulan thiophen disambungkan kepada carbazol pada kedudukan 3- dan 6- kedudukan dan  $\pi$ -konjugasi dalam sebatian meningkat seperti dijangka. Selepas carbazole ditambah kumpulan berfungsi, "fluorescence" maksimum secara beransur-ansur ( $\lambda_{em}$ ) beralih kearah "red shift" apabila kumpulan thiophene ditambah menyebabkan anjakan "red shift" yang ketara dalam spectrum pancaran. Nilai  $E_{pa}$  values bagi **2.38 (P1)**, **2.39 (P2)**, **2.40 (P3)**, **2.41 (P4)**, **2.42 (P5)**, **2.43 (P6)**, **2.44 (P7)**, **2.45 (P8)**, **2.46 (P9)** dan **2.47 (P10)** adalah beralih kearah katod berbanding **1.4 (CBP)**, **2.36 (CDBP)** dan **2.37 (BCP)** dengan penambahan molekul thiophene, menunjukkan bahawa penambahan thiophen pada 3-

dan 6- kedudukan pada carbazol dalam sebatian **1.4 (CBP)**, **2.36 (CDBP)** dan **2.37 (BCP)** menyebabkan kestabilan elektrokimia adalah tinggi dan berkesan meningkatkan keupayaan sebagai unit penderma. Carbazol dengan kumpulan thiophen tertukarganti pada kedudukan 3- dan 6- membawa kestabilan yang lebih besar pada level tenaga HOMO dan LUMO di mana jurang jalur ( $\Delta E$ ) semua sebatian semakin berkurangan, kumpulan thiophene tersebut boleh dimasukkan pada sebatian kecil  $\pi$ -conjugasi **1.4 (CBP)**, **2.36 (CDBP)** dan **2.37 (BCP)** bagi membina sebatian-sebatian baru dengan jurang jalur rendah yang mungkin mempunyai potensi aplikasi dalam bidang optoelektronik. Satu pengenalan ringkas mengenai pengiraan teori diberikan. Pengiraan teori ringkas mengenai sebatian carbazol-thiophen dengan mengoptimumkan geometri dan pengiraan frontier orbital molekul dibincang. Semua pengiraan telah dilakukan dengan menggunakan perisian GAUSSION 09W pakej dan kaedah "Density Functional Theory (DFT)" dengan fungsi korelasi B3LYP dan 6-31G sebagai set asas berfungsi.

## ACKNOWLEDGEMENTS

This thesis arose in part out of years of research that has been done and I would like to record my gratitude to my supervisor Professor Dr. Azhar Ariffin for his supervision, advice and guidance from the very early stage of this research as well as giving me extraordinary experiences throughout the work.

I gratefully acknowledge my co-supervisor, Associate Professor Dr. Khaulah Sulaiman for her advice, supervision and crucial contribution, which made her a backbone of this research and so to the thesis.

My special thanks to the Chemistry Department of University Malaya, for providing me the opportunities to fully utilize the lab facilities and the staff members of Chemistry Department for their cooperation.

Furthermore, thankful for the support of the Chemistry Department, Faculty of Science University Malaya, Kuala Lumpur, Malaysia, and for financial support from the Long term Research Grant Scheme (LRGS) (LR003-2011A), High Impact Research Grant (HIR) (UM.C/625/1/HIR/208) (J-21001-73865) and Postgraduate Research Grant (PPP) (PG021-2013A) for the financial support.

My parents Damit Haji Mojitar and Zaitun Mohd Zain deserve special mention for their inseparable support and prayers. Mohd Dzul Alfian, Ahmad Tharmizi and Deen Khairee, thanks for being supportive and caring siblings.

Words fail me to express my appreciation to my husband Azmi Ahmad whose dedication, love and persistent confidence in me. My beloved children Siti Aisyah and Afiq Haikal, who bring a smile to my face and joy to my heart.

Finally I would like to thank everybody who was important to the successful realization of thesis, as well as expressing my apology that I could not mention personally one by one.

## TABLES OF CONTENTS

<b>ABSTRACT</b>	iii
<b>ABSTRAK</b>	v
<b>ACKNOWLEDGEMENT</b>	vii
<b>TABLE OF CONTENTS</b>	viii
<b>LIST OF FIGURES</b>	xiii
<b>LIST OF TABLES</b>	xv
<b>LIST OF SYMBOLS AND ABBREVIATIONS</b>	xvi
<b>LIST OF APPENDICES</b>	xx
<b>CHAPTER 1: INTRODUCTION</b>	
1.1 Introduction	1
1.2 Organic Photovoltaic versus Polymer Photovoltaic	2
1.3 Organic Photovoltaic Operation Principal	3
1.4 Thiophene-Based for Organic Solar Cells (OSCs)	7
1.5 Literature Review	8
1.6 Objective of the Study	24

## CHAPTER 2: SYNTHESIS OF CARBAZOLE-THIOPHENE BASED DERIVATIVES

2.1 Introduction	25
2.2 Suzuki-Miyaura Coupling	36
2.2.1 Suzuki Miyaura Reaction	
2.2.1.1 Biphenylene System	29
2.2.1.2 Binaphthyl System	30
2.2.1.3 Reaction Involving 9-BBN Derivatives	31
2.2.1.4 Formation of Carbon-Heteroatom (C-N, C-O and C-S) Bonds	32
2.3 Ullmann Coupling	33
2.3.1 Reductive Coupling	
2.3.1.1 Symmetrical Coupling	36
2.3.1.2 Unsymmetrical Coupling	38
2.4 Results and Discussion	
2.4.1 Targeted Compounds	39
2.4.2 Synthesis of Compound 1.4 (CBP), 2.36 (CDBP) and 2.37 (BCP)	46
2.4.3 Synthesis of Compound 2.38 (P1), 2.39 (P2) and 2.40 (P3)	47
2.4.4 Synthesis of Compound 2.41 (P4), 2.42 (P5) and 2.43 (P6)	49
2.4.5 Synthesis of Compound 2.44 (P7), 2.45 (P8) and 2.48 (P11)	50
2.4.6 Synthesis of Compound 2.46 (P9), 2.47 (P10) and 2.49 (P12)	51
2.5 Suzuki Coupling Reaction	53

## CHAPTER 3: PHYSICAL PROPERTIES

3.1 Introduction	62
3.1.1 Absorption Spectroscopy	64
3.1.2 Bandgap, $E_g$	69
3.1.3 Electronic Spectroscopy	71
3.2 Literature review	75
3.3 Objective	79
3.4 Results and Discussion	
3.4.1 Optical Properties - Electronic Absorption Spectroscopy (Effect of Thiophenes)	81
3.4.2 Optical Properties – Electronic Absorption Spectroscopy (Effect of Core Unit)	86
3.4.3 Optical Properties – Fluorescence Spectroscopy (Effect of Thiophenes)	91
3.4.4 Optical Properties – Fluorescence Spectroscopy (Effect of Core Unit)	95
3.4.5 Electrochemical Properties	102



## CHAPTER 4: THEORITICAL CALCULATION

4.1 Introduction	109
4.2 Literature Review	111
4.3 Objective	117
4.4 Results and Discussion	118

## CHAPTER 5: EXPERIMENTAL

5.1 Materials	128
5.2 General Procedures	
5.2.1 Synthesis and Characterization	130
5.2.2 Physical and Theoretical Properties Analysis	130
5.3 Details Procedure for the synthesis of Starting Materials	
5.3.1 Synthesis of compound 2.54 (3-Iodocarbazole)	131
5.3.2 Synthesis of compound 2.57 (3,6-Diiodocarbazole)	132
5.3.3 Synthesis of compound 2.51 (4,4-Diiodobiphenyl)	133
5.3.4 Synthesis of compound 2.56 (3-(Thiophen-2-yl)carbazole)	134
5.3.5 Synthesis of compound 2.58	135
5.3.6 Synthesis of compound 2.60	136
5.3.7 Synthesis of compound 2.62	137
5.3.8 Synthesis of compound 2.64	138
5.4 Synthesis of end products	
5.4.1 Synthesis of compound 4,4'-Di(9H-carbazol-9-yl)-1,1'-biphenyl (1.4 (CBP))	139

5.4.2 Synthesis of compound 9,9'-(2,2'-dimethyl-[1,1'-biphenyl]-4,4'-diyl)bis(9H-carbazole) ( 2.36 (CDBP))	140
5.4.3 Synthesis of 1,4-di(9H-carbazol-9-yl)benzene (2.37 (BCP))	141
5.4.4 Synthesis of compound 2.38 (P1)	142
5.4.5 Synthesis of compound 2.39 (P2)	143
5.4.6 Synthesis of compound 2.40 (P3)	144
5.4.7 Synthesis of compound 2.41 (P4)	145
5.4.8 Synthesis of compound 2.42 (P5)	146
5.4.9 Synthesis of compound 2.43 (P6)	147
5.4.10 Synthesis of compound 2.44 (P7)	148
5.4.11 Synthesis of compound 2.45 (P8)	150
5.4.12 Synthesis of compound 2.46 (P9)	152
5.4.13 Synthesis of compound 2.47 (P10)	154
5.4.14 Synthesis of compound 2.48 (P11)	156
5.4.15 Synthesis of compound 2.49 (P12)	157
<b>CONCLUSIONS</b>	158
<b>REFERENCES</b>	159
<b>LIST OF PUBLICATIONS AND PAPERS PRESENTED</b>	179
<b>APPENDIX</b>	181

## LIST OF FIGURES

Figure 2.1: Catalytic cycle for cross-coupling of organic halides and organoboranes

Figure 2.2: Two alternative oxidative addition/ reductive elimination mechanistic pathways for copper catalyzed nucleophilic aromatic substitutions with aryl halides

Figure 2.3: Structure of compounds

Figure 2.4: Proposed mechanism of Suzuki Miyaura cross coupling reaction for compound 2.56 (s = solvent)

Figure 2.5: Proposed mechanism of Ullmann cross coupling reaction for compound 2.38 (s = solvent)

Figure 3.1: Electromagnetic spectrum

Figure 3.2: Absorption spectra of Benzene, Naphthalene and Anthracene

Figure 3.3: Bandgap energy of metal, semiconductor and insulator

Figure 3.4 Partial Jablonski diagram for absorption, fluorescence and phosphorescence

Figure 3.5: Wavelength intensities of absorption, fluorescence and phosphorescence

Figure 3.6: Structure of organic dyes (M1-M6)

Figure 3.7: (a) UV-Vis absorption and (b) normalized emission spectra of M1-M6 recorded in THF solutions ( $1 \times 10^{-5}$  M).

Figure 3.8: Molecular structures of MK dyes

Figure 3.9: Normalized UV-Vis absorption spectra for different compound MK dye-loaded TiO<sub>2</sub> films using a bare TiO<sub>2</sub> film as reference.

Figure 3.10: Electronic absorption spectra at fixed bridging core unit of a) (Biphenyl) CBP, P1, P4, P7 and P9, b) (Dimethylbiphenyl) CDBP, P2, P5, P8 and P10, and c) (phenyl) BCP, P3 and P6 recorded in DMF at 30 °C

Figure 3.11: Electronic absorption spectra by the change of bridging core unit of  
a) CBP, CDBP, and BCP b) P1, P2, P3 c) P4, P5 and P6 d) P7 and P8  
e) P9 and P10 recorded in DMF at 30 °C

Figure 3.12: Emission spectra of a) CBP, P1, P4, P7 and P9, b) CDBP, P2, P5, P8  
and P10, and c) BCP, P3 and P6 recorded in DMF at 30 °C. Excitation  
at 300 nm.

Figure 3.13: Emission spectra by the change of bridging core unit a) CBP, CDBP  
and BCP b) P1, P2, P3 c) P4, P5 and P6 d) P7 and P8  
e) P9 and P10 recorded in DMF at 30 °C. Excitation at 300 nm.

Figure 3.14: Cyclic Voltammogram (0.1 Vs<sup>-1</sup>) for a) CBP, P1, P4, P7 and P9,  
b) CDBP, P2, P5, P8 and P10, and c) BCP, P3 and P6 with  
ferrocene as an internal standard in DMF - 0.05 M <sup>n</sup>Bu<sub>4</sub>NPF<sub>6</sub>

Figure 4.1: Plots of HOMO and LUMO of compounds 4.1 and 4.2

Figure 4.2: Plots of HOMO and LUMO of compounds 4.3 and 4.4

Figure 4.3: Plots of HOMO and LUMO of compounds 4.5 and 4.6

Figure 4.4: Plots of HOMO and LUMO of compounds 4.7, 4.8, 4.9 and 4.10

Figure 4.5: HOMO and LUMO frontier molecular orbitals of compounds 1.4 (CBP),  
2.36 (CDBP), 2.37 (BCP) and 2.41 (P1) - 2.47 (P10) that were calculated  
in vacuo at B3LYP/6-31G level of approximation.

## LIST OF TABLES

Table 2.1: Suzuki cross-coupling of aryl iodide with thiopheneboronic acid

Table 3.1: UV-Vis –Spectroscopic Data and Fluorescence on 300 nm excitation

Table 3.2: Oxidation potential ( $E_{pa}$ ) and Onset ( $E_{onset}$ ) by Cyclic Voltammetry

in DMF ( $0.05 \text{ mol L}^{-1}$  n-Bu<sub>4</sub>NPF<sub>6</sub>) and Optical HOMO-LUMO

Gaps ( $\Delta E_{opt}$ )

University of Malaya

## LIST OF SYMBOLS AND ABBREVIATIONS

AcOH	glacial acetic acid
$A_{\text{calcd}}$	calculated absorbance
abs	absorbance
9-BBN	9-borabicyclo[3.3.1]nonane
CH <sub>3</sub> CN	acetonitrile
CuI	copper(I) iodide
CDCl <sub>3</sub>	chloroform-d <sub>6</sub>
CCl <sub>4</sub>	carbon tetrachloride
CB	conduction band
°C	degree Celsius
CBP	(4,4'-bis(9-carbazolyl)biphenyl)
CDBP	(4,4'-bis(9-carbazolyl)-2,2'-dimethylbiphenyl)
CV	cyclic voltammogram
BCP	1,4-di(9H-carbazol-9-yl)benzene
VB	valence band
DFT	density functional theory
DSSC	dye-sensitized solar cell
Eq.	equation
eq	equivalent
em	emission
$E_{\text{pa}}$	oxidation potential
EtOH	ethanol
$E_{\text{opt}}$	optical gap
eV	electron volt

h	hour
s	second
MHz	Megahertz
MS	mass spectroscopy
HOMO	highest occupied molecular orbital
LUMO	lowest unoccupied molecular orbital
HF	Hartree-Fock
IR	infrared
ITO	indium-tin-oxide
<i>J</i>	coupling constant
LED	light emitting diodes
M	mole per liter
Min	minute
mA	mili Amphere
MP2	Moller-Plesset perturbation theory
NMR	nuclear magnetic resonance
nm	nanometer
PV	photovoltaic
OPV	organic photovoltaic
OLED	organic light emitting diode
OSC	organic solar cell
PCE	power conversion efficiency
PPh <sub>3</sub>	triphenylphosphine
Pd(PPh <sub>3</sub> ) <sub>4</sub>	palladium triphenylphosphine
PdCl <sub>2</sub> (PPh <sub>3</sub> ) <sub>2</sub>	dichlorobis(triphenylphosphine)palladium
PdCl <sub>2</sub> (dppf)	[1,1-bis(diphenylphosphino)ferrocene]dichloropalladium(II)

SnMe <sub>3</sub> Cl	trimethyltin chloride
TiCl <sub>4</sub>	titanium tetrachloride
n-Bu <sub>4</sub> NPF <sub>6</sub>	tetrabutylammoniumhexafluorophosphate
K <sub>2</sub> CO <sub>3</sub>	potassium carbonate
NaOH	sodium hydroxide
NBS	N-bromosuccinimide
KI	potassium iodide
KIO <sub>3</sub>	potassium iodate
HIO <sub>4</sub>	periodic acid
H <sub>2</sub> SO <sub>4</sub>	sulfuric acid
Na <sub>2</sub> SO <sub>4</sub>	sodium sulphate
n-BuLi	n-butyllithium
THF	tetrahydrofuran
TMSA	trimethylsilylacetylene
TiCl <sub>4</sub>	titanium tetrachloride
DMF	dimethylformamide
DCM	dichloromethane
DME	dimethoxyethane
DMS	dimethyl sulfide
H <sub>2</sub> O	water
<i>o</i> -DCB	1,2-dichlorobenzene
ppm	part per million
rt	room temperature
s	singlet
d	doublet
t	triplet



m	multiplet
dd	doublet of doublet
dt	doublet of triplet
UV	ultraviolet
v/v	volume per volume
V	volt
$\lambda$	wavelength
$\pi$	Pi
%	percent

University of Malaya

## LIST OF APPENDICES

### APPENDIX A: $^1\text{H}$ NMR AND $^{13}\text{C}$ NMR

Figure A1:  $^1\text{H}$  NMR and  $^{13}\text{C}$  NMR of 3-iodocarbazole (2.54) in  $\text{CDCl}_3$

Figure A2:  $^1\text{H}$  NMR and  $^{13}\text{C}$  NMR of 3,6-Diiodocarbazole (2.57) in  $\text{CDCl}_3$

Figure A3:  $^1\text{H}$  NMR and  $^{13}\text{C}$  NMR of 4,4-diiodobiphenyl (2.51) in  $\text{CDCl}_3$

Figure A4:  $^1\text{H}$  NMR and  $^{13}\text{C}$  NMR of 3-(Thiophen-2-yl)carbazole (2.56) in  $\text{CDCl}_3$

Figure A5:  $^1\text{H}$  NMR and  $^{13}\text{C}$  NMR of 3,6-Di(thiophen-2-yl)-9H-carbazole (2.58)  
in  $\text{CDCl}_3$

Figure A6:  $^1\text{H}$  NMR and  $^{13}\text{C}$  NMR of compound 2.60 in  $\text{CDCl}_3$

Figure A7:  $^1\text{H}$  NMR and  $^{13}\text{C}$  NMR of compound 2.62 in  $\text{CDCl}_3$

Figure A8:  $^1\text{H}$  NMR and  $^{13}\text{C}$  NMR of compound 2.64 in  $\text{CDCl}_3$

Figure A9:  $^1\text{H}$  NMR and  $^{13}\text{C}$  NMR of 4,4'-Di(9H-carbazol-9-yl)-1,1'-biphenyl  
(1.4 (CBP)) in  $\text{CDCl}_3$

Figure A10:  $^1\text{H}$  NMR and  $^{13}\text{C}$  NMR of 9,9'-(2,2'-dimethyl-[1,1'-biphenyl]-4,4'-  
diyl)bis(9H-carbazole) (2.36 (CDBP)) in  $\text{CDCl}_3$

Figure A11:  $^1\text{H}$  NMR and  $^{13}\text{C}$  NMR of 1,4-di(9H-carbazol-9-yl)benzene  
(2.37 (BCP)) in  $\text{CDCl}_3$

Figure A12:  $^1\text{H}$  NMR and  $^{13}\text{C}$  NMR of compound 2.38 (P1) in  $\text{CDCl}_3$

Figure A13:  $^1\text{H}$  NMR and  $^{13}\text{C}$  NMR of compound 2.39 (P2) in  $\text{CDCl}_3$

Figure A14:  $^1\text{H}$  NMR and  $^{13}\text{C}$  NMR of compound 2.40 (P3) in  $\text{CDCl}_3$

Figure A15:  $^1\text{H}$  NMR and  $^{13}\text{C}$  NMR of compound 2.41 (P4) in  $\text{CDCl}_3$

Figure A16:  $^1\text{H}$  NMR and  $^{13}\text{C}$  NMR of compound 2.42 (P5) in  $\text{CDCl}_3$

Figure A17:  $^1\text{H}$  NMR and  $^{13}\text{C}$  NMR of compound 2.43 (P6) in  $\text{CDCl}_3$

Figure A18:  $^1\text{H}$  NMR and  $^{13}\text{C}$  NMR of compound 2.44 (P7) in  $\text{CDCl}_3$

Figure A19:  $^1\text{H}$  NMR and  $^{13}\text{C}$  NMR of compound 2.45 (P8) in  $\text{CDCl}_3$

Figure A20:  $^1\text{H}$  NMR of compound 2.46 (P9) in  $\text{CDCl}_3$

Figure A21:  $^{13}\text{C}$  NMR of compound 2.46 (P9) in  $\text{CDCl}_3$

Figure A22:  $^1\text{H}$  NMR of compound 2.47 (P10) in  $\text{CDCl}_3$

Figure A23:  $^{13}\text{C}$  NMR of compound 2.47 (P10) in  $\text{CDCl}_3$

Figure A24:  $^1\text{H}$  and  $^{13}\text{C}$  NMR of compound 2.48 (P11) in  $\text{CDCl}_3$

Figure A25:  $^1\text{H}$  and  $^{13}\text{C}$  NMR of compound 2.49 (P12) in  $\text{CDCl}_3$

## APPENDIX B: THEORITICAL CALCULATION

Table B1: Cartesian Coordinates ( $\text{\AA}$ ) of the Optimized Structure of compound 1.4 (CBP) at the B3LYP/6-31G Level

Table B2: Cartesian Coordinates ( $\text{\AA}$ ) of the Optimized Structure of compound 2.36 (CDBP) at the B3LYP/6-31G Level

Table B3: Cartesian Coordinates ( $\text{\AA}$ ) of the Optimized Structure of compound 2.37 (BCP) at the B3LYP/6-31G Level.

Table B4: Cartesian Coordinates ( $\text{\AA}$ ) of the Optimized Structure of compound 2.38 (P1) at the B3LYP/6-31G Level

Table B5: Cartesian Coordinates ( $\text{\AA}$ ) of the Optimized Structure of compound 2.39 (P2) at the B3LYP/6-31G Level

Table B6: Cartesian Coordinates ( $\text{\AA}$ ) of the Optimized Structure of compound 2.40 (P3) at the B3LYP/6-31G Level

Table B7: Cartesian Coordinates ( $\text{\AA}$ ) of the Optimized Structure of compound 2.41 (P4) at the B3LYP/6-31G Level.

Table B8: Cartesian Coordinates (Å) of the Optimized Structure of compound  
2.42 (P5) at the B3LYP/6-31G Level

Table B9: Cartesian Coordinates (Å) of the Optimized Structure of compound  
2.43 (P6) at the B3LYP/6-31G Level

Table B10: Cartesian Coordinates (Å) of the Optimized Structure of compound  
2.44 (P7) at the B3LYP/6-31G Level

Table B11: Cartesian Coordinates (Å) of the Optimized Structure of compound  
2.45 (P8) at the B3LYP/6-31G Level

Table B12: Cartesian Coordinates (Å) of the Optimized Structure of compound  
2.46 (P9) at the B3LYP/6-31G Level

Table B13: Cartesian Coordinates (Å) of the Optimized Structure of compound  
2.47 (P10) at the B3LYP/6-31G Level

#### APPENDIX C: UV, FLUORESCENCE SPECTRA AND FERROCENE CV CURVE

Figure C1: Electronic absorption spectra of a) CBP, P1, P4, P7 and P9, b) CDBP, P2,  
P5, P8 and P10 and c) BCP, P3 and P6.

Figure C2: Emission spectra of a) CBP, P1, P4, P7 and P9, b) CDBP, P2, P5, P8 and  
P10 and c) BCP, P3 and P6.

Figure C3: Cyclic voltammogram of ferrocene in 0.1 M Bu<sub>4</sub>NPF<sub>6</sub> THF.

## CHAPTER 1: INTRODUCTION

### 1.1 Introduction

The most promising approaches to provide neat energy is by converting sunlight into electricity, which is an ample and renewable energy resource. Organic photovoltaic (OPV) can be fabricated by comparatively simpler and cost-effective processing system, such as screen printing, ink jet printing, dip coating and roll to roll processing for achieving low cost solar energy conversion devices. Additionally, lightweight and mechanically flexible is an extra advantages.

The greatest challenges of OPV are relatively low power conversion efficiency (PCE) compared to their single crystal silicon counterparts and the relative of electron accepting materials, which paired with hole conducting polymers to induce exciton dissociation at the interface.

In last four years, photovoltaic (PV) market showed average growth of 100 %. 87 % of the worldwide solar cell productions are primarily silicon based solar technologies. Further upstream, within the last couple of years to upgrade and maintain their respective in current market shares was by installation of new facilities in which polysilicon procedures kept up the PV market (European Photovoltaic Industry, 2010; Steeman *et al.*, 2012).

Despite the growth in the PV industry, the particular PV market remains its dependency on beneficial government incentives. As a result, continuously lower costs along with improve cell efficiencies are the main challenge in manufactured silicon PV.

Simple processing techniques to make low-cost with lightweight products and fabricated on large-area represent organic solar cells (OSCs) as the potential candidate. Langmuir-Blodgett (LB) technique was used in the manufacture of high quality ultrathin, anisotropic organic film in sensorics, electrooptics and electronic devices and also biomimetic system (Brook & Narayanaswamy, 1998; Cabala *et al.*, 1997; Iraqi & Wataru, 2004; Nguyen & Potje-Kamloth, 1999; Selampinar *et al.*, 1995; Swager, 1998).

Throughout early April 2011, according to the Nikkei, a Japanese business daily, Mitsubishi Chemical reportedly 9.2 % conversion efficiency of organic solar cells. Three other firms – Konarka Technologies in Lowell, Massachusetts; SolarmerEnergy Inc. in El Monte, California; and Heliatek in Dresden, Germany reporting greater efficiency of 8 %. The figure could soon top up to 10 % and possibly reach 15 %. The technologies of organics efficiency is lower than others but they are catching up at fast pace. Another concern is lifetime of organic solar cells where sun can degrade many of organic solar cells (Service, 2011).

## **1.2 Organic Photovoltaic versus Polymer Photovoltaic**

Organic photovoltaics (OPVs) were among the low cost alternatives to the silicon-based PV technology. Organic material based was utilized for the sensitive and specific chemical sensor of human exposure to chemical present in environment. A specific popular feature of organic cells in some applications where silicon technology is less capable has extremely developed. Under investigation of material science, band gap of PV polymer has successfully forced from near UV or visible towards near infrared region (NIR). Today, band gap of several PV polymers centered close to the

maximum of sun photon flux known as low band gap polymers (Blouin *et al.*, 2008). Most research could not demonstrate schematic studies to improve OPV cell for optimal performance in most application of transparent PV cell over long time scale (Romero-Gómez *et al.*, 2015).

In recent years, most polymer solar cells makers focused on polymer designing which absorb all visible light down into the reds, the low- energy of the spectrum. The amount of light absorbed would improve the cells' energy conversion. Polymer tandem makers try to make a barrier layer between two cells but the right barrier can be hard to make, because they must be not only conductive to collect electrical charges in the cells but also optically transparent. (Service, 2011)

### **1.3 Organic Photovoltaic Operation Principal**

Mobility of charge carriers in molecular semiconductor critically determined the performance of organic cells. Charge transport properties in terms of material parameters is complicated due to the complex phenomena between range of length and scales control of charge transport in disordered organic semiconductors. Until now, trial and error efforts were done rather than schematic design in order to strengthen charge mobilities in molecular semiconductor. Nevertheless, recently the very first predictive simulation advancement reviews of charge transport in disordered organic semiconductors (Nelson *et al.*, 2009).

Planar-layered framework of organic light-absorbing layer is sandwiched in two different electrodes in most organic solar cells. The two electrodes are (semi-) transparent, often Indium-tin-oxide (ITO) or a thin metal layer and aluminium (calcium, magnesium, gold and others are also used) is frequently used. The development of light emitting diodes (LEDs) and OPV are connected to each other, however the fundamental theory of light-harvesting organic PV cell is reverse of the particular principle in LEDs (Figure 1.1). Standard electrode materials are shown in the Figure 1.1. Within each instances, an organic material is sandwiched between two electrodes. In PVs electrons tend to be gathered at the metal electrode and holes are collected at the ITO electrode. The reverse happens in a LED: electrons are introduced at the metal electrode (cathode), that recombined with holes introduced at the ITO electrode (anode) (Spanggaard & Krebs, 2004).

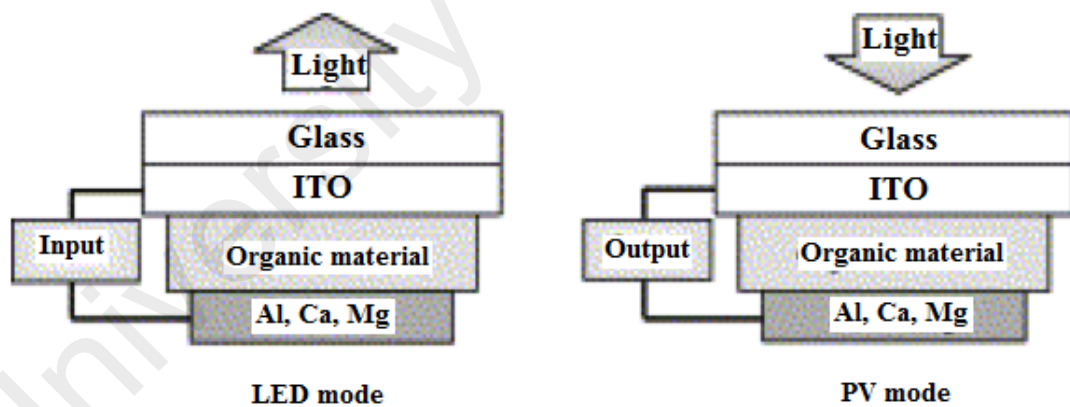


**Figure 1.1:** A PV device (right) is the reverse of LED (left).

In LEDs an electron is introduced at the low-workfunction electrode (cathode) and a hole at the high-workfunction (anode). Light was emitted upon recombination of electron and the hole (Burroughes *et al.*, 1990; Friend *et al.*, 1997; Greenham *et al.*, 1993). In contrast with a PV device, light is absorbed an



electron and then promoted from the highest occupied molecular orbital (HOMO) towards the lowest unoccupied molecular orbital (LUMO) creating an exciton (Figure 1.2). On irradiation an electron is promoted to the LUMO leaving a hole behind in the HOMO. Electrons are collected at the Al electrode and holes at the ITO electrode.

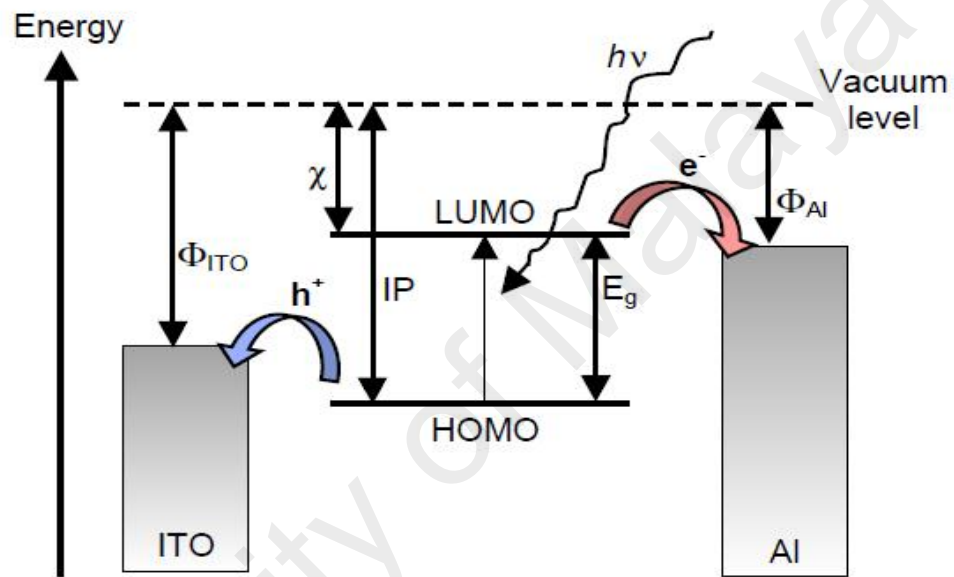


**Figure 1.2:** Energy levels and light harvesting.  $\Phi$ : workfunction,  $\chi$ : electron affinity, IP: ionisation potential,  $E_g$ : optical band gap.

Exciton dissociation in the PV device is where electron have to reach one electrode and the hole must reach the other electrode. Electrical field is necessary in order to attain charge separation that offered by the asymmetrical ionisation energy/workfunctions of the electrodes. Electron-flow is more favored from the low-workfunction electrode towards the high-workfunction electrode (forward bias) caused by the asymmetry, which this phenomenon referred to as rectification. Positioning levels of energy in light harvesting process is depicted in Figure 1.2.

Three-dimensional crystal lattice the individual LUMOs as well as HOMOs inside a crystalline inorganic semiconductor form a conduction band (CB) and valence band (VB). Weak intermolecular between LUMOs and HOMOs in three-dimensional crystal lattice could not form a CB and VB, which is fundamentally different from most organic dye semiconductor. For instance, charge carrier mobility within organic and polymeric semiconductor is generally low compared with inorganic semiconductors due to localized hopping charge transport, instead of transport within a band.

Low dielectric constant makes charge separation is more difficult within organic semiconductor. Photon absorption creates a totally free electron along with a hole (sometimes called charge carriers) in several inorganic semiconductors, whereas the excited electron is bound to the hole (at room temperature) within organic semiconductors. Approximately, conjugated polymers lay between the inorganic semiconductor and organic dyes. Generally, excitons tend to be localized and in some cases they are delocalized on specific chain segments which known as polarons (Frankevich *et al.*, 1992; Rauscher *et al.*, 1990).

Depending on organic semiconductors in simple PV devices and diodes, the electrode interface site reach by main exciton (other sites consist defects in the crystal lattice, absorbed oxygen or even impurities) (Rothberg, Yan, Papadimitrakopoulos, *et al.*, 1996; Rothberg, Yan, Son, *et al.*, 1996). The effectiveness of light harvesting limit by the thickness of the device, if the layer is too thick, the exciton never reaches the electrode interface since excitons created in the center of the organic layer. Instead they recombine as describe above. Distances of standard exciton diffusion are on the order of 10 nm.

## 1.4 Thiophene-Based for Organic Solar Cells (OSCs)

Thiophene draws a substantial interest in advanced materials such as organic TFTs, light emitting devices, and dye-sensitized organic solar cells. Thiophene derivatives possess an interesting behavior in spectroscopic properties, electrochemical behaviors, as well as liquid crystalline characteristic (Facchetti *et al.*, 2003; Funahashi *et al.*, 2007; Koumura *et al.*, 2006; McCullough, 1998; Murphy *et al.*, 2005; Tour, 1996; Yamashiro *et al.*, 1999; Yasuda *et al.*, 2006). A wide variety of thiophene derivatives developed through artificial methods has been a significant issue in organic functionality (Briehn *et al.*, 2001; Izumi *et al.*, 2003; Kobayashi *et al.*, 2006; Masui *et al.*, 2004; Satoh & Miura, 2007; Sugie *et al.*, 2006; Takahashi *et al.*, 2006; Yokooji *et al.*, 2004; F. Zhang & Bäuerle, 2007).

Design and synthesis of conjugated materials utilized thiophene as the importance building block because they have amazing optic, electronic and redox properties in addition to prominent supramolecular behavior on the solid surface or in the bulk. Thiophene is a heterocyclic rings which could be selectively modified at the  $\alpha$ - and  $\beta$ -position as well as the sulfur atom to establish flexible structures. For example, solution processibility and self-assembly capability guarantees by affixing long alkyl side-chains at the  $\alpha$ - or even  $\beta$ -position which incorporation from the  $\alpha$ -linked thiophene units into oligomers makes a competent conjugation across the primary chain backbone. Higher polarizability possess by the soft sulfur atoms in thiophene rings make the prominent contribution towards the electron-donating and charge-transport properties. Formerly, oligothiophenes as donor materials in OSCs have been widely investigated as the narrow absorption of sunlight spectra indicated low PCEs (Noma *et al.*, 1995b).

## 1.5 Literature Review

Fascinating in new  $\pi$ -conjugated organic materials are caused by their potential applications in numerous electronic devices (Klauk, 2006; Sheats, 2004), such as organic photovoltaics (OPVs) (Klauk, 2006; Sheats, 2004), organic light emitting diodes (OLEDs) (Klauk, 2006; Sheats, 2004), organic field effect transistor (OFETs) (Anthony, 2008; Dimitrakopoulos & Malenfant, 2002; Mas-Torrent & Rovira, 2008; Murphy & Frechet, 2007; Newman *et al.*, 2004; Yamashita, 2009) and sensors (J. Chen *et al.*, 2003; Thomas *et al.*, 2007). A remarkable electrochemical and optoelectrical properties possess by thiophene, a sulfur-containing aromatic heterocycle due to their various potential applications in a wide range of the organic electronic devices (Cheng *et al.*, 2009; Guo *et al.*, 2009; Haas *et al.*, 2009; Okamoto *et al.*, 2008; Shinamura *et al.*, 2010; Sista *et al.*, 2010; L. Zhang *et al.*, 2009). Thiophene derivatives are now excellent applicants and crucial precursors for the design and synthesis variety of advanced novel material (Mishra *et al.*, 2009; Perepichka & Perepichka, 2009). Carbazole moiety an excellent hole-transporting material has been widely used in organic light-emitting diodes (OLEDs) (Kato, Shimizu, *et al.*, 2012).

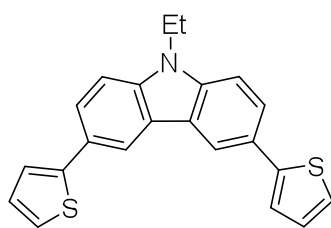
Rigorous research in organic low band gap materials has been the subject owing to their light-harvesting capability for organic photovoltaics (OPVs) (Boudreault *et al.*, 2010; Brabec *et al.*, 2011; Bundgaard & Krebs, 2007; Cheng *et al.*, 2009; Inganäs *et al.*, 2009; Rasmussen *et al.*, 2011; Thompson & Fréchet, 2008; Van Mullekom *et al.*, 2001; Zhou *et al.*, 2012). Factors that counteract the decrease in band gap are steric hindrance, which preventing a completely planar configuration in conjugated compounds (Havinga *et al.*, 1992, 1993).

Synthesizing short-chain conjugated compounds have become interesting researches, as they are not amorphous and could be synthesized as well-defined structures (Y. Lei *et al.*, 2013). The size and shape of molecules are as much a part of molecular structure as is the order in which the component atoms are bonded. Contrary to the impression from structural formulas, complex molecules are not flat and formless, but have well-defined spatial arrangements that are determined by the lengths and directional characters of their chemical bonds. This means that it is often possible to design ionic compounds having certain well-defined and desirable properties. Furthermore, the distinctive electronic properties, high photoluminescence quantum effectiveness and thermal stability have attracted much attention on shorter conjugated molecules models (Brownell *et al.*, 2013; Morvillo & Bobeico, 2008).

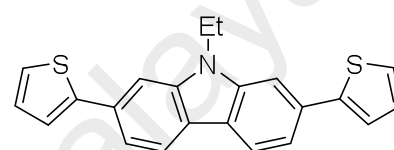
Carbazole known as hole-transporting as well as electroluminescent unit. This unique properties permit numerous photonic application (photoconductivity, electroluminescence and photorefractive) for polymers that contains carbazole moieties in the primary or side chain (Mello *et al.*, 2002; Sanda *et al.*, 2004). A large number of 3,6-functionalized carbazole derivatives have been analyzed as carbazole easily functionalized through electrophilic aromatic substitution at its 3,6-positions (para position from the nitrogen atom) with high electron density (Gauthier & Frechet, 1987). Consequently, due to the extremely electron donating ability of mixed  $\pi$ -conjugated polymers and oligomers made of carbazoles and thiophenes are a brand new course of functional compounds (Melucci *et al.*, 2007; Zhan *et al.*, 2001; Zotti *et al.*, 2002).

The 3,6-di(2-thienyl) substituent of compound **1.1** can be found at the para positions in accordance with the nitrogen atom of the carbazole moiety, while the 2,7-di(thienyl) substituent of compound **1.2** are at the meta positions. Therefore, the

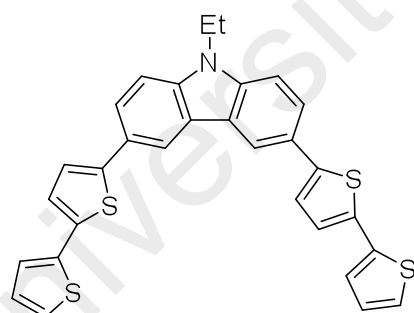
electron-donating capability of the carbazole moiety in **1.1** is actually improved through the 3,6-di(2-thienyl) groups compared to **1.2** due to the cross-conjugation. The electronic effects of thienyl groups in the carbazole moiety **1.1** and **1.3** had been acquired at the B3LYP/6-311G\*\*//B3LYP/6-31G\* level of theory which provide considerably different value 4.09 and 3.47 eV respectively, where most of LUMO density on **1.3** resides on 2,2'-bithiophen-5-yl unit (Kato, Shimizu, *et al.*, 2012).



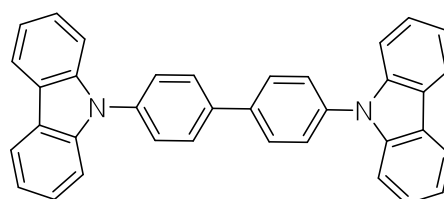
**1.1**



**1.2**



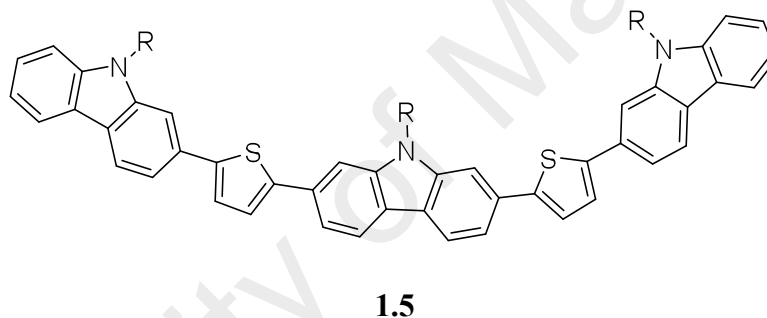
**1.3**



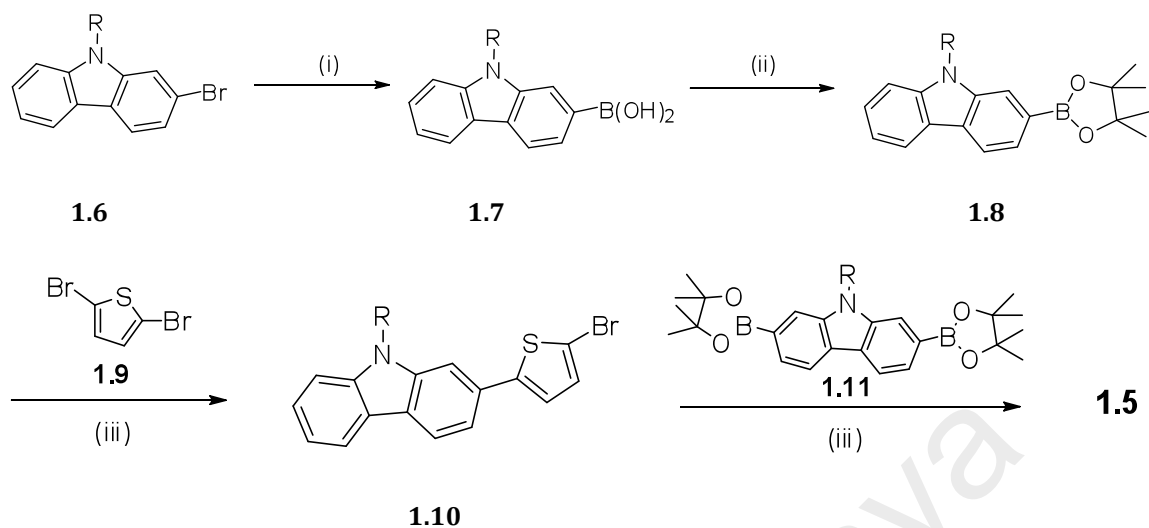
**1.4 (CBP)**

Carbazole-based materials exhibit hole-transport properties even though numerous acceptor moieties such as 4,4'-bis(carbazol-9-yl)biphenyl (Matsusue *et al.*, 2005) **1.4 (CBP)** synthesized by Ullmann reaction have been popular as donors in a number of electronic devices (Koene *et al.*, 1998).

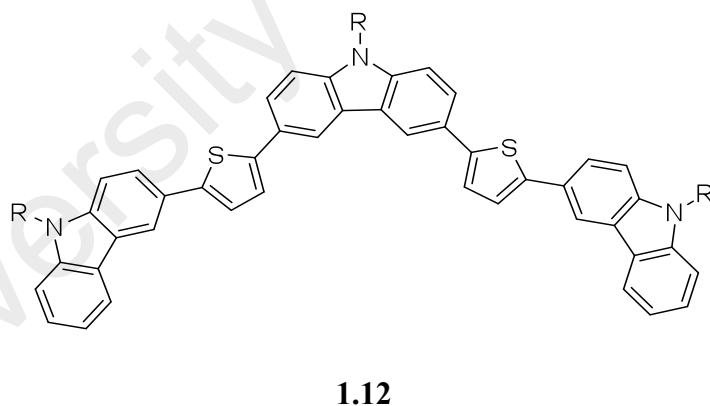
Shin-ichiro Kato *et al.* (2014) prepared a number of systematically elongated alternating 2,7-linked and 3,6-linked carbazole-thiophene oligomers which has been synthesized by Suzuki-Miyaura coupling in Scheme 1.1 and Scheme 1.2, respectively. Higher degree of  $\pi$ -conjugation and high fluorescence quantum yields was observed in connection with thiophene at 2,7-position of carbazole (**1.5**) and donor ability improved at 3,6-positions (**1.12**). 2,7-linked oligomers successfully extend  $\pi$ -conjugation as the increase in the molecular length.



The synthesis of **1.5** was outlined in Scheme 1.1. The lithium-bromine exchange between **1.6** and n-BuLi followed by the successive addition of trimethoxyborane and aqueous HCl gave boronic acid **1.7** which was converted to boronic acid pinacol ester **1.8** in 48% yield in two steps. Bromide **1.10** was prepared by the coupling reaction of **1.8** and 3 eq of 2,5-dibromothiophene (**1.9**) in 20% yield and then was subjected to the coupling reaction with **1.11** to furnish **1.5** in 63% yield.

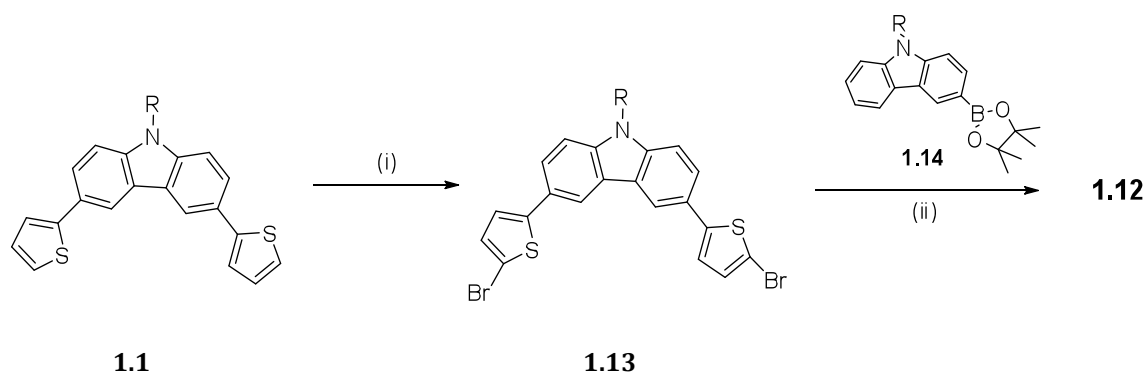


**Scheme 1.1:** Synthesis of **1.5**. Reaction conditions: (i) a) n-Buli, THF, -98 °C b) B(OMe)<sub>3</sub>, THF, -98 °C c) HCl aq. (ii) Pinacol, THF, reflux (iii) [Pd(PPh<sub>3</sub>)<sub>4</sub>], K<sub>2</sub>CO<sub>3</sub>, DME / water, reflux.



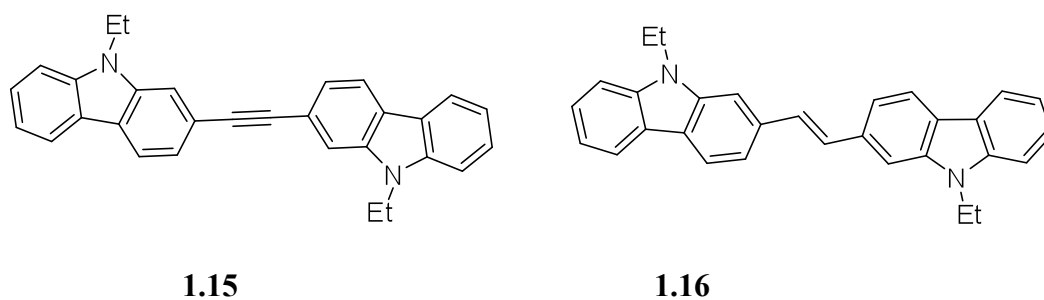
The synthesis of compound **1.12** was outlined in Scheme 1.2. The synthesized following a two-step transformation from **1.1**. Thus, the bromination of **1.1** with NBS was carried out and then the cross-coupling reaction of dibromide **1.13** with **1.14** afforded the desired **1.12** in 64% yield.



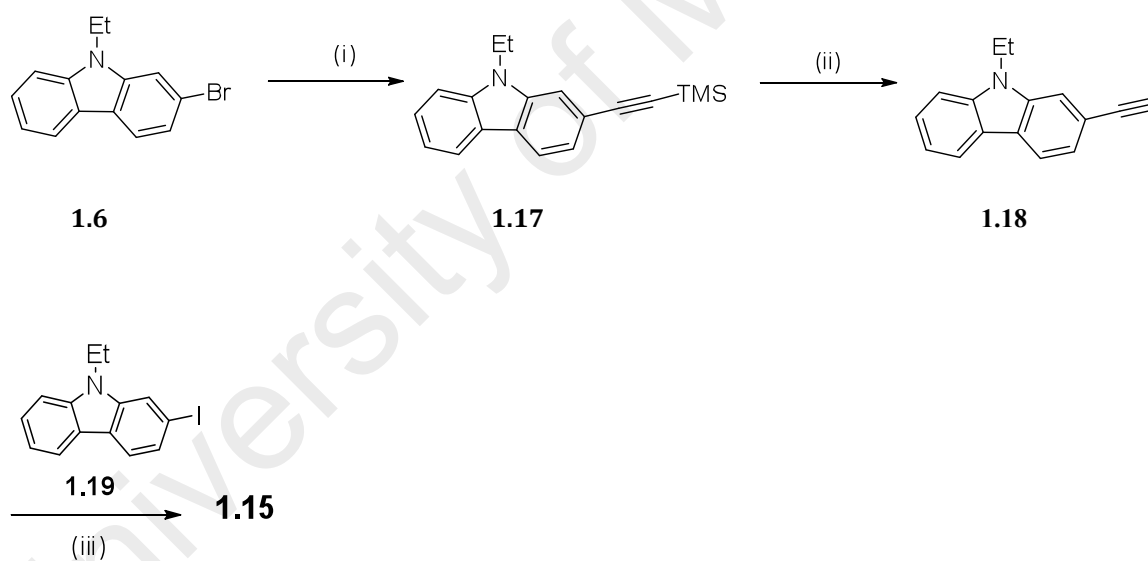


**Scheme 1.2:** Synthesis of **1.12**. Reaction conditions: (i) NBS, DMF, rt (ii)  $[\text{Pd}(\text{PPh}_3)_4]$ ,  $\text{K}_2\text{CO}_3$ , DME / water, reflux.

Shin-ichiro Kato *et al.* (2012) also report bicarbazoles in a large series of conjugated carbazole dimmers, which had been synthesized through Suzuki-Miyaura, Sonogashira, Hay and McMurry coupling reaction. Connection at the 1-,2-, or 3-position directly or *via* an acetylenic (**1.15**) (Scheme 1.3) or olefinic (**1.16**) (Scheme 1.4) spacer in both carbazole ensures high extent of  $\pi$ -conjugation at the 1-position of carbazole, while electron-donating ability improves at the 3-position and both acetylenic and olefinic spacers extend  $\pi$ -conjugation, which also leads to the increase of the donor ability.

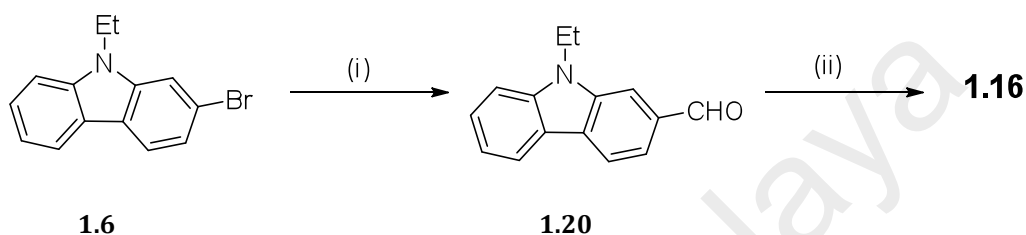


The synthesis of compound **1.15** was outlined in Scheme 1.3. For the synthesis of **1.15**, compound **1.17**, was synthesized by the Sonogashira reaction of **1.6** and trimethylsilylacetylene (TMSA) followed by the removal of TMS group with  $K_2CO_3$ . The Sonogashira reaction of **1.18** and **1.6**, however, produced no desired **1.15**. Therefore, bromide **1.6** was converted to iodide **1.19** with excess amounts of CuI/LiI in DMSO. The reaction of **1.18** and **1.19** with  $Pd(PPh_3)_4$  catalyst and CuI cocatalyst was first examined, but **1.15** was again not isolated. Finally, when  $Pd(PPh_3)_4$  was employed as the sole catalyst in the absence of CuI, the homocoupling reaction of **1.18** was suppressed to some extent and **1.15** was obtained.



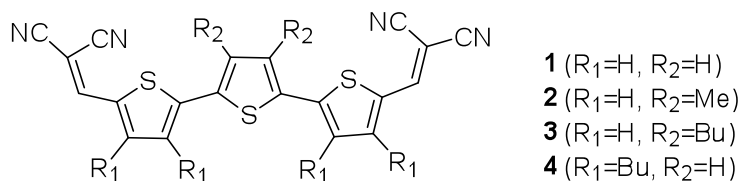
**Scheme 1.3:** Synthesis of compound **1.15**. Reaction conditions: (i) TMSA,  $PdCl_2(PPh_3)_2$ , CuI,  $PPh_3$ , piperidine, 100 °C. (ii)  $K_2CO_3$ , THF / MeOH, rt. (iii)  $Pd(PPh_3)_4$ , THF /  $Et_3N$ , reflux (based on **1.17**).

The synthesis of compound **1.16** was outlined in Scheme 1.4. The preparation of **1.16** rely on McMurry coupling reactions (1989). Thus, lithium–bromine exchange between **1.6** and n-BuLi followed by the successive addition of piperidine-1-carbaldehyde and aqueous NH<sub>4</sub>Cl gave aldehyde **1.20**, which was allowed to react with TiCl<sub>4</sub> and zinc powder in THF to furnish **1.16** in 78% yield.



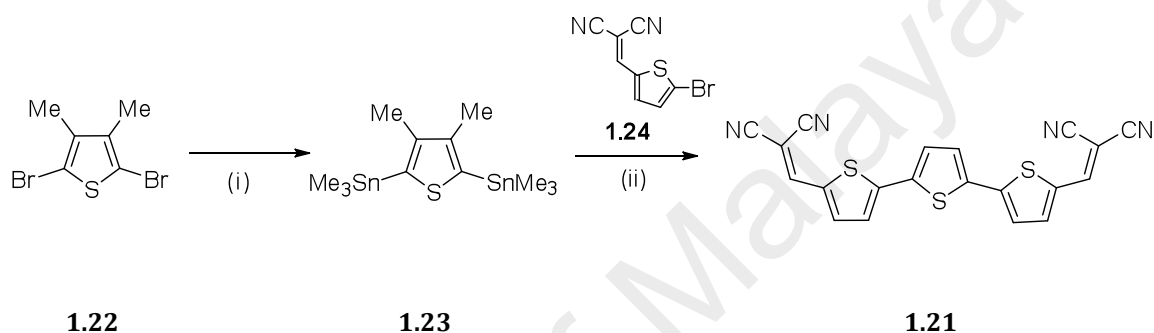
**Scheme 1.4:** Synthesis of compound **1.16**. Reaction conditions: (i) a) n-BuLi, THF, -78 °C b) Piperidine-1-carbaldehyde, 78 °C to rt c) NH<sub>4</sub>Cl aq. (ii) Zn, TiCl<sub>4</sub>, THF / pyridine, reflux.

Hannah Ziehlke *et al.* (2011) documented a series of dicyanovinyl-terthiophenes (**1.21**) with various alkyl side chains. Absorption, energy levels, and thin film roughness were affected by the variance of side chain substitution patterns where the morphology of the evaporated thin film was depending on the length of the substances. The effectiveness of energy transfers is dependence on the type of side chain.



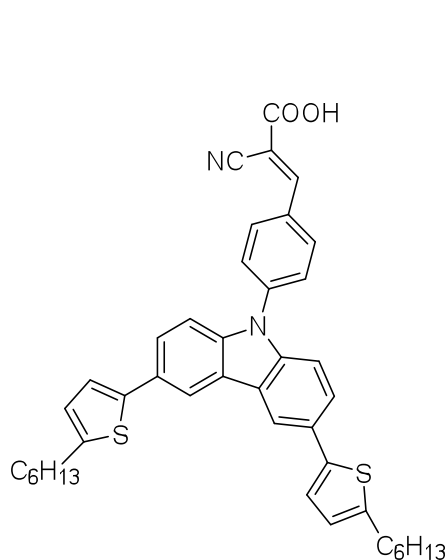
**1.2**

Synthesis of compound **1.21** was outlined in Scheme 1.5. Dis- tannylated dimethylthiophene **1.23** is prepared from 2,5-dibromo- 3,4-dimethylthiophene **1.22** by lithiation with n-butyllithium and subsequent quenching with trimethylstannyl chloride. Two-fold Pd0-catalyzed Stille-type coupling reaction of central building block **1.23** and dicyanovinyl-substituted bromothiophene **1.24** gives **1.21** in 80% yield.

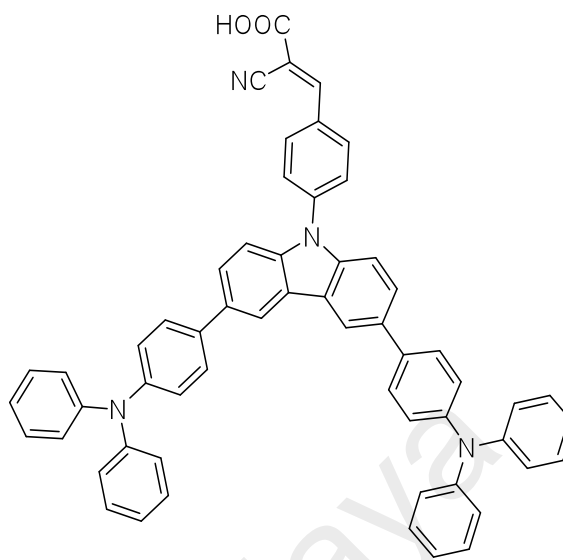


**Scheme 1.5:** Synthesis of compound **1.21**. Reaction conditions: (i) a) n-BuLi b) SnMe<sub>3</sub>Cl (ii) Pd(PPh<sub>3</sub>)<sub>4</sub>.

Naresh Duvva *et al.* (2015) have synthesized two push-pull substances employing carbazole alkyl thiophene (**1.25**) and carbazole triphenylamine (**1.26**) as donor moieties. They have used the cyanoacrylic group as the acceptor. The moderate photovoltaic efficiency of the sensitizers may be related to the poor light absorption of the sensitizers in the visible area. Density functional theory (DFT) calculations have shown a powerful intramolecular charge transfer character, with the HOMOs of both the sensitizers exclusively localized on the corresponding donor moieties and LUMOs on the cyanoacrylic acid acceptor. However, less extended and intense absorption spectra in the visible region caused by the calculated high dihedral angle between the carbazole donor and the phenyl bridge impedes the conjugation across the dyes backbone.



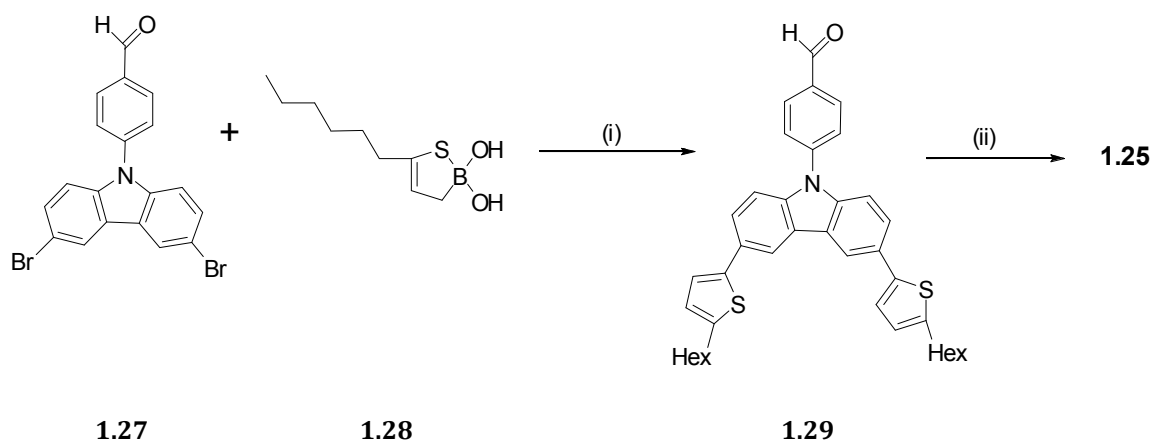
**1.25**



**1.26**

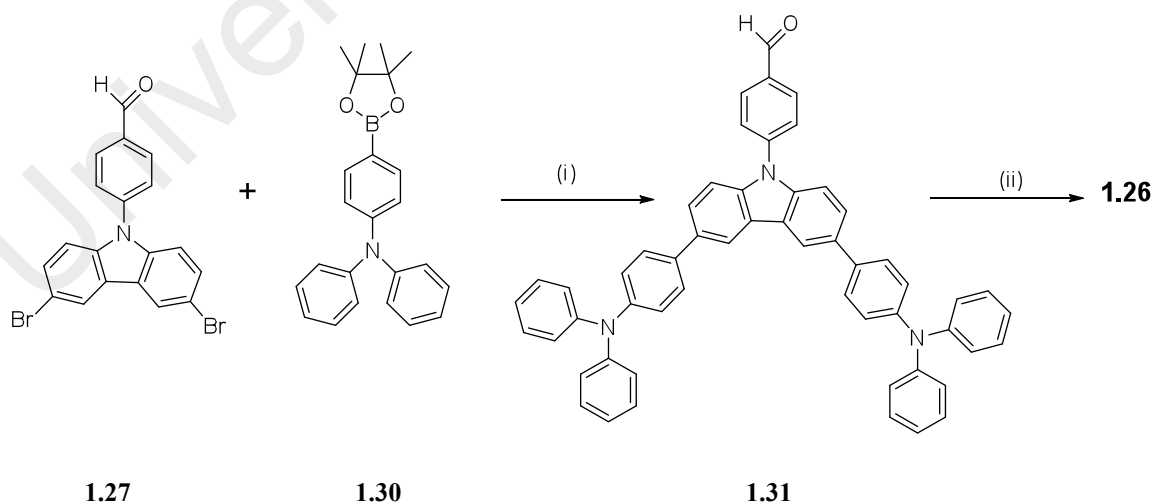
The synthetic approach to these single donor (**1.25**) and double donor (**1.26**) metal-free organic sensitizers involves Miyaura borylation, Suzuki and Knoevenagel reactions and the synthetic routes are outlined in Schemes 1.6 and 1.7.

Compound **1.25** was synthesized by Suzuki coupling reaction of compound **1.27**. In a typical synthesis, compound **1.27** and 5-hexylthiophene-2-yl-2-boronic acid **1.28** were dissolved in DME and  $\text{Na}_2\text{CO}_3$  solution.  $\text{Pd}(\text{PPh}_3)_4$  were added and reaction mixture refluxed for 18 h gives **1.29**. Compound **1.29**, cyanoacetic acid and ammonium acetate were dissolved in acetic acid and refluxed for 14 h gives **1.25** in 76 % yield.



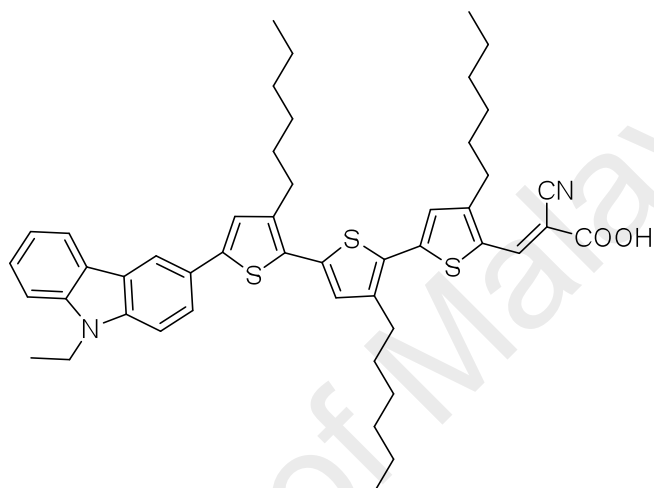
**Scheme 1.6:** Synthesis of compound **1.25**. Reaction conditions: (i)  $\text{Pd}(\text{PPh}_3)_4$ ,  $\text{Na}_2\text{CO}_3$ , DME,  $\text{H}_2\text{O}$ . (ii) AcOH, cyanoacetic acid,  $\text{CH}_3\text{COO}^-\text{NH}_4^+$ , reflux 14 h.

Compound **1.26** was synthesized similar to the procedure adopted for preparing compound **1.25**. Compound **1.31** was synthesized by palladium catalyzed Suzuki coupling between compound **1.27** and compound **1.30**. KOAc and  $\text{Pd}(\text{PPh}_3)_2\text{Cl}_2$  were dissolved in DMF reflux for 6 h give **1.31**. Compound **1.31**, cyanoacetic acid and ammonium acetate were dissolved in acetic acid and refluxed for 14 h gives **1.26** in ~76 % yield.

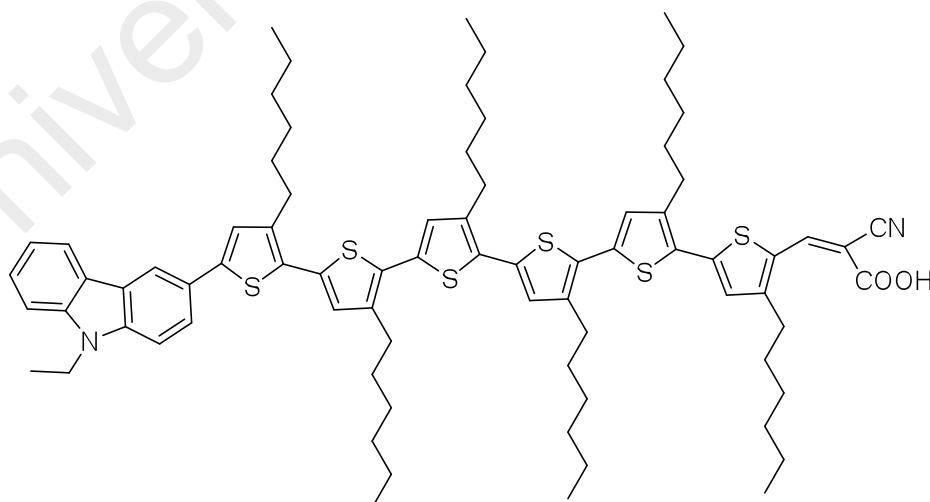


**Scheme 1.7:** Synthesis of compound **1.26**. Reaction conditions: (i)  $\text{Pd}(\text{PPh}_3)_2\text{Cl}_2$ , KOAc (ii) AcOH, cyanoacetic acid,  $\text{CH}_3\text{COO}^-\text{NH}_4^+$ , reflux 14 h.

Koumura and co-workers (Koumura *et al.*, 2006; Z.-S. Wang *et al.*, 2008) systematically investigated the effect of  $\pi$ -conjugated system series of n-hexyl-substituted oligothiophenes (**1.32** and **1.33**), which are carbazole sensitizers with regard to DSSCs overall performance.



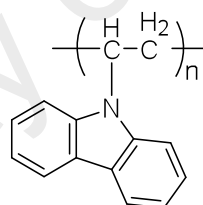
**1.32**



**1.33**

The molecular structure of the dyes in DSSCs substantially depends on the number and position of thiophene moieties. The existence of n-hexyl chains linked to the thiophene groups cause retardation of charge recombination, which led to an increase in electron lifetime. The addition of n-hexyl chains to the thiophene groups has improved open-circuit photovoltage ( $V_{oc}$ ) and the solar to electric power conversion efficiency ( $\eta$ ) of DSSCs.

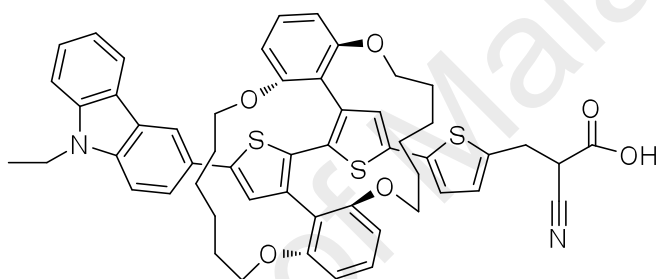
For the very first time, Miyasaka and co-workers used the carbazole based polymer (poly(N-vinyl-carbazole)) (PVK) (**1.34**) in dye-sensitized solar cell as a hole transporting layer and the cell demonstrated power efficiency of 2.4 and 2.0 % at 0.25 and 1 sun (AM 1.5) light irradiation, respectively (Ikeda & Miyasaka, 2005).



**1.34**

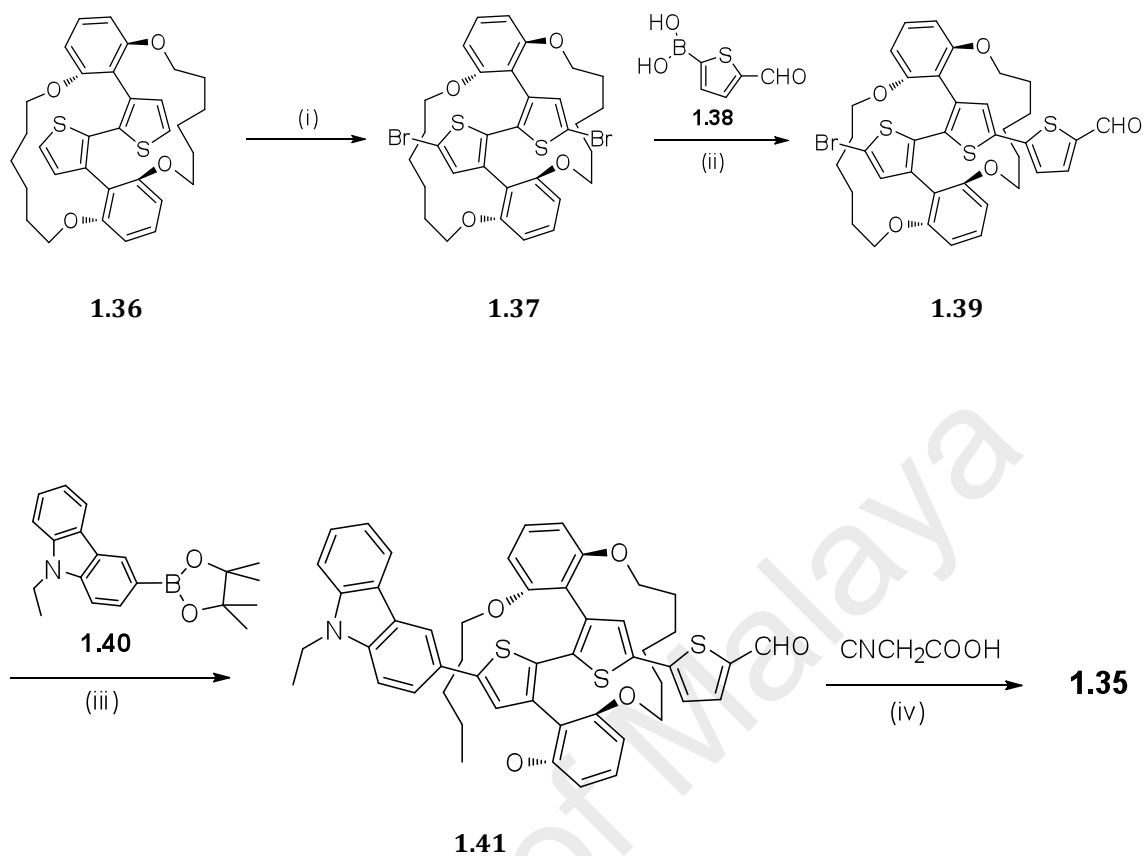


Recently, Han and co-workers reported efficient carbazole based sensitizer showing versatile flexible circle chain embracing  $\pi$ -spacer (**1.35**), that has an efficiency of 9.2 %. In the majority of the carbazole sensitizers, cyanoacrylic group is often utilized as an anchoring group (J. Liu *et al.*, 2013). Chemical substituents that can act as an anchor, enabling their adsorption onto a metal oxide substrate. This adsorption provides a means for electron injection, which the process that initiates the electrical circuit in a DSSCs.



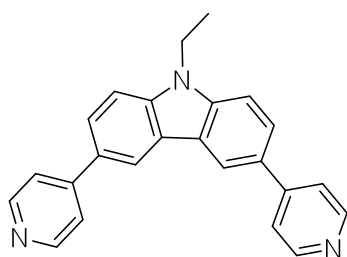
**1.35**

Synthesis of compound **1.35** was outlined in Scheme 1.8. Bromination of **1.36** with NBS was carried out and then the cross-coupling reaction of dibromide **1.37** with **1.38** afforded compound **1.39**. Compound **1.41** was synthesized by palladium catalyzed Suzuki coupling between compound **1.39** and compound **1.40**. A solution of aldehyde **1.41**, cyanoacetic acid, piperidine in  $\text{CHCl}_3$  was reflux for 10 h to afford the desired dye **1.35** as a purple solid in 87 % yield.

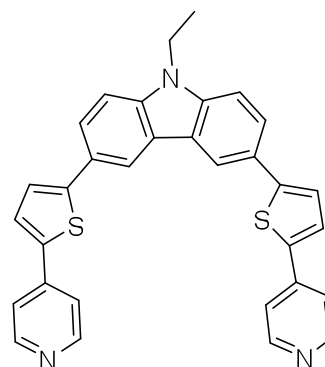


**Scheme 1.8:** Synthesis of compound **1.35**. Reaction conditions: (i) NBS (ii)  $\text{K}_2\text{CO}_3$ ,  $\text{Pd}(\text{PPh}_3)_4$ , THF,  $\text{H}_2\text{O}$ ,  $50\text{ }^\circ\text{C}$  (iii)  $\text{K}_2\text{CO}_3$ ,  $\text{Pd}(\text{PPh}_3)_4$ , 1,4-dioxane,  $\text{H}_2\text{O}$ ,  $90\text{ }^\circ\text{C}$ . (iv) piperidine,  $\text{CHCl}_3$ , reflux for 10 h.

Nevertheless, Harima and co-workers (2013) reported new carbazole based sensitizers bearing pyridine anchoring group along with a thiophene (**1.42** and **1.43**) unit as a  $\pi$ -bridge, accomplished the efficiency of 1.61 %. By substituting correct functional groups at C3, C6 and N9 positions of the carbazole scaffold, it is possible to tune the optoelectronic properties and therefore the device performance.



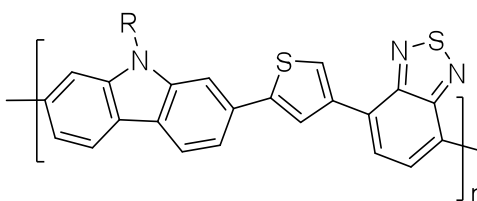
**1.42**



**1.43**

Xinliang Feng (2011) reported thiophene-based conjugated oligomer with molecular architectures from 1D to 3D in developing high-performance OSCs. This represent an enormous source of materials for OSCs and have taken aggressive benefits more polymeric materials. A well balanced device overall performance depending on their synthetic reproducibility and the ability to form long range crystalline ordering in the solid state which is beneficial for the charge carrier transport. Furthermore, low molecular weights, great thermal stabilities and device fabrication could be done by vacuum-deposited or solution-processable (or both) method. Currently, oligothiophene-based donor materials in organic solar cells have achieved excellent PCEs of over 8 % ("Heliatek GmbH Press Release," 2010).

High PCE over 7 % for OPVs had been achieved with 2,7-carbazole-containing polymer such as poly(2,7-carbazole-alt-dithienylbenzothiadiazole) (**1.44**) (T.-Y. Chu *et al.*, 2011).



**1.44**

Over the past three years, a considerable investigation associated with new building blocks in developing high end polymer semiconductors has been an extensive research (He *et al.*, 2014). For instance, the film morphology and molecular stacking could be control by the side chain in order to significantly enhance the charge carrier mobility (T. Lei *et al.*, 2012). The energy levels might reduce while maintaining the band gaps almost unchanged by fluorinated building blocks (H.-Y. Chen *et al.*, 2009; Liang *et al.*, 2009). However, development of new building blocks still needs a lot of work.

### **1.6 Objective of the Study**

One strategy to design new functional materials would be to imitate the actual framework from the well-known as well as well-studied substances, even though their synthesis may be a great challenge. Structurally, CBP can be viewed as a carbazole end-capped biphenyl. To design new semiconducting compound for OPV application, we investigate the behaviors associated with a series of thiophene-carbazole-based derivatives. The objective of this research are i) to synthesize a series of symmetric carbazole-thiophene based derivatives, ii) to investigate their electronic behavior by varying the conjugation connectivity as well as the number of thiophene units to study the actual structure-property relationships associated with carbazole-thiophene-based materials that have taken biphenyl, benzene and dimethylbiphenyl as core and iii) to provide theoretical calculation of the electron distribution for HOMO and LUMO of carbazole-thiophene derivatives. In this context, we report the synthesis and fundamental properties, such as the structure features as well as electronic, photophysical properties on the basis of UV-Vis, fluorescence emission, cyclic voltammetry, supported by quantum chemical calculation (DFT) had been utilized in characterization of these new compounds.

## CHAPTER 2: SYNTHESIS OF CARBAZOLE-THIOPHENE BASED DERIVATIVES

### 2.1 Introduction

Organic electronic devices have drawn a lot of interest for their properties. They could be easily tuned by suitable molecular design and could be produced on a large scale at low prices.

Formations of new carbon-carbon bonds are important reactions in development of complex bio-active drugs, agrochemicals and also ingeniously-designed organic materials. These bio-active materials show novel electronic, optical or mechanical properties, which can play significant role in the development of nanotechnology.

During the past forty years, the most crucial carbon-carbon bond-forming methodologies included utilizing transition metals to mediate the reactions in a controlled and selective method. Probably the most favored of those chemistries is Suzuki coupling, that is cross-coupling reaction of numerous organoboron compounds with organic electrophiles catalyzed by a palladium complex. It is now the fundamental element of any synthetic route to construct organic complex. This reaction turned out to be extremely versatile.

Since it was discovered a century ago (Ullmann, 1903), products of Ullmann-type aryl are essential in the pharmaceutical and material world, which has been observed on industrial-scale applications. The range of this reaction, nevertheless, is

significantly restricted to its high reaction temperature (Ley & Thomas, 2003). Classic Ullmann methods have been recognized for a complete hundred years for C-N, C-S, C-O and plus other bond formation. The entire evidence acquired demonstrated that copper noticeably much similar to palladium in cross-coupling chemistry.

Main method for the synthesis of novel heterocyclic compounds have been developed by copper-catalyzed C-N, C-O, and C-S bond formations between aryl halides and NH, OH, SH-containing heterocyclic (Beletskaya & Cheprakov, 2004; Klapars *et al.*, 2002; Kunz *et al.*, 2003; Kwong & Buchwald, 2003; Ley & Thomas, 2003; Lindley, 1984; Okano *et al.*, 2003). Wide range of compounds from simple to complex molecules were regularly prepared by utilized copper-mediated C(aryl)-O, C(aryl)-N, and C(aryl)-S bond formation.

## 2.2 Suzuki-Miyaura Coupling

Common strategy and effective way for the formation of carbon-carbon bonds are palladium-catalyzed cross-coupling reaction between organoboron compounds and organic halides. Recently, this particular reaction may be known as Suzuki coupling, Suzuki reaction, or Suzuki-Miyaura coupling (SM). The coupling reaction offers several extra benefits. For an example, it is unaffected by the existence of water and also tolerate an extensive selection of functional groups, and generally regio- and stereoselective. Furthermore, the inorganic by-product from the reaction mixture is non-toxic and can be removed easily, therefore making the Suzuki coupling appropriate for commercial procedures (Akira Suzuki, 1999).

Recently, SM cross coupling that produces biaryls was the most popular even though other methods are also available, for examples, Kharash coupling, Negishi coupling, Stille coupling, Himaya coupling, Liebeskind-Srogl coupling and Kumuda coupling. Moderate reaction conditions and the industrial accessibility of variety boronic acids which are environmentally safer compared to other organometallic reagents were the key benefit of SM coupling (Kotha *et al.*, 2002). Additionally in large-scale synthesis, the elimination of boron-containing byproducts is easy to handle. The SM reaction has become dominance within the last couple of years, which responsive in industrial synthesis of pharmaceuticals and fine chemicals since the conditions have many desirable features for large-scale synthesis (Kotha *et al.*, 2002).

Aryl bromides, aryl iodide and aryl triflate frequently utilized in the Suzuki reaction. Aryl chlorides only utilized along with electron-deficient groups (Miyaura & Suzuki, 1995). However triflates are thermally labile, susceptible hydrolysis and costly in preparation. Aryl sulphonates tend to be a better choice and inexpensive compared to triflates because there are readily available starting materials. They could be find easily through phenol and more stable.

The different in the SM cross coupling reaction between coupling rate of the iodo- versus bromo-function offers some advantages in organic synthesis. Stepwise functionalisation procedure could be used for multifunctional substrates. This specificity of the reaction only for the iodinated carbon if the coupling partner is not utilized in excess.

In SM cross-coupling reaction,  $\text{Na}_2\text{CO}_3$  base was typically used but often inadequate with sterically challenging substrates. In many cases,  $\text{Ba}(\text{OH})_2$  or  $\text{K}_3\text{PO}_4$  were used which produce better yields. Other bases such as  $\text{K}_2\text{CO}_3$ ,  $\text{CS}_2\text{CO}_3$ ,  $\text{KF}$  and  $\text{NaOH}$  are also have been utilized. Within the coordination sphere of the palladium and the formation of the  $\text{Ar-Pd(II)-OH}$  from  $\text{Ar-Pd(II)-X}$ , the active base may speed up the transmetallation step (Figure 2.1) (Kotha *et al.*, 2002). Pd-mediated SM cross-coupling reaction has several disadvantages. Only aryl bromides and iodides may be utilized. Chlorides only react gradually. In many cases, coupling products of phosphine-bound aryls byproducts are often formed such as self-coupling products. Particular disadvantage has formed scrambled derivatives which most probably  $\text{Pd}(\text{PPh}_3)_4$  catalyst and phenyl group of the  $\text{PPh}_3$  becomes affected in the product. Homocoupling products can be prevented under oxygen free conditions by de-gas the solvents to remove dissolved oxygen.

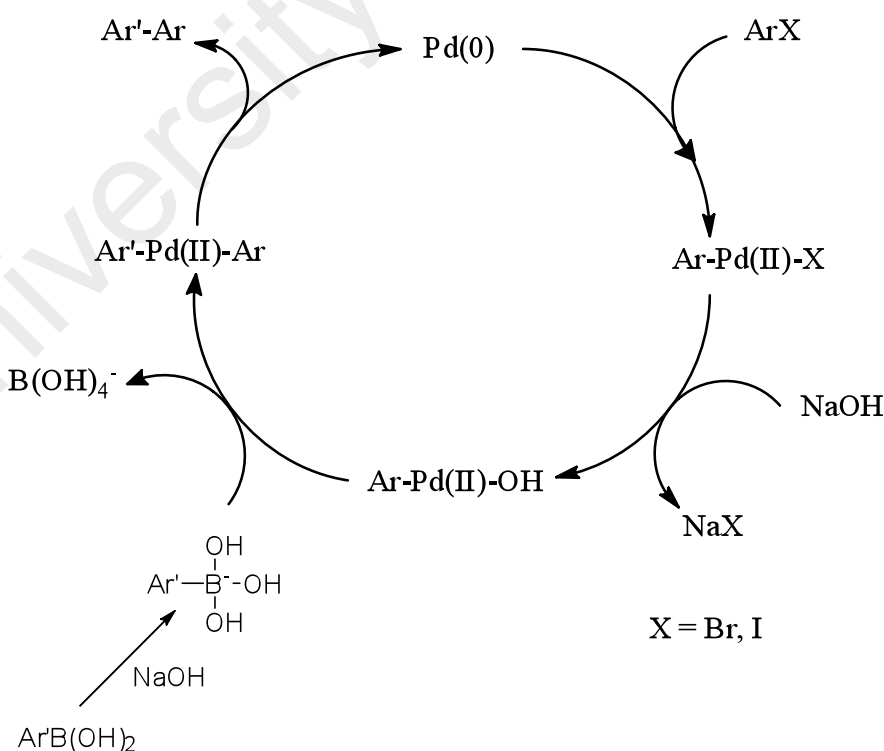


**Figure 2.1:** Catalytic cycle for cross-coupling of organic halides and organoboranes.



In the past ten years, numerous options in Suzuki reaction continually to develop such as solid phase Suzuki coupling may be created by utilizing either resin-bound aryl halides with solution phase boronic acids (A. Suzuki & Brown, 2003) or vice versa (Carboni *et al.*, 1999).

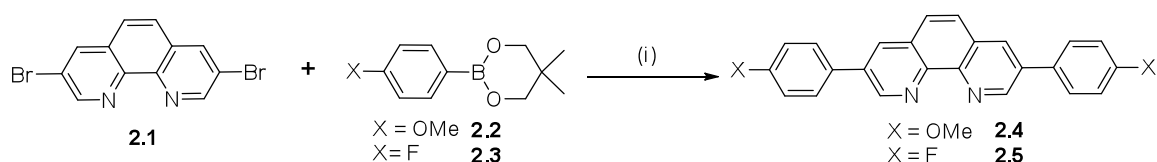
Industry is trying to make use of much more environmentally-friendly procedures in which Suzuki coupling well suited. The adjustment of reaction either in aqueous media or with trace amounts of catalyst was actively investigated.

## 2.2.1 Suzuki Miyaura Reaction

### 2.2.1.1 Biphenylene System

SM cross-coupling reaction has become a useful tool for assembling biphenyl (paraphenyl) systems. They are important structural element in most liquid crystal, fluorescent compounds and conducting polymer (Kotha *et al.*, 2002).

The Pd(PPh<sub>3</sub>)<sub>4</sub> – catalysed SM cross coupling reaction of 3,8-dibromo-1,10-phenanthroline **2.1** with the arylboronic acids **2.2** and **2.3** to give the coupling products **2.4** and **2.5** (Scheme 2.1) (Dietrich-Buchecker *et al.*, 1999).

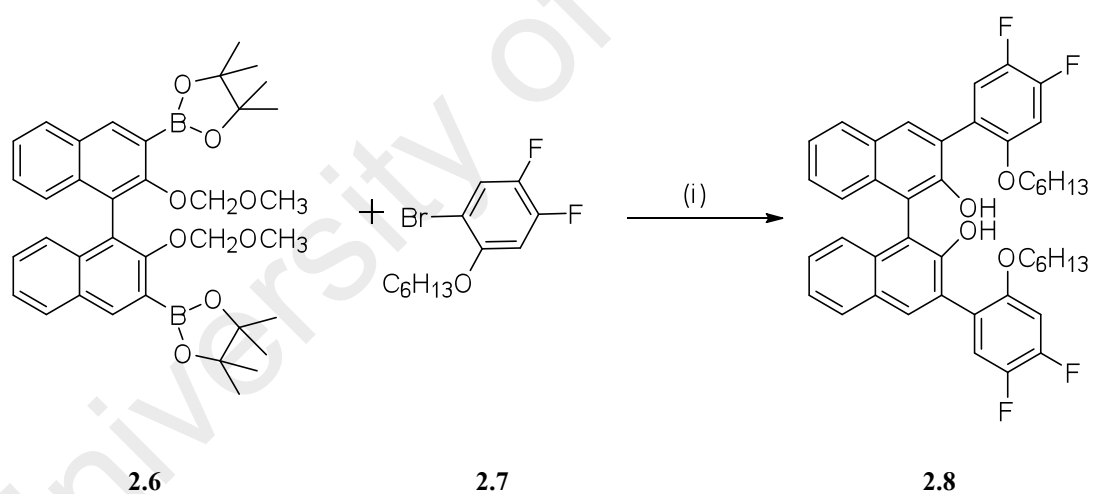


**Scheme 2.1:** Synthesis of **2.4** and **2.5**. Reaction conditions: (i) Pd(PPh<sub>3</sub>)<sub>4</sub> (10%), Na<sub>2</sub>CO<sub>3</sub>, toluene, 80 °C, 12 h.

### 2.2.1.2 Binaphthyl System

Chiral binaphthyl-based ligands are useful for enantio- and diastereo-selective synthesis of organic molecules. Recent example of the synthesis of binaphthyl ligands *via* the SM cross-coupling reaction.

Pu et. al. have used the Pd(PPh<sub>3</sub>)<sub>4</sub>-catalysed SM cross-coupling of a fluorine containing binaphthyl ligand **2.8** by using the SM cross-coupling of the preformed binaphthyl-based bispinacolboronate **2.6** with the fluorine-substituted halobenzene **2.7** (Scheme 2.2) (Huang & Pu, 2000).

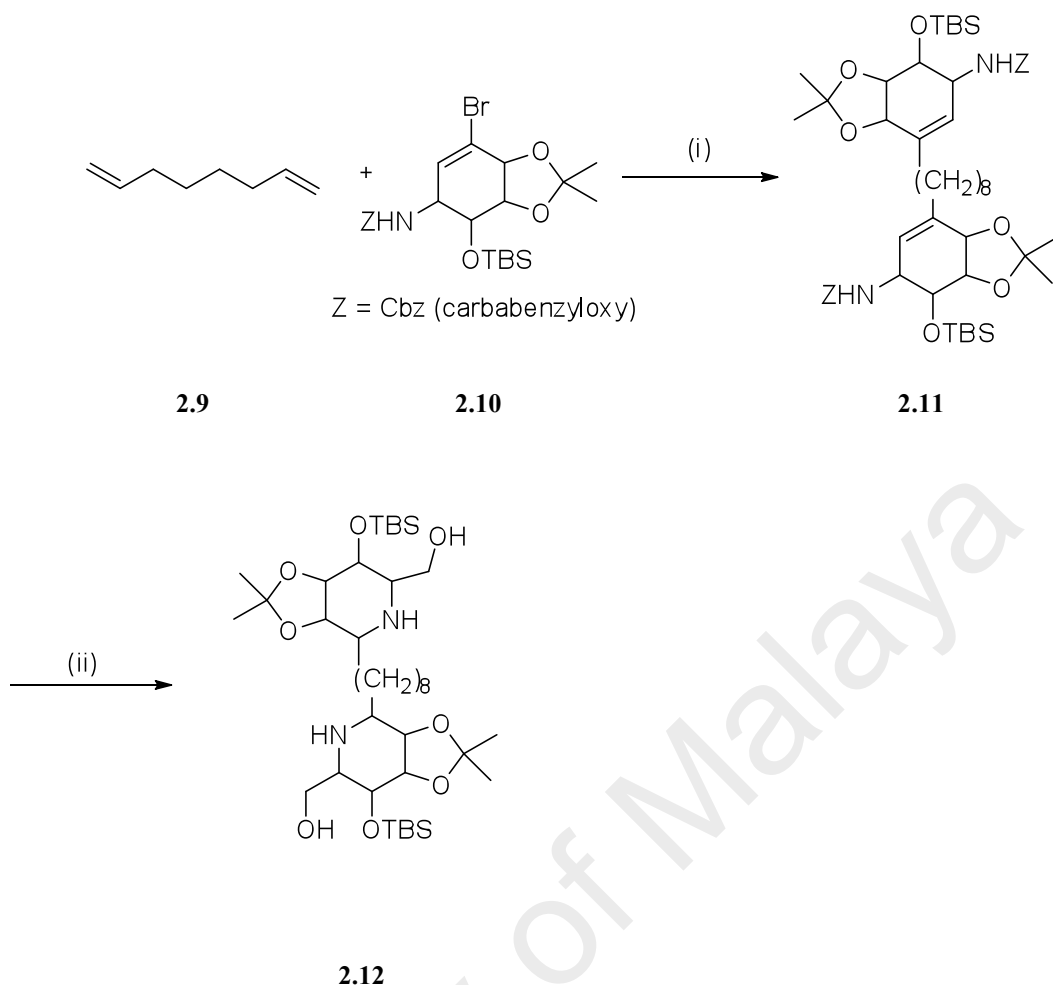


**Scheme 2.2:** Synthesis of **2.8**. Reaction conditions: (i) a) Pd(PPh<sub>3</sub>)<sub>4</sub> aq., KOH, THF, (ii) 6N HCl, THF, reflux.

### 2.2.1.3 Reaction Involving 9-BBN Derivatives

The SM cross-coupling reaction has played an important role in the synthesis of complex natural products like ciguatoxin, gambierol, epothilone, phomactin, and halichlorine. In this regard, hydroboration of alkenes followed by the SM cross-coupling reaction has been used as a key step.

Johnson and Johns have reported the synthesis of the glycosidase inhibitor bis-aza sugar **2.12** by using the double SM cross-coupling reaction. The required borane is prepared from the terminal diene **2.9** and is coupled with the vinyl bromide **2.10**. Peperidine ring formation was initiated by cleavage of trisubstituted olefin **2.11** and cyclization was accomplished *via* an intramolecular reductive amination to yield aza sugar **2.12** (Scheme 2.3) (Johns & Johnson, 1998).

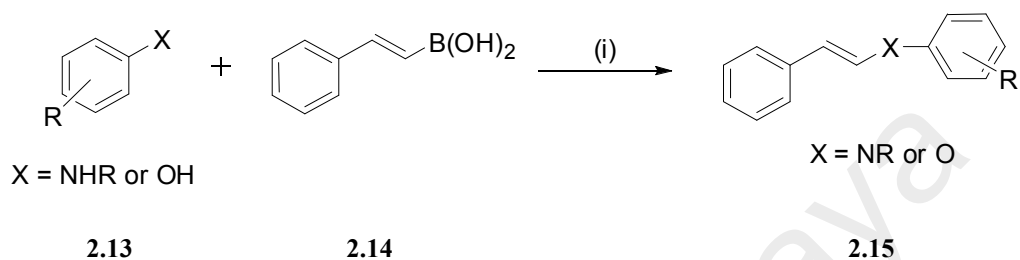


**Scheme 2.3:** Synthesis of **2.11** and **2.12**. Reaction conditions: (i) a) 9-BBN-H, THF b) PdCl<sub>2</sub>(dppf), K<sub>3</sub>PO<sub>4</sub>, DMF. (ii) a) O<sub>3</sub>, CH<sub>2</sub>Cl<sub>2</sub>/CH<sub>3</sub>OH, -78 °C, DMS b) NaBH<sub>3</sub>CN, pH 4 buffer, THF c) Pd/C (Degussa type), H<sub>2</sub>, MeOH.

#### 2.2.1.4 Formation of Carbon–Heteroatom (C–N, C–O and C–S) Bonds

Lam and co-workers reported the Cu(OAc)<sub>2</sub>-catalysed N-arylation of different NH-containing functional groups including amines, anilines and phenols with aryl **2.13** and vinylboronic acids **2.14** by using N-methyl-morpholine oxide, pyridine N-oxide, 2,2,6,6-tetramethyl-1-piperidinyloxy and etc. as additives which facilitates the oxidation of Cu(II) to Cu(III) and easy reductive elimination to form the C – N and C –

O cross-coupled products **2.15** (Scheme 2.4) (Lam *et al.*, 2001). SM cross-coupling reaction is more user-friendly than other coupling reactions and is widely employed in the synthesis of various natural and non-natural products.



**Scheme 2.4:** Synthesis of **2.15**. Reaction condition: (i)  $Cu(OAc)_2$  additive (1:1 eq) base (2 eq)  $CH_2Cl_2$ .

### 2.3 Ullmann Coupling

Aryl-aryl bond formation has been known for more than a century and was one of the first reactions using a transition metal (copper in its higher oxidation states should be considered a transition metal). The evolution of this field is also a good illustration of the development of modern organic chemistry, particularly the increasing importance of transition-metal catalysis. Indeed, during the first 70 years of the 20th century, copper was almost the only metal usable for aryl-aryl bond formation, initially as copper metal in the reductive symmetrical coupling of aryl halides (the Ullmann reaction). Several modifications and improvements of this reaction still justify today the use of copper derivatives in several synthetic cases.

For hundred years copper-promoted arylation of aromatic amines, initially diarylamines recognized as the classical Ullmann reaction (Ullmann, 1903). Demands severe extended heating at 200 °C or higher, in the existence of Cu(I) and Cu(II) salts, oxides, or Cu bronze, etc. and polar high-boiling solvents in the presence of base. Until now, copper-catalyzed cross-coupling only limited to iodo and bromo derivatives, while chloro-derivatives have not likely focus on regarded as for this chemistry with only a few exception (Beletskaya & Cheprakov, 2004).

Two conceivable mechanism are those involving radical intermediates and oxidative addition/reductive elimination (Figure 2.2) which have been suggested in the literature (Lindley, 1984) for such Ullmann-type condensation.

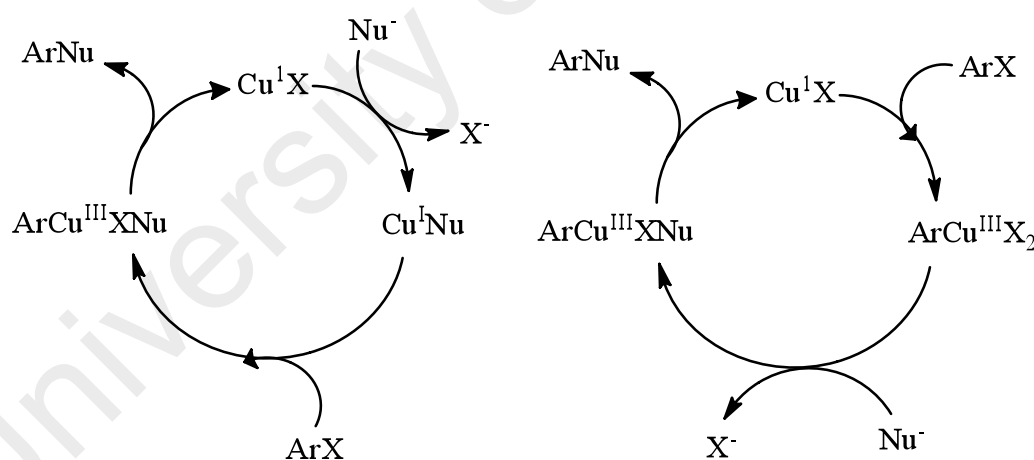
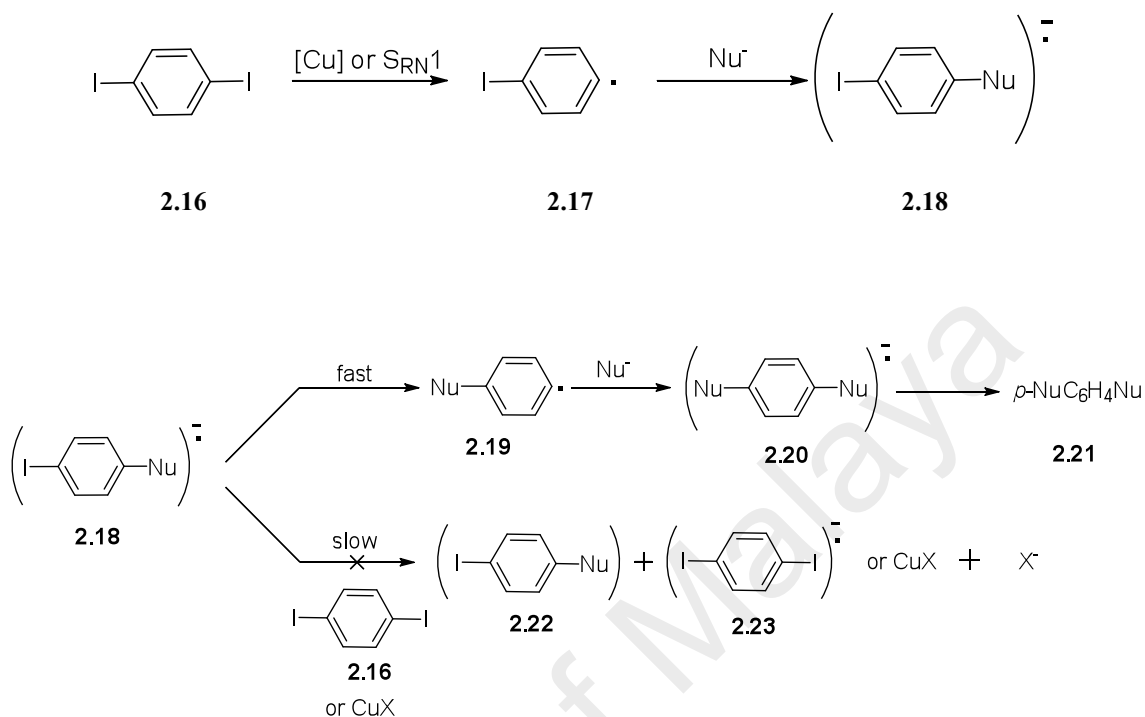


**Figure 2.2:** Two alternative oxidative addition/ reductive elimination mechanistic pathways for copper catalyzed nucleophilic aromatic substitutions with aryl halides.



**Scheme 2.5:** Expected behavior of 1,4-diiodobenzene **2.16** in the event that mechanism might involve radical anion intermediates.

According to literature (Bowman *et al.*, 1984; Paine, 1987; Rossi & de Rossi, 1983), unimolecular pathway considerably faster even at brief reaction times, result in quasi-exclusive disubstitution. The nucleophile with halo-aryl radical **2.17** produced radical anion **2.18**. Compound **2.18** does not undergo bimolecular electron transfer (to copper (II) or 1,4-diiodobenzene) to provide monosubstitution product, but instead formed aryl radical **2.20** by losing the second iodide ion (Scheme 2.5).

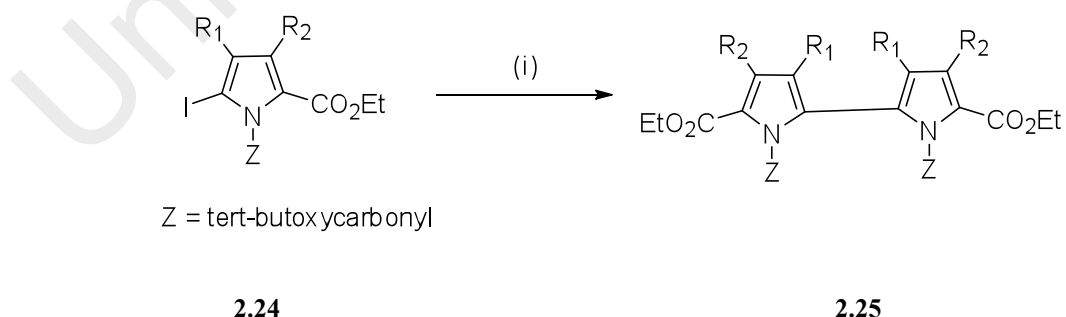
## 2.3.1 Reductive Coupling of Aromatic Halides (The Ullmann Reaction)

### 2.3.1.1 Symmetrical Coupling

The Ullmann reaction, initially was first reported in 1901. It has long been employed by chemists to generate a C-C bond between two aromatic rings. Typically two molecular equivalents of aryl halide are reacted with one equivalent of finely divided copper at high temperature (above 200 °C) to form a biaryl and a copper halide.

Symmetrical coupling of substituted benzene rings and aromatic heterocycles using copper as the reducing and coupling agent can be performed in both inter- and intramolecular reactions.

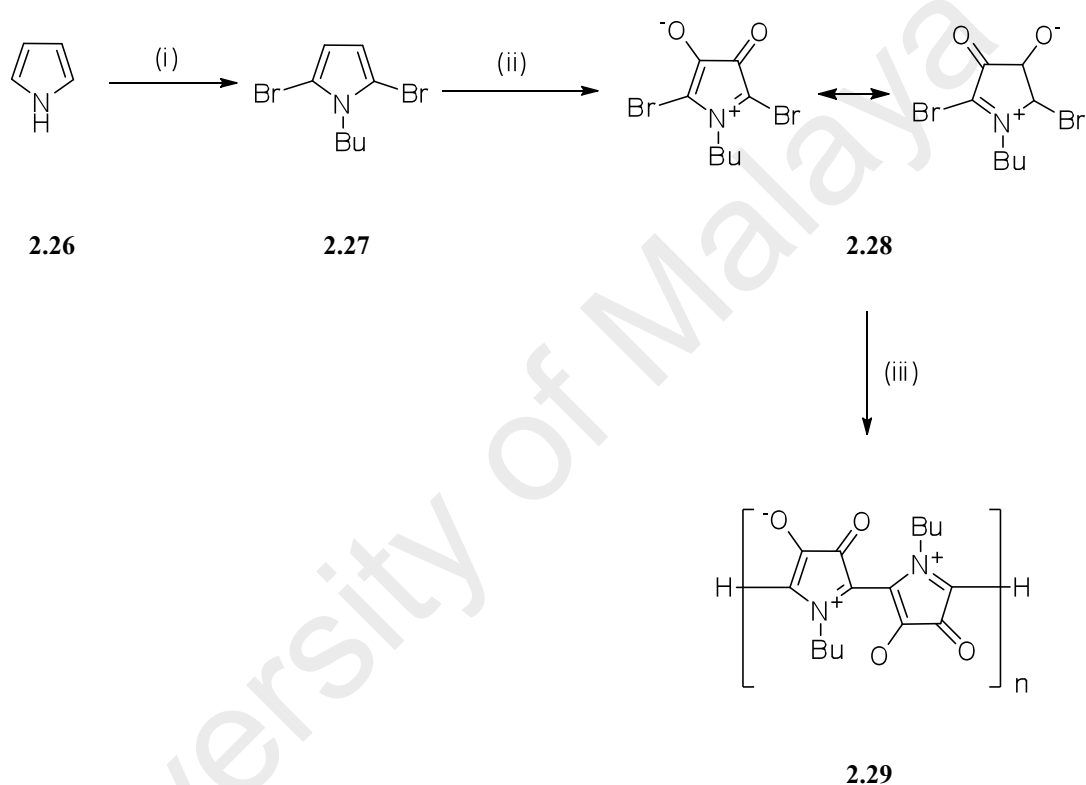
Sessler *et al.* (1994) developed an efficient procedure for the preparation of alkyl-substituted 2,2''-bipyrroles **2.25**. It involved first the protection of the nitrogen atom (with di-*tert*-butyl-dicarbonate) **2.24** as the key step, then an Ullmann-type coupling, followed by the deprotection of the resulting 2,2''-bipyrroles **2.25**.



**Scheme 2.6:** Synthesis of **2.25**. Reaction condition: (i) 4.7 eq Cu(0), DMF, 100 °C.



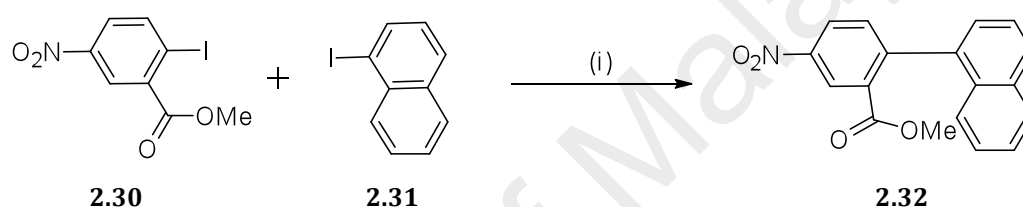
In an effort to maximize the extended  $\pi$ -conjugation in polymers and to study their corresponding optical and electronic properties, Tour *et al.* (1994) performed the synthesis of a zwitterionic pyrrole-derived polymer **2.29** using the Ullmann reaction (Scheme 2.7).



**Scheme 2.7:** Synthesis of **2.29**. Reaction conditions: (i) n-BuBr, PTC, NBS, THF (ii) HNO<sub>3</sub>, H<sub>2</sub>SO<sub>4</sub> (fuming) (iii) Cu bronze, DME, 200 °C.

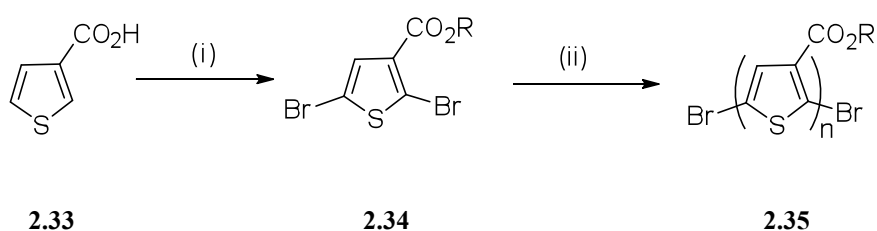
### 2.3.1.2 Unsymmetrical Coupling

A new class of suspected mutagens in the atmospheric environment, Suzuki et al.(1997) reported an Ullmann cross coupling between nitro-substituted iodobenzoates **2.30** and iodonaphthalenes **2.31** to synthesize polynitrobenzanthrones **2.32** (Scheme 2.8). To obtain those high yields of unsymmetrical coupling a large excess of 4 eq iodonaphthalene **2.31** has to be used.



**Scheme 2.8:** Synthesis of **2.32**. Reaction condition: 7 eq Cu(0), DMF, 140-150 °C, 4 h.

General synthesis of polythiophenes **2.35** bearing a carbonyl group (or other strongly electron- withdrawing substituents) directly attached to the 3-position of the thiophene ring **2.33**, Pomerantz *et al.* (1995) naturally thought about using the Ullmann reaction (Scheme 2.9). Furthermore, polymers obtained by this route had better properties (i.e., lower polydispersity and longer conjugation lengths) than polymers prepared by a Ni(0) coupling reaction.



**Scheme 2.9:** Synthesis of **2.35**. Reaction conditions: (i) a) Br<sub>2</sub>, AcOH b) SOCl<sub>2</sub> c) ROH, pyridine (ii) Cu, DMF, 140 – 150 °C, 7 days.

## 2.4 Results and Discussion

### 2.4.1 Targeted Compounds

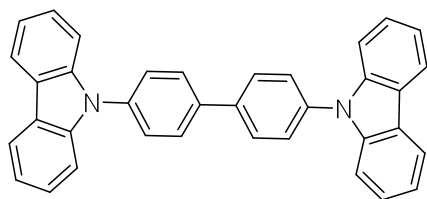
The explorations of green, affordable and renewable energy have obtained substantial improvement in harvesting sunlight energy. Low-cost and lightweight product of organic solar cells (OSCs) signify the guaranteeing prospect for versatile substrate potential to be fabricated on large-area.

A variety of application for example solar cells, displays, sending or radio frequency identification tags (RFIDs) (Dennler *et al.*, 2007) make frequently used of organic semiconductor host materials. Carbazole structures such as **1.4 (CBP)** (4,4'-bis(9-carbazolyl)biphenyl), **2.36 (CDBP)** (4,4'-bis(9-carbazolyl)-2,2'-dimethylbiphenyl) (Hoffmann *et al.*, 2010; Tanaka *et al.*, 2004) and **2.37 (BCP)** 1,4-di(9H-carbazol-9-yl)benzene (Kaafarani *et al.*, 2013; Koene *et al.*, 1998) are current interest which

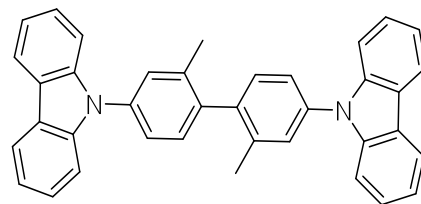
promising possibilities for solid-state lighting. The architectural of these carbazole derivatives gives the effective white organic light emitting devices (WOLEDs) (Kamtekar *et al.*, 2010).

Wide range of donor materials of conjugated small molecules own powerful absorption of sunlight spectra and great charge mobility. The most promising materials for OSCs are thiophene-based  $\pi$ -conjugated oligomers (Mishra *et al.*, 2009; Noma *et al.*, 1995a). Thiophenes posses remarkable optic, electronic and redox properties which become promising foundation for the design and synthesis of conjugated materials. Additionally, they have a prominent supramolecular behavior on the solid surface or in the bulk. For instance, competent conjugation along the primary chain backbone through  $\alpha$ -linked thiophene units into oligomers.

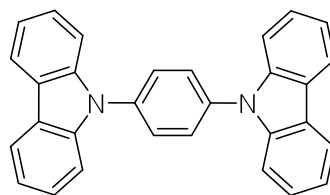
We present here in depth the synthesis of carbazole-thiophene derivatives and the spectroscopic and quantum mechanical study on the electronic structures of these compounds, focusing on the impact associated with electron donor thiophene group on the **1.4 (CBP)**, **2.36 (CDBP)** and **2.37 (BCP)** on the nature of the optical transitions and discuss the relationship between the molecular architectures and photovoltaic properties. The structural features and the electronic photophysical properties of **1.4 (CBP)**, **2.36 (CDBP)**, **2.37 (BCP)**, **2.38 (P1)**, **2.39 (P2)**, **2.40 (P3)**, **2.41 (P4)**, **2.42 (P5)**, **2.43 (P6)**, **2.44 (P7)**, **2.45 (P8)**, **2.46 (P9)**, **2.47 (P10)**, **2.48 (P11)** and **2.49 (P12)** (Figure 2.3) based on UV-vis, fluorescence spectroscopies, cyclic voltammetry and theoretical calculation were investigated by evaluating these compound with the documented compound of **1.4 (CBP)**, **2.36 (CDBP)** and **2.37 (BCP)**.



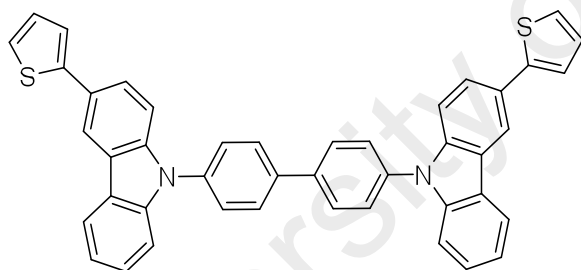
**1.4 (CBP)**



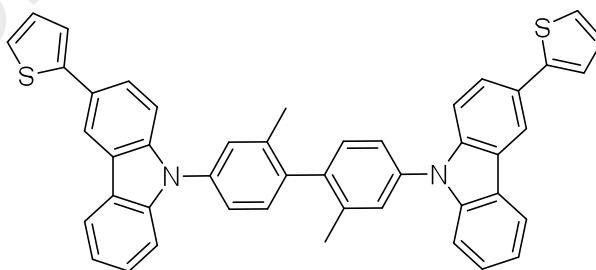
**2.36 (CDBP)**



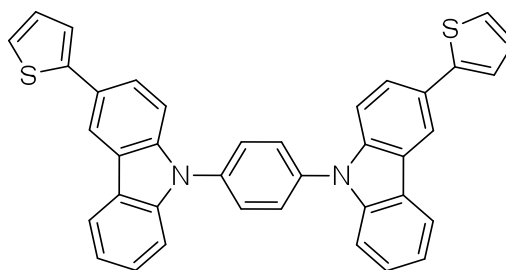
**2.37 (BCP)**



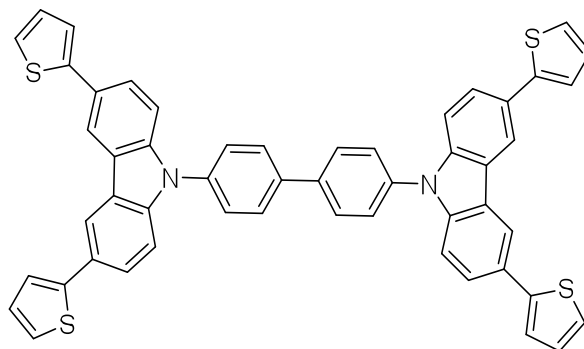
**2.38 (P1)**



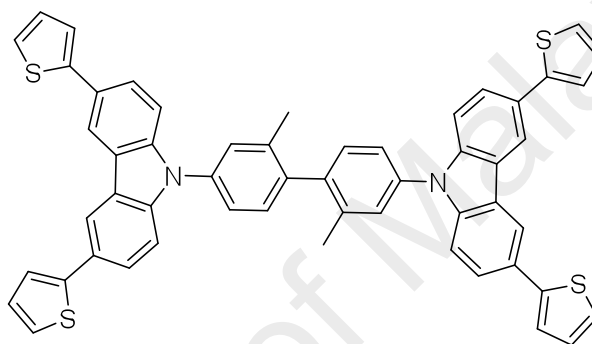
**2.39 (P2)**



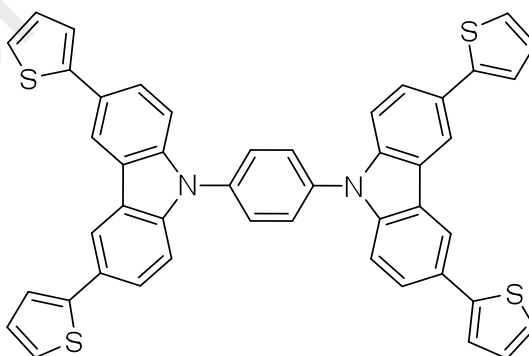
**2.40 (P3)**



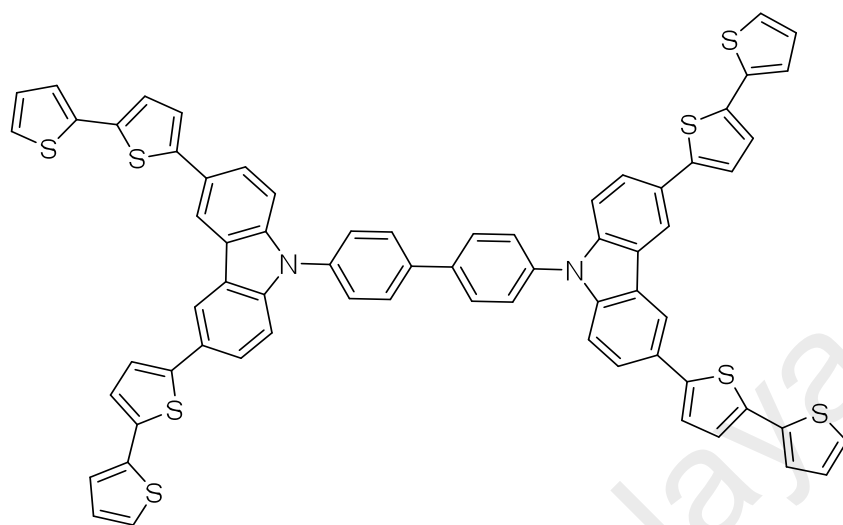
**2.41 (P4)**



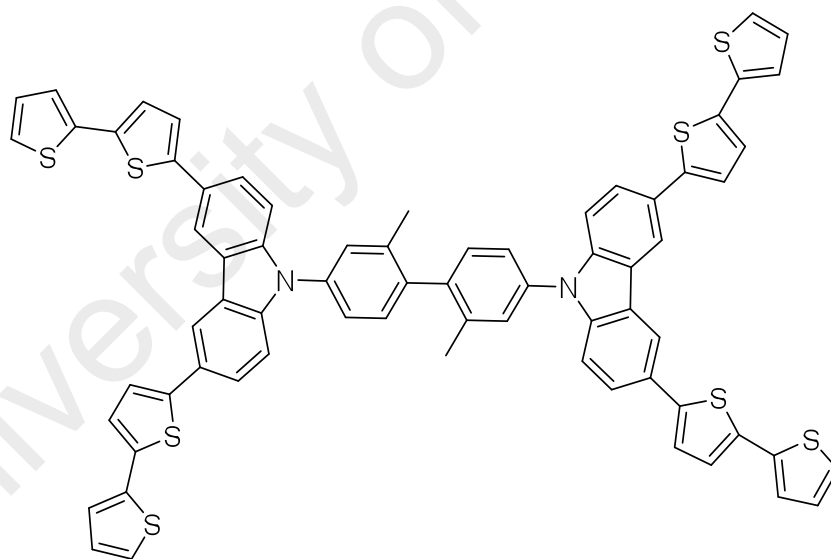
**2.42 (P5)**



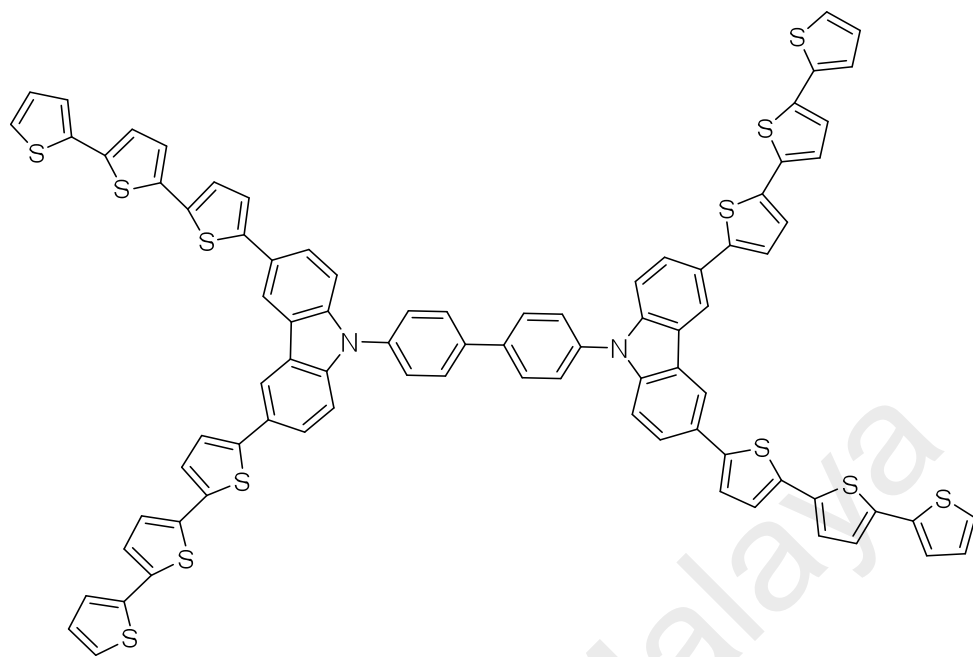
**2.43 (P6)**



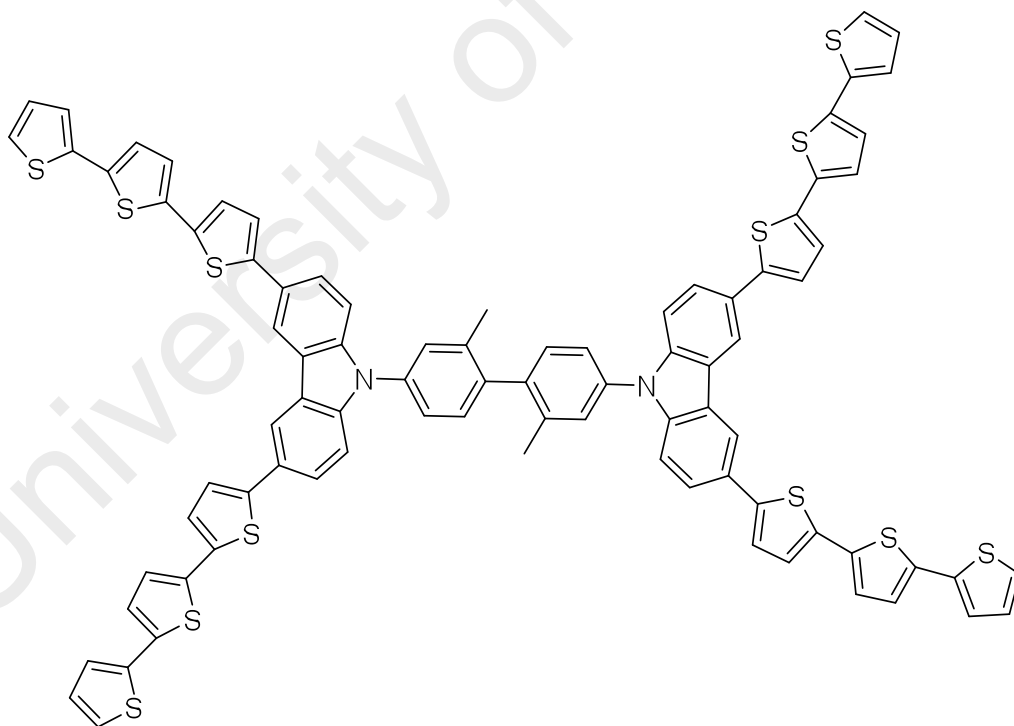
2.44 (P7)



2.45 (P8)

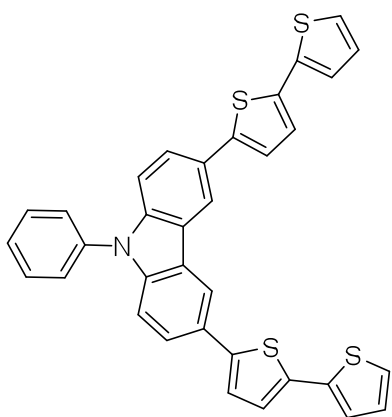


2.46 (P9)

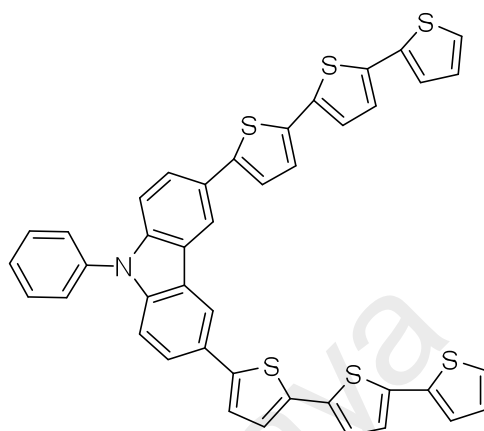


2.47 (P10)





**2.48 (P11)**



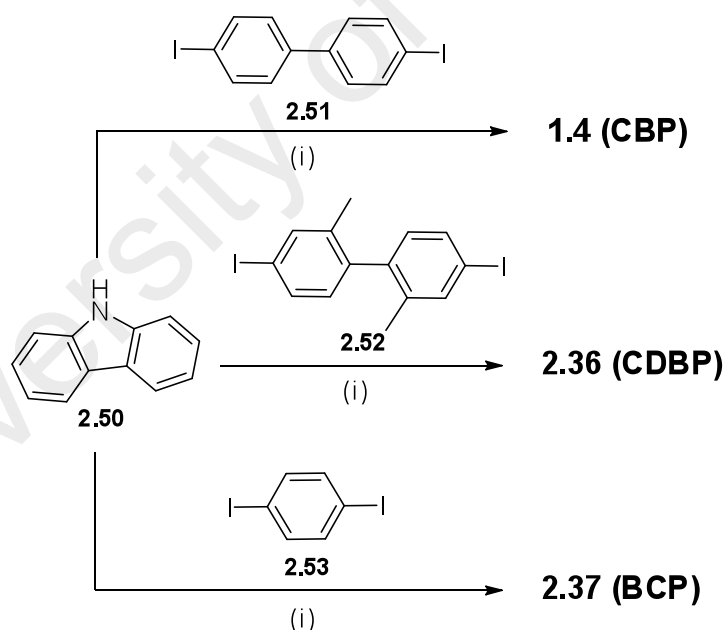
**2.49 (P12)**

**Figure 2.3:** Structure of compounds.

University of Malaya

## 2.4.2 Synthesis of Compound 1.4 (CBP), 2.36 (CDBP) and 2.37 (BCP).

Scheme 2.10 outlined the synthesis of compounds **1.4 (CBP)**, **2.36 (CDBP)** and **2.37 (BCP)**. The Ullmann coupling reaction were performed on carbazole (**2.50**) with either 4,4-diiodobiphenyl (**2.51**), 4,4-diiido-2'2'-dimethyl-1,1'-biphenyl (**2.52**) or 1,4-diiodobenzene (**2.53**) to give **1.4 (CBP)**, **2.36 (CDBP)** and **2.37 (BCP)** in 50 %, 60 %, and 80 % yields, respectively. Compounds **1.4 (CBP)** (Kaafarani *et al.*, 2013; Koene *et al.*, 1998), **2.36 (CDBP)** (Schrögel *et al.*, 2011) and **2.37 (BCP)** (Kaafarani *et al.*, 2013; Koene *et al.*, 1998) are known compounds. The procedure that we use have been adopted from the literature procedure reported by Schrögel *et al.* (2011).



**Scheme 2.10:** Synthesis of **1.4 (CBP)**, **2.36 (CDBP)** and **2.37 (BCP)**. Reaction condition: (i)  $K_2CO_3$ , Cu, 18-crown-6, *o*-dichlorobenzene (DCB), and reflux for 3 days.

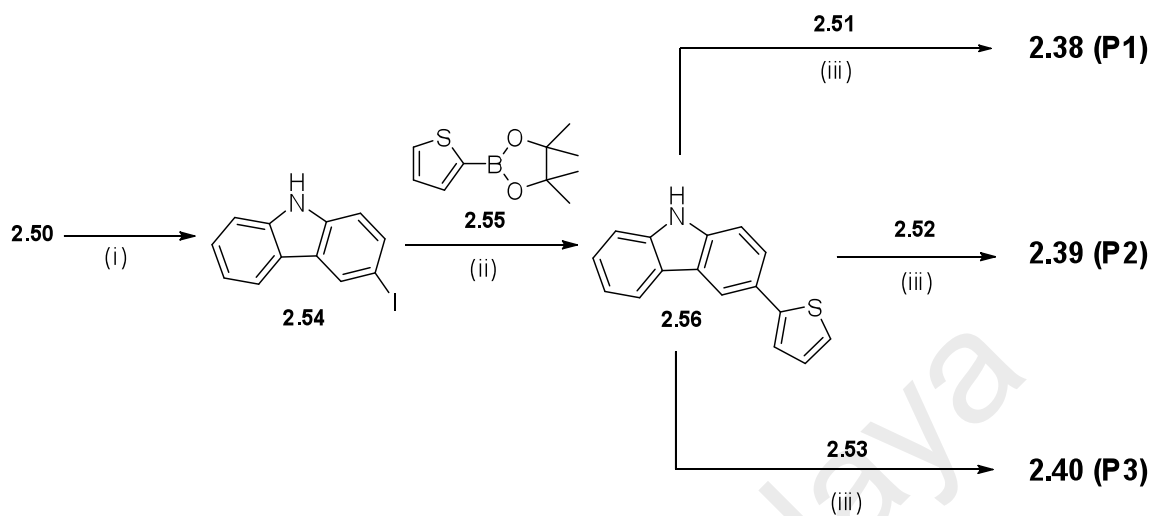
### 2.4.3 Synthesis of Compound 2.38 (P1), 2.39 (P2) and 2.40 (P3).

The synthesis of compounds **2.38 – 2.49 (P1-P12)** was described in Scheme 2.11– 2.14. The key steps in the synthesis of the compounds involved Suzuki Miyaura (Miyaura & Suzuki, 1995) and Ullmann coupling (Beletskaya & Cheprakov, 2004) reactions. The detailed procedures for the synthesis of the compound are described in the experimental section.

The syntheses of compounds **2.38 (P1)**, **2.39 (P2)** and **2.40 (P3)** were achieved in three steps starting from carbazole (**2.50**) as described in Scheme 2.11. The first step involved iodination of **2.50** using 0.5 eq of iodine to give 3-iodocarbazole (**2.25**). This was followed by Suzuki Miyaura cross coupling of **2.54** with thiophene-2-boronic acid pinacol ester (**2.55**) to produce monothieryl-substituted carbazole (**2.56**). Ullmann coupling of compound **2.56** with compounds **2.51**, **2.52** and **2.53** afforded compounds **2.38 (P1)**, **2.39 (P2)** and **2.40 (P3)** in 26 %, 35 % and 48 % yields, respectively (Damit *et al.*, 2016). Proposed mechanism of Suzuki Miyaura cross coupling reaction for compound **2.56** and Ullmann coupling reaction for compound **2.38** were showed in Figure 2.4 and 2.5, respectively. All other compounds were followed similar reaction mechanisms.

Many of drawbacks of the classical Ullmann reaction such as high reaction temperatures, long reaction times, high metal loadings and low conversion proved unsatisfactory yield (Evano *et al.*, 2008; Mangione & Spanevello, 2015; Wipf & Lynch, 2003). Certain functional groups such as free NH or OH are not adequate and may cause side reactions, Pd-based methods are sensitive to moisture and oxygen and large

scale applications of this type of chemistry is restrictive because of the cost of the metal catalysts and ligands (Mangione & Spanevello, 2015).



**Scheme 2.11:** Synthesis of **2.38 (P1)**, **2.39 (P2)** and **2.40 (P3)**. Reaction conditions: (i)  $I_2$  (0.5 eq), AcOH and reflux for 10 min (ii)  $K_2CO_3$ ,  $Pd(PPh_3)_4$ , EtOH, and reflux for 24 h (iii)  $K_2CO_3$ , copper powder, 18-crown-6, *o*-DCB, and reflux for 3 days.

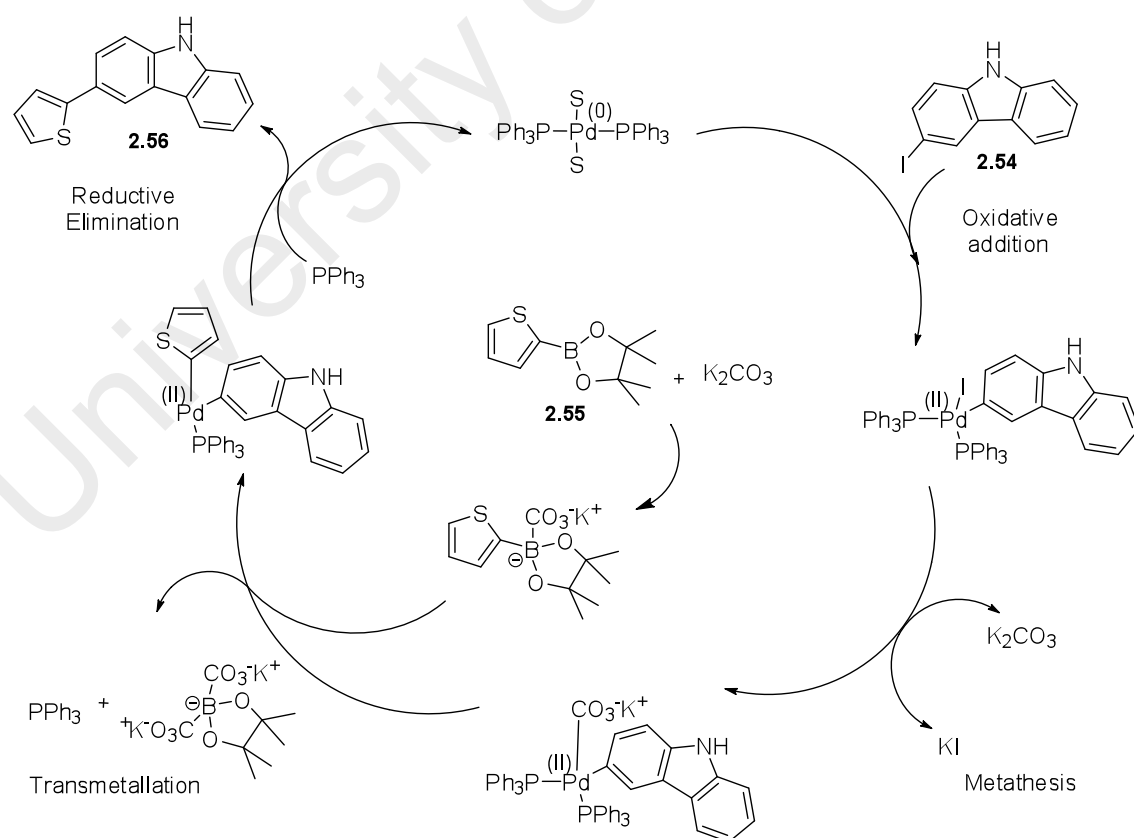


**Figure 2.4:** Proposed mechanism of Suzuki Miyaura cross coupling reaction for compound **2.56**. (s = solvent).

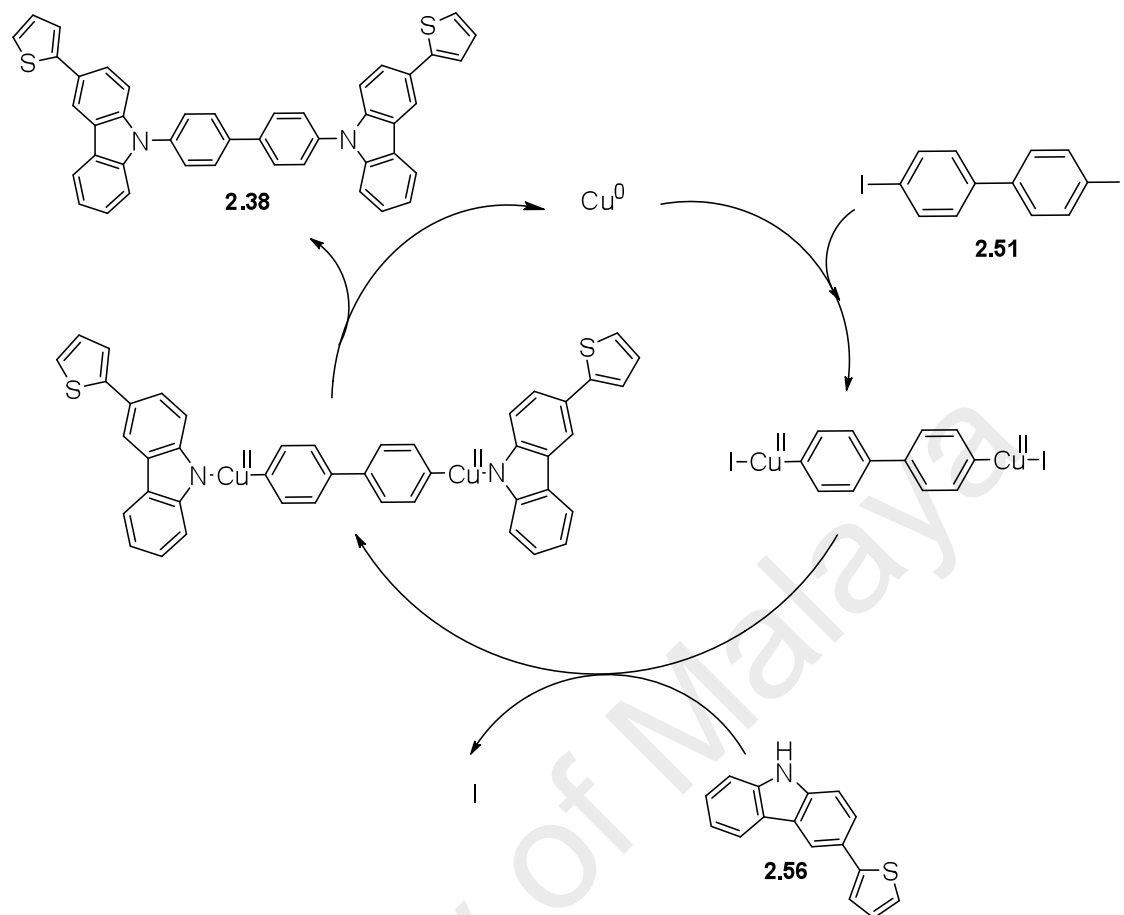
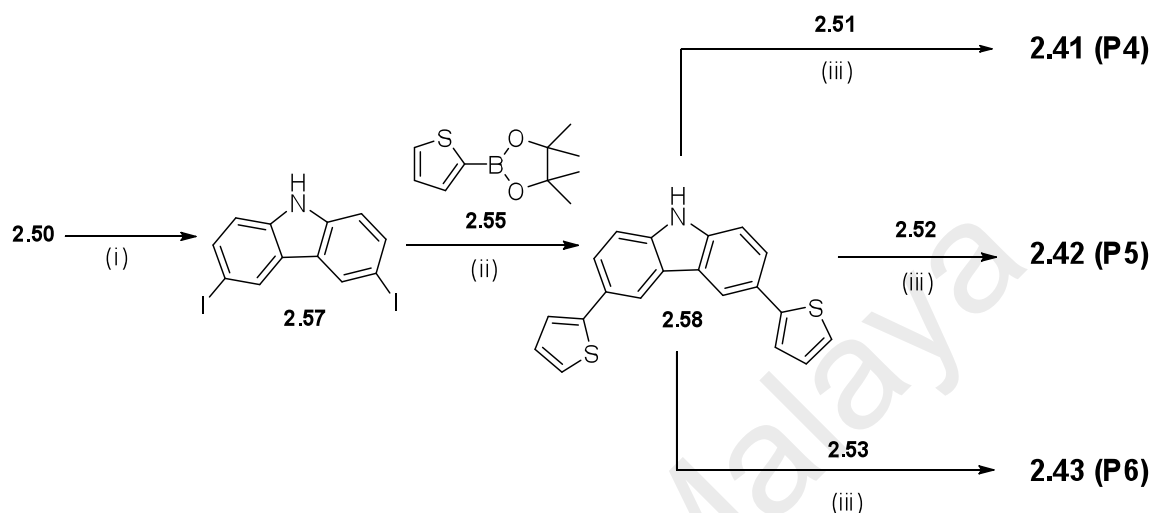


**Figure 2.5:** Proposed mechanism of Ullmann cross coupling reaction for compound **2.38**. (s = solvent).

#### 2.4.4 Synthesis of Compound **2.41** (P4), **2.42** (P5) and **2.43** (P6).

In a similar approach, compounds **2.41** (P4), **2.42** (P5) and **2.43** (P6) were synthesized in three steps from compound **2.50** as described in Scheme 2.12. Iodination of compound **2.50** using 1 eq of iodine gave 3,6-diiodocarbazole (**2.57**), which was then refluxed with compound **2.55** to give dithienyl-substituted carbazole (**2.58**). Ullmann

coupling of **2.58** with **2.51**, **2.52** and **2.53**, gave compounds **2.41 (P4)**, **2.42 (P5)** and **2.43 (P6)** in 75 %, 60 % and 50 % yields, respectively (Damit *et al.*, 2016).

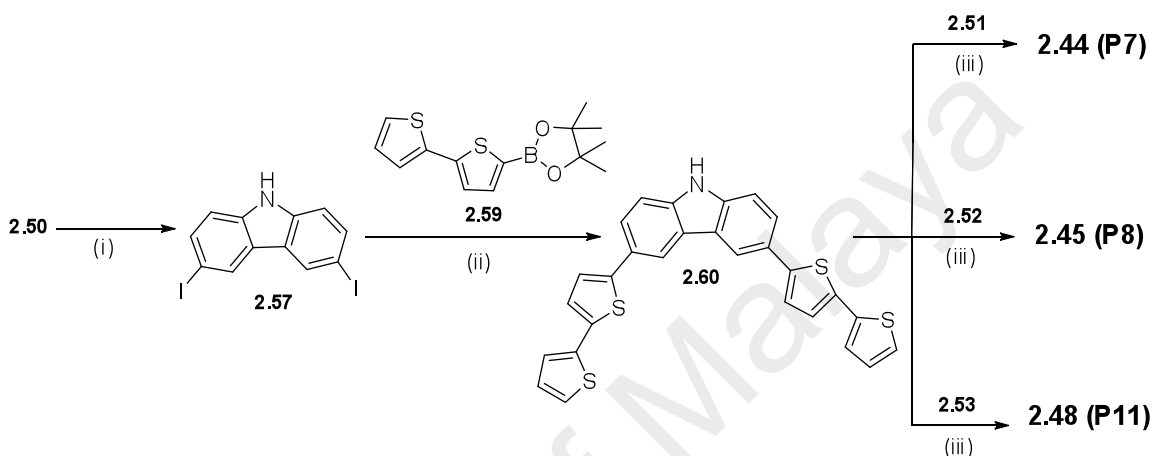


**Scheme 2.12:** Synthesis of **2.41 (P4)**, **2.42 (P5)** and **2.43 (P6)**. Reaction conditions (i)  $I_2$  (1 eq), AcOH and reflux for 10 min. (ii)  $K_2CO_3$ ,  $Pd(PPh_3)_4$ , EtOH, and reflux for 24 h. (iii)  $K_2CO_3$ , Cu, 18-crown-6, *o*-DCB, and reflux for 4 days.

#### 2.4.5 Synthesis of Compound **2.44 (P7)**, **2.45 (P8)** and **2.48 (P11)**.

In a similar approach, compounds **2.44 (P7)**, **2.45 (P8)** and **2.48 (P11)** were synthesized in three steps from compound **2.50** as described in Scheme 2.13. Iodination of compound **2.50** using 1 eq of iodine gave 3,6-diiodocarbazole (**2.57**), which was then refluxed with compound **2.59** to give dithienyl-substituted carbazole (**2.60**). Ullmann coupling of **2.60** with **2.51**, **2.52** and **2.53**, gave compounds **2.44 (P7)**, **2.45 (P8)** and **2.48 (P11)** in 40 %, 38 % and 40 % yields, respectively. Compound **2.48 (P11)** was synthesized under Ullmann coupling reaction between **2.60** with 1,4-diiodobenzene

(**2.53**) undergoes selective single coupling reaction due to the steric hinderance. The presence of bulkier groups at the reaction centre, cause mechanical interference and resulted attacking reagent difficult to reach the reaction site and thus slow down the reaction.

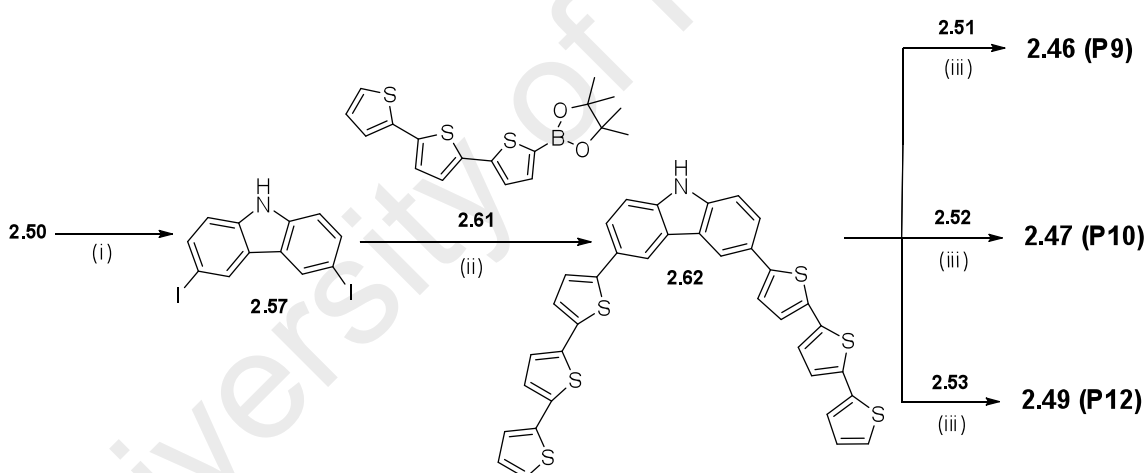


**Scheme 2.13:** Synthesis of **2.17 (P7)**, **2.18 (P8)** and **2.48 (P11)**. Reaction conditions (i)  $I_2$  (1 eq), AcOH and reflux for 10 min. (ii)  $K_2CO_3$ ,  $Pd(PPh_3)_4$ , EtOH, and reflux for 24 h. (iii)  $K_2CO_3$ , Cu, 18-crown-6, *o*-DCB, and reflux for 4 days.

#### 2.4.6 Synthesis of Compound **2.46 (P9)**, **2.47 (P10)** and **2.49 (P12)**.

In a similar approach, compounds **2.46 (P9)**, **2.47 (P10)** and **2.49 (P12)** were synthesized in three steps from compound **2.50** as described in Scheme 2.14. Iodination of compound **2.50** using 1 eq of iodine gave 3,6-diiodocarbazole (**2.57**), which was then refluxed with compound **2.61** to give dithienyl-substituted carbazole (**2.62**). Ullmann coupling of **2.62** with **2.51**, **2.52** and **2.53** gave compounds **2.46 (P9)**,

**2.47 (P10)** and **2.49 (P12)** in 40 %, 36 % and 40 % yields, respectively. Compound **2.49 (P12)** was synthesized under Ullmann coupling reaction between **2.62** with 1,4-diiodobenzene (**2.53**) undergoes selective single coupling reaction due to the steric hinderance. Similar observation was found with compound **2.48 (P11)** as described previously. All of the compounds were fully characterized by spectroscopic methods such as  $^1\text{H}$  NMR,  $^{13}\text{C}$  NMR and mass spectroscopy. For compounds **2.48 (P11)** and **2.49 (P12)**, their electronic studies were not further discussed because these compound undergoes selective single coupling reaction, where the trend of these compounds structures did not followed compounds **P1** to **P10** of carbazole-thiophene derivatives series.



**Scheme 2.14:** Synthesis of **2.46 (P9)**, **2.47 (P10)** and **2.49 (P12)**. Reaction conditions (i)  $\text{I}_2$  (1 eq), AcOH and reflux for 10 min. (ii)  $\text{K}_2\text{CO}_3$ ,  $\text{Pd}(\text{PPh}_3)_4$ , EtOH, and reflux for 24 h. (iii)  $\text{K}_2\text{CO}_3$ , Cu, 18-crown-6, *o*-DCB, and reflux for 5 days.



## 2.5 Suzuki Coupling Reactions

Order of reactivity is usually  $I > Br \gg Cl$  in palladium-catalyzed Suzuki (Miyaura *et al.*, 1985; Watanabe, 1992) and Stille (1986) coupling of aryl halides. Great yield has been reported in aqueous condition for cross coupling of 4-iodoanisole with phenylboronic acid with water-soluble Pd-TPPTS (triphenylphosphinetrisulfonate sodium salt) catalyst (Gene<sup>^</sup>t *et al.*, 1995). Furthermore, the displacement reaction (i.e.  $S_N2$ ) in the liquid-liquid phase-transfer catalysis system (LL-PTC) system, aryl iodide give incomplete transformation (Starks *et al.*, 1978; Starks & Owens, 1973).

Mechanism of Pd-catalyzed Suzuki reaction of aryl halides with aryl boronic acids involve oxidative addition of Pd(0) to aryl halide, transmetallation of the Ar-Pd-X with  $Ar_1B(OH)_3^-M^+$  and reductive elimination to give Ar-Ar<sub>1</sub> (Negishi *et al.*, 1987). Under “classical” conditions, oxidative addition proved to be the slow step when utilizing aryl bromides (Smith *et al.*, 1994), while the rate-determining is the transmetallation step. An extremely wide range of palladium (0) catalyst and precursor were utilized, however PdCl<sub>2</sub>(PPh<sub>3</sub>)<sub>2</sub> and Pd(OAc) in addition PPh<sub>3</sub> or other phosphine ligands employed for cross coupling are also effective which are stable to air and readily reduced to active Pd(0) complexes with organometallics or phosphines (Miyaura & Suzuki, 1995).

All experiments were refluxed for 24 hours. 1 eq of aryl iodide with boronic acid with 1eq (entry 1 to 3) or 2 eq (entry 4 to 15) of boronic acid. All ratio of mixed cosolvent of organic solvent : water was maintained at 5:1. The representative synthesis and reaction conditions are summarized in Table 2.1.

Recently, water was used as solvent for the Suzuki reaction obtained much interest (Arcadi *et al.*, 2003; DeVasher *et al.*, 2004; Dupuis *et al.*, 2001; Leadbeater, 2005; L. Liu *et al.*, 2006; Shaughnessy & Booth, 2001; Uozumi & Nakai, 2002). Considering its safety, cost, and importance to eco harmless procedures, water as solvent offers advantages in organic synthesis (C.-J. Li & Chan, 1997). As shown in Table 2.1, remarkably we discovered that good yields was obtained in most aryl iodide coupling with boronic acid where sodium hydroxide as base in benzene/H<sub>2</sub>O cosolvent (benzene is non-polar solvent) (Deloux *et al.*, 1994; Miyaura *et al.*, 1986; Miyaura *et al.*, 1979; Punji *et al.*, 2006), however the reaction stop at about 75 % conversion (entries 3, 6, 9, 12 and 15). Furthermore, the addition of strong bases of NaOH in benzene exerts an amazing impact of acceleration of the coupling rate (Daku *et al.*, 2003; Guillier *et al.*, 1994; Kelly *et al.*, 1994; Rocca *et al.*, 1993). Other cosolvents EtOH/H<sub>2</sub>O and Dioxane/H<sub>2</sub>O with weak base K<sub>2</sub>CO<sub>3</sub> had been very ineffective (entries 2, 5, 7, 10 and 13) where less than 20 % and none of products had been discovered. Polar protic solvents (EtOH/H<sub>2</sub>O) with K<sub>2</sub>CO<sub>3</sub> weak base give much better outcomes for less hindered mono-thiophene boronic acid (entries 1 and 4) which give more than 80 % yield of products.

Cross coupling reaction of organoboron yielding nontoxic byproduct, tolerate an extensive of functionality and unaffected by the existence of water offers diverse application in laboratories and within sectors.

**Table 2.1: Suzuki cross-coupling of aryl iodide with thiopheneboronic acid.<sup>a</sup>**

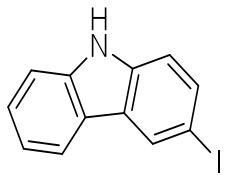
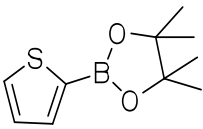
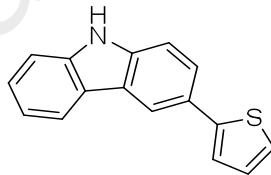
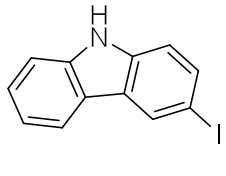
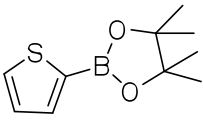
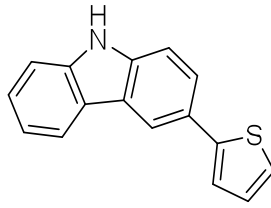
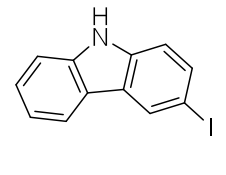
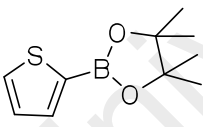
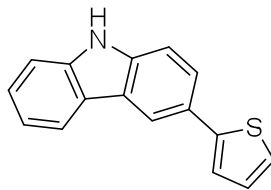
Entry	Aryl iodide	Boronic acid	Condition	Products	Percentage yield /(%) <sup>d</sup>
1 <sup>b</sup>	 <b>2.54</b>	 <b>2.55</b>	EtOH / H <sub>2</sub> O 2 eq K <sub>2</sub> CO <sub>3</sub> 0.5 mol % Pd(PPh <sub>3</sub> ) <sub>4</sub>	 <b>2.56</b>	95 %
2 <sup>b</sup>			Dioxane / H <sub>2</sub> O 2 eq K <sub>2</sub> CO <sub>3</sub> 0.5 mol % Pd(PPh <sub>3</sub> ) <sub>4</sub> H <sub>2</sub> O		None detected
3 <sup>b</sup>			Benzene / H <sub>2</sub> O 3 eq NaOH 3 mol % Pd(PPh <sub>3</sub> ) <sub>4</sub>		75 %

Table 2.1 continued

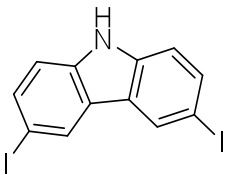
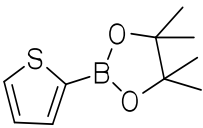
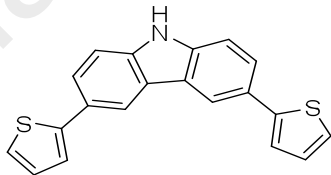
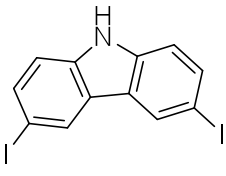
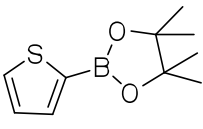
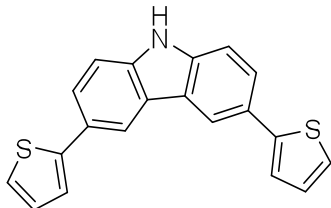
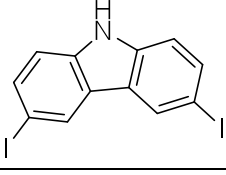
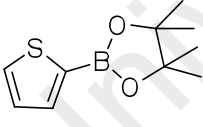
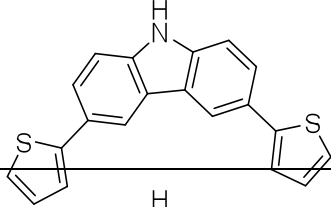
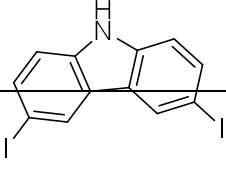
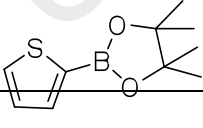
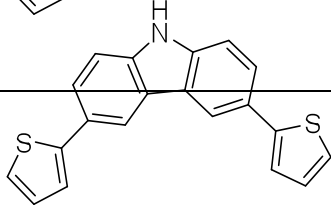
Entry	Aryl iodide	Boronic acid	Condition	Products	Percentage yield /(%) <sup>d</sup>
4 <sup>c</sup>	 <b>2.57</b>	 <b>2.55</b>	EtOH / H <sub>2</sub> O 2 eq K <sub>2</sub> CO <sub>3</sub> 0.5 mol % Pd(PPh <sub>3</sub> ) <sub>4</sub>	 <b>2.58</b>	80 %
5 <sup>c</sup>			Dioxane / H <sub>2</sub> O 2 eq K <sub>2</sub> CO <sub>3</sub> 0.5 mol % Pd(PPh <sub>3</sub> ) <sub>4</sub> H <sub>2</sub> O		None detected
6 <sup>c</sup>			Benzene / H <sub>2</sub> O 3 eq NaOH 3 mol % Pd(PPh <sub>3</sub> ) <sub>4</sub>		70 %
6 <sup>c</sup>			Benzene / H <sub>2</sub> O 3 eq NaOH 3 mol % Pd(PPh <sub>3</sub> ) <sub>4</sub>		70 %

Table 2.1, continued.

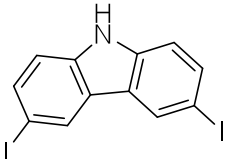
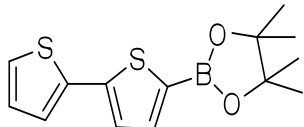
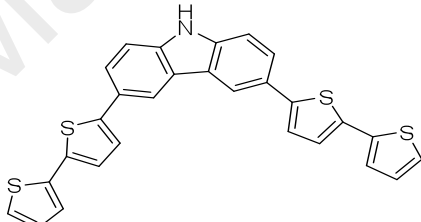
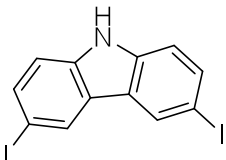
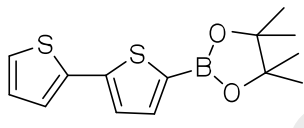
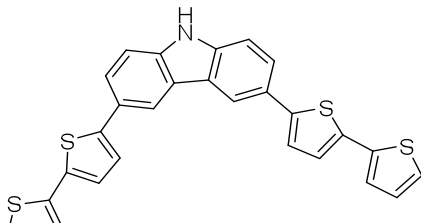
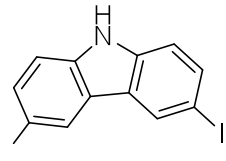
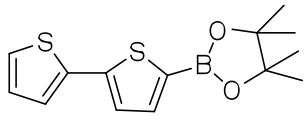
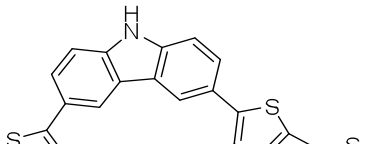
Entry	Aryl iodide	Boronic acid	Condition	Products	Percentage yield / (%) <sup>d</sup>
7 <sup>c</sup>	 <b>2.57</b>	 <b>2.59</b>	EtOH / H <sub>2</sub> O 2 eq K <sub>2</sub> CO <sub>3</sub> 0.5 mol % Pd(PPh <sub>3</sub> ) <sub>4</sub>	 <b>2.60</b>	None detected
8 <sup>c</sup>	 <b>2.57</b>	 <b>2.59</b>	Dioxane/H <sub>2</sub> O 2 eq K <sub>2</sub> CO <sub>3</sub> 0.5 mol % Pd(PPh <sub>3</sub> ) <sub>4</sub> H <sub>2</sub> O	 <b>2.60</b>	10 %
8 <sup>c</sup>	 <b>2.57</b>	 <b>2.59</b>	Dioxane/H <sub>2</sub> O 2 eq K <sub>2</sub> CO <sub>3</sub> 0.5 mol % Pd(PPh <sub>3</sub> ) <sub>4</sub> H <sub>2</sub> O	 <b>2.60</b>	10 %

Table 2.1, continued.

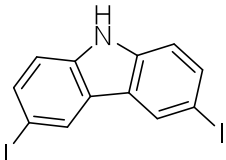
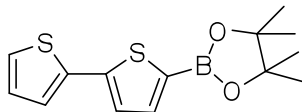
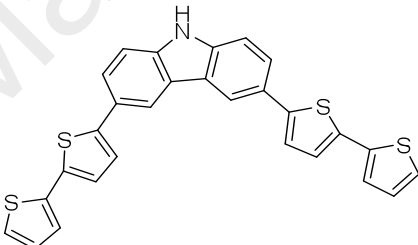
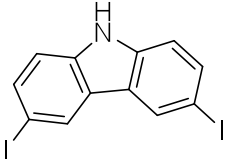
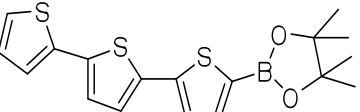
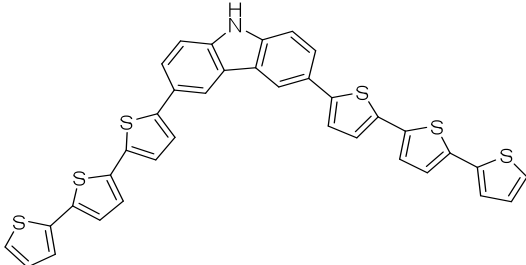
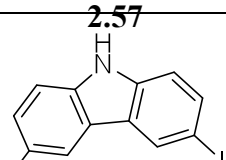
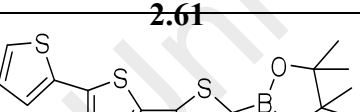
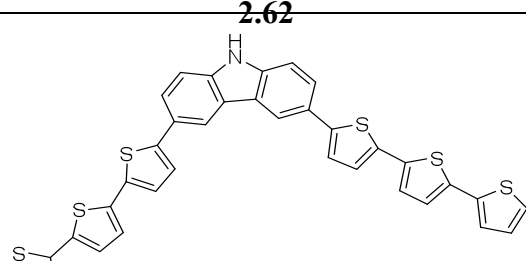
Entry	Aryl iodide	Boronic acid	Condition	Products	Percentage yield / (%) <sup>d</sup>
9 <sup>c</sup>			Benzene/H <sub>2</sub> O 3 eq NaOH 3 mol % Pd(PPh <sub>3</sub> ) <sub>4</sub>		80 %
10 <sup>c</sup>			EtOH/H <sub>2</sub> O 2 eq K <sub>2</sub> CO <sub>3</sub> 0.5 mol % Pd(PPh <sub>3</sub> ) <sub>4</sub>		None detected
10 <sup>c</sup>	 <b>2.57</b>	 <b>2.61</b>	EtOH/H <sub>2</sub> O 2 eq K <sub>2</sub> CO <sub>3</sub> 0.5 mol % Pd(PPh <sub>3</sub> ) <sub>4</sub>	 <b>2.62</b>	None detected
	<b>2.57</b>	<b>2.61</b>		<b>2.62</b>	

Table 2.1, continued.

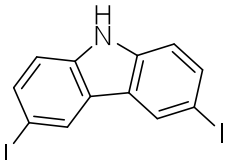
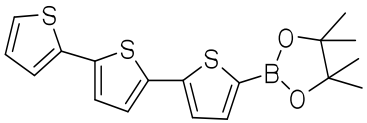
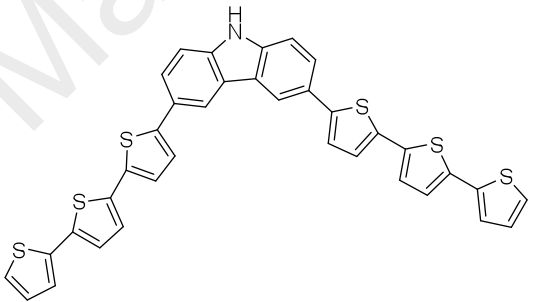
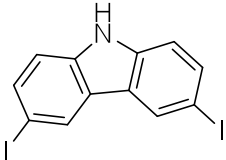
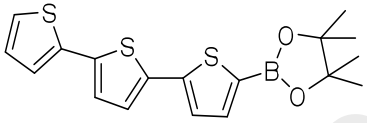
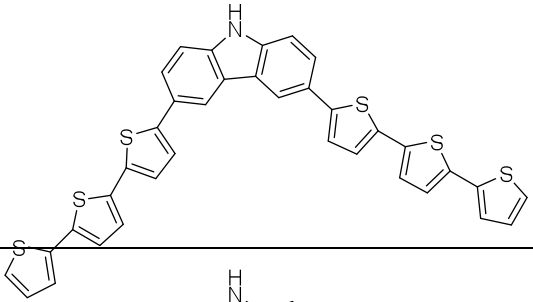
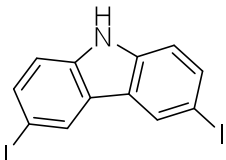
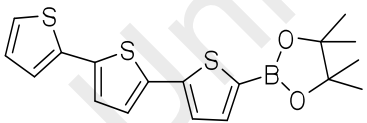
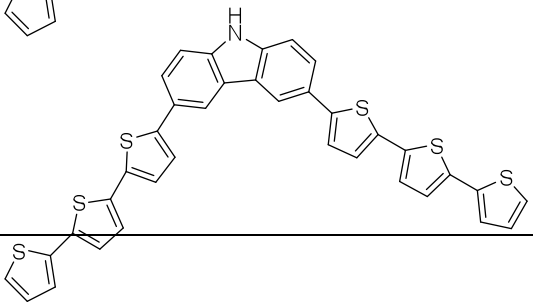
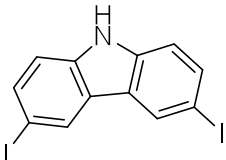
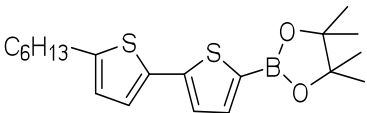
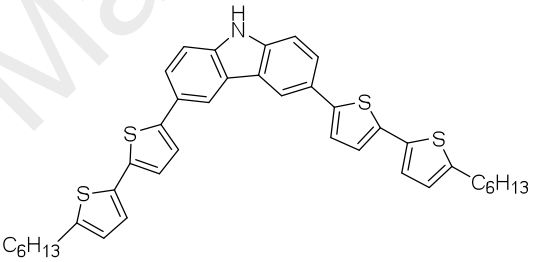
Entry	Aryl iodide	Boronic acid	Condition	Products	Percentage yield /(%) <sup>d</sup>
11 <sup>c</sup>			Dioxane/H <sub>2</sub> O 2 eq K <sub>2</sub> CO <sub>3</sub> 0.5 mol % Pd(PPh <sub>3</sub> ) <sub>4</sub> H <sub>2</sub> O		15 %
12 <sup>c</sup>			Benzene/H <sub>2</sub> O 3 eq NaOH 3 mol % Pd(PPh <sub>3</sub> ) <sub>4</sub>		75 %
12 <sup>c</sup>			Benzene/H <sub>2</sub> O 3 eq NaOH 3 mol % Pd(PPh <sub>3</sub> ) <sub>4</sub>		75 %

Table 2.1, continued.

Entry	Aryl iodide	Boronic acid	Condition	Products	Percentage yield / (%) <sup>d</sup>
13 <sup>c</sup>			EtOH/H <sub>2</sub> O 2 eq K <sub>2</sub> CO <sub>3</sub> 0.5 mol % Pd(PPh <sub>3</sub> ) <sub>4</sub>		None detected
14 <sup>c</sup>			Dioxane/H <sub>2</sub> O 2 eq K <sub>2</sub> CO <sub>3</sub> 0.5 mol % Pd(PPh <sub>3</sub> ) <sub>4</sub> H <sub>2</sub> O		10 %
14 <sup>c</sup>			Dioxane/H <sub>2</sub> O 2 eq K <sub>2</sub> CO <sub>3</sub> 0.5 mol % Pd(PPh <sub>3</sub> ) <sub>4</sub> H <sub>2</sub> O		10 %



Table 2.1, continued.					
Entry	Aryl iodide	Boronic acid	Condition	Products	Percentage yield / (%) <sup>d</sup>
15 <sup>c</sup>			Benzene/H <sub>2</sub> O 3 eq NaOH 3 mol % Pd(PPh <sub>3</sub> ) <sub>4</sub>		86 %

<sup>a</sup> All coupling were carried at 80 °C of 1 eq of aryl iodide with boronic acid with <sup>b</sup>1 eq of boronic acid and <sup>c</sup>2 eq of boronic acid. All ratio of mixed cosolvent was maintained at 5:1. <sup>d</sup> Isolated percentage yield.

## CHAPTER 3: PHYSICAL PROPERTIES

### 3.1 Introduction

While organic semiconductor materials are of current interest for a range of application such as solar cells, displays, sending or radio frequency identification tags (RFIDs) (Dennler *et al.*, 2007), they offer particularly promising opportunities for solid-state lighting since they allow for the engineering of efficient white organic light emitting devices (WOLEDs) (Kamtekar *et al.*, 2010). Host materials that are considered suitable and therefore used frequently for WOLED applications are often based on carbazole structures, such as **1.4 (CBP)** 4,4'-bis(9-carbazolyl)biphenyl, **2.36 (CDBP)** 4,4'-bis(9-carbazolyl)-2,2'-dimethylbiphenyl (Hoffmann *et al.*, 2010; Tanaka *et al.*, 2004) and **2.37 (BCP)** 1,4-di(9H-carbazol-9-yl)benzene (Kaafarani *et al.*, 2013; Koene *et al.*, 1998).

A large number of applications exist based on electrochromism, which relies on the reproducible switching characteristics of conjugated compounds (Beaujuge & Reynolds, 2010; Durmus *et al.*, 2007; Schwendeman *et al.*, 2002; Sonmez *et al.*, 2005; H. M. Wang *et al.*, 2010). All these applications usually require the modification of the structure to tune the properties of the compounds (electronic, optical, conductivity, etc.) with respect to desired applications. In addition, the physical and chemical properties of the conjugated compound can be controlled by some basic factors such as bond length alteration (Jean Roncali, 1997; J. Roncali, 2007). Besides, the attachment of electron-withdrawing and /or electron-donating moieties onto conjugated system is the most promising way to control the properties of the electroactive compounds (Asil *et al.*, 2008; Ferraris & Lambert, 1991; Hsieh *et al.*, 2001; McQuade *et al.*, 2000; Toussaint &

Brédas, 1993). This new formation has created a strong change in point of view regarding the molecular engineering of the electronic properties of materials derived from conjugated system and hence control of their band gap (Koyuncu *et al.*, 2011).

The exploration of donor materials conjugated small molecules that own strong absorption of sunlight spectra covering an extensively broad range and good charge mobility. From the view of these points, thiophene-based  $\pi$ -conjugated oligomers are among the most promising materials for OSCs (Mishra *et al.*, 2009; Noma *et al.*, 1995a). Thiophenes are promising building blocks for the design and synthesis of conjugated materials because they possess remarkable optic, electronic and redox properties as well as prominent supramolecular behavior on the solid surface or in the bulk. For instance, the incorporation of the  $\alpha$ -linked thiophene units into oligomers renders an efficient conjugation along the main chain backbone. An impressive library of thiophene oligomers has been built and explored over the past two decades (Allard *et al.*, 2008; Murphy & Frechet, 2007). Symmetrical donor-acceptor (DA) small molecules appended with solubilizing substituents and consisting of an electron-deficient core flanked with electron-rich groups, are now being considered as alternatives to their all-donor counterparts (Beaujuge & Fréchet, 2011).

Organic (both low molecular weight compounds and polymers) conjugated materials have recently received much attention due to their potential application in light-emitting diodes, field effect transistors, charge storage devices, photodiodes, sensors, etc (Bernier *et al.*, 1999; Skotheim *et al.*, 1997). These organic electroactive and photoactive materials are usually based on thiophene, pyrrole, phenylene fluorene, or carbazole moieties.

In the case of carbazole-based conjugated oligomers and polymers, all previous studies were devoted to 3,6-linked N-substituted carbazole units (Ambrose & Nelson, 1968; Desbene-Monvernay *et al.*, 1981; Hwang & Chen, 2001; Romero *et al.*, 1996; Wellinchoff *et al.*, 1984; Y. Zhang *et al.*, 1997; Zotti *et al.*, 1999). Indeed, the most reactive sites for coupling are the 3- and 6-positions (Ambrose & Nelson, 1968). Despite a relatively short effective conjugation length (dimeric units), studies on carbazole-thiophene moieties have revealed interesting electrochemical properties.

It is well-known that carbazole compounds exhibit photoconductive properties and have internal donor group in the 9-position. After the various acceptor groups are introduced to 3- and 6-positions, carbazole compounds show both photoconductivity and second order nonlinearity (Y. Zhang *et al.*, 1996).

### **3.1.1 Absorption Spectroscopy**

Electromagnet energy travels in waves spans a broad spectrum from very long radio waves to very short gamma rays. Human eye can only detect a small portion of this spectrum called visible light (Figure 3.1). Sun is a source of energy across the full spectrum, and its electromagnetic radiation bombards our atmosphere constantly. However, the Earth's atmosphere protects us from exposure to a range of higher energy waves that can be harmful to life.

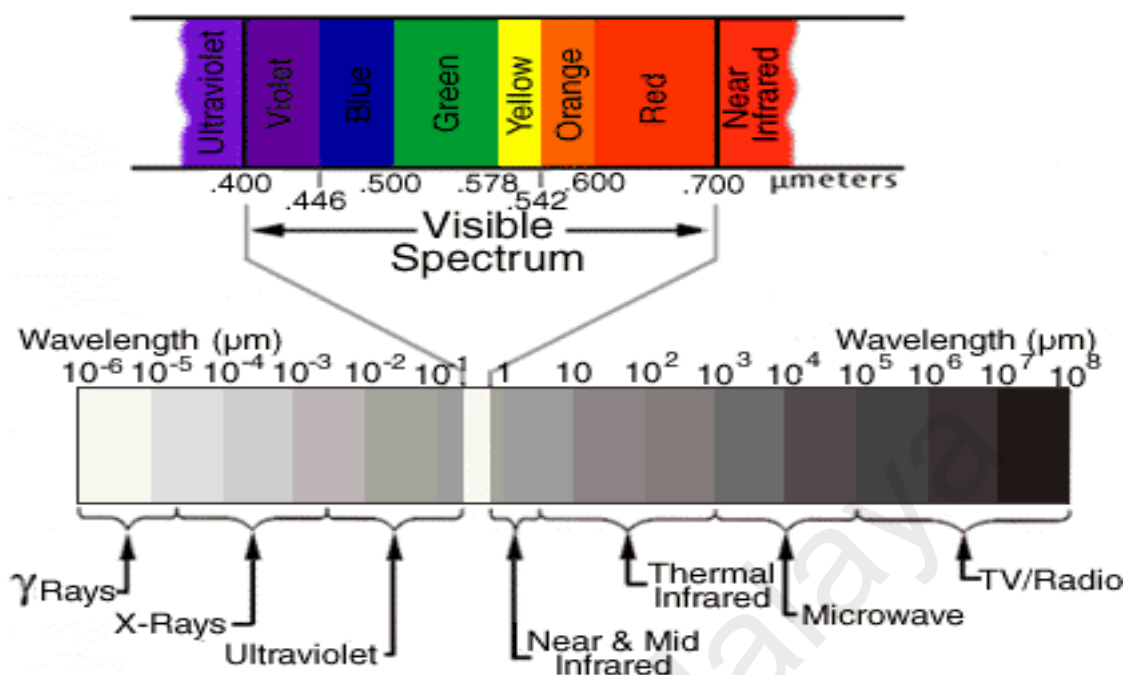


**Figure 3.1:** Electromagnetic spectrum.

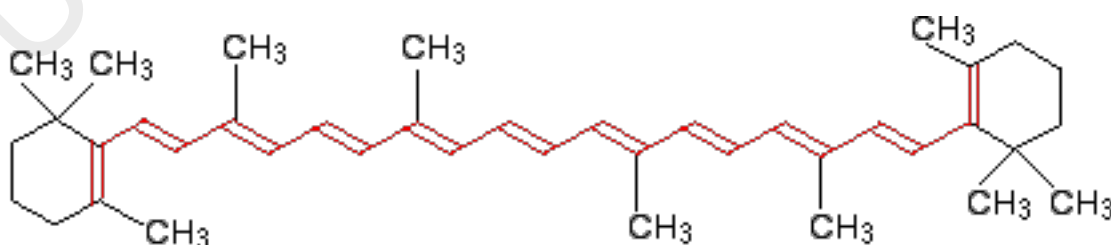
Sunlight is effectively an inexhaustible energy source, which motivated the interest in photochemical synthesis. However, most simple organic molecules absorb only ultraviolet (UV) light and cannot be activated by the visible wavelengths that comprise most of the solar energy. Consequently, UV light source has generally required for organic photochemistry.

Over the past several years, transition metal chromophores were productively exploited in synthetic photochemistry for the design of solar energy technologies. Solar energy conversion can also convert visible light energy into useful chemical potential for synthetic purposes. Productive photoreactions of compounds possessing weak bonds which are sensitive toward UV photodegradation can be enable by visible light. Furthermore, visible light photoreactions can be conducted by using any source of white light, including sunlight. This feature has expanded to a broad range of the accessibility

of photochemical reactions. Visible light photocatalysis of variety reaction types have been enable via photoinduced electron transfer or from the transition metal chromophore, as well as energy-transfer processes. Application of these reactions towards complex target molecules was possible by the predictable reactivity of the intermediates generated and the tolerance of the reaction conditions to a wide range of functional groups (Schultz & Yoon, 2014).

Many problems arising in research, development and manufacturing activities require the analytical examination of complex materials. Certain resonating groups called chromophores within molecules arises from the excitation of electronic energy levels of ultraviolet absorption (Shreve, 1952).

All molecules give similar UV-visible absorption spectra. The only difference is as the amount of delocalization in the molecule increases, the maximum absorptions moves to longer and longer wavelengths. Therefore there must be less energy gap between the bonding and anti-bonding orbitals. Beta-carotene (**3.1**) has the sort of delocalization but on a much greater scale with eleven conjugated carbon-carbon double bonds (shown in red).

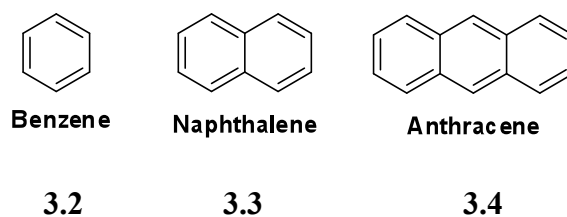


**3.1**

The gap between the highest energy  $\pi$ -bonding orbital and the lowest energy  $\pi$ -anti-bonding orbital become smaller as the delocalization increase. Therefore, it takes less energy in beta-carotene to promote an electron because the gap between the levels is less. Less energy means a lower frequency of light gets absorbed and that is equivalent to a longer wavelength. Beta-carotene strongly absorbs in the visible region between about 400 and 500 nm with a peak about 470 nm.

There are many organic compounds that have conjugated double bond systems in which every other bond is a double bond called as conjugated system. These conjugated systems have a large influence on peak wavelengths and absorption intensities (Tsuda & Osuka, 2001).

Figure 3.2 shows the absorption spectra of benzene (3.2), naphthalene (3.3), and anthracene (3.4). The maximum peak wavelengths tend to be shifted toward the long wavelength (red shift) region as the conjugated system gets larger (Coulson, 1948). Larger conjugated systems, the absorption peak wavelengths tend to be shifted toward the long wavelength region (red shift) and the absorption peaks tend to be larger.



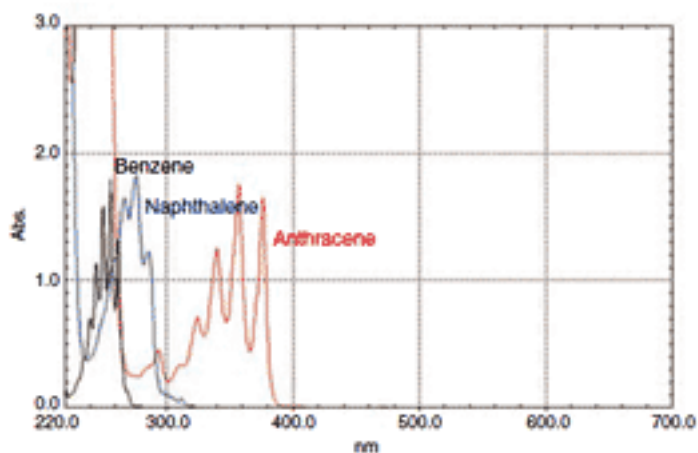


**Figure 3.2:** Absorption spectra of Benzene, Naphthalene and Anthracene

Why does the peak wavelength tend to be shifted toward the long wavelength region (red shift) as the size of the conjugated system increases? Light exhibits properties of both waves and particles (photons). The energy of one photon is expressed as  $hc/\lambda$ , where  $h$  is Planck's constant,  $c$  is the speed of light, and  $\lambda$  is the wavelength. Absorption in the ultraviolet and visible regions is related to the transition of electrons. "Transition" refers to the switching of an electron from one state of motion to another. The state of motion of the  $\pi$  electrons in the conjugated system changes more easily than that of the  $\sigma$  electrons that form the molecular frameworks. If a photon collides with a  $\pi$  electron, that  $\pi$  electron readily changes to a different state of motion. This is true even if the photon has only a small amount of energy. The  $\pi$  electrons in relatively large conjugated systems are more easily affected by low-energy photons. Transition expresses the way that electrons absorb the energy of photons. If a photon has a relatively small amount of energy, the value of  $hc/\lambda$  for that photon is relatively small, and therefore the value of  $\lambda$  is relatively large.  $\lambda$  is observed as the absorption wavelength and so, if there is a conjugated system, peaks tend to appear in regions where  $\lambda$  is large, i.e., the long wavelength region (Lin *et al.*, 1994).



### 3.1.2 Bandgap, $E_g$

Why do some materials work well for making solar cells or light-emitting diodes (LEDs), while other materials don't? One key factor is having the right bandgap. The bands closest to the atomic nucleus, called core levels, and the furthest band from the nucleus that has electrons in it, called the valence band, all keep their electrons tightly in place. The next band out from that is called the "conduction band," and there, the electrons are free to roam around freely.

In some materials, called metals, a valence band and a conduction band overlap, and electricity flows freely and easily through them. In other materials, called insulators, there is a wide gap between the valence band and the conduction band, making it almost impossible for an electron to get excited enough to jump from one to the other, so they block the flow of electricity.

There's a third category, and that's where the most interesting stuff happens. These are materials that have a narrower gap between the two bands, and they are called semiconductors. Sometimes they can act like metals, sometimes they can act like insulators, and sometimes they can have properties in between. When first discovered, they were considered useless because of their erratic, variable behavior until physicists figured out the mystery of the bandgap (Figure 3.3) (Capasso, 1987). Tonio Buonassisi, MIT's SMA Assistant Professor of Mechanical Engineering and Manufacturing said that is the idea of the bandgap which allowed people to understand and harness semiconductors for optoelectronic devices which is work with light and electricity.

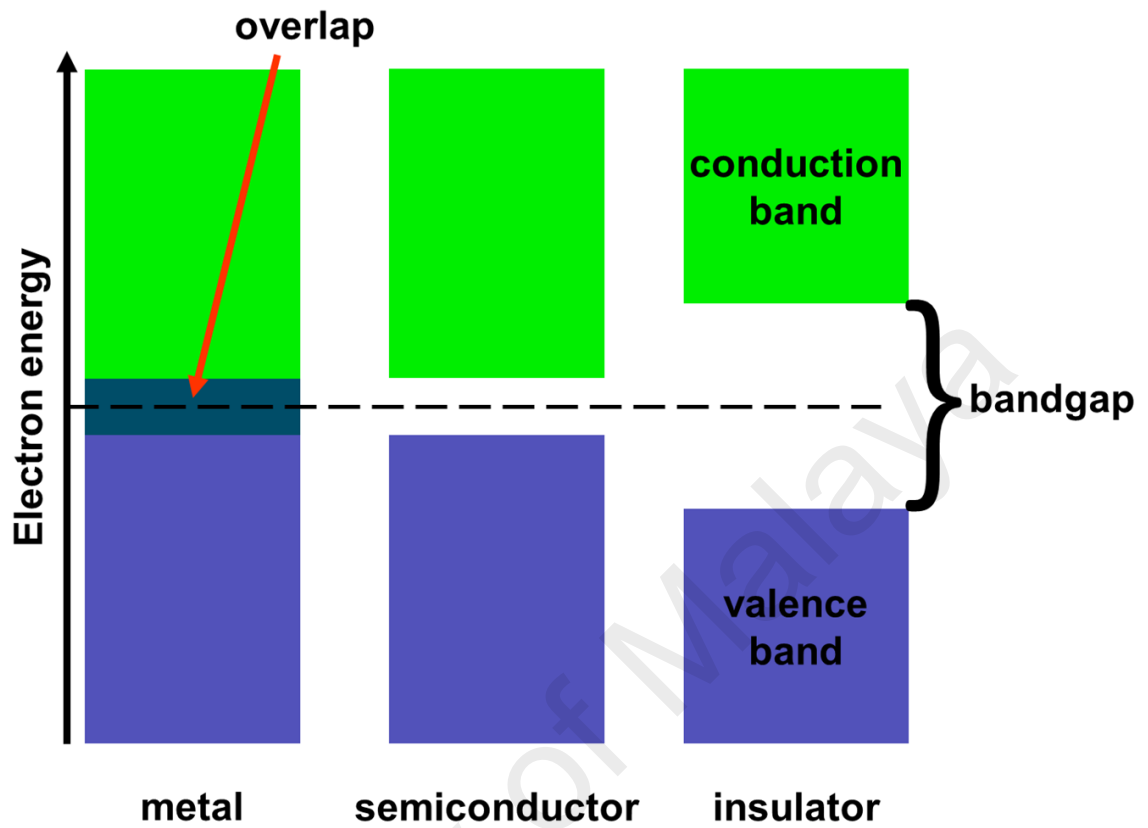


**Figure 3.3:** Bandgap energy of metal, semiconductor and insulator.

When electrons get excited (by getting heated, or by being hit with a particle of light, known as a photon), they can jump across the gap. If an electron in a crystal gets hit by a photon that has enough energy, it can get excited enough to jump from the valence band to the conduction band, where it is free to form part of an electric current. That's what happens when light strikes a solar cell, producing a flow of electrons.

Silicon, a semiconductor, is the material of choice for solar cells in large part because of its bandgap. Silicon's bandgap is just wide enough so that electrons can easily cross it once they are hit by photons of visible light.

The same process also works in reverse. When electricity passes through a semiconductor, it can emit a photon, whose color is determined by the material's bandgap. That's the basis for light-emitting diodes, which are increasingly being used for displays and computer screens, and are seen as the ultimate low-power light bulbs (Chandler, 2012).

Molecular design of high efficiency photovoltaic materials needs broad and strong absorption band in visible and near infrared region to match the solar spectrum, that is why we need smaller bandgap ( $E_g$ ). In addition, the absorption properties of the photovoltaic materials depend on their bandgap.

### 3.1.3 Electronic Spectroscopy

Fluorescence and phosphorescence are types of molecular luminescence methods. A molecule of analyte absorbs a photon and excites a species. Qualitative and quantitative analyze can be provided by the emission spectrum. The term fluorescence and phosphorescence are usually referred as photoluminescence because both are alike in excitation brought by absorption of a photon. Electronic energy transition in fluorescence differs from phosphorescence. Electron spin does not change in the excited state of fluorescence, which results in short-live electrons ( $<10^{-5}$  s). In phosphorescence, there is a change in electron spin, which results in a longer lifetime of the excited state (second to minutes). Fluorescence and phosphorescence occurs at longer wavelength than the excitation radiation.

The Jablonski diagram (Figure 3.4) is a partial energy diagram that represents the energy of photoluminescent molecule in its different energy states. The lowest and darkest horizontal line represents the ground-state electronic energy of the molecule which is the singlet state labeled as  $S_0$ . At room temperature, majority of the molecules in a solution are in this state. The upper lines represent the energy state of the three excited electronic states:  $S_1$  and  $S_2$  represent the electronic singlet state (left) and  $T_1$  represents the first electronic triplet state (right). The upper darkest line represents the ground vibrational state of the three excited electronic state. The energy of the triplet state is lower than the energy of the corresponding singlet state.

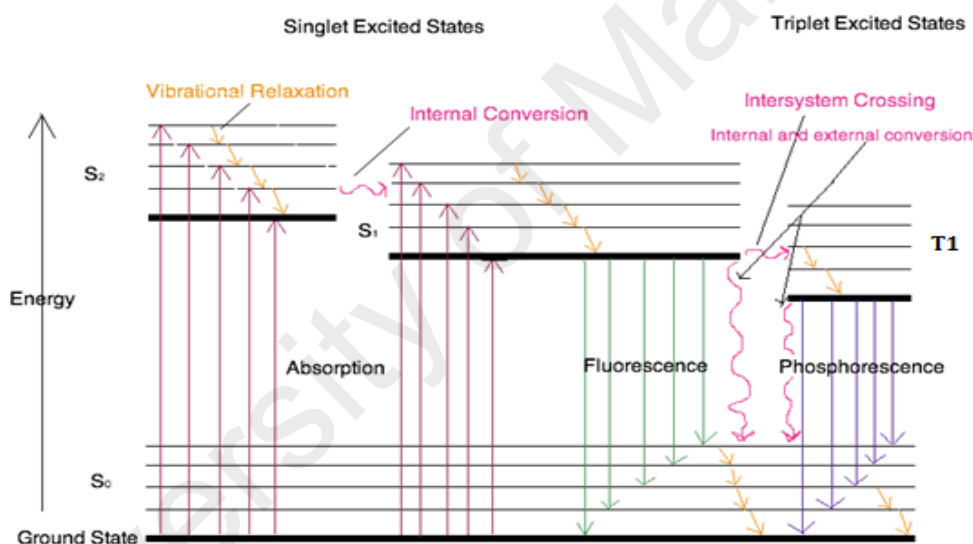


**Figure 3.4:** Partial Jablonski diagram for absorption, fluorescence, and phosphorescence.

There are numerous vibrational levels that can be associated with each electronic state as denoted by the thinner lines. Absorption transitions (red lines in Figure 3.4) can occur from the ground singlet electronic state ( $S_0$ ) to various vibrational levels in the singlet excited vibrational states. It is unlikely that a transition from the

ground singlet electronic state to the triplet electronic state because the electron spin is parallel to the spin in its ground state (Figure 3.4). This transition leads to a change in multiplicity and thus has a low probability of occurring, which is a forbidden transition. Molecules also go through vibration relaxation to lose any excess vibrational energy that remains when excited to the electronic states ( $S_1$  and  $S_2$ ) as demonstrated in orange in Figure 3.4. The knowledge of forbidden transition is used to explain and compare the peaks of absorption and emission.

Compounds containing aromatic group with low-energy  $\pi \rightarrow \pi^*$  transitions have the most intense fluorescence. A few aliphatic, alicyclic carbonyl, highly conjugated double-bond and most unsubstituted aromatic hydrocarbons structures also exhibit fluorescence as well. The quantum efficiency increases as the number of rings and the degree of condensation increases (Skoog *et al.*).

One of the ways to visually distinguish the difference between each photoluminescence is to compare the relative intensities of emission/excitation at each wavelength. An example of the three types of photoluminescence (absorption, fluorescence and phosphorescence) is shown for phenanthrene in the spectrum (Figure 3.5). The spectrum in red represents the excitation spectrum, which is identical to the absorption spectrum because in order for fluorescence emission to occur, radiation needs to be absorbed to create an excited state. The spectrum in blue represent fluorescence and green spectrum represents the phosphorescence.

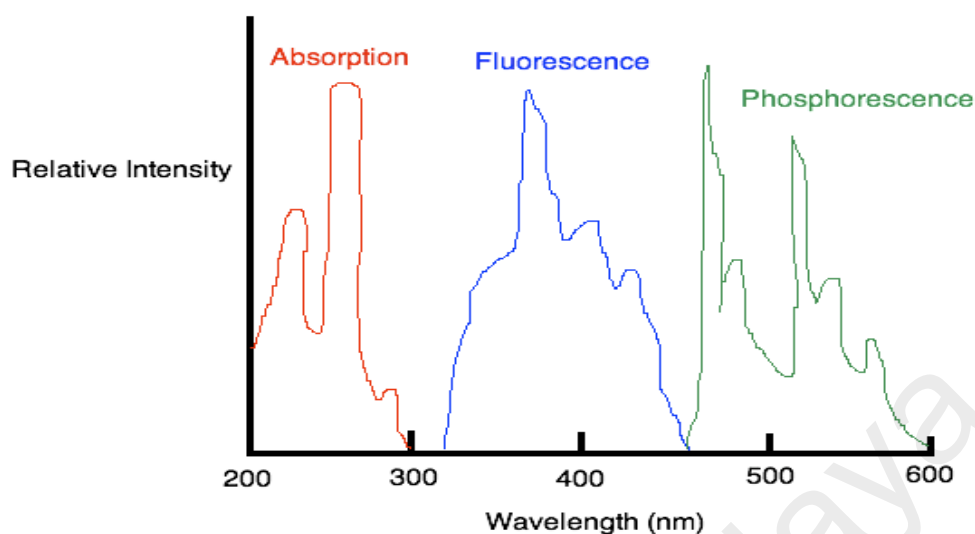


**Figure 3.5:** Wavelength intensities of absorption, fluorescence, and phosphorescence.

Fluorescence and Phosphorescence occur at wavelengths that are longer than their absorption wavelengths. Phosphorescence bands are found at a longer wavelength than fluorescence band because the excited triplet state is lower in energy than the singlet state. The difference in wavelength could also be used to measure the energy difference between the singlet and triplet state of the molecule. The wavelength ( $\lambda$ ) of a molecule is inversely related to the energy ( $E$ ) by the equation,  $E = hc / \lambda$ . As the wavelength increases, the energy of the molecule decrease and vice versa (Harris & Bertolucci, 1978). Less energy means a lower frequency of light gets absorbed and that is equivalent to a longer wavelength. Therefore less energy gap between the bonding and anti-bonding orbitals as the amount of delocalization increases.

### 3.2 Literature Review

In the design of an efficient light harvesting small molecular architecture, the donor/acceptor (D/A) concept has been utilized. Where the p-electron distribution between electron rich and electron deficient moieties leads to low energy optical transitions. Depending on the electronic offset between the donor and acceptor, a wide range of band gaps can be achieved and thus the optical absorption can be tailored (Welch *et al.*, 2011). For organic solar cells, it is important that the active layer components absorb from 300 to 800 nm, the maximum photon flux in the solar spectrum.

In general as shown in Figure 3.7, all dyes **M1-M6** (Figure 3.6) showed two prominent absorption band: a) a small absorption band at  $\lambda_{\text{max}}$  of 312-387 nm, which attributed to the localized  $\pi$ - $\pi^*$  transition, and b) a large absorption band in the visible region, corresponding to an ICT transition from the central electron-donating carbazole unit to both electron-accepting cyanoacrylic acid. Because of their structural similarities, **M1-M6** exhibited similar ICT transition peaks located in the range ( $\lambda_{\text{max}}$ ) from 455 to 488 nm.

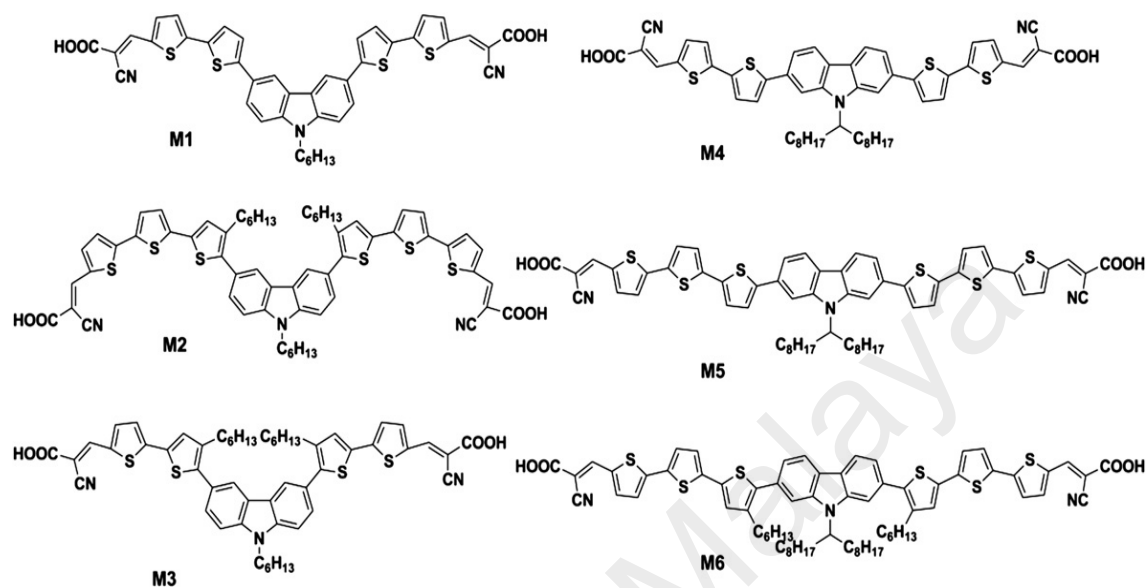


**Figure 3.6:** Structure of organic dyes (**M1-M6**).

They also display consistent red-shifted absorptions and emissions upon increasing the number of thiophene units. For instance, red shifts occurred upon increasing the number of conjugated thiophene units from **M3** to **M2** and from **M4** to **M5** (in the 3,6- and 2,7- functionalized carbazole-based systems), respectively. As expected, elongation of the p-conjugation length decreased the  $\pi$ - $\pi^*$  band gap energy and led to spectral red shifts of the  $\pi$ - $\pi^*$  transitions (H.-C. Chu *et al.*, 2012).



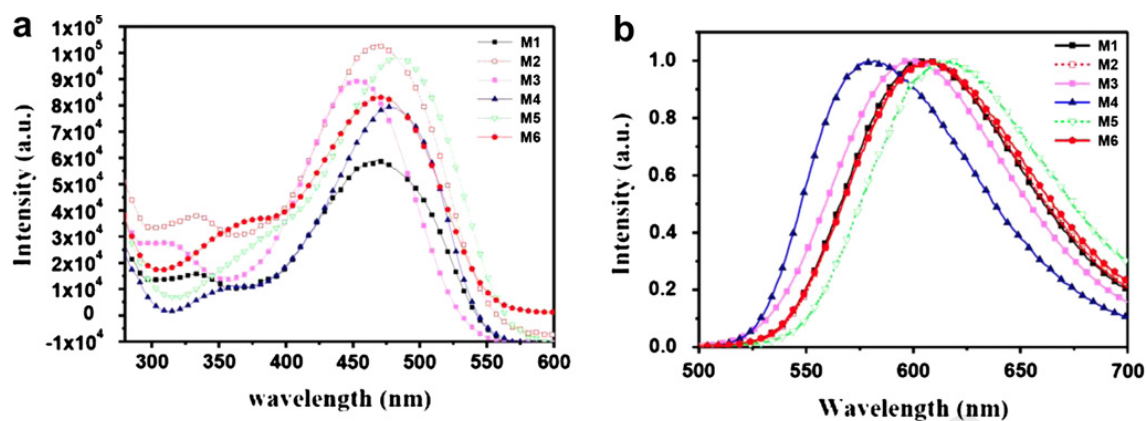


**Figure 3.7:** (a) UV-Vis absorption and (b) normalized emission spectra of **M1-M6** recorded in THF solutions ( $1 \times 10^{-5}$  M).

Dye-sensitized solar cells (DSSCs), which are one of the promising molecular photovoltaic, have been attracting considerable attention since the pioneering study because of the potential of low cost production and high efficiency. All **MK** dyes (Figure 3.8) exhibit similar  $\pi$ - $\pi^*$  electron transition peaks located in the range of 470 – 485 nm. It is clearly seen from Figure 3.9 that the maximum absorption peak gradually shifts to the longer wavelength with increasing number of thiophene group as a result of expanded  $\pi$ -conjugation (Z.-S. Wang *et al.*, 2008).

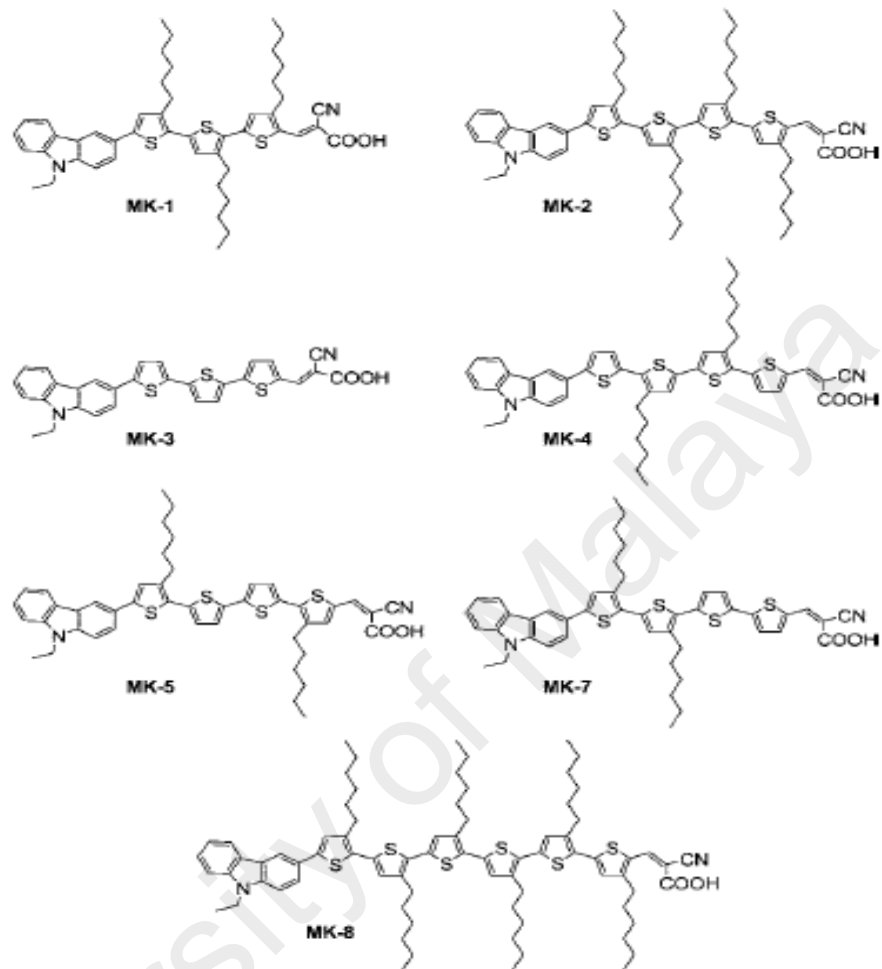


**Figure 3.8:** Molecular structures of MK dyes.

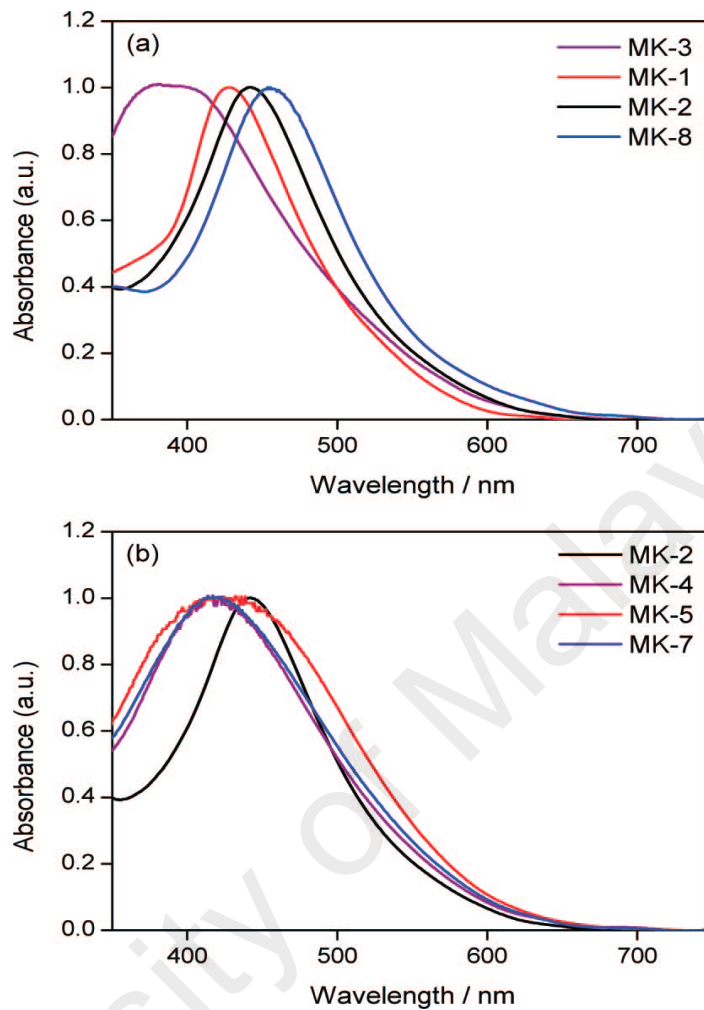


**Figure 3.9:** Normalized UV-Vis absorption spectra for different compound MK dye-loaded TiO<sub>2</sub> films using a bare TiO<sub>2</sub> film as reference.

### 3.3 Objective

Our attention mainly on tuning the electronic energy levels and absorption spectra of the photovoltaic materials. The absorption properties of the photovoltaic materials depend on their bandgap ( $E_g$ ). A unique advantage of the conjugated photovoltaic materials is that their physicochemical properties can be easily tuned by

attaching functional substituents on the main chains. For an example, attaching flexible side chains such as alkyl and alkoxy groups will improve the solubility of the conjugated compound, and substituents of electron-donating or electron-withdrawing functional groups can tune the electronic energy levels of the compounds (Y. Li, 2012).

Bredas and Heeger (1994) studied the effect of the functional substituents on the electronic energy levels of poly(p-phenylene vinylene) (PPV). They found that the bandgap of the conjugated polymers can be reduced to some extent by both electron-donating groups and the electron-withdrawing. HOMO level up-shifted more than the LUMO level by the electron-donating groups, while LUMO level down-shifted more than the HOMO level by the electron-withdrawing groups. Obviously, HOMO and LUMO level can be up-shift or down-shift by suitable electron-withdrawing or electron donating substituents.

Hou et al. tuned the HOMO level of the narrow bandgap copolymers of benzodithiophene and thieno[3,4-b]-thiophene (H.-Y. Chen *et al.*, 2009). By change of the ester group on the unit to a strong electron withdrawing ketone group, the LUMO and HOMO levels of the polymer dropped by 0.11 eV. Obviously, electron-withdrawing groups played an important role in lowering the HOMO level.

Absorption, bandgaps and HOMO energy levels of the studied compounds were tuned effectively by the addition of thiophene units at 3,6-position on carbazole. For high-efficiency conjugated materials, narrower  $E_g$ , broad absorption, and relatively lower-lying HOMO level are of most importance.

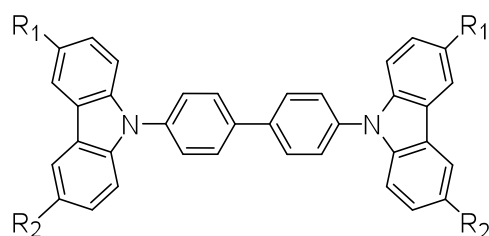
### 3.4 Results And Discussion

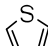
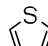
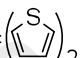
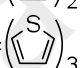
#### 3.4.1 Optical Properties - Electronic Absorption Spectroscopy (Effect of Thiophenes)

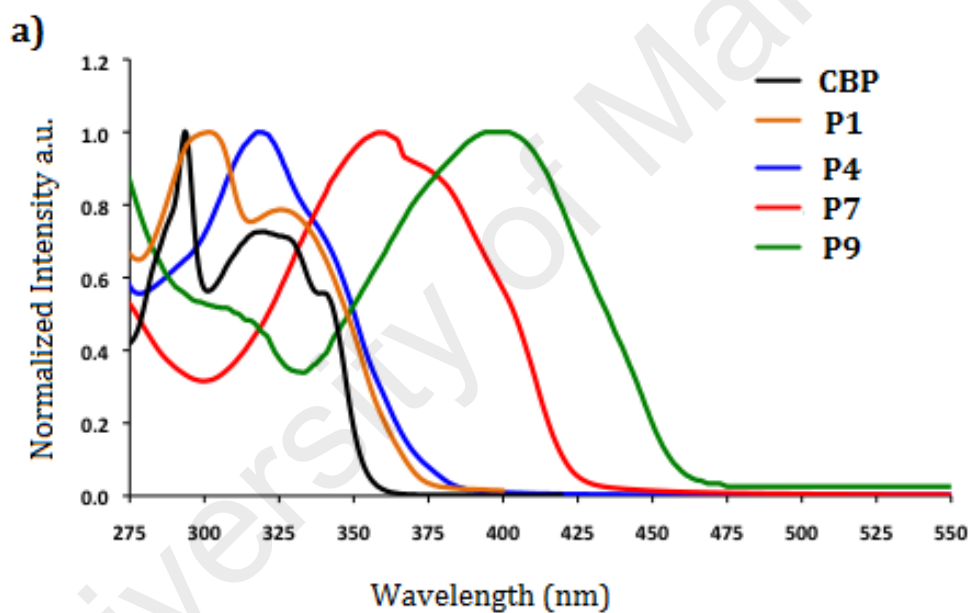
The UV-Vis absorption spectra of **1.4 (CBP)**, **2.36 (CDBP)**, **2.37 (BCP)**, **2.38 (P1)**, **2.39 (P2)**, **2.40 (P3)**, **2.41 (P4)**, **2.42 (P5)**, **2.43 (P6)**, **2.44 (P7)**, **2.45 (P8)**, **2.46 (P9)** and **2.47 (P10)** were measured in DMF solutions (Figure 3.10(a), 3.10(b) and 3.10(c)) and  $\lambda_{\max}^{\text{abs}}$  values for quantifying on the extension of  $\pi$ -conjugation are summarized in Table 3.1. It is clearly seen from Figure 3.10(a), 3.10(b) and 3.10(c) that the maximum absorption bands of all compounds were gradually red shifts to the longer wavelength with the increasing number of thiophene unit on **1.4 (CBP)**, **2.36 (CDBP)**, **2.37 (BCP)** backbone, which are connected to the carbazole at the 3- and 6- positions and the extent of  $\pi$ -conjugation in the compounds increased as expected. Compounds **2.44 (P7)**, **2.45 (P8)**, **2.46 (P9)** and **2.47 (P10)** show the longest wavelength absorptions at 422, 423, 458 and 532 nm, respectively (Figure 3.10), which were considerably red-shifted in comparison to those of compounds **1.4 (CBP)** (360 nm), **2.36 (CDBP)** (353 nm) and **2.37 (BCP)** (352 nm) (Damit *et al.*, 2016). The attachment of two to three unit of thiophenes on each position significantly enhances the optical properties for photovoltaic materials.

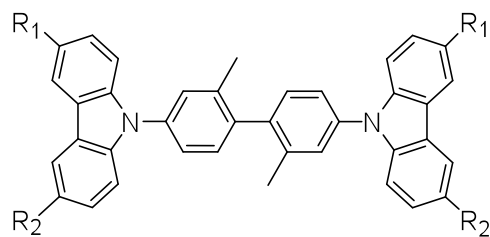
It is well-known that  $\pi$ -conjugated thiophene oligomers and polymers tend to  $\pi$ -stack because of the strong intermolecular interaction between  $\pi$ -electrons (Z.-S. Wang *et al.*, 2008). The difference in intermolecular  $\pi$ - $\pi$  interaction for these compounds would account for the differences in the broadness of their UV-vis absorption spectra,

as shown in Figure 3.6. We also observe that the broadness increased slightly as the numbers of thiophene groups increased (Hara *et al.*, 2005).



- CBP.** R<sub>1</sub> = R<sub>2</sub> = H  
**P1.** R<sub>1</sub> =  R<sub>2</sub> = H  
**P4.** R<sub>1</sub> = R<sub>2</sub> =   
**P7.** R<sub>1</sub> = R<sub>2</sub> =   
**P9.** R<sub>1</sub> = R<sub>2</sub> = 





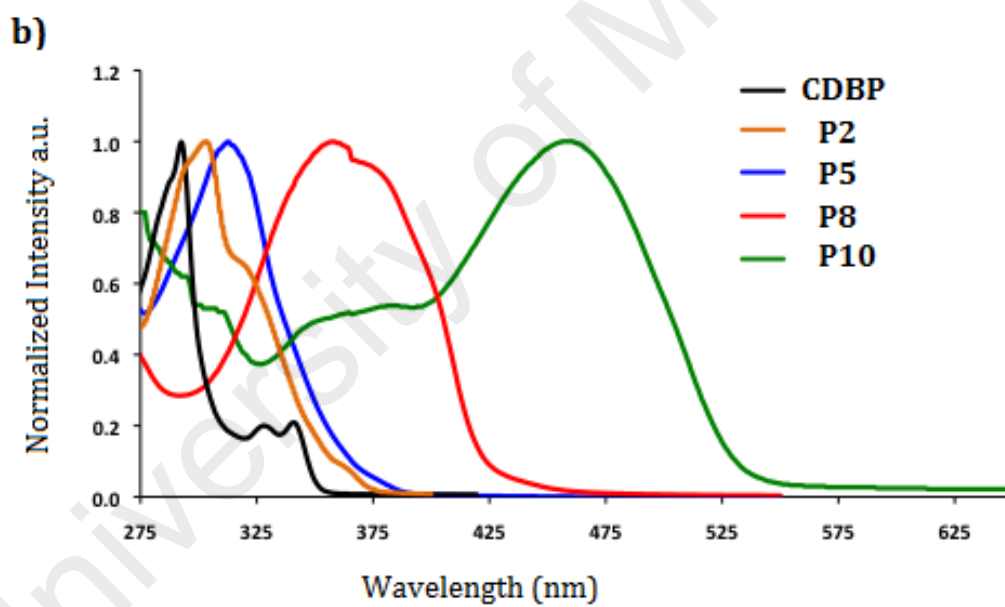
**CDBP.**  $R_1 = R_2 = H$

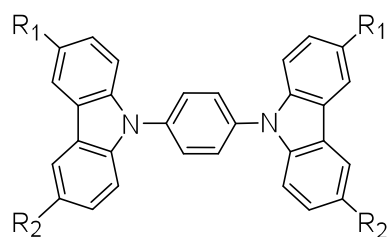
**P2.**  $R_1 = \text{thiophene}$   $R_2 = H$

**P5.**  $R_1 = R_2 = \text{thiophene}$

**P8.**  $R_1 = R_2 = (\text{thiophene})_2$

**P10.**  $R_1 = R_2 = (\text{thiophene})_3$





**BCP.**  $R_1 = R_2 = H$

**P3.**  $R_1 = \text{thiophene}$   $R_2 = H$

**P6.**  $R_1 = R_2 = \text{thiophene}$

**c)**

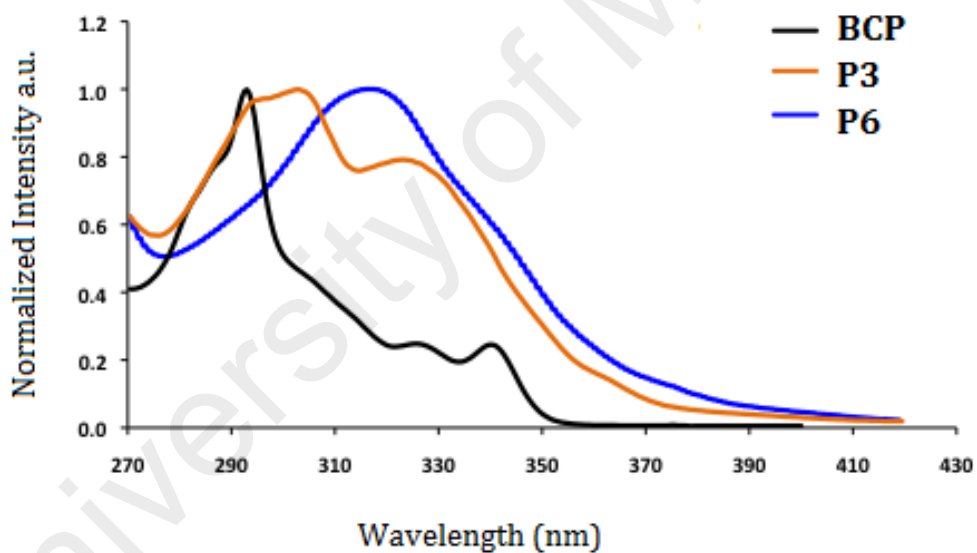


**Figure 3.14:** Electronic absorption spectra at fixed bridging core unit of a) (Biphenyl) **CBP**, **P1**, **P4**, **P7** and **P9**, b) (Dimethylbiphenyl) **CDBP**, **P2**, **P5**, **P8** and **P10**, and c) (phenyl) **BCP**, **P3** and **P6** recorded in DMF at 30 °C.



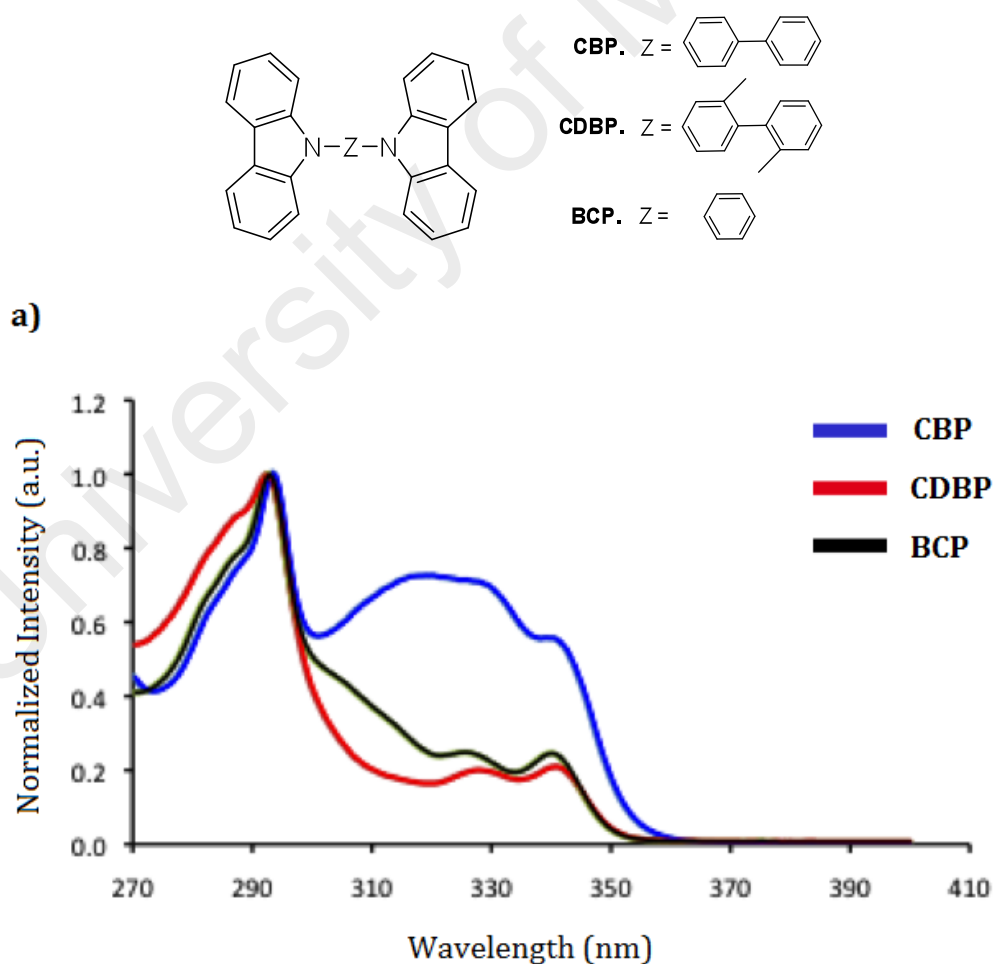
**Table 3.1: UV-Vis –Spectroscopic Data and Fluorescence on 300 nm excitation.<sup>a</sup>**

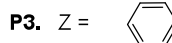
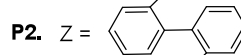
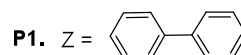
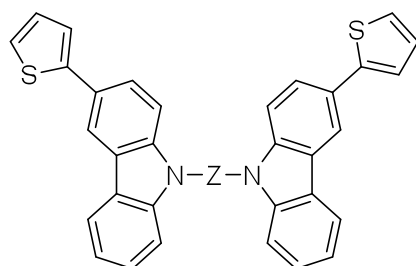
	$\lambda_{\max}^{\text{abs}}$ [nm]	$\lambda_{\text{onset}}$ [nm]	$\lambda_{\text{em}}^{\text{c}}$ [nm]
<b>CBP</b>	293, 317 <sup>b</sup> , 340 <sup>b</sup>	360	390
<b>P1</b>	301, 325 <sup>b</sup>	377	413
<b>P4</b>	318, 344 <sup>b</sup>	390	412
<b>P7</b>	358	422	443
<b>P9</b>	398	458	486
<b>CDBP</b>	293, 328 <sup>b</sup> , 341 <sup>b</sup>	353	351
<b>P2</b>	293 <sup>b</sup> , 303, 322 <sup>b</sup>	373	396
<b>P5</b>	313	393	410
<b>P8</b>	358	423	446
<b>P10</b>	458	532	554
<b>BCP</b>	293, 326 <sup>b</sup> , 340 <sup>b</sup>	352	355
<b>P3</b>	294 <sup>b</sup> , 303, 324 <sup>b</sup>	372	394
<b>P6</b>	316	414	421

<sup>a</sup> Measured in DMF. <sup>b</sup> Peak as shoulder. <sup>c</sup> Wavelength of the intensity maxima of the fluorescence at 300 nm excitation at room temperature.

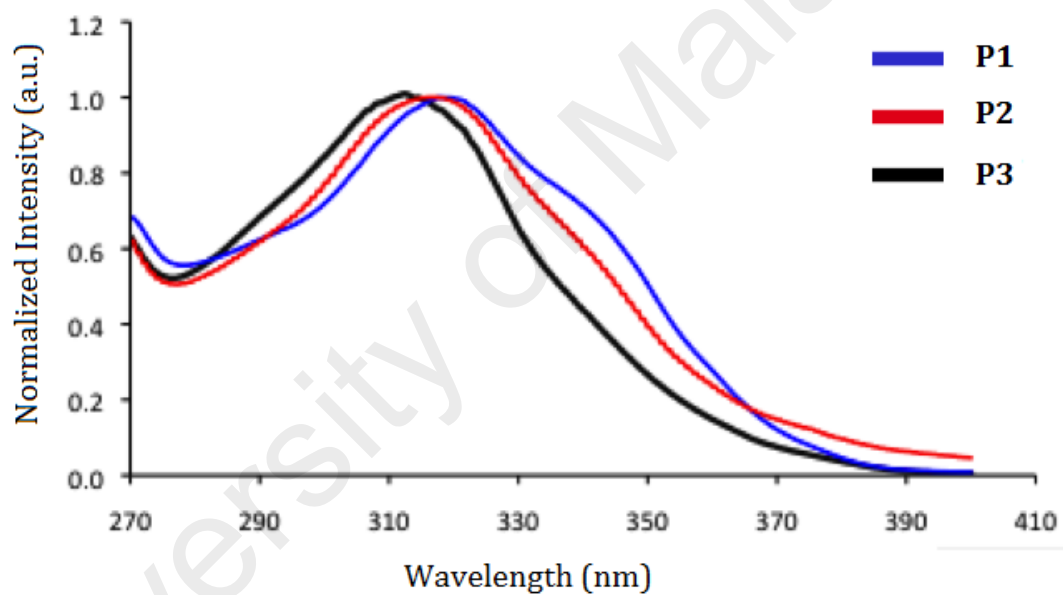
### 3.4.2 Optical Properties - Electronic Absorption Spectroscopy (Effect of Core unit)

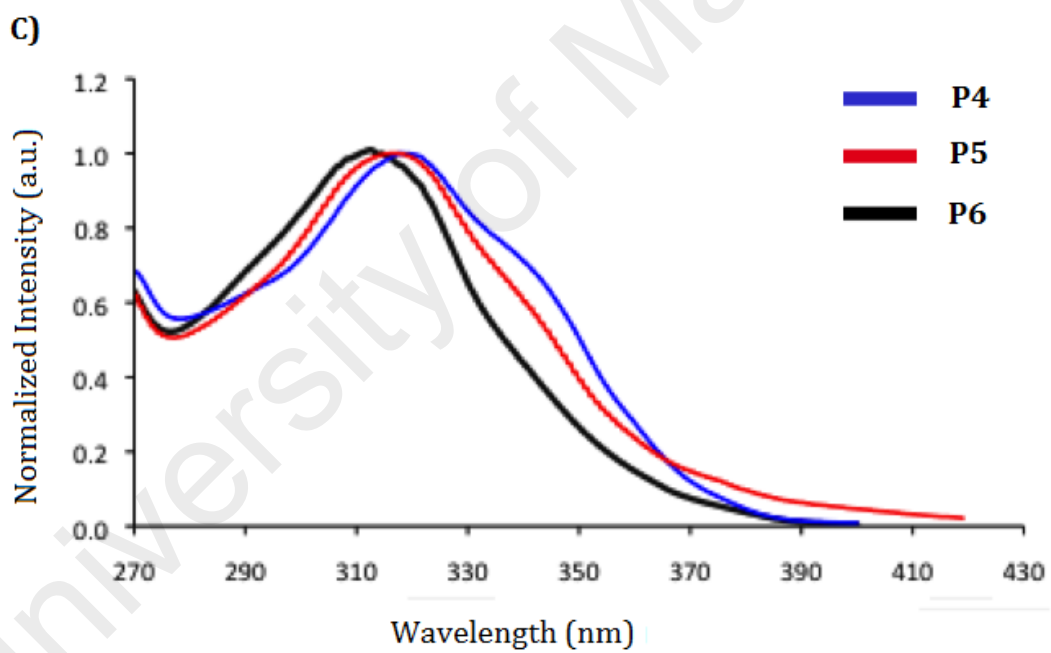
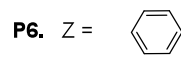
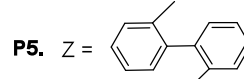
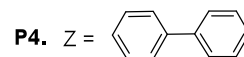
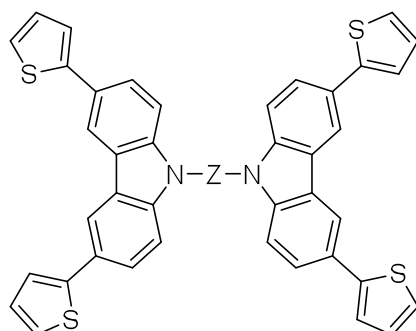
Furthermore, the slight shift of wavelength for a fixed number of thiophene groups, bridging biphenyl groups, dimethylbiphenyl and phenyl suggests that the differences in core groups in the compounds affect the optical properties. Noticeably,  $\lambda_{\max}^{\text{abs}}$  are not affected by the changes of core groups (Figure 3.11(a), 3.11(b), 3.11(c) and 3.2(d), however, the attachment of trienyl on compounds **2.46 (P9)** and **2.47 (P10)**, a significant change on  $\lambda_{\max}^{\text{abs}}$  was observed when bridging core unit was change from biphenyl **2.46 (P9)** to dimethylbiphenyl **2.47 (P10)** as shown in Figure 3.11(e).

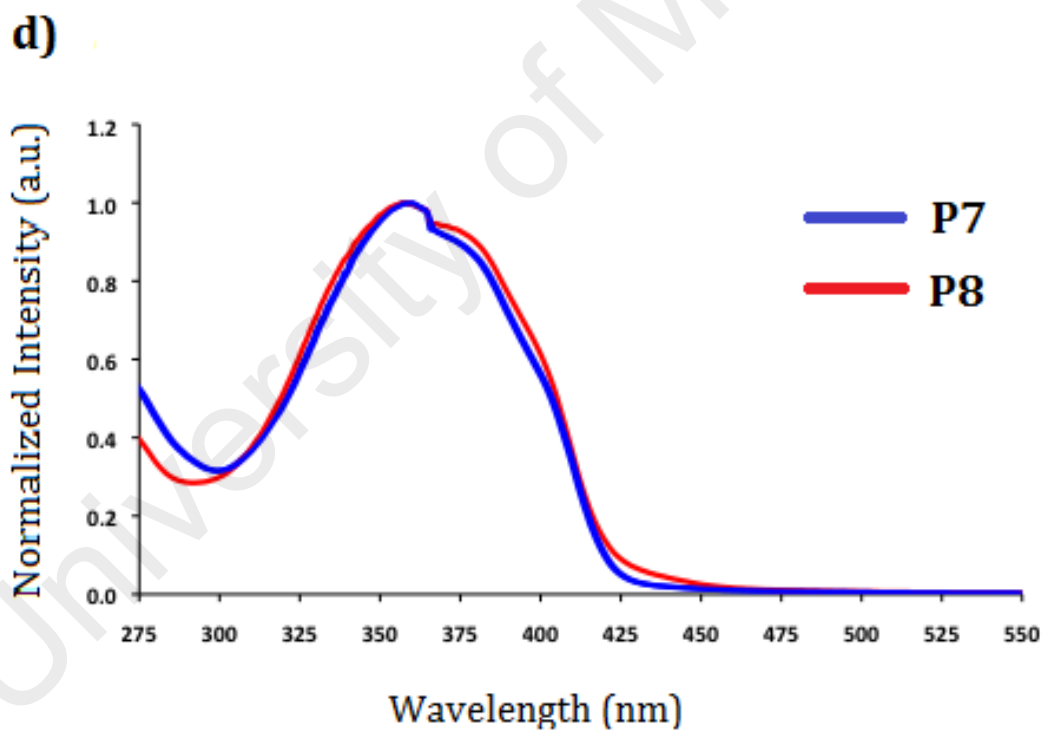
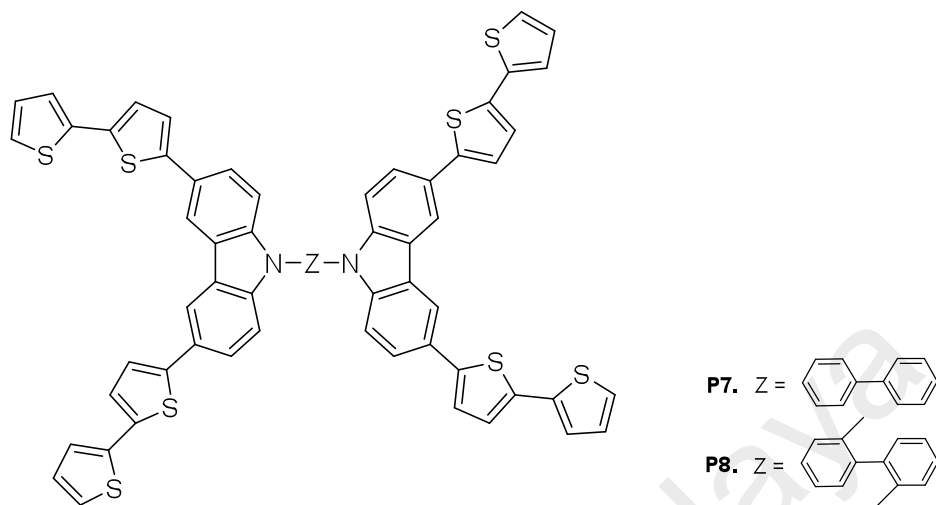




**b)**







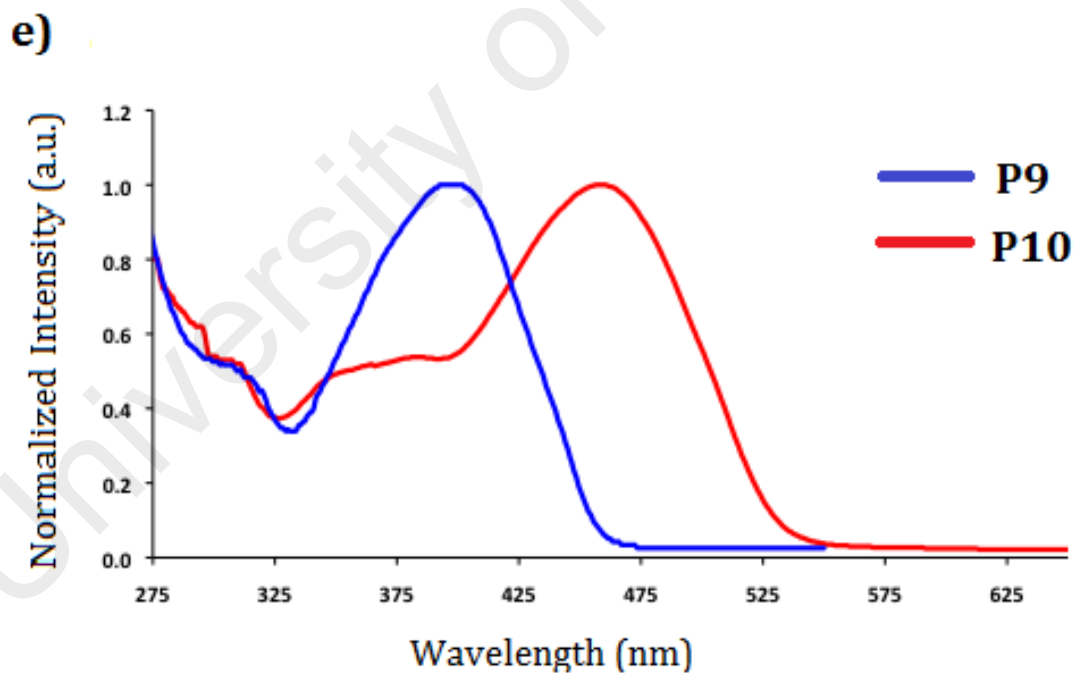
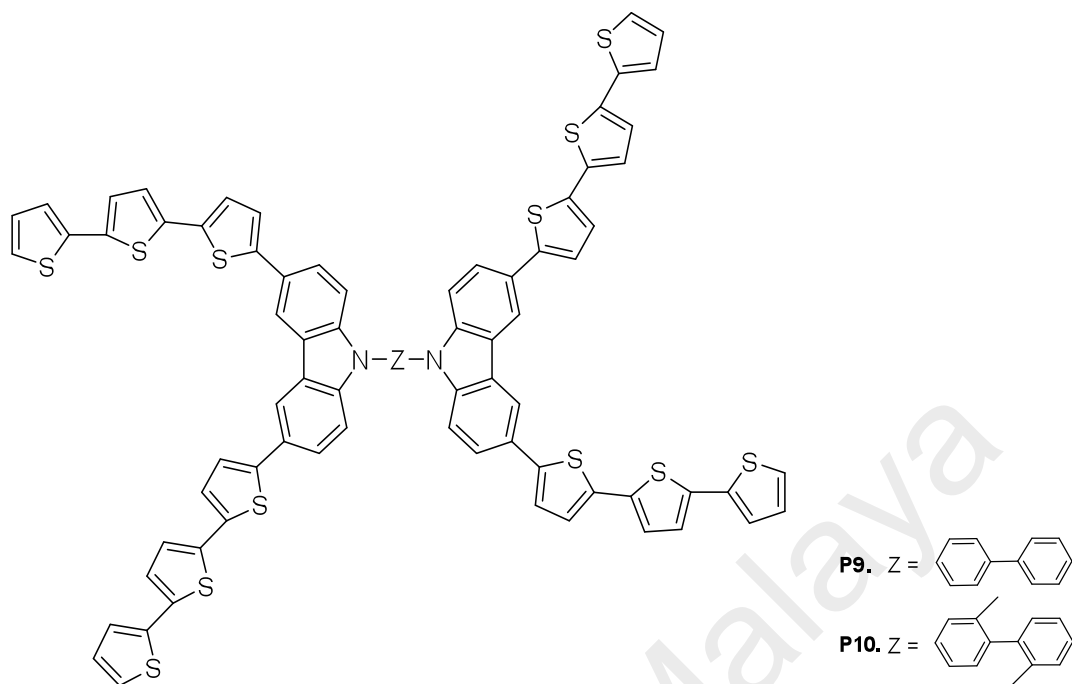


**Figure 3.11:** Electronic absorption spectra by the change of bridging core unit of a) CBP, CDBP, and BCP b) P1, P2, P3 c) P4, P5 and P6 d) P7 and P8 e) P9 and P10 recorded in DMF at 30 °C.

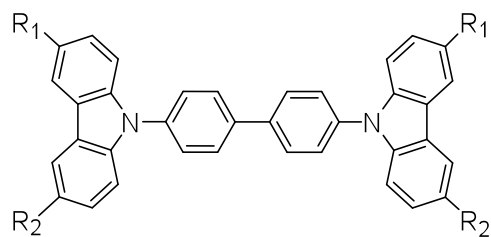
### 3.4.3 Optical Properties - Fluorescence Spectroscopy (Effect of Thiophenes)

All the compounds **1.4 (CBP)**, **2.36 (CDBP)**, **2.37 (BCP)**, **2.38 (P1)**, **2.39 (P2)**, **2.40 (P3)**, **2.41 (P4)**, **2.42 (P5)**, **2.43 (P6)**, **2.44 (P7)**, **2.45 (P8)**, **2.46 (P9)** and **2.47 (P10)** are fluorescent. After the functionalization of the carbazole groups, the fluorescence maxima ( $\lambda_{em}$ ) gradually red shifted upon the addition of thiophene group, resulting a significant red shift in the emission spectrum as shown in Figure 3.12(a), 3.12(b) and 3.12(c), and the spectral data are summarized in Table 3.1. The broad absorption band in the fluorescence spectra of **2.38 (P1)**, **2.39 (P2)**, **2.40 (P3)**, **2.41 (P4)**, **2.42 (P5)**, **2.43 (P6)**, **2.44 (P7)**, **2.45 (P8)**, **2.46 (P9)** and **2.47 (P10)** suggest the contribution of a more rigid structure in the excited state, namely the quinoid state, than the ground state (Cao *et al.*, 2005). Carbazole-thiophene possess nonplanar structures in their ground state ( $S_0$ ) and become almost planar in the lowest excited state ( $S_1$ ) (Belletête *et al.*, 2004; Yang *et al.*, 2006). This is expected because, with the addition of each thiophene group, these compounds more conformationally flexible and thus produce a more diffuse spectrum (Radke *et al.*, 2005). The larger the number of  $\pi$ -electron in a chromophore, the greater the shift to the red of the fluorescence and absorption spectra. Thus, the characteristics of a planar chromophore can be interpreted as being because, in this configuration, the number of functional  $\pi$ -electron is a maximum (Berlman, 1970).

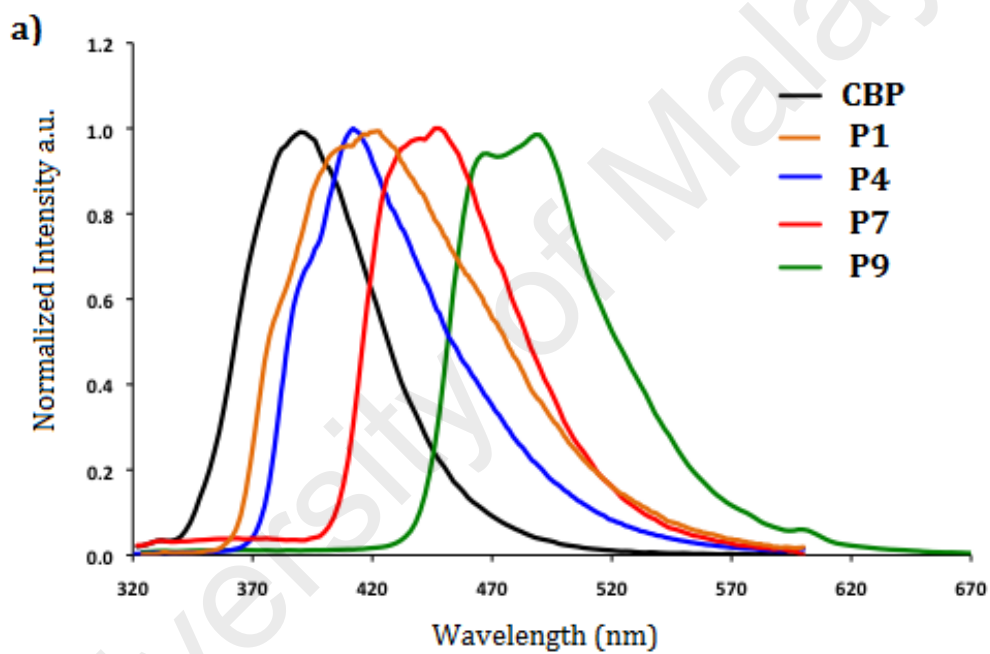
The addition of thiophene unit at 3,6-position of the carbazole, there are no significant changes on  $\lambda_{em}$  of **2.38 (P1)**, **2.39 (P2)**, **2.40 (P3)**, **2.41 (P4)**, **2.42 (P5)** and **2.43 (P6)**. A significant red shift was observed on the di-thienyl-substituted (**2.44 (P7)**, **2.45 (P8)**) and ter-thienyl-substituted carbazole (**2.46 (P9)**, **2.47 (P10)**) suggest that  $\alpha$ -oligothiophene improve the planarity of the compound. Furthermore, the planarity

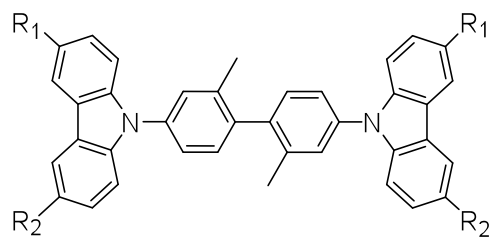
between **1.4 (CBP)**, **2.36 (CDBP)** and **2.37 (BCP)** backbone and oligothiophene linkage would be more increased. By adding electron rich of five-membered thiophene ring, has increased the planarity between electron rich group and electron deficient group carbazole for the enhancement of intramolecular charge transfer (ICT) effect was expected to result in improved  $\pi$ -electron delocalization, low band gap and increased ability of light harvesting of the organic photovoltaic cells (OPVs) (Lo *et al.*, 2014; X.-H. Zhang *et al.*, 2010). The larger the number of  $\pi$ -electron in a chromophore, the greater the shift to the red of the fluorescence and the absorption spectra. Thus the characterization of a planar chromophore can be interpreted as being due to the fact that in this configuration the number of functional  $\pi$ -electron is a maximum (Berlman, 1970). More thiophenes units attached at 3,6-carbazole of **1.4 (CBP)**, **2.36 (CDBP)** and **2.37 (BCP)** backbone was expected to have stronger electron donating ability, which could lead to the more efficient low-band gap materials.





- CBP.**  $R_1 = R_2 = H$   
**P1.**  $R_1 = \text{C}_4\text{H}_3\text{S}$   $R_2 = H$   
**P4.**  $R_1 = R_2 = \text{C}_4\text{H}_3\text{S}$   
**P7.**  $R_1 = R_2 = (\text{C}_4\text{H}_3\text{S})_2$   
**P9.**  $R_1 = R_2 = (\text{C}_4\text{H}_3\text{S})_3$





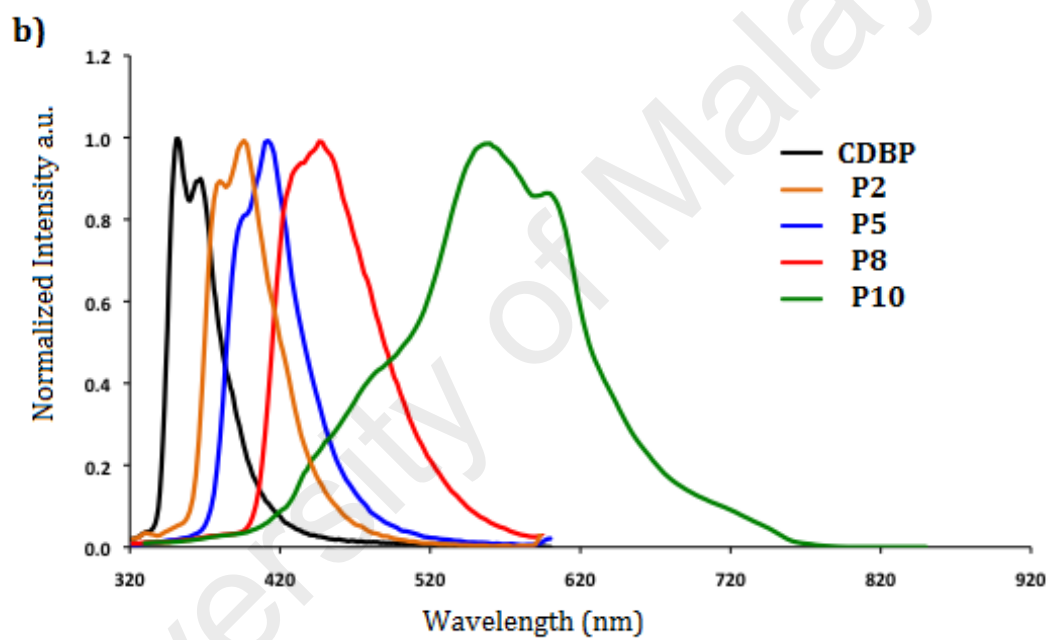
**CDBP.**  $R_1 = R_2 = H$

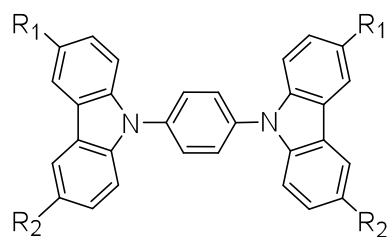
**P2.**  $R_1 = \text{thiophene}$   $R_2 = H$

**P5.**  $R_1 = R_2 = \text{thiophene}$

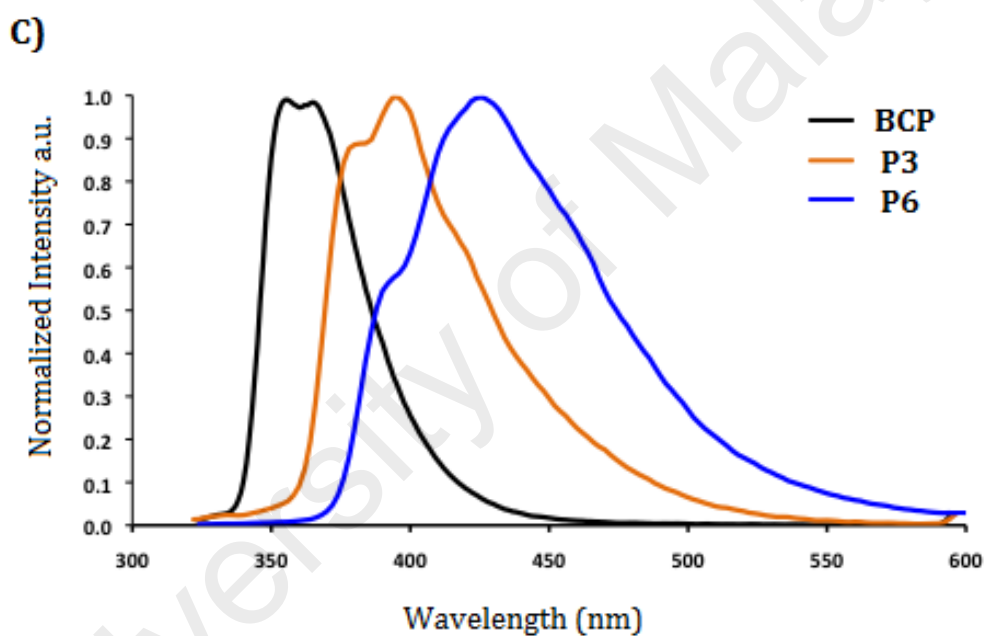
**P8.**  $R_1 = R_2 = (\text{thiophene})_2$

**P10.**  $R_1 = R_2 = (\text{thiophene})_3$





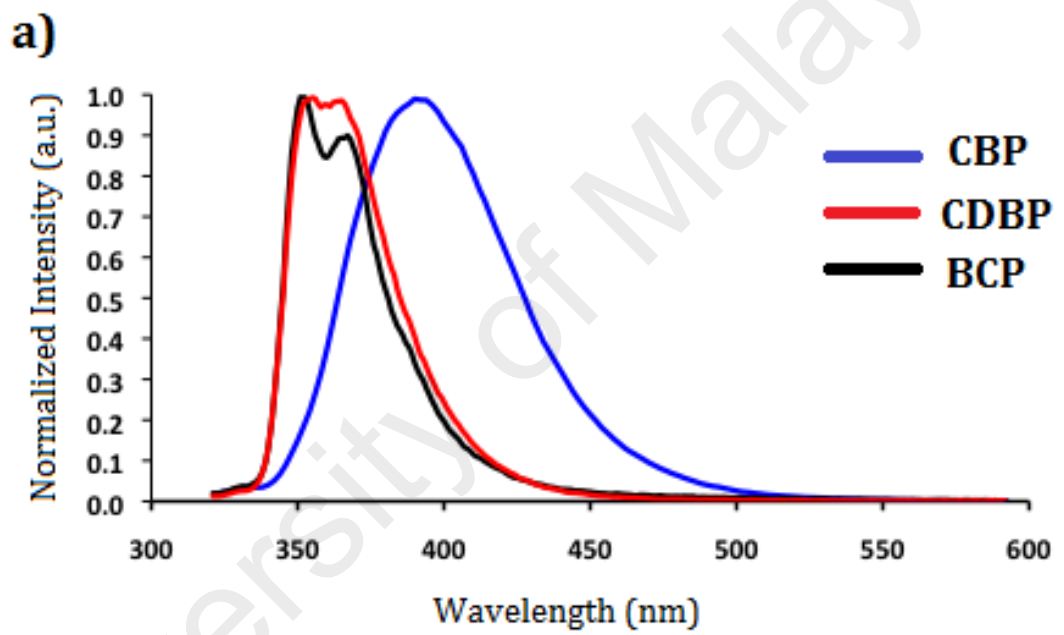
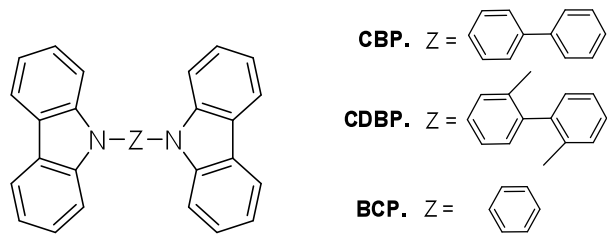
- BCP.**  $R_1 = R_2 = H$   
**P3.**  $R_1 = \text{thiophene-2-yl}$   $R_2 = H$   
**P6.**  $R_1 = R_2 = \text{thiophene-2-yl}$

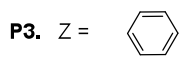
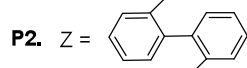
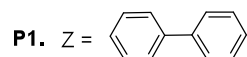
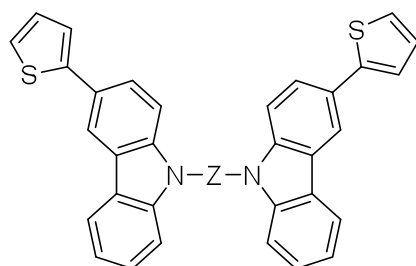


**Figure 3.12:** Emission spectra of a) CBP, P1, P4, P7 and P9, b) CDBP, P2, P5, P8 and P10, and c) BCP, P3 and P6 recorded in DMF at 30 °C. Excitation at 300 nm.

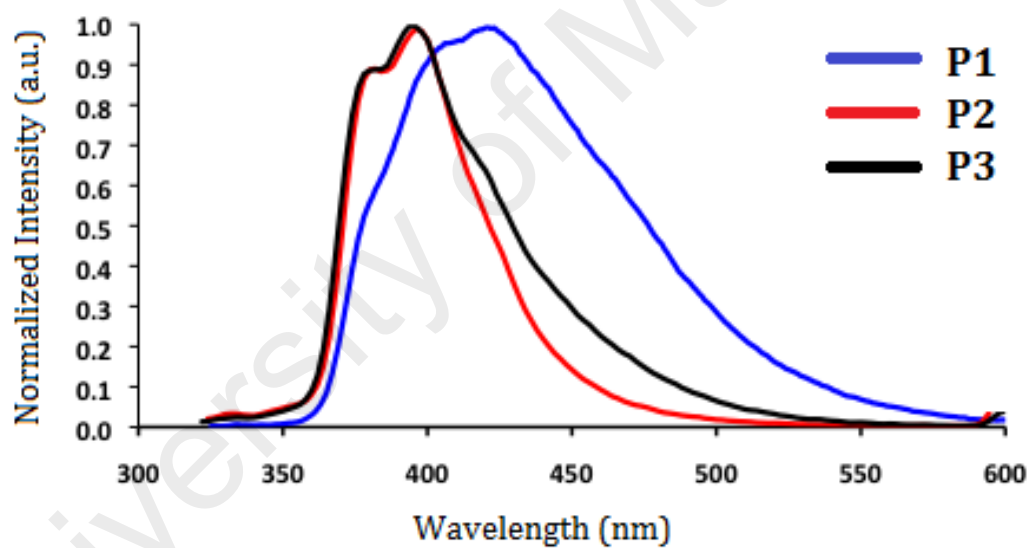
### 3.4.4 Optical Properties - Fluorescence Spectroscopy (Effect of Core Unit)

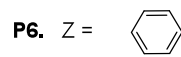
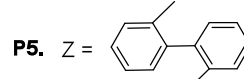
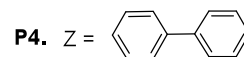
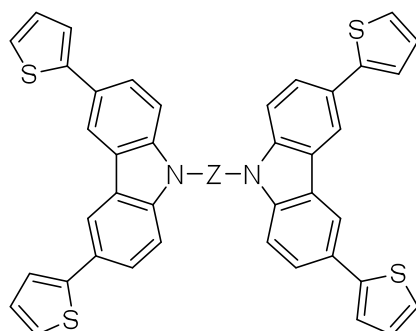
In contrast to the absorption, we note that the emission of **1.4 (CBP)** is red shifted compared to **2.36 (CDBP)** and **2.37 (BCP)**, which is attributed to the planarization of **1.4 (CBP)** after the transition state to the excited state. Such a geometric relaxation is not possible for **2.36 (CDBP)** due to the bulkier side on the introduction of methyl group at core group (Figure 3.13(a)) (Hoffmann *et al.*, 2010). Similarly, **2.38 (P1)** is red shifted compared to **2.39 (P2)** and **2.40 (P3)** (Figure 3.13(b)). As the attachment of thiophene at 3- and 6- on the carbazole for compounds **2.41 (P4)**, **2.42 (P5)**, **2.43 (P6)**, **2.44 (P7)**, **2.45 (P8)**,  $\lambda_{em}$  are not significantly affected by the changed of core groups (Figure 3.13(c) and 3.13(d)). However, a significant change was observed for compounds **2.46 (P9)** and **2.47 (P10)** as the attachment of ter-thienyl at 3- and 6- position of **1.4 (CBP)** and **2.36 (CDBP)**, which is expected that the overall planarity have been affected by the conformation of compounds (Figure 3.13(e)).



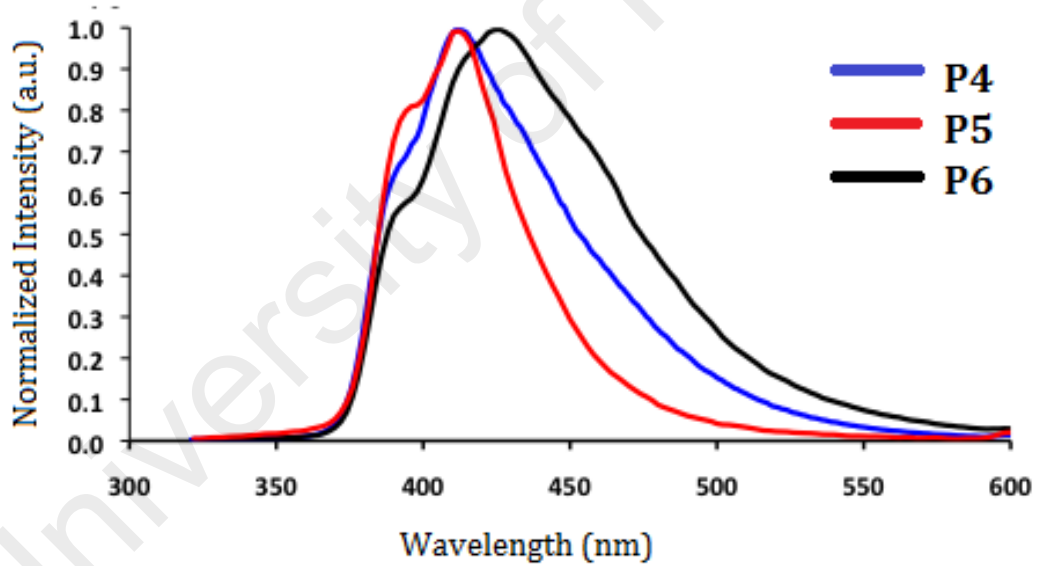


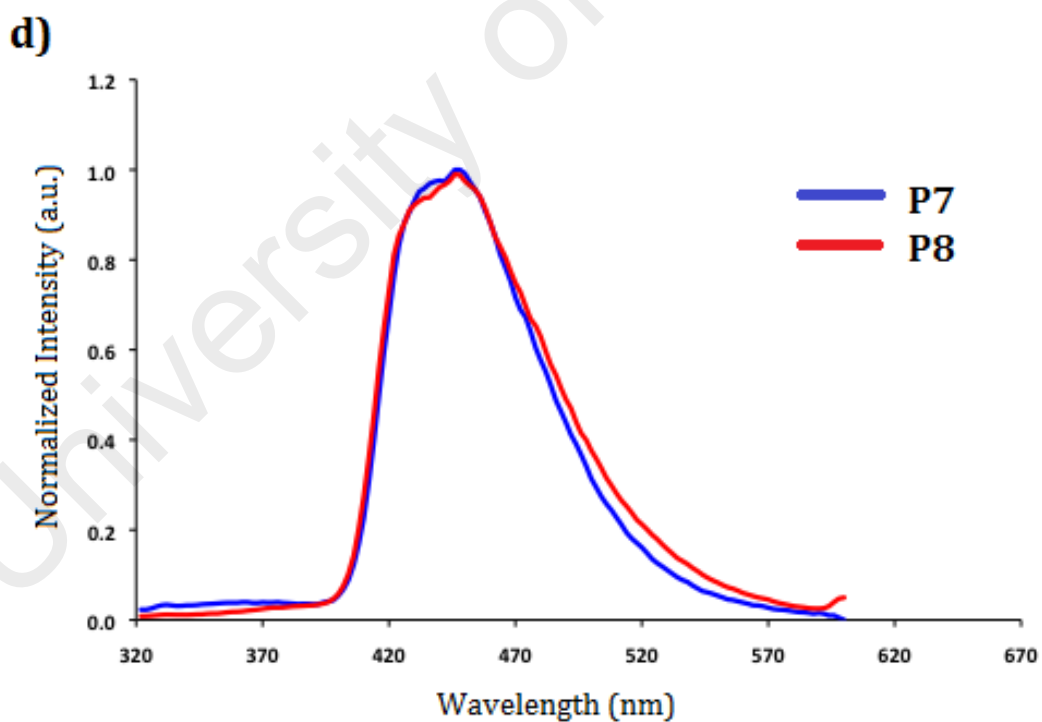
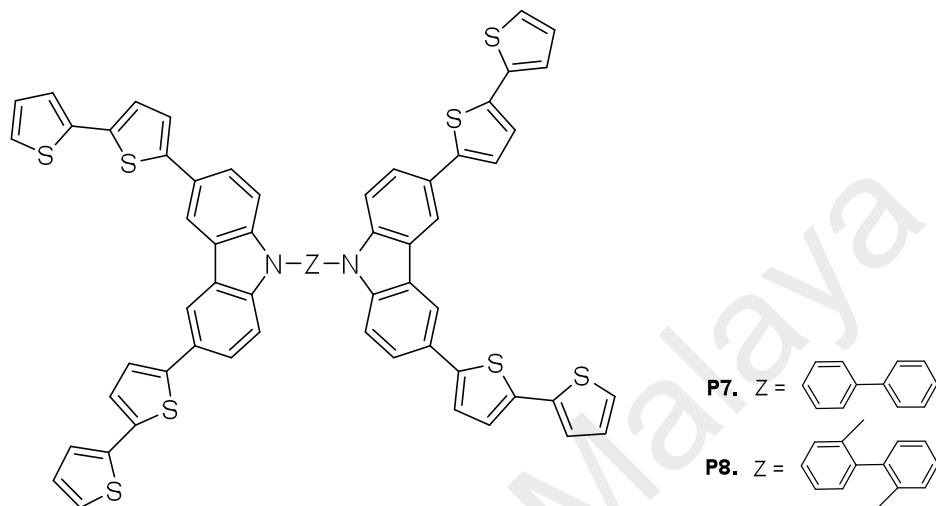
b)





c)







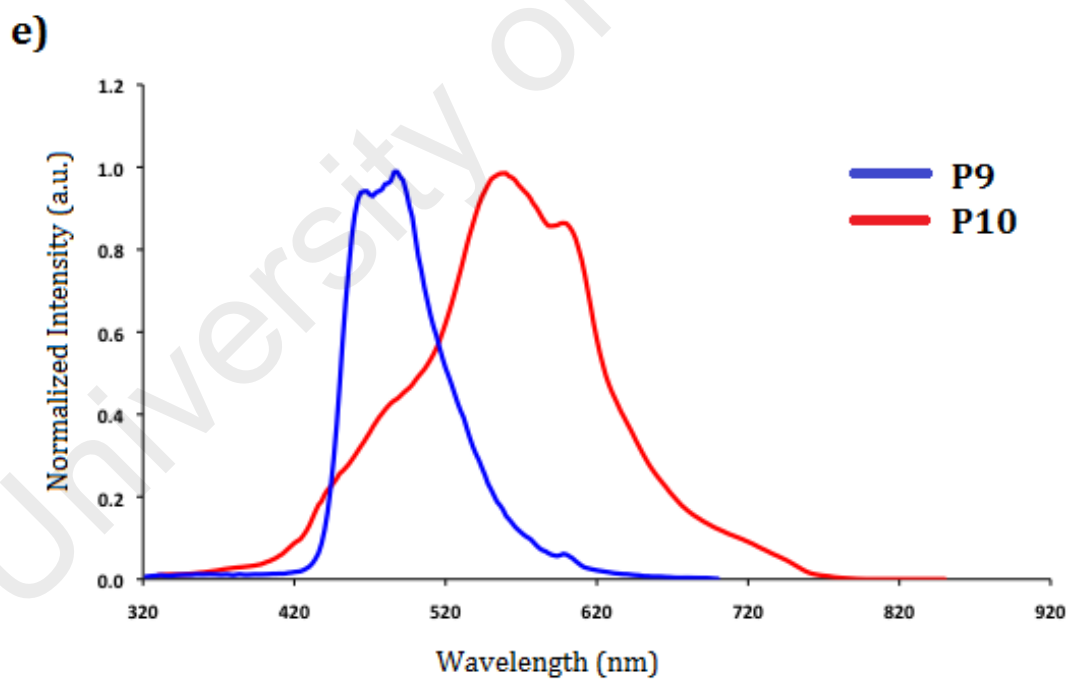
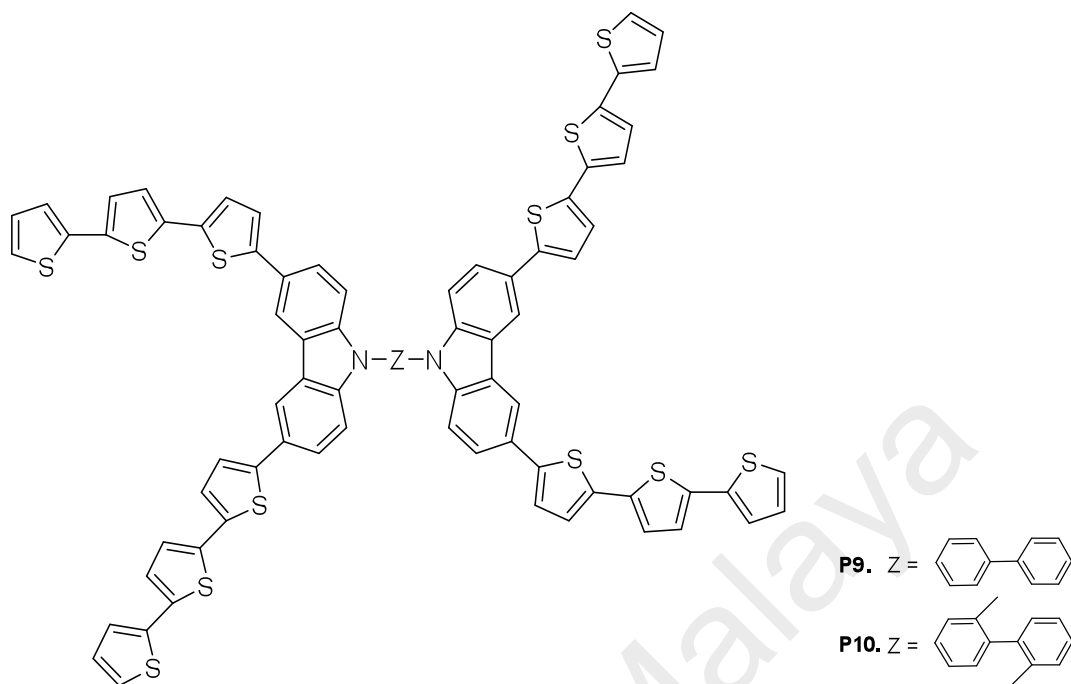
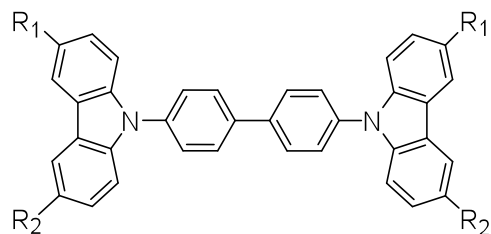


**Figure 3.13:** Emission spectra by the change of bridging core unit a) **CBP**, **CDBP** and **BCP** b) **P1**, **P2**, **P3** c) **P4**, **P5** and **P6** d) **P7** and **P8** e) **P9** and **P10** recorded in DMF at 30 °C. Excitation at 300 nm.

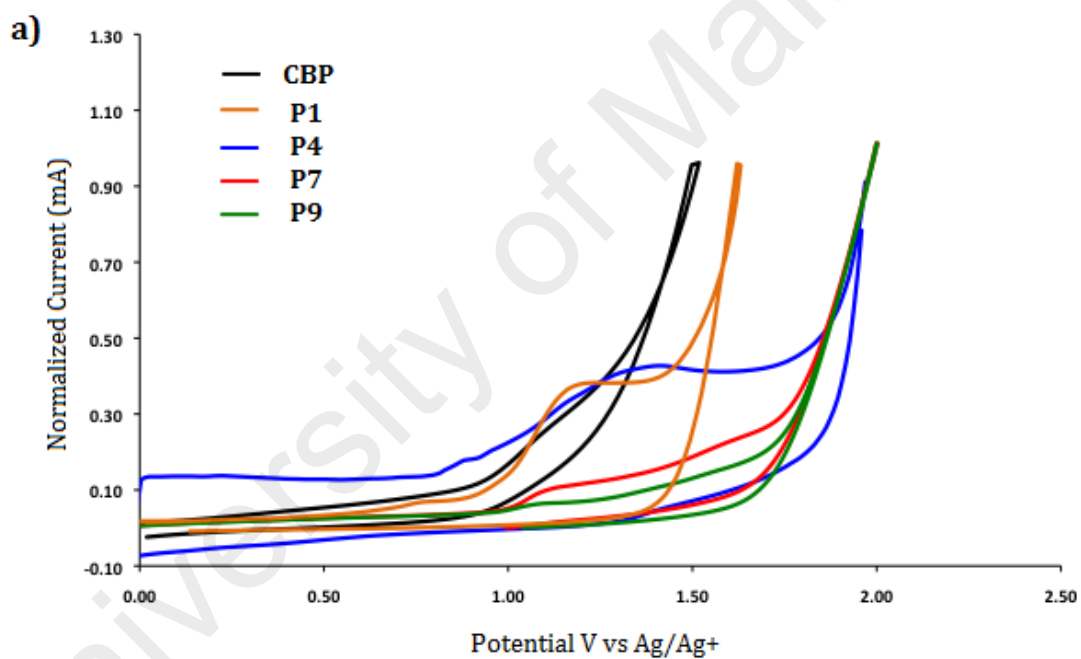
### 3.4.5 Electrochemical Properties

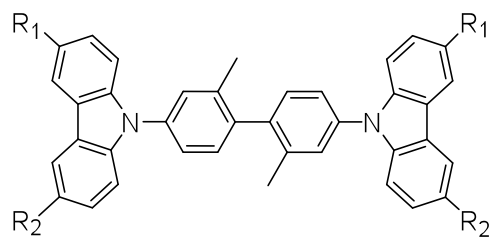
To elucidate the effects of the degree of conjugation between the core, carbazole and thiophene groups and the elongation of the molecular length on donor ability and electrochemical stability, we performed cyclic voltammetry (CV) in a conventional three-electrode cell using platinum working electrode, a platinum wire counter electrode, and a Ag/AgNO<sub>3</sub> reference electrode. In particular, the oxidation processes for **1.4 (CBP)**, **2.36 (CDBP)**, **2.37 (BCP)**, **2.38 (P1)**, **2.39 (P2)**, **2.40 (P3)**, **2.41 (P4)**, **2.42 (P5)**, **2.43 (P6)**, **2.44 (P7)**, **2.45 (P8)**, **2.46 (P9)** and **2.47 (P10)** were investigated in a DMF solution containing 0.05 mol L<sup>-1</sup> of n-Bu<sub>4</sub>NPF<sub>6</sub> as a supporting electrolyte (Figure 3.14). The oxidation potential ( $E_{pa}$ ) and onset ( $E_{onset}$ ) versus Fc<sup>+</sup>/Fc (ferrocenium/Ferrocene couple) are listed in Table 3.2.

Noticeably,  $E_{pa}$  values for **2.38 (P1)**, **2.39 (P2)**, **2.40 (P3)**, **2.41 (P4)**, **2.42 (P5)**, **2.43 (P6)**, **2.44 (P7)**, **2.45 (P8)**, **2.46 (P9)** and **2.47 (P10)** are cathodically shifted compared to those for **1.4 (CBP)**, **2.36 (CDBP)** and **2.37 (BCP)** (Figure 3.14) by the subsequent addition of thiophene molecules, demonstrating that the connection with thiophene at the 3- and 6-positions on carbazole of **1.4 (CBP)**, **2.36 (CDBP)** and **2.37 (BCP)** gives rise to high electrochemical stability and effectively enhances donor ability, which should result from the effective resonance stabilization of the cationic species (Kato *et al.*, 2014). These results indicate that the increase in the molecular length is substantially effective for the enhancement of the donor ability. Moreover increasing the numbers of the thiophene units stabilize the LUMO levels and narrows the HOMO-LUMO gap of the carbazole-thiophene-based obviously. Noticeably, the HOMO-LUMO gap  $\Delta E$  decrease with the increment of the number of thiophene electro-donor groups in the molecule, which may favor light harvesting.

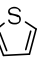


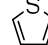
- CBP.**  $R_1 = R_2 = H$   
**P1.**  $R_1 = \text{C}_4\text{H}_3\text{S}$   $R_2 = H$   
**P4.**  $R_1 = R_2 = \text{C}_4\text{H}_3\text{S}$   
**P7.**  $R_1 = R_2 = (\text{C}_4\text{H}_3\text{S})_2$   
**P9.**  $R_1 = R_2 = (\text{C}_4\text{H}_3\text{S})_3$

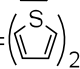


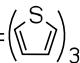


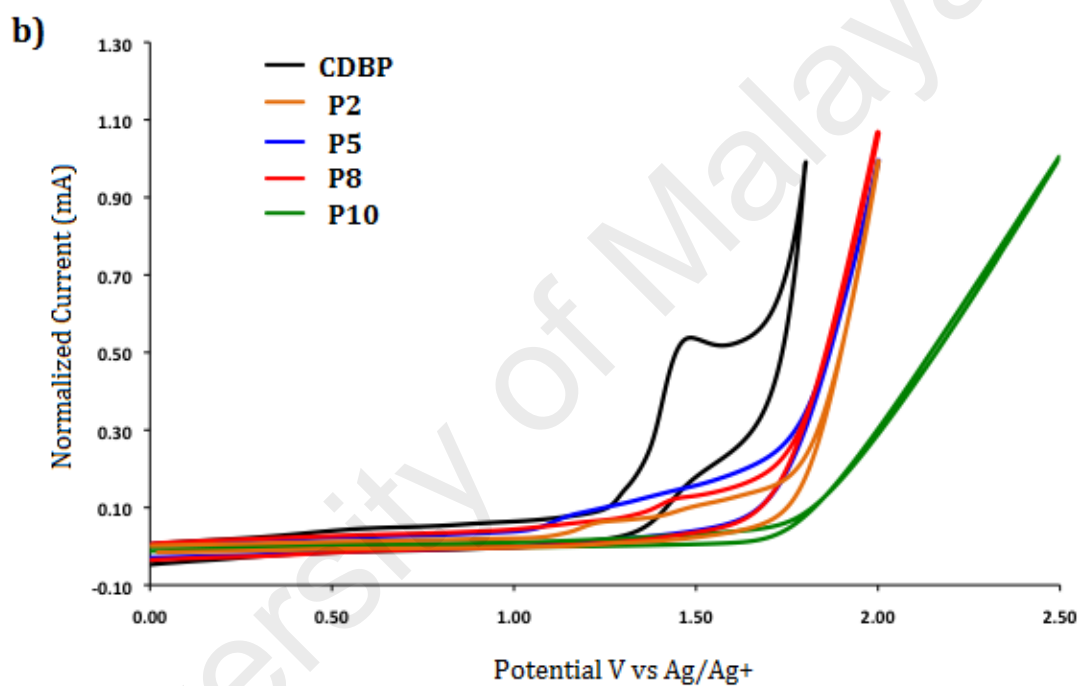
**CDBP.** R<sub>1</sub> = R<sub>2</sub> = H

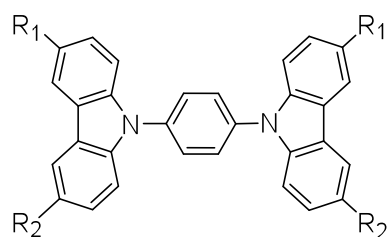
**P2.** R<sub>1</sub> =  R<sub>2</sub> = H

**P5.** R<sub>1</sub> = R<sub>2</sub> = 

**P8.** R<sub>1</sub> = R<sub>2</sub> = 

**P10.** R<sub>1</sub> = R<sub>2</sub> = 





- BCP.**  $R_1 = R_2 = H$   
**P3.**  $R_1 = \text{thiophene}$   $R_2 = H$   
**P6.**  $R_1 = R_2 = \text{thiophene}$

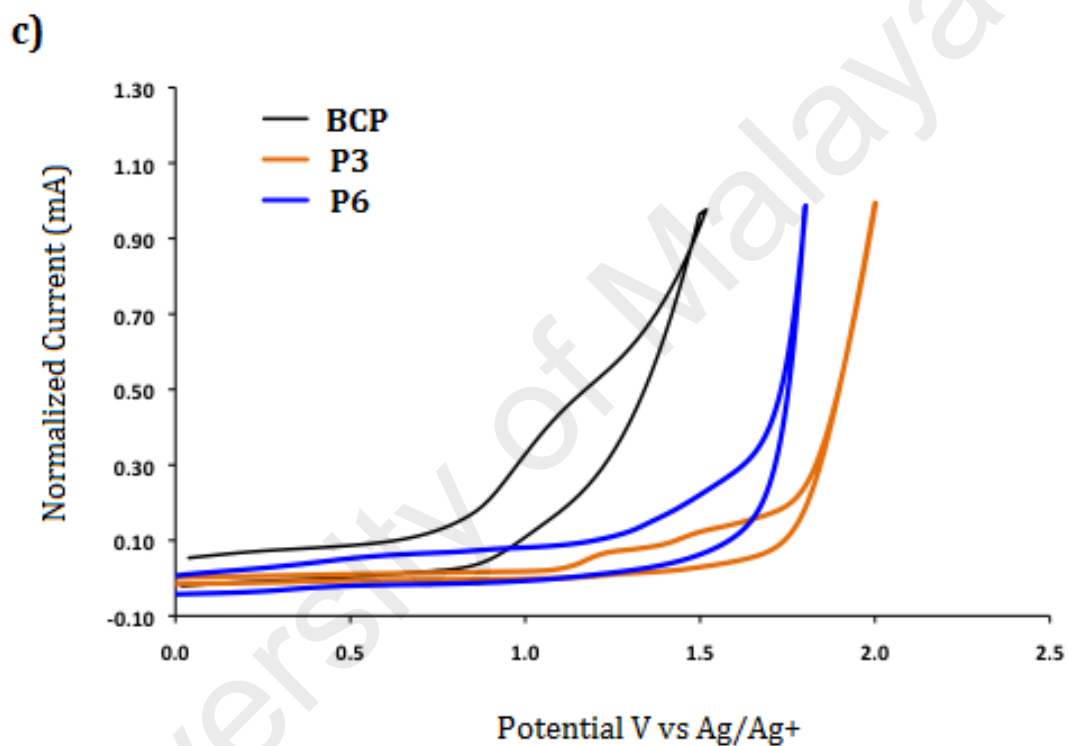


**Figure 3.14:** Cyclic Voltammogram ( $0.1 \text{ Vs}^{-1}$ ) for a) **CBP**, **P1**, **P4**, **P7** and **P9**, b) **CDBP**, **P2**, **P5**, **P8** and **P10**, and c) **BCP**, **P3** and **P6** with ferrocene as an internal standard in DMF -  $0.05 \text{ M } ^n\text{Bu}_4\text{NPF}_6$ .

**Table 3.2: Oxidation potential ( $E_{pa}$ ) and Onset ( $E_{onset}$ ) by Cyclic Voltammetry in DMF (0.05 mol L<sup>-1</sup> n-Bu<sub>4</sub>NPF<sub>6</sub>),<sup>a</sup> and Optical HOMO-LUMO Gaps ( $\Delta E_{opt}$ )<sup>b</sup>**

	$E_{pa}$ [V]	$E_{onset}$ [V]	HOMO <sup>c</sup> [eV]	LUMO <sup>d</sup> [eV]	$\Delta E_{opt}$ <sup>b</sup> [eV]
<b>CBP</b>	+1.04	+0.89	-5.69,-5.63 <sup>e</sup>	-2.25	3.44,3.47 <sup>e</sup>
<b>P1</b>	+1.16	+0.90	-5.70	-2.41	3.29
<b>P4</b>	+1.28	+0.92	-5.72	-2.54	3.18
<b>P7</b>	+1.38	+0.97	-5.77	-2.83	2.94
<b>P9</b>	+1.39	+0.97	-5.77	-3.07	2.70
<b>CDBP</b>	+1.13	+0.90	-5.70,-5.64 <sup>e</sup>	-2.18	3.52,3.51 <sup>e</sup>
<b>P2</b>	+1.41	+1.09	-5.89	-2.56	3.33
<b>P5</b>	+1.38	+1.05	-5.85	-2.69	3.16
<b>P8</b>	+1.42	+1.13	-5.93	-3.00	2.93
<b>P10</b>	+1.47	+1.18	-5.98	-3.65	2.33
<b>BCP</b>	+1.04	+0.82	-5.62	-2.09	3.53
<b>P3</b>	+1.44	+1.14	-5.94	-2.60	3.34
<b>P6</b>	+1.44	+1.19	-5.99	-2.99	3.00

<sup>a</sup>All potential are given versus the Fc<sup>+</sup>/Fc couple used as the external standard; scan rate 100mV s<sup>-1</sup>. <sup>b</sup>The values are obtained from UV/Vis absorption onset  $\lambda_{onset}$ . <sup>c</sup>The values in the parentheses are those deduced from the  $E_{onset}$  values according to the following equation: HOMO = - (4.8 +  $E_{onset}$ ) eV (Chi & Wegner, 2005; Pommerehne *et al.*, 1995). <sup>d</sup>Estimated from the HOMO values and the optical band gap  $\Delta E_{opt}$ . <sup>e</sup>(Schrögel *et al.*, 2011).

The HOMO levels of the compound were estimated from the half-wave potential of the first oxidation relative to the ferrocene group. As the reduction peaks are out of our scan range, the LUMO levels were calculated by adding the optical band gap to the HOMO levels. Table 3.2 lists the values for the HOMO and LUMO levels. In the CV-experiments, by the increment number of thiophene groups at the carbazole moieties in compounds **2.38 (P1)**, **2.39 (P2)**, **2.40 (P3)**, **2.41 (P4)**, **2.42 (P5)**, **2.43 (P6)**, **2.44 (P7)**, **2.45 (P8)**, **2.46 (P9)** and **2.47 (P10)** causes decreases in the HOMO levels -5.70, -5.89, -5.94, -5.72, -5.85, -5.99, -5.77, -5.93, -5.77 and -5.98 eV respectively, compared to -5.69 (**1.4 (CBP)**), -5.70 (**2.36 (CDBP)**) and -5.62 eV (**2.37 (BCP)**) (Dमित *et al.*, 2016). The lower HOMO level indicating that the introduction of thiophene leads to more stabilization of HOMO energy levels (Hlel *et al.*, 2015). LUMO levels of **2.38 (P1)**, **2.39 (P2)**, **2.40 (P3)**, **2.41 (P4)**, **2.42 (P5)**, **2.43 (P6)**, **2.44 (P7)**, **2.45 (P8)**, **2.46 (P9)** and **2.47 (P10)** decreased significantly with the increment number of thiophene where **2.46 (P9)** and **2.47 (P10)** are the lowest LUMO level -3.07 and -3.65 eV respectively, indicating that the compounds improve the electron-accepting ability. A lower LUMO level suggest stronger intramolecular charge transfer interaction which result in lower band gap (Table 3.2) (Lu *et al.*, 2014).

Band gap values ( $\Delta E$ ) decrease significantly with the increment number of thiophene unit on **1.4 (CBP)**, **2.36 (CDBP)** and **2.37 (BCP)**. The HOMO-LUMO gap 2.70 and 2.33 eV of **2.19 (P9)** and **2.20 (P10)** respectively, are the narrowest among these ten new compounds, which is expected to have the most outstanding photophysical properties. Therefore, **1.4 (CBP)**, **2.36 (CDBP)** and **2.37 (BCP)** connecting with thiophenes at 3,6-position of carbazole leads to more stabilization of HOMO and LUMO level energy where the  $\Delta E$  of all compounds significantly reduced.

These considerations show that the energy levels of **1.4 (CBP)**, **2.36 (CDBP)** and **2.37 (BCP)** derivatives can be finely tuned to some extent by the variation of the substitution pattern at 3,6-positions of carbazole.  $\pi$ -Functional small molecules benefit from the fact they are easy to purify, tend to possess high intrinsic carrier mobilities, and are able to self-assemble to achieve long-range order. Particularly, the HOMO levels can be varied. Thus, through these slight variations in the molecular structure, the energy of the different layers in optoelectronic devices can be adjusted to minimize energy barriers within the devices (Schrögel *et al.*, 2011).

University of Malaya



## CHAPTER 4: THEORITICAL CALCULATION

### 4.1 Introduction

Finding the solution of time-independent Schrodinger equation for a molecular system within the Born-Oppenheimer (fixed-nuclei) approximation is the fundamental goal of quantum chemistry. For instance, some properties can be calculated from first principle such as potential energy surfaces, heats of reaction, equilibrium geometries, activation barriers, excitation energies, infrared and Raman Spectra, electric properties such as dipole moments and polarizabilities, and magnetic properties such as chemical shift.

In the development of modern computational quantum chemistry, Gaussian orbital have played a central role since 50 years ago (Boys, 1950). Gaussian orbitals posses a fundamental advantage over the types of one-electron function even though certain basic properties of the electronic wave function, such as the electron-nuclear cusp and the exponential tail could not be satisfied.

In order to preserve conceptual simplicity and afford efficient computation, the quest for the best possible representation of the molecular wave function was related to the history of quantum chemistry. Independent particle models such as Hartree-Fock (HF) or Kohn-Sham density functional theory (DFT) (Dreizler & Gross, 1990; P. Hohenberg & PhysRev, 1965; Parr & Yang, 1989) are built upon a *single* Slater determinant wave function. DFT is now much more accurate than HF which is firmly establish in the literature. Furthermore, DFT is more accurate than the second order Moller-Plesset perturbation theory (MP2), even though they are not systematically but

plenty of evidences have been discovered. Potential comparison are dimensionality, HOMO – LUMO gap, desired accuracy and basis set are the most significant elements which have to be taken into account (Scuseria, 1999).

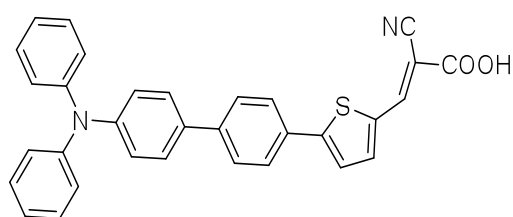
In summary, DFT was effective, efficient and has a great performance for the accurate calculation of molecular properties, structure, and spectra. Density functional method has been gaining popularity in the past decade (Pierre Hohenberg & Kohn, 1964; Kohn & Sham, 1965). Among the ever increasing number of DFT methods, the hybrid functional B3LYP(Devlin *et al.*, 1995; El-Azhary & Suter, 1995; Johnson *et al.*, 1993; Langhoff, 1996; Rauhut & Pulay, 1995; Stephens *et al.*, 1994; Tirado-Rives & Jorgensen, 2008; Wheelless *et al.*, 1995), first developed to study vibrational absorption and circular dichroism, has emerged as good compromise between computational cost, coverage, and accuracy of results. It has become a standard method used to study organic chemistry in the gas phase.

Quantum chemical calculation is popular tool for the prediction of properties of molecules and materials in their ground and excited states. The elucidation of chemical and photochemical reaction pathways and the interpretation of experimental results. Especially density functional theory (DFT) calculations have become a standard tool in the development of new materials for organic electronic. Computational chemistry can help to access the feasibility of reaction pathways that molecules can undergo. Energies and geometries of the participating electronics states can be predicted thus contribute to the understanding of charge and exciton induced processes in the organic materials (Treboux *et al.*, 2008).

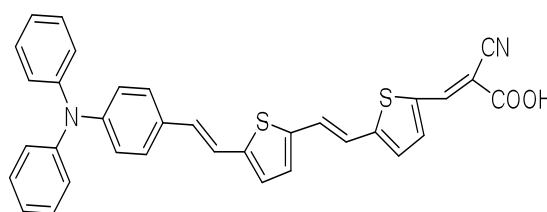
However, some major failures found in DFT calculations such as underestimate the barriers of chemical reactions, the band gaps of materials, the energies of dissociating molecular ions and charge transfer excitation energies. Furthermore, binding energies of charge transfer complexes were overestimate and the response to an electric field in molecules and materials. Surprisingly, all of these diverse issues share the same root, the delocalization error of approximate functionals, due to the dominating Coulomb term that pushes electrons apart (Cohen *et al.*, 2008).

## 4.2 Literature Review

Licheng Sun *et al.* (2007) tuning HOMO and LUMO energy levels of organic chromophores for dye sensitized solar cells by varying the conjugation between the triphenylamine donor and cyanoacetic acid acceptor (**4.1** and **4.2**) (Figure 4.1). The HOMO orbital is delocalized over the entire molecule. The LUMO orbital also has  $\pi$ -character, electron density has been shifted toward the other end of the molecule indicates that the dipole moment should be considerably larger in the first excited state compared to the ground state. Consequently, the absorption wavelength increases (red shift) with linker length in agreement with experimental absorption spectra.



**4.1**



**4.2**

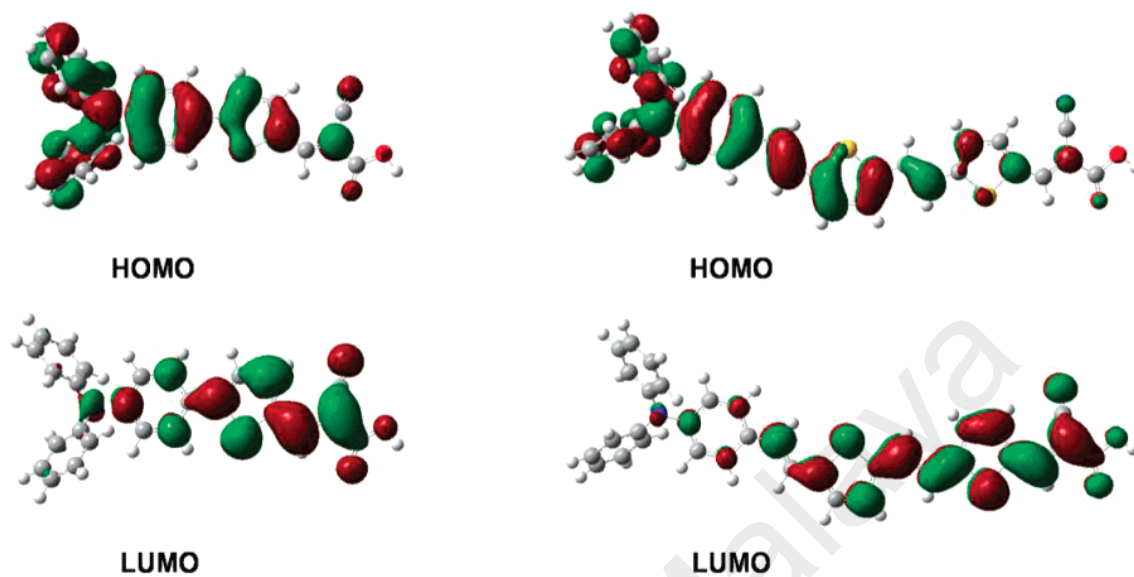
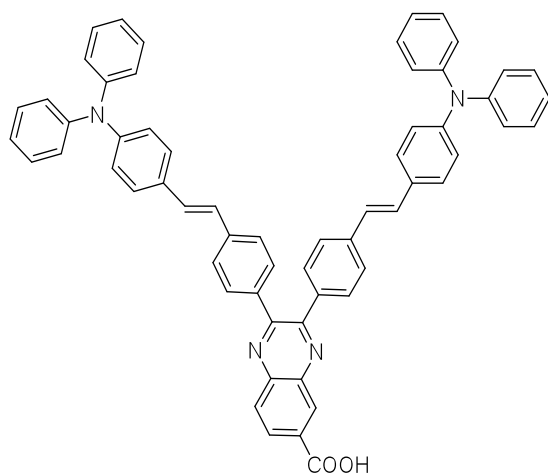
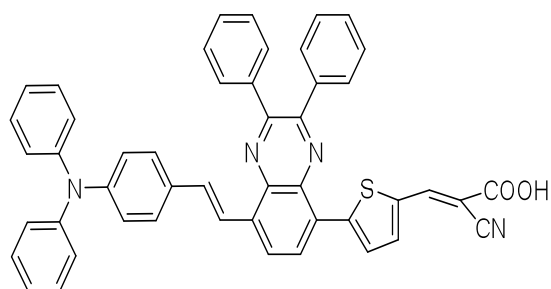


**Figure 4.1:** Plots of the HOMO and LUMO of compounds **4.1** and **4.2**.

Jong-Beom Baek et al.(Chang *et al.*, 2011) synthesized quinoxaline-based organic sensitizers using vertical (**4.3**) and horizontal (**4.4**) conjugation between an electron-donating triphenylamine unit and electron-accepting quinoxaline unit. In both dyes, the HOMO shows the highest electron density near the electron-donating triphenylamine moieties, while in LUMO, it is located near electron-withdrawing quinoxaline and cyanoacrylic acid units (Figure 4.2). Thus the efficient photoexcited electron transfer from the LUMO to the conduction band of TiO<sub>2</sub> is expected through the close position of LUMO to the anchoring group in the excited state.(Hagberg *et al.*, 2006)



4.3



4.4

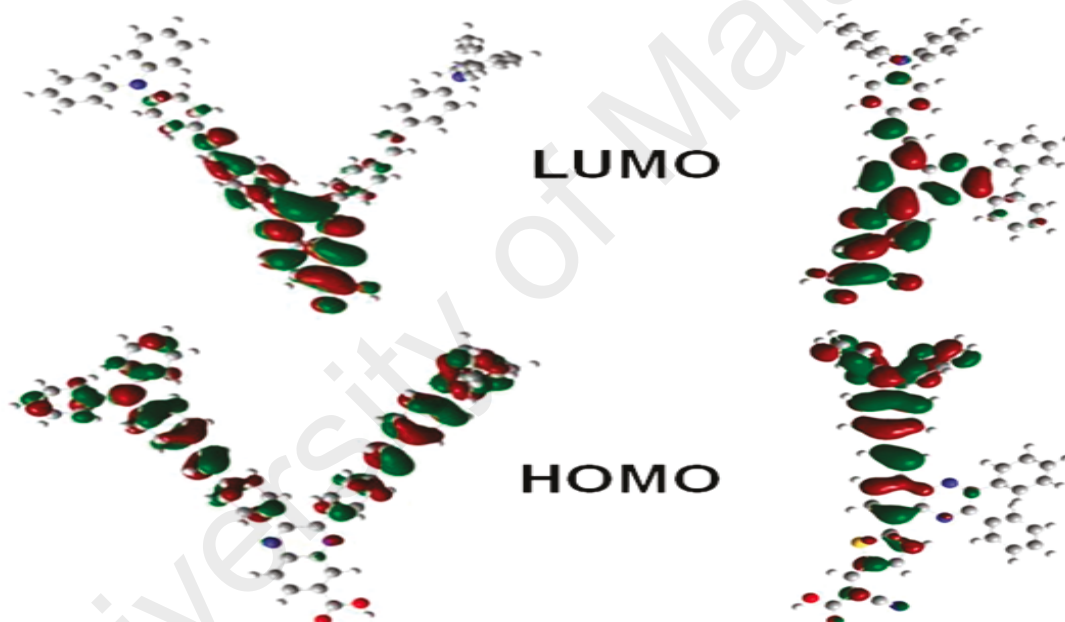


**Figure 4.2:** Plots of the HOMO and LUMO of compounds 4.3 and 4.4.

Kim *et al.* (2007) report two new organic dyes (4.5 and 4.6) containing [bis(9,9-dimethylfluorene-2-yl)amino]benzene as electron donor and cyano acrylic acid as electron acceptor bridged by thiophene-vinylene units. The HOMO is delocalized over pi conjugated system via the amino phenyl unit, and LUMO is delocalized over the cyanoacrylic unit through methine units (Figure 4.3). Examination of the HOMO and

LUMO of **4.5** and **4.6** indicates that HOMO–LUMO excitation moved the electron distribution from the bis-dimethylfluorenyl amino phenyl unit to the vinylene cyanoacrylic acid group. The change in electron distribution induced by photo-excitation results in an efficient charge separation.

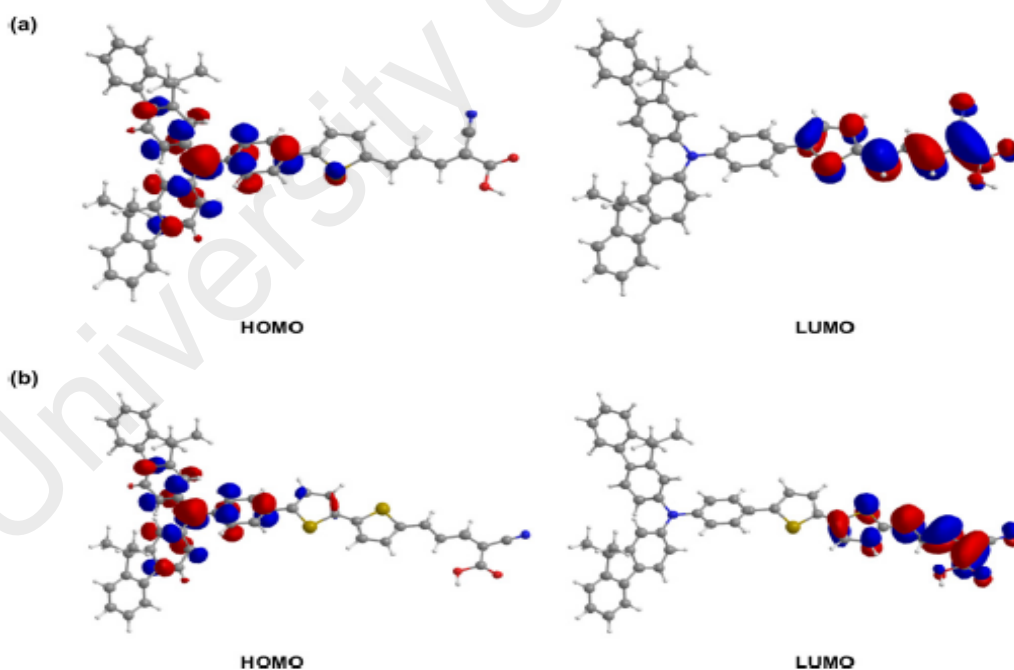
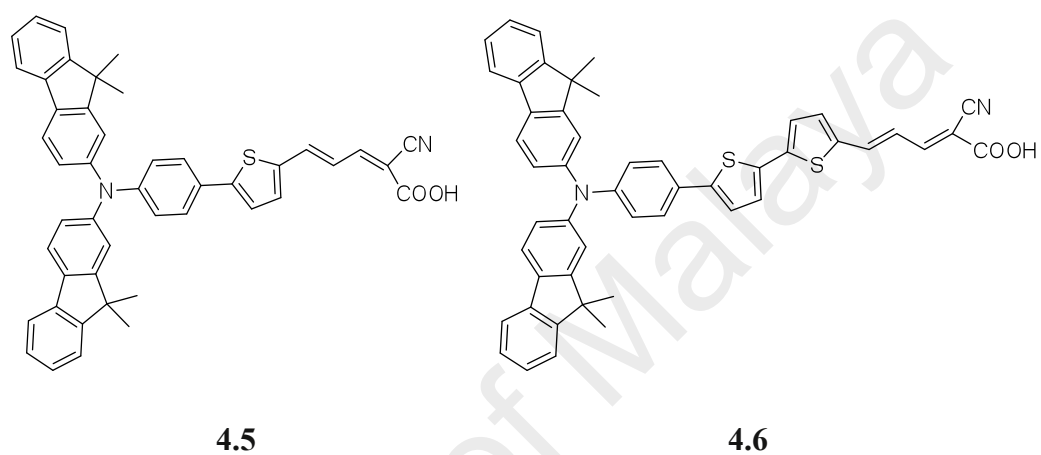


**Figure 4.3:** Plots of the HOMO and LUMO of compounds a) **4.5** and b) **4.6**.

Tan *et al.* (2014) synthesized four organic photosensitizers (**4.7**, **4.8**, **4.9** and **4.10**) incorporating 3,6-diodocarbazole units as the electron donor, a benzene/thiophene or oligothiophene moiety as the conjugated spacer and 2-cyanoacrylic acid as the electron acceptor have been synthesized. Clearly, the HOMOs of these compounds are delocalized over the carbazole pi system with the highest electron density located at the nitrogen atoms of the carbazole moiety. It can be seen that the HOMOs in **4.8** are more delocalized than those in **4.7**, due to the better coplanarity in conjugated pathway (Figure 4.4). The LUMOs are located in the anchoring group through the pi bridge constituted by the benzene and/or thiophene moieties. Thus, the HOMO-LUMO excitation induced by light irradiation could move the electron distribution from the carbazole segment to the anchoring unit through the conjugation pathway.

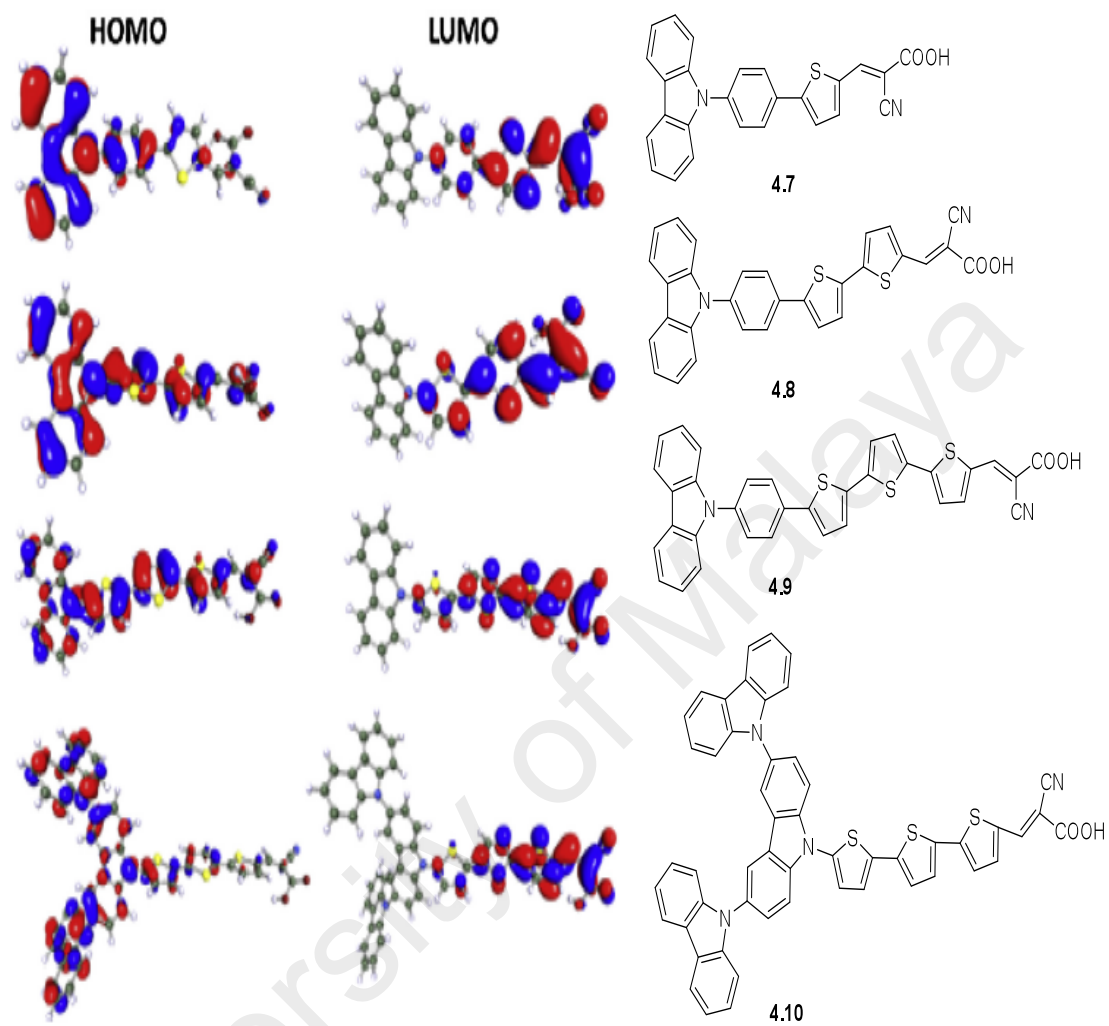


**Figure 4.4.** Plots of the HOMO and LUMO of compounds **4.7**, **4.8**, **4.9** and **4.10**.



### 4.3 Objective

An efficient method to obtain conjugated compounds is based on the strategy of donor – acceptor by combining  $\pi$ -electron-rich (donor) and  $\pi$ -electron-deficient (acceptor) conjugated moieties. Choosing appropriate donor and acceptor moieties allows control of the band gap and energy levels of conjugated compounds. Energy level of the highest occupied molecular orbital (HOMO) determine by donor and the lowest unoccupied molecular orbital (LUMO) determine by the acceptor.

However, the performance of the photovoltaic cells is considerably limited by relatively large band gaps, which are not yet optimized with respect to the solar spectrum. Therefore, the development of low band gap organic compound becomes very important for better harvesting of the solar spectrum, especially in the red and near-infrared ranges, which leads to a possible enhancement in the photovoltaic devices.

To get further insight on these new carbazole-thiophene derivatives compounds. Here, we calculated the geometry and electron distribution structure of HOMO and LUMO of these compounds by using DFT method. Our aim is to provide a theoretical explanation to the relationship between the electronic and the molecular structure.

#### 4.4 Results and Discussion

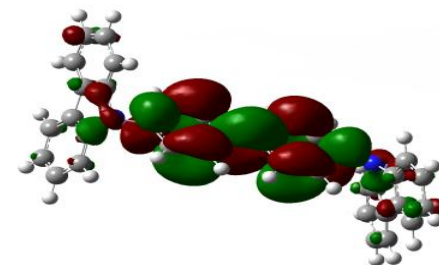
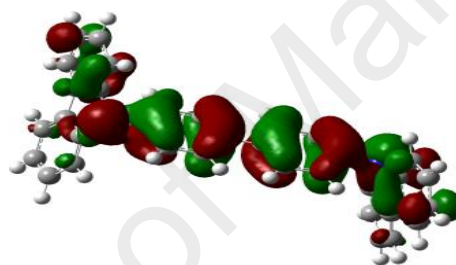
To obtain further insight into the electronic properties on the effect of the addition donor group (on carbazole scaffold), **1.4 (CBP)**, **2.36 (CDBP)**, **2.37 (BCP)**, **2.38 (P1)**, **2.39 (P2)**, **2.40 (P3)**, **2.41 (P4)**, **2.42 (P5)**, **2.43 (P6)**, **2.44 (P7)**, **2.45 (P8)**, **2.46 (P9)** and **2.47 (P10)** compounds have been theoretically modeled; the optimized structures are shown in Figure 4.5. We performed geometrical optimization and frontier molecular orbital calculations. All of the computations were performed using the GAUSSIAN 09W software package (Appendix B). The images presented in the figures were generated using ChemDraw and GaussView visualization programs. The geometries of the compounds in their ground state were optimized employing the Density Functional Theory (DFT) method with restricted Becke's three parameter hybrid functional and the nonlocal Lee, Yang and Parr gradient-corrected correlation functional B3LYP (Acar *et al.*, 2003; Lee *et al.*, 1988) combined with the 6-31G functional basis set. This method has been found to be an accurate formalism for calculating the characteristic parameters of many molecular systems (Tretiak & Mukamel, 2002).

University of Malaya

HOMO

LUMO

1.4 (CBP)



2.38 (P1)

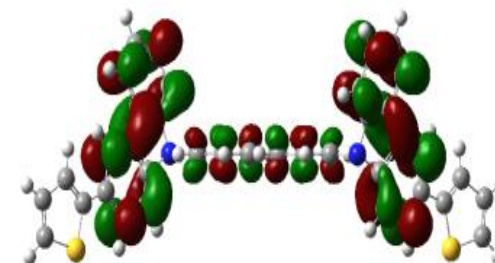
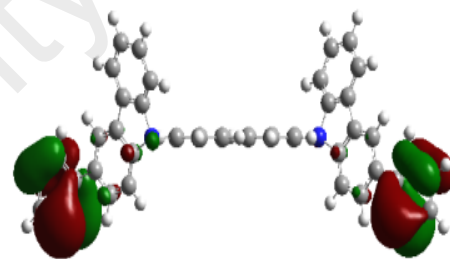
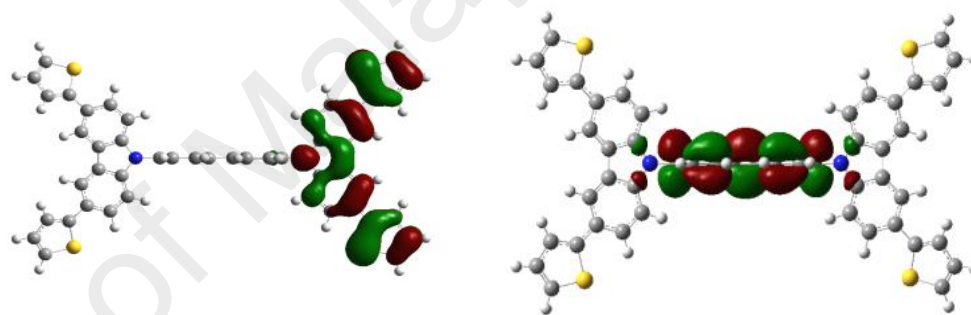


Figure 4.5, continued.

HOMO

LUMO

2.41 (P4)



2.44 (P7)

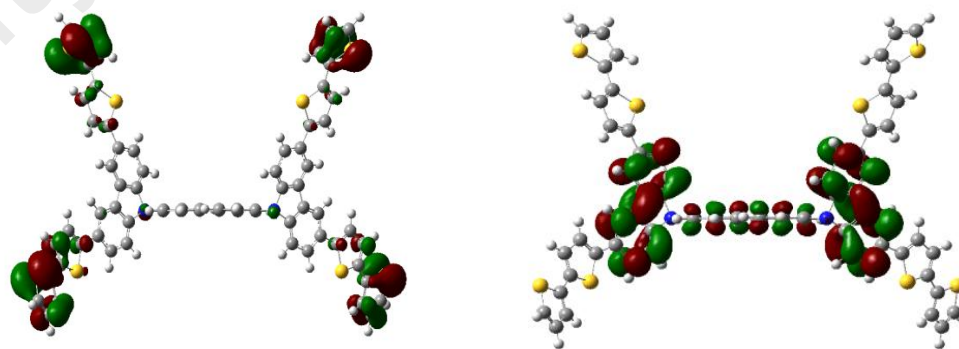
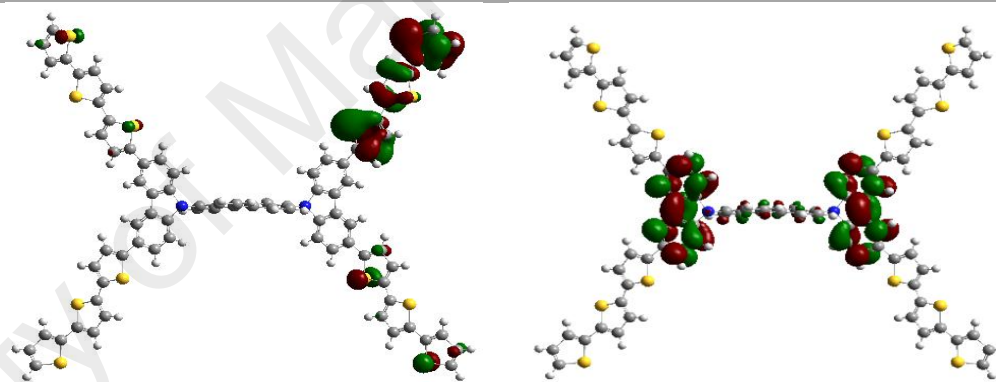


Figure 4.5, continued.

HOMO

LUMO

2.46 (P9)



2.36 (CDBP)

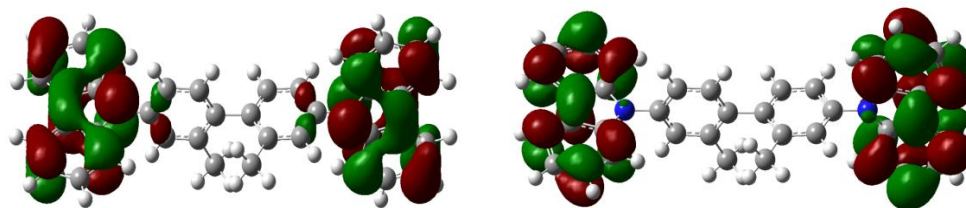
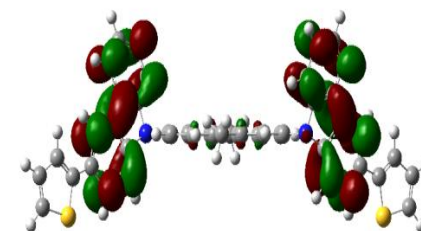
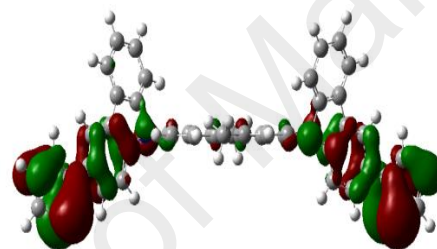


Figure 4.5, continued.

HOMO

LUMO

2.39 (P2)



2.42 (P5)

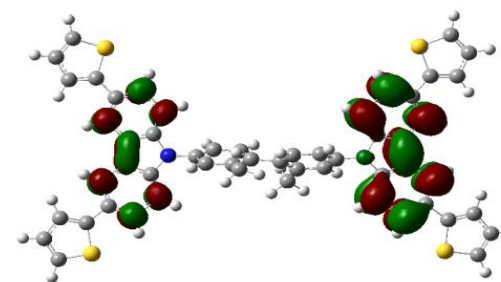
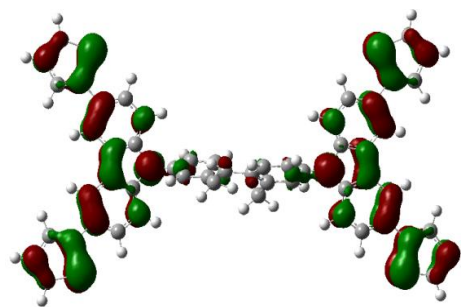
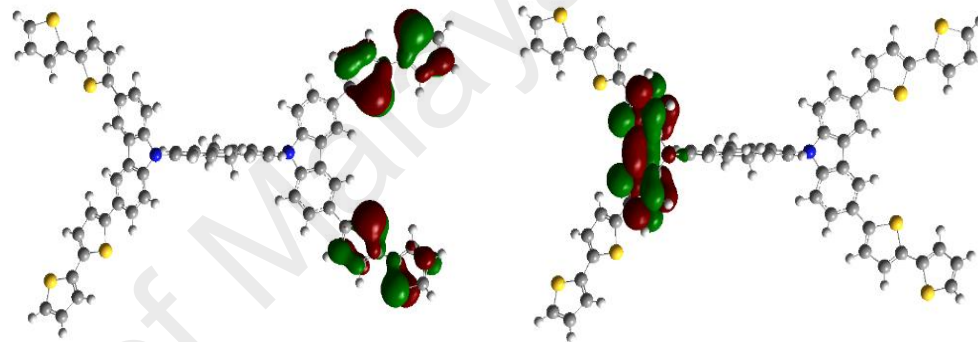


Figure 4.5, continued.

HOMO

LUMO

2.45 (P8)



2.47 (P10)

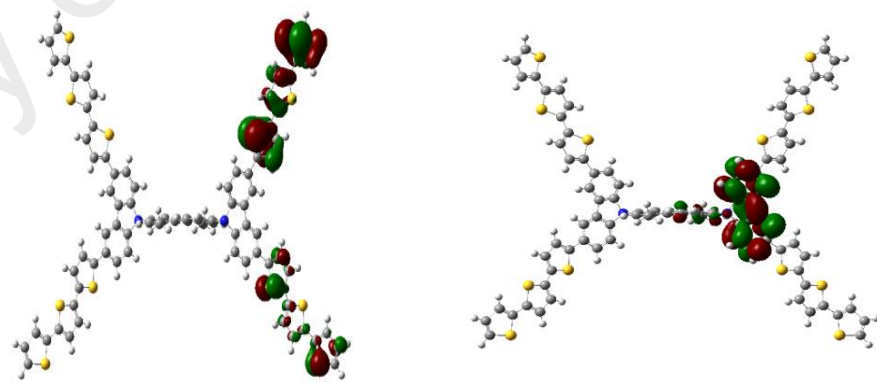




Figure 4.5, continued.

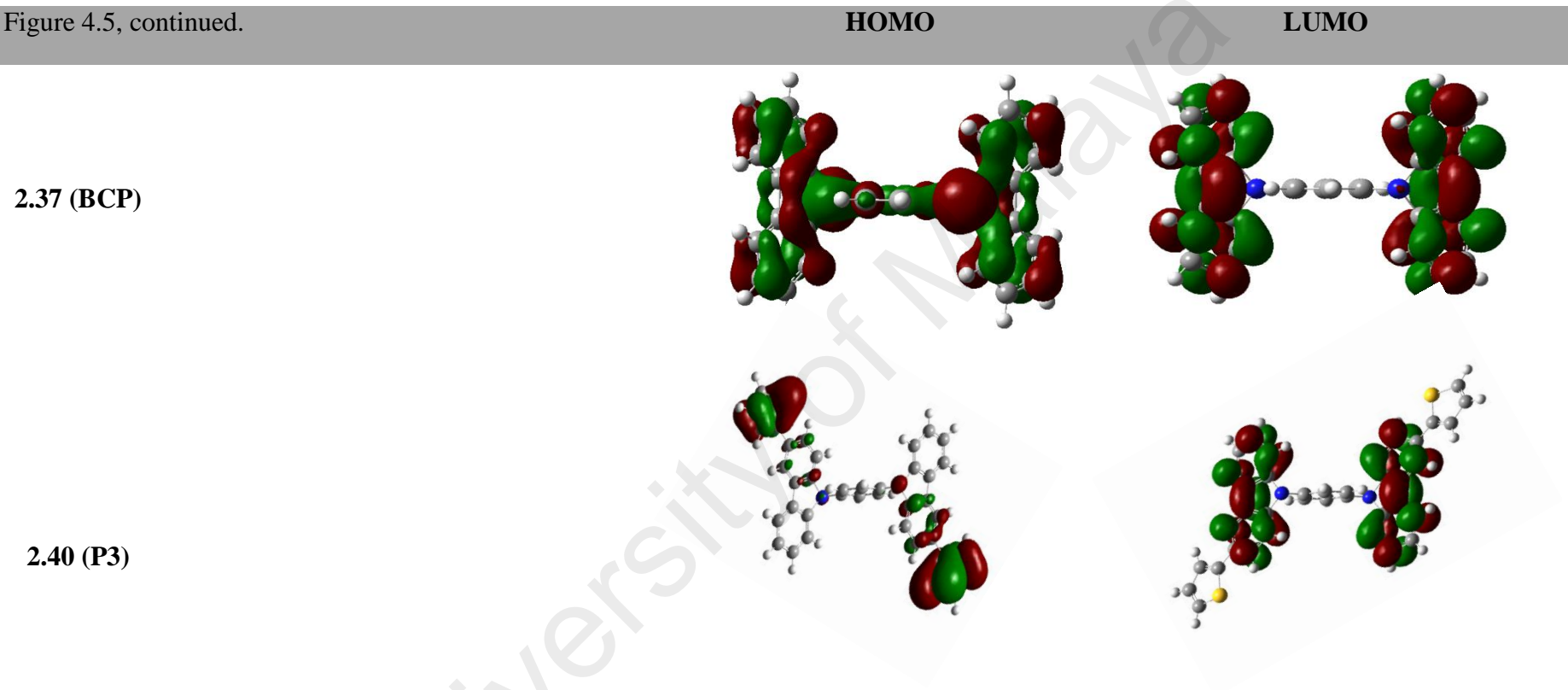
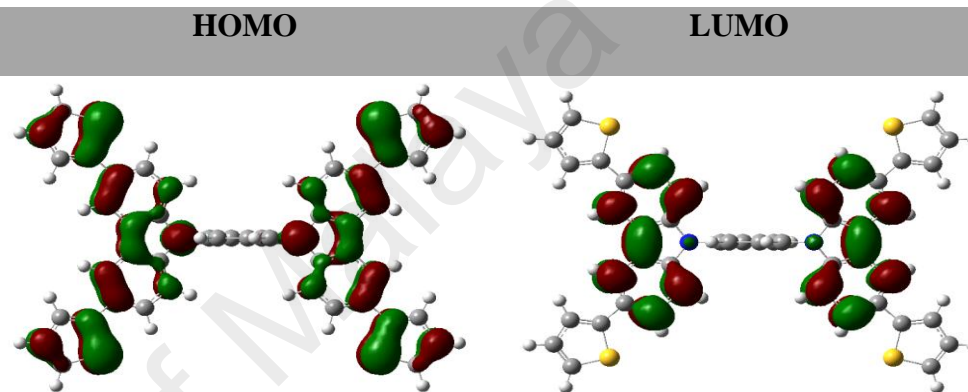


Figure 4.5, continued.

2.43 (P6)



**Figure 4.5:** HOMO and LUMO frontier molecular orbitals of compounds **1.4 (CBP)**, **2.36 (CDBP)**, **2.37 (BCP)** and **2.38 (P1) - 2.47 (P10)** that were calculated in vacuo at B3LYP/6-31G level of approximation.

The contour plots of the HOMO and LUMO determined at the DFT/B3LYP/6-31G level for all of the compounds are shown in Figure 4.5. The HOMO is expected to lie on the electron-rich groups, affording an effective hole-transporting property. The energy of the HOMO and LUMO orbitals is an important molecularly correlated parameter. The molecules with lower HOMO orbital energy levels have weaker electron donating abilities. Moreover, the electronic density distribution in these orbitals permits prediction of the most probable sites of attack by reactive agents in the molecules investigated.

We note that all compounds have a similar structure. From the HOMO and LUMO orbitals shown in Figure 4.5, the HOMO is predominantly determined by the carbazole groups for **1.4 (CBP)**, **2.36 (CDBP)** and **2.37 (BCP)**, whereas for **2.38 (P1)**, **2.39 (P2)**, **2.40 (P3)**, **2.41 (P4)**, **2.42 (P5)**, **2.43 (P6)**, **2.44 (P7)**, **2.45 (P8)**, **2.46 (P9)** and **2.47 (P10)** the HOMO are mainly determined by the thiophene groups and their  $\pi$ -bonding orbitals, although the carbazoles also exert their influence; however, the LUMOs are predominantly localized on and primarily determined by the carbazole and biphenyl core groups and their  $\pi^*$ -bonding orbitals (Damit *et al.*, 2016). The carbazole plane is  $47^\circ$  twisted with respect to the biphenyl ring bonded at N9-position (Duvva *et al.*, 2015). The strong deviation from the planarity between the carbazole donor and biphenyl, dimethylbiphenyl and phenyl bridge hinders the conjugation along the compound backbone, thus leading to an increase of the band gap and less extended absorption spectra (refer Figure 3.7 (b)-absorption spectra) toward the visible region (compounds **2.38 (P1)**, **2.39 (P2)**, **2.40 (P3)**).

Compounds **2.15 (P5)** and **2.16 (P6)** demonstrate an overlap between HOMO and LUMO on the acceptor carbazole group, which facilitates the charge transfer from the four electron-donating thiophene groups to the two electron-withdrawing carbazoles (Lu *et al.*, 2014). In addition to the stronger electron-donating ability of the thiophene, compounds **2.14 (P4)**, **2.15 (P5)**, **2.16 (P6)**, **2.17 (P7)**, **2.18 (P8)**, **2.19 (P9)** and **2.20 (P10)**, exhibit more planar structures and more effective  $\pi$ -conjugation, which result in strengthened intra-molecular interactions and lower band gaps. These results are consistent with the experimentally observed absorption properties of the resulting compound (refer Figure 3.6-absorption spectra).

In fact, for N-carbazole end-capped- $\pi$ -conjugated molecules, the introduction of carbazole moieties at the terminal group of the conjugated backbone would result in a less planar molecule due to the planar character of carbazole groups. This fact is manifested by a perpendicular orientation to the backbone chain, which decreases the bond length between the core and the carbazole group. This decrease is attributed to the size and the electro-negativity of the nitrogen atom. These large dihedral angles could minimize the degree of  $\pi$ -aggregation and thus improve the photoluminescence intensity (Hlel *et al.*, 2015). Particularly, the 3,6-disubstituted structures present high dipole moments, indicating the presence of a significant charge transfer. This effect is more pronounced in the case of D-A structures **2.38 (P1)**, **2.39 (P2)**, **2.40 (P3)**, **2.41 (P4)**, **2.42 (P5)**, **2.43 (P6)**, **2.44 (P7)**, **2.45 (P8)**, **2.46 (P9)** and **2.47 (P10)** (Hlel *et al.*, 2015). It reveals that the oligothiophenes is essentially coplanar with carbazole group. There are effective electron separations between HOMO and LUMO of these dyes induced by light irradiation.

## CHAPTER 5: EXPERIMENTAL DETAILS

### 5.1 Materials

All reagents used were reagent grade products obtained from either Aldrich or Merck with highest purity and used without further purification unless otherwise stated. The purity of some reagents used is shown below.

- i. Acetone-D6 (Merck  $\geq$  99.8%)
- ii. Benzene (Merck  $\geq$  98%)
- iii. Biphenyl (Merck  $\geq$  99.8%)
- iv. 2,2-Bithiopheneboronic acid (Aldrich  $\geq$  98%)
- v. Carbazole (Merck  $\geq$  98%)
- vi. Chloroform-D6 (Merck  $\geq$  99.8%)
- vii. Chloroform AR grade (Merck  $\geq$  98%)
- viii. Concentrated Sulfuric Acid (Merck  $\geq$  98%)
- ix. Copper powder (Aldrich  $\geq$  98%)
- x. 18-Crown-6 (Aldrich  $\geq$  98%)
- xi. Dichloromethane (Merck  $\geq$  98%)
- xii. 1,2-Dichlorobenzene (Merck  $\geq$  98%)
- xiii. 1,4-Diiodobenzene (Aldrich  $\geq$  98%)
- xiv. 1,4-Dioxane (Merck  $\geq$  98%)
- xv. 1,3-Dimethylbiphenyl (Aldrich  $\geq$  98%)
- xvi. Ethyl Acetate (Merck  $\geq$  98%)
- xvii. Glacial Acetic acid (Merck)
- xviii. Hexane (Merck  $\geq$  98%)

- xix. 2,5-Hexylthiopheneboronic acid (Aldrich  $\geq$  98%)
- xx. Iodine Resublimed (Merck  $\geq$  98%)
- xxi. Iodobenzene (Aldrich  $\geq$  98%)
- xxii. Nitrogen 99.99% purity
- xxiii. Potassium Carbonate (Merck  $\geq$  98%)
- xxiv. Sodium Hydroxide (Merck  $\geq$  98%)
- xxv. Tetrakis(triphenylphosphine)palladium (0) (Aldrich  $\geq$  98%)
- xxvi. Tetrahydrofuran (Merck  $\geq$  98%)
- xxvii. 2-Thiopheneboronic acid (Aldrich  $\geq$  98%)
- xxviii. 2,5-Hexylthiopheneboronic acid (Aldrich  $\geq$  98%)
- xxix. Terthiopheneboronic acid (Aldrich  $\geq$  98%)
- xxx. Water - high purity

University of Malaya

## 5.2 General Procedures

### 5.2.1 Synthesis and Characterization

All chemicals were commercially available and used as received unless otherwise specified.  $^1\text{H}$  NMR (400 and 600 MHz) and  $^{13}\text{C}$  NMR (100 MHz) spectra were recorded using a Spectrometer (Bruker FT-NMR AVANCE III 400 and 600 MHz). Chemical shifts are reported in parts per million (ppm) relative to the residual solvent protons ( $^1\text{H}$ ) or the solvent carbon ( $^{13}\text{C}$ ) as internal standards. The Mass spectra and high-resolution mass spectra (HRMS) were obtained using either electrospray ionization (ESI), atmospheric pressure chemical ionization (APCI) techniques or MALDI-TOF. Melting point was measured using Differential Scanning Calorimetry (DSC) (TA-instrument DSC Q20).

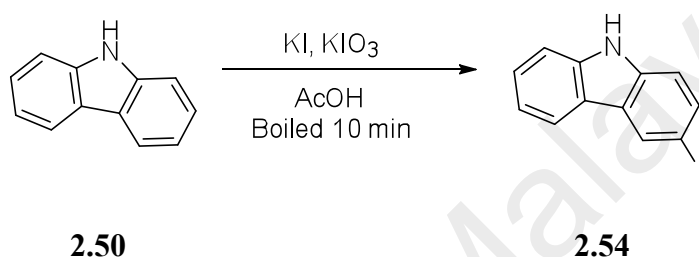
### 5.2.2 Physical and Theoretical Properties Analysis

UV-Vis spectra and fluorescence spectral measurements of all samples were performed in DMF Solution at room temperature in a standard 1 cm quartz cell using Shimadzu UV-1601 UV-Vis Spectrophotometer and Cary Eclipse Fluorescence Spectrophotometer, respectively. Cyclic voltammetry (CV) were carried out at room temperature using Autolab PGSTAT101 with NOVA software. The samples were examined employing three conventional working electrodes as glassy carbon, counter electrode was platinum electrodes and  $\text{Ag}/\text{Ag}^+$  (0.10 M  $\text{AgNO}_3$  in DMF) as reference electrode. The electrochemical potential was calibrated against  $\text{Fc}/\text{Fc}^+$ . All samples were investigated in a DMF solution containing  $0.05 \text{ mol L}^{-1}$  of  $\text{n-Bu}_4\text{NP}_6$  as supporting electrolyte. Theoretical Density Functional Theory (DFT) calculation was performed

using GAUSSIAN 09W software package using the B3LYP method and 6-31G basis set.

### 5.3 Details Procedure for the synthesis of Starting Materials

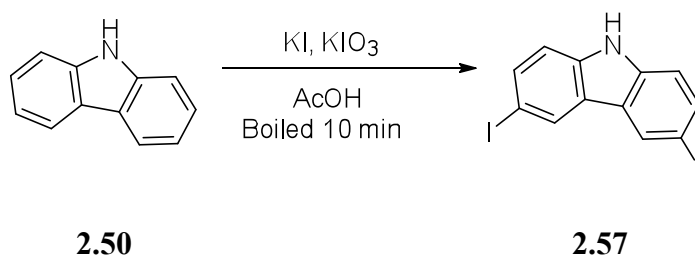
#### 5.3.1 Synthesis of compound 2.54 (3-Iodocarbazole)



Carbazole **2.50** (16.7 g, 101 mmol) was dissolved in boiling glacial acetic acid (250 ml), and KI (11.73 g, 135 mmol) was added. The solution was cooled, ground potassium iodate (23.42 g, 150 mmol) was added, and the mixture was boiled until it acquired a clear straw-colored tint (10 min). The hot solution was decanted from the undissolved potassium iodate, and it was allowed to cool to 45 °C. The faintly brown plates were rapidly filtered off and recrystallized from alcohol, and the solution was allowed to cool to 45 °C. The faintly brown plates were rapidly filtered off and recrystallized from ethanol, the solution was allowed to cool to 45 °C and filtered, yielding 9.73 g (47 %) of **2.54** as a brown solid (Wu *et al.*, 2011); mp 202 °C (mp<sup>lit.</sup> 202 °C) (Tucker, 1926), <sup>1</sup>H NMR (600 MHz, CDCl<sub>3</sub>) δ ppm 8.41 (s, 1 H), 8.11 (br. s., 1 H), 8.04 (d, *J*=7.70 Hz, 1 H), 7.68 (dd, *J*=8.53, 1.74 Hz, 1 H), 7.42 - 7.49 (m, 2 H), 7.22 - 7.28 (m, 2 H); <sup>13</sup>C NMR (100 MHz, CDCl<sub>3</sub>) δ ppm 139.5, 138.6, 134.1, 129.2, 126.6, 125.9, 122.1, 120.5, 119.9, 112.4, 112.6, 110.7. Maldi-Tof MS: *m/z* calcd for [M<sup>+</sup>] = C<sub>12</sub>H<sub>8</sub>IN 292.970; found 292.971.

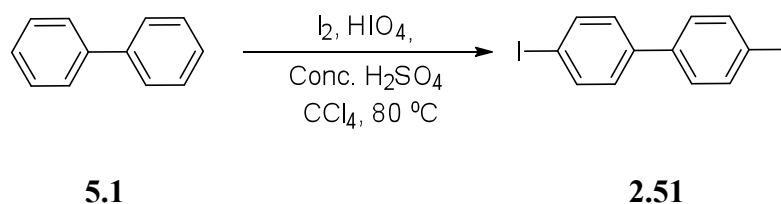


### 5.3.2 Synthesis of compound 2.57 (3,6-Diiodocarbazole)



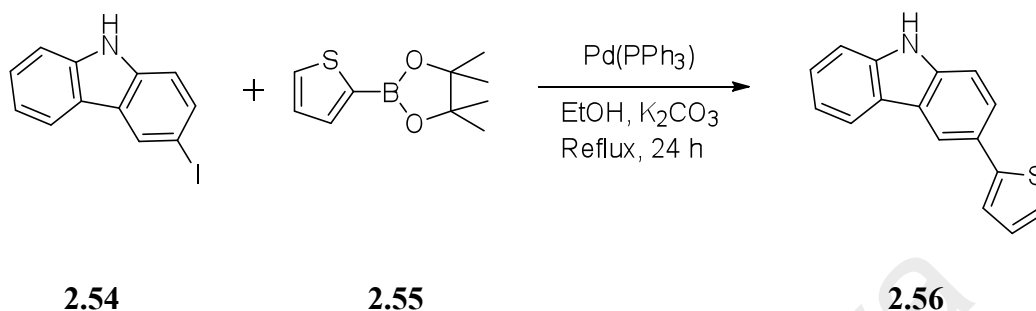
Carbazole **2.50** (12.23 g, 73 mmol) was dissolved in boiling glacial acetic acid (300 ml), and KI (15.84 g, 95 mmol) was added. The solution was cooled, ground potassium iodate (23.42 g, 150 mmol) was added, and the mixture was then boiled until it acquired a clear straw-colored tint (10 min). The hot solution was decanted from the undissolved potassium iodate, and it was allowed to cool to 45 °C. The faintly brown plates were rapidly filtered off and recrystallized from alcohol, and the solution was allowed to cool to 45 °C and filtered, yielding 5.75 g of **2.57** as a brown solid (18.79 %) (Tucker, 1926): mp 202 °C (mp<sup>lit.</sup> 202 °C), <sup>1</sup>H NMR (400 MHz, CDCl<sub>3</sub>) δ ppm 8.34 (s, 2 H), 8.16 (br. s., 1 H), 7.70 (dd, *J*=8.53, 1.63 Hz, 2 H), 7.23 (d, *J*=8.41 Hz, 2 H); <sup>13</sup>C NMR (100 MHz, CDCl<sub>3</sub>) δ ppm 138.5, 134.8, 129.4, 124.5, 112.7 and 82.5. Maldi-Tof MS: *m/z* calcd for [M<sup>+</sup>] = C<sub>12</sub>H<sub>7</sub>I<sub>2</sub>N 418.867; found 418.868.

### 5.3.3 Synthesis of compound 2.51 (4,4-Diiodobiphenyl)



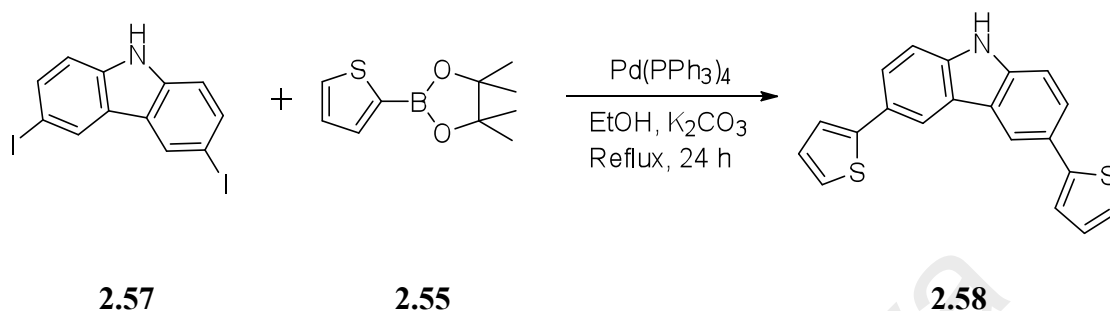
A mixture of biphenyl **5.1** (4.62 g, 30 mmol), acetic acid 30 ml, water 3 ml, concentrated sulfuric acid 3 ml, iodine 8.37 g, periodic acid (3.75 g, 16.5 mmol) and carbon tetrachloride (CCl<sub>4</sub>, 4 ml) was stirred and maintained at 80 °C. for 4 hours. Afterwards, the slurry product was cooled to room temperature, poured into water and extracted with dichloromethane. The combined dark purple organic layer was decolorized with sodium sulfite, dried with anhydrous sodium sulfate, filtered and evaporated to dryness yielding 3.99 g of **2.51** pale yellow shiny powder (33 %): mp 200-202 °C (mp<sup>lit.</sup> 200-201 °C) (Tucker, 1926). <sup>1</sup>H NMR (400 MHz, CDCl<sub>3</sub>) δ ppm 7.78 (d, *J*=8.56 Hz, 4 H) 7.30 (d, *J*=8.56 Hz, 4 H); <sup>13</sup>C NMR (100 MHz, CDCl<sub>3</sub>) δ 139.6, 137.7, 128.7, 93.5. HR-ESI-MS: *m/z* calcd for [M+H]<sup>+</sup> = C<sub>12</sub>H<sub>8</sub>I<sub>2</sub> 406.8795; found 406.8793.

### 5.3.4 Synthesis of compound 2.56 (3-(Thiophen-2-yl)carbazole)



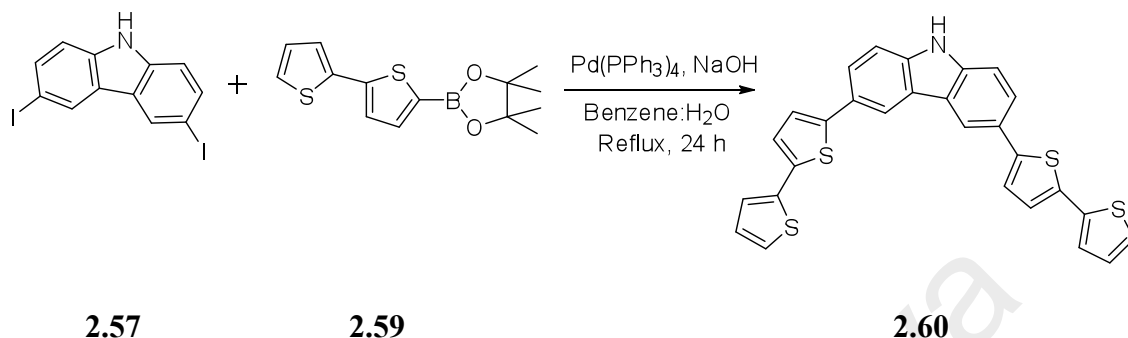
3-Iodocarbazole **2.54** (2.4 g, 8.0 mmol) was dissolved in 80 ml absolute ethanol, a few drops of dry THF, and 1.2 eq thiophene-2-boronic acid pinacol ester **2.55** (2.02 g, 9.6 mmol) was added to the solution. Then 2 eq  $K_2CO_3$  (2.21 g, 16.0 mmol) added to the mixture. Bring mixture to reflux for 10 minutes, when the solution was homogenous, add required quantity of catalyst 0.5 mol %  $Pd(PPh_3)_4$  (0.05 g, 0.04 mmol) into reaction mixture and start refluxed for 24 hours under nitrogen. White precipitates appeared in the reaction mixture and filter the residue. Take filtrate and washed with DCM (3 x 25 ml) and water (2 x 15ml). The organic layer was dried with  $Na_2SO_4$  and evaporated to dryness give yellowish powder. Recrystallization from hexane and dichloromethane give **2.56** as off-white solid (1.60 g, 80%) (Wu *et al.*, 2011): mp 196 °C; mp lit. 197 °C (D. Kim *et al.*, 2007).  $^1H$  NMR (600 MHz,  $CDCl_3$ )  $\delta$  ppm 8.32 (s, 1 H), 8.14 (d,  $J=7.79$  Hz, 1 H), 8.10 (br. s., 1 H), 7.72 (d,  $J=8.34$  Hz, 1 H), 7.42 - 7.50 (m, 4 H), 7.37 (d,  $J=3.48$  Hz, 1 H), 7.29 - 7.33 (m, 1 H), 7.13 (ddd,  $J=5.02, 3.55, 1.42$  Hz, 1 H);  $^{13}C$  NMR (100 MHz,  $CDCl_3$ )  $\delta$  ppm 145.7, 140.0, 139.0, 128.0, 126.4, 126.2, 124.6, 123.8, 123.7, 123.3, 122.2, 120.5, 119.7, 117.9, 110.9, 110.8; HR-ESI-MS  $m/z$  calcd for  $[M+H]^+ = C_{16}H_{11}NS$  250.0692, found 250.0690.

### 5.3.5 Synthesis of compound 2.58 (3,6-di(thiophen-2-yl)-9H-carbazole)



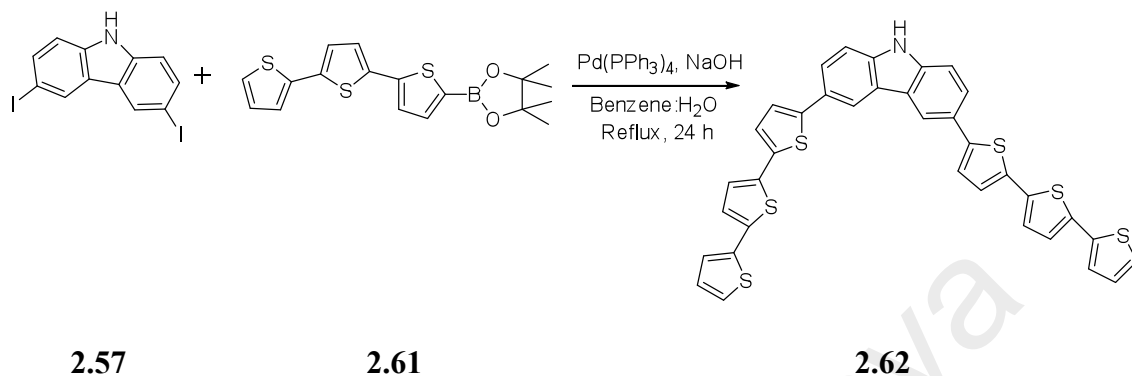
3,6-Diiodocarbazole **2.57** (1.5 g, 3.6 mmol) was dissolved in 36 ml absolute ethanol, a few drops of dry THF, and 2.1 eq thiophene-2-boronic acid pinacol ester **2.55** (1.80 g, 7.5 mmol) was added to the solution. Then 2 eq  $K_2CO_3$  (1.0 g, 7.2 mmol) was added to the mixture. Bring mixture to reflux for 10 minutes, when the solution was homogenous, add required quantity of catalyst 0.5 mol %  $Pd(PPh_3)_4$  (0.21 g, 0.02 mmol) into reaction mixture and start reflux for 24 hours under nitrogen. White precipitates appeared in the reaction mixture and filter the residue. Take filtrate and wash with DCM (3 x 25 ml) and water (2 x 15 ml). The organic layer was dried with  $Na_2SO_4$  and evaporated to dryness give **2.58** as yellowish powder. Recrystallization from hexane and dichloromethane give **2.58** as white solid (0.70 g, 59 %): mp 127 °C.  $^1H$  NMR (600 MHz,  $CDCl_3$ )  $\delta$  ppm 8.35 (s, 2 H), 8.13 (br. s., 1 H), 7.73 (dd,  $J=8.39$ , 1.70 Hz, 2 H), 7.44 (d,  $J=8.53$  Hz, 2 H), 7.38 (d,  $J=3.48$  Hz, 2 H), 7.30 (d,  $J=5.04$  Hz, 2 H), 7.12 - 7.16 (m, 2 H);  $^{13}C$  NMR (100 MHz,  $CDCl_3$ )  $\delta$  ppm 145.5, 139.4, 128.0, 126.7, 124.9, 123.9, 123.8, 122.3, 118.0, 111.1. HR-ESI-MS  $m/z$  calcd for  $[M+H]^+ = C_{20}H_{13}NS_2$  332.0569; found 332.0569.

### 5.3.6 Synthesis of compound **2.60** (3,6-di([2,2'-bithiophen]-5-yl)-9H-carbazole)



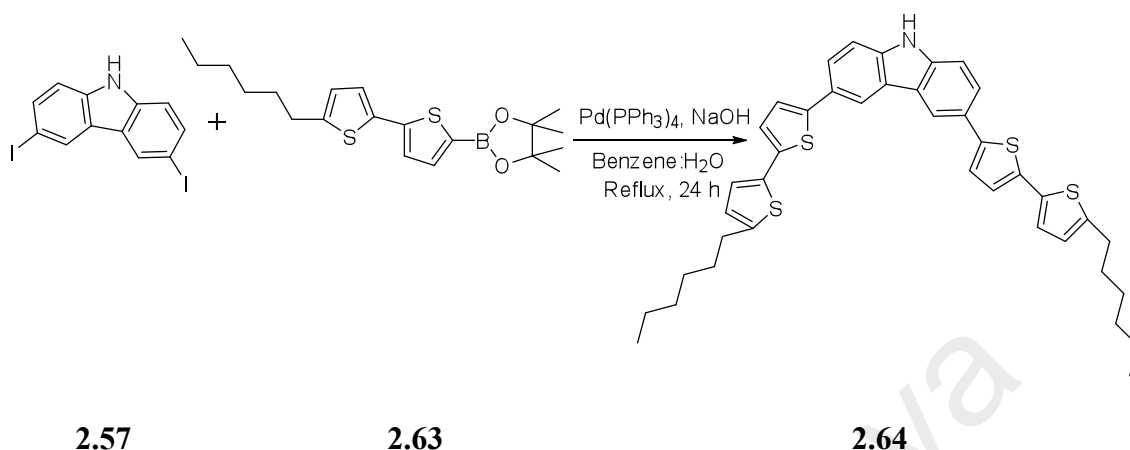
3,6-Diiodocarbazole **2.57** (0.25 g, 0.6 mmol) was dissolved in 10 ml benzene, a few drops of dry THF, and 2.2 eq 2,2-bithiophene-5-boronic acid pinacol ester **2.59** (0.38 g, 1.3 mmol) was added to the solution. Then 3 eq NaOH (0.07 g, 1.8 mmol) in 2 ml water added to the mixture. Bring mixture to reflux for 10 minutes, when the solution was homogenous, add required quantity of catalyst 3 mol % Pd(PPh<sub>3</sub>)<sub>4</sub> (0.05 g, 0.04 mmol) into reaction mixture and start reflux for 24 hours under nitrogen. After the slurry dark green reaction mixture was cooled at room temperature, washed with ethyl acetate (3 x 25 ml) and water (2 x 15 ml). The organic layer was dried with Na<sub>2</sub>SO<sub>4</sub> and evaporated to dryness give dark brown liquid. The residue was purified on silica gel column chromatography using ethyl acetate and hexane as eluent yielding **2.60** in green solid (0.24 g, 80 %). <sup>1</sup>H NMR (400 MHz, CDCl<sub>3</sub>) δ ppm 8.36 (s, 2 H), 8.17 (s, 1 H), 7.73 (dd, *J*=8.44, 1.83 Hz, 2 H), 7.47 (d, *J*=8.44 Hz, 2 H), 7.30 (d, *J*=3.67 Hz, 2 H), 7.23 - 7.27 (m, 4 H), 7.22 (d, *J*=3.67 Hz, 2 H), 7.07 (dd, *J*=4.89, 3.79 Hz, 2 H); <sup>13</sup>C NMR (100 MHz, CDCl<sub>3</sub>) δ ppm 141.2, 139.5, 137.7, 135.7, 127.8, 126.4, 124.7, 124.6, 124.1, 123.8, 123.3, 122.8, 117.9, 111.2. Maldi-Tof MS: *m/z* calcd for [M<sup>+</sup>] = C<sub>28</sub>H<sub>17</sub>NS<sub>4</sub> 495.024; found 495.020.

### 5.3.7 Synthesis of compound **2.62** (3,6-di([2,2':5',2''-terthiophen]-5-yl)-9H-carbazole)



3,6-Diiodocarbazole **2.57** (0.13 g, 0.3 mmol) was dissolved in 10 ml benzene, a few drops of dry THF, and 2.1 eq 2,2':5',2''-terthiophene-5-boronic acid pinacol ester **2.61** (0.24 g, 0.6 mmol) was added to the solution. Then 3 eq NaOH (0.036 g, 1.8 mmol) in 2 ml water added to the mixture. Bring mixture to reflux for 10 minutes, when the solution was homogenous, add required quantity of catalyst 3 mol % Pd(PPh<sub>3</sub>)<sub>4</sub> (0.05 g, 0.04 mmol) into reaction mixture and start reflux for 24 hours under nitrogen. After the slurry dark green reaction mixture was cooled at room temperature, washed with ethyl acetate (3 x 25 ml) and water (2 x 15 ml). The organic layer was dried with Na<sub>2</sub>SO<sub>4</sub> and evaporated to dryness give dark brown liquid. The residue was purified on silica gel column chromatography using ethyl acetate and hexane as eluent yielding **2.62** in green solid (0.15 g, 75 %); <sup>1</sup>H NMR (400 MHz, CDCl<sub>3</sub>) δ ppm 8.35 (s, 2 H), 8.13 (br. s., 1 H), 7.70 (dd, *J*=8.44, 1.71 Hz, 2 H), 7.55 (d, *J*=3.55 Hz, 2 H), 7.23 - 7.27 (m, 5 H), 7.18 - 7.23 (m, 3 H), 7.16 (d, *J*=3.79 Hz, 2 H), 7.10 (d, *J*=3.79 Hz, 2 H), 7.04 (dd, *J*=5.14, 3.67 Hz, 2 H); <sup>13</sup>C NMR (100 MHz, CDCl<sub>3</sub>) δ ppm 143.8, 138.5, 138.0, 137.9, 136.9, 136.8, 136.7, 136.0, 134.8, 129.4, 127.9, 124.9, 124.8, 124.6, 124.4, 123.8. Maldi-Tof MS: *m/z* calcd for [M<sup>+</sup>] = C<sub>36</sub>H<sub>21</sub>NS<sub>6</sub> 658.999; found 659.010.

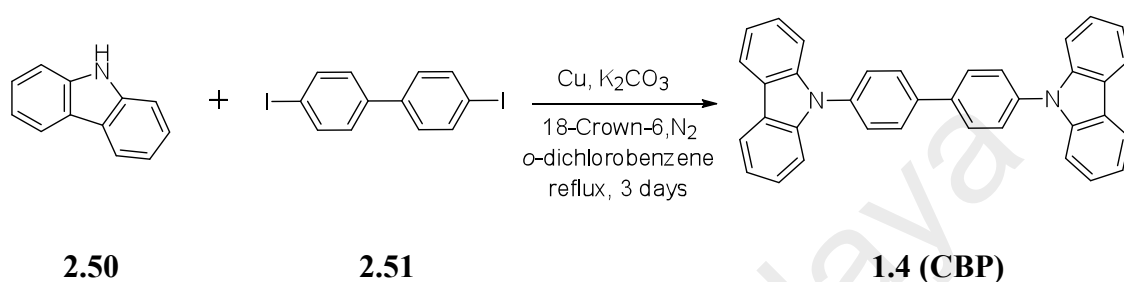
### 5.3.8 Synthesis of compound 2.64 (3,6-bis(5'-hexyl-[2,2'-bithiophen]-5-yl)-9H-carbazole)



3,6-Diiodocarbazole **2.57** (1.5 g, 3.6 mmol) was dissolved in 20 ml benzene, a few drops of dry THF, and 2.1 eq 5-hexyl-2,2-bithiophene-5-boronic acid pinacol ester **2.63** (2.82 g, 7.5 mmol) was added to the solution. Then 3 eq NaOH (0.43 g, 10.8 mmol) in 4 ml water added to the mixture. Bring mixture to reflux for 10 minutes, when the solution was homogenous, add required quantity of catalyst 3 mol % Pd(PPh<sub>3</sub>)<sub>4</sub> (0.26 g, 0.11 mmol) into reaction mixture and start reflux for 24 hours under nitrogen. After the slurry dark green reaction mixture was cooled at room temperature, washed with ethyl acetate (3 x 30 ml) and water (2 x 20 ml). The organic layer was dried with Na<sub>2</sub>SO<sub>4</sub> and evaporated to dryness give dark green liquid. The residue was purified on silica gel column chromatography using ethyl acetate and hexane as eluent yielding **2.64** in dark green solid (2.05 g, 86 %); <sup>1</sup>H NMR (400 MHz, CDCl<sub>3</sub>) δ ppm 8.32 (s, 2 H), 8.12 (br. s., 1 H), 7.70 (d, *J*=8.44 Hz, 2 H), 7.43 (d, *J*=8.19 Hz, 2 H), 7.27 (d, *J*=3.30 Hz, 2 H), 7.12 (d, *J*=3.67 Hz, 2 H), 7.05 (d, *J*=3.42 Hz, 2 H), 6.73 (d, *J*=3.42 Hz, 2 H), 2.84 (t, *J*=7.52 Hz, 4 H), 1.67 - 1.80 (m, 4 H), 1.30 - 1.49 (m, 12 H), 0.92 (t, *J*=6.80 Hz, 6 H); <sup>13</sup>C NMR (100 MHz, CDCl<sub>3</sub>) δ ppm 145.1, 143.6, 139.4, 136.2, 135.0, 126.2, 124.7, 124.3, 123.8, 123.6, 122.9, 122.6, 117.3, 111.1, 31.6, 30.2, 28.8, 24.5, 22.6, 14.1. Maldi-Tof MS: *m/z* calcd for [M<sup>+</sup>] = C<sub>40</sub>H<sub>41</sub>NS<sub>4</sub> 663.212; found 663.227.

## 5.4 Synthesis of end products

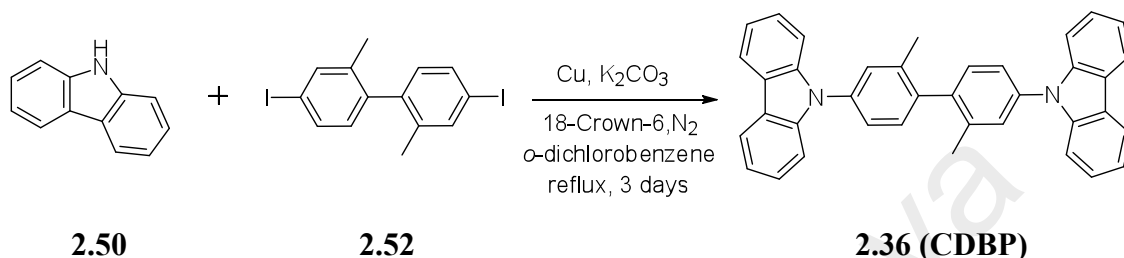
### 5.4.1 Synthesis of compound 4,4'-Di(9H-carbazol-9-yl)-1,1'-biphenyl (1.4 (CBP))



Carbazole **2.50** 2 eq (0.09 g, 0.50 mmol), 1 eq 4,4'-diiodobiphenyl **2.51** (0.10 g, 0.25 mmol), 1 eq K<sub>2</sub>CO<sub>3</sub> (0.03 g, 0.50 mmol), 2 eq copper powder (0.03 g, 0.50 mmol) and 20 mol % 18-crown-6 (0.01 g) were dissolved in *o*-dichlorobenzene (10 ml). The system was purged under nitrogen for 30 minutes and start reflux for 3 days. The solution was filtered and the solvent removed under vacuo. Purified by column chromatography (silica, chloroform-hexane) afforded **1.4 (CBP)** in white shiny powder (0.07 g, 50%). Mp 283 (Schrögel *et al.*, 2011). <sup>1</sup>H NMR (400 MHz, CDCl<sub>3</sub>) δ ppm 8.21 (d, *J*=7.70 Hz, 4 H), 7.95 (d, *J*=8.44 Hz, 4 H), 7.74 (d, *J*=8.56 Hz, 4 H), 7.55 (d, *J*=7.90 Hz, 4 H), 7.48 (td, *J*=7.10, 1.00 Hz, 4 H), 7.35 (td, *J*=6.80, 1.00 Hz, 4 H); <sup>13</sup>C NMR (100 MHz, CDCl<sub>3</sub>) δ ppm 140.8, 139.3, 137.3, 128.5, 127.5, 126.0, 123.5, 120.4, 120.1, 109.8. HR-ESI-MS: *m/z* calcd for [M+H]<sup>+</sup> = C<sub>36</sub>H<sub>24</sub>N<sub>2</sub> 485.2017; found 485.2015.

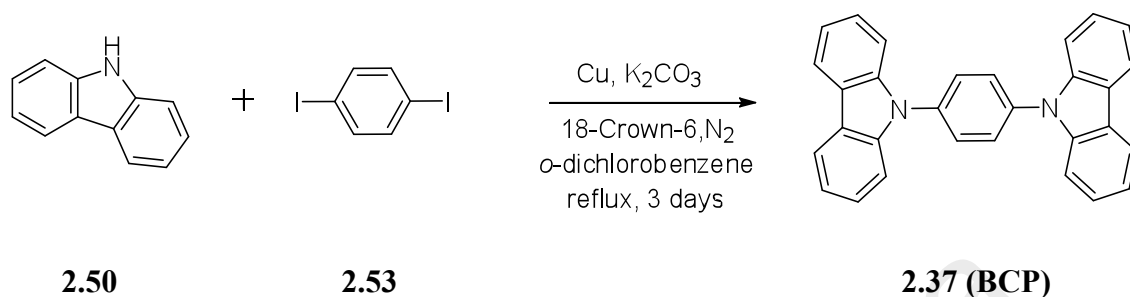


#### 5.4.2 Synthesis of compound 9,9'-(2,2'-dimethyl-[1,1'-biphenyl]-4,4'-diyl)bis(9H-carbazole) ( **2.36 (CDBP)** )



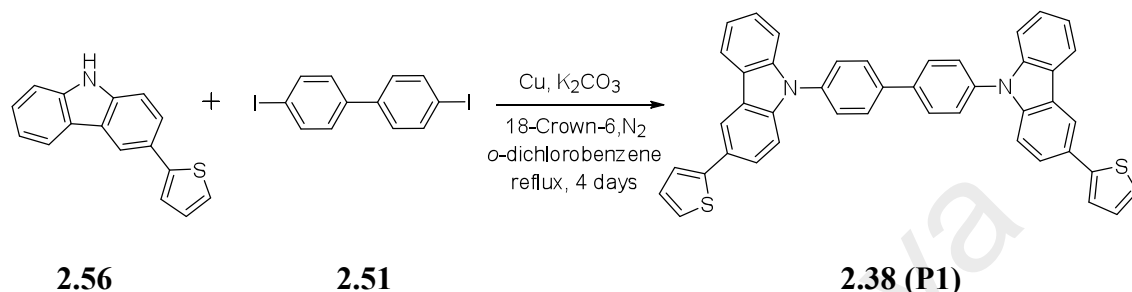
Carbazole **2.50** 2.2 eq (0.17 g, 0.05 mmol), 1 eq 4,4'-diiodo-2,2'-dimethyl-1,1'-biphenyl **2.52** (0.10 g, 0.02 mmol), 1 eq K<sub>2</sub>CO<sub>3</sub> (0.03 g), 2 eq copper powder (0.03 g) and 20 mol % 18-crown-6 (0.01 g) were dissolved in *o*-dichlorobenzene (20 ml). The system was purged under nitrogen for 30 minutes and start reflux for 3 days. The solution was filtered and the solvent removed under vacuo. Purified by column chromatography (silica, dichloromethane-hexane) to give **2.36 (CDBP)** as white powder (0.01 g, 60%) (Schrögel *et al.*, 2011). <sup>1</sup>H NMR (400 MHz, CDCl<sub>3</sub>) δ ppm 8.21 (d, *J*=7.70 Hz, 4 H), 7.55 - 7.60 (m, 6 H), 7.45 - 7.55 (m, 8 H), 7.35 (td, *J*=7.40, 0.98 Hz, 4 H), 2.32 (s, 6 H). <sup>13</sup>C NMR (100 MHz, CDCl<sub>3</sub>) δ ppm 140.9, 140.0, 137.9, 136.9, 130.8, 128.3, 125.9, 124.3, 123.4, 120.3, 119.9, 109.9, 20.13. HR-ESI-MS: *m/z* calcd for [M+H]<sup>+</sup> = C<sub>38</sub>H<sub>28</sub>N<sub>2</sub> 513.2330; found 513.2332.

### 5.4.3 Synthesis of 1,4-di(9H-carbazol-9-yl)benzene (**2.37** (BCP))



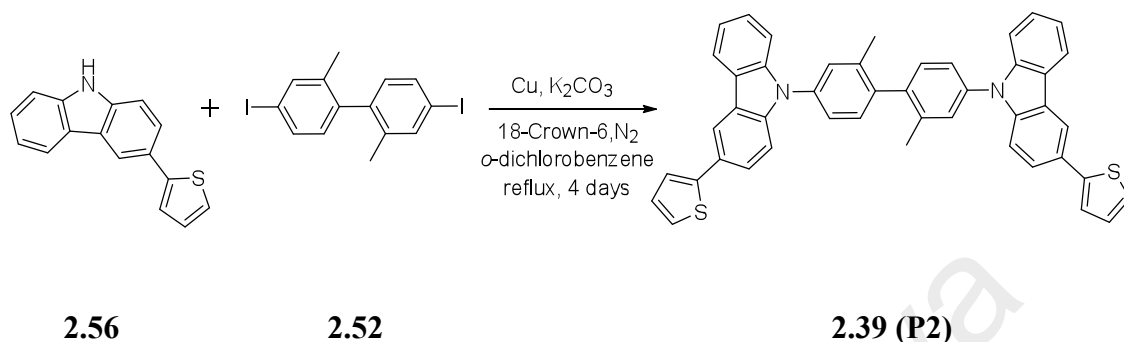
Carbazole **2.50** 2 eq (0.08 g, 0.50 mmol), 1 eq 1,4-diodobenzene **2.53** (0.10 g, 0.23 mmol), 1 eq K<sub>2</sub>CO<sub>3</sub> (0.03 g), 2 eq copper powder (0.03 g) and 20 mol % 18-crown-6 (0.01 g) were dissolved in *o*-dichlorobenzene (10 ml). The system was purged under nitrogen for 30 minutes and start reflux for 3 days. The solution was filtered and the solvent removed under vacuo. Purified by column chromatography (silica, dichloromethane-hexane) give **2.37** as white solid (0.08 g, 80%). Mp 323 °C. <sup>1</sup>H NMR (400 MHz, CDCl<sub>3</sub>) δ ppm 8.22 (d, *J*=7.58 Hz, 4 H), 7.85 (s, 4 H), 7.60 (d, *J*=8.20 Hz, 4 H), 7.51 (td, *J*=7.67, 1.16 Hz, 4 H), 7.37 (td, *J*=7.40, 0.98 Hz, 4 H). <sup>13</sup>C NMR (100 MHz, CDCl<sub>3</sub>) δ ppm 140.8, 136.9, 128.4, 126.1, 123.6, 120.4, 120.3, 109.7. HR-ESI-MS: *m/z* calcd for [M+H]<sup>+</sup> = C<sub>30</sub>H<sub>20</sub>N<sub>2</sub> 409.1704; found 409.1706.

#### 5.4.4 Synthesis of compound **2.38 (P1)** (4,4'-bis(3-(thiophen-2-yl)-9H-carbazol-9-yl)-1,1'-biphenyl)



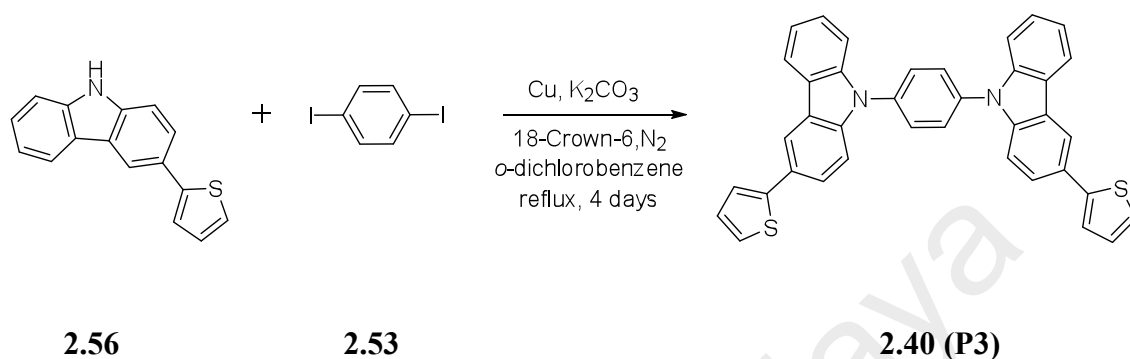
3-(thiophene-2-yl)-9H-carbazole **2.56** 2 eq (0.3241 g, 1.3 mmol), 1 eq 4,4'-diiodobiphenyl **2.51** (0.25g, 0.6 mmol), 1 eq  $K_2CO_3$  (0.2 g), 2 eq Cu powder (0.25 g) and 18-crown-6 (0.05 g) were dissolved in *o*-dichlorobenzene (35 ml). The system was purged under nitrogen for 30 minutes and start reflux for 4 days. The solution was filtered and the solvent removed under vacuo. Purified by column chromatography (silica, ethyl acetate-hexane) to give **2.38 (P1)** as off-white solid (0.1 g, 26%).  $^1H$  NMR (400 MHz,  $CDCl_3$ )  $\delta$  ppm 8.41 (s, 2 H), 8.24 (d,  $J=8.31$  Hz, 2 H), 7.97 (d,  $J=8.07$  Hz, 4 H), 7.75 (dd,  $J=8.62, 3.12$  Hz, 6 H), 7.50 - 7.58 (m, 5 H), 7.33 - 7.43 (m, 5 H), 7.31 (d,  $J=4.77$  Hz, 2 H), 7.15 (t,  $J=4.20$  Hz, 2 H);  $^{13}C$  NMR (100 MHz,  $CDCl_3$ )  $\delta$  ppm 145.6, 141.4, 140.4, 140.1, 138.0, 136.7, 130.8, 128.3, 128.0, 126.8, 126.3, 124.6, 124.2, 123.9, 123.3, 122.3, 120.5, 120.2, 117.9, 110.3, 110.1. HR-ESI-MS:  $m/z$  calcd for  $[M+H]^+ = C_{44}H_{28}N_2S_2$  649.1772; found 649.1775.

#### 5.4.5 Synthesis of compound **2.39 (P2)** (9,9'-(2,2'-dimethyl-[1,1'-biphenyl]-4,4'-diyl)bis(3-(thiophen-2-yl)-9H-carbazole))



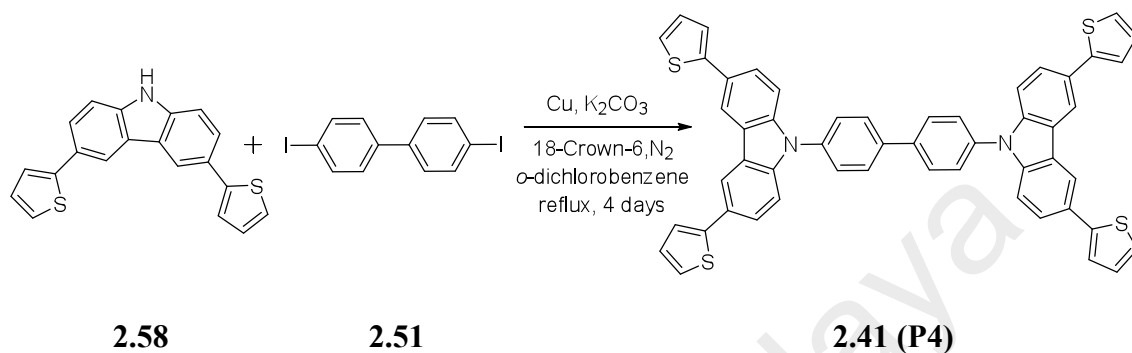
3-(thiophene-2-yl)-9H-carbazole **2.56** 2 eq (0.12 g, 0.48 mmol), 1 eq 4,4'-diiodo-2,2'-dimethyl-1,1'-biphenyl **2.52** (0.10 g, 0.23 mmol), 1 eq  $K_2CO_3$  (0.03 g), 2 eq copper powder (0.03 g) and 20 mol % 18-crown-6 (0.01 g) were dissolved in *o*-dichlorobenzene (10 ml). The system was purged under nitrogen for 30 minutes and start reflux for 4 days. The solution was filtered and the solvent removed in vacuo. Purified by column chromatography (silica, ethyl acetate-hexane) to give **2.39 (P2)** as pale yellow solid (0.05 g, 35 %).  $^1H$  NMR (400 MHz,  $CDCl_3$ )  $\delta$  ppm 8.42 (s, 2 H), 8.24 (d,  $J=7.46$  Hz, 2 H), 7.75 (d,  $J=8.56$  Hz, 2 H), 7.46 - 7.60 (m, 12 H), 7.41 (dd,  $J=3.55$ , 1.10 Hz, 2 H), 7.36 (td,  $J=7.43$ , 0.92 Hz, 2 H), 7.31 (dd,  $J=5.14$ , 1.10 Hz, 2 H), 7.16 (dd,  $J=5.14$ , 3.55 Hz, 2 H), 2.33 (s, 6 H);  $^{13}C$  NMR (100 MHz,  $CDCl_3$ )  $\delta$  ppm 145.6, 141.4, 140.4, 140.1, 138.0, 136.7, 130.8, 128.3, 128.0, 126.8, 126.6, 126.3, 124.6, 124.2, 123.9, 123.3, 122.3, 120.5, 120.2, 117.9, 110.3, 110.1, 20.2. HR-ESI-MS:  $m/z$  calcd for  $[M+H]^+ = C_{46}H_{32}N_2S_2$  677.2085; found 677.2080.

#### 5.4.6 Synthesis of compound 2.40 (P3) (1,4-bis(3-(thiophen-2-yl)-9H-carbazol-9-yl)benzene)



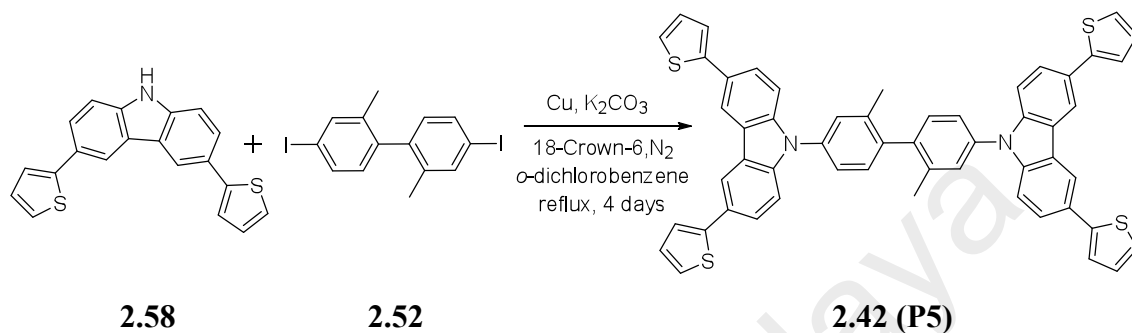
3-(thiophene-2-yl)-9H-carbazole **2.56** 2 eq (0.16 g, 0.60 mmol), 1 eq 1,4-diiodobenzene **2.53** (0.10 g, 0.30 mmol), 1 eq  $K_2CO_3$  (0.10 g), 2 eq copper powder (0.04 g) and 20 mol % 18-crown-6 (1.60 mg) were dissolved in *o*-dichlorobenzene (10 ml). The system was purged under nitrogen for 30 minutes and start reflux for 4 days. The solution was filtered and the solvent removed under vacuo. Purified by column chromatography (silica, chloroform-hexane) give **2.40 (P3)** as pale yellow solid (0.08 g, 48%).  $^1H$  NMR (600 MHz,  $CDCl_3$ )  $\delta$  ppm 8.42 (s, 2 H), 8.25 (d,  $J=7.52$  Hz, 2 H), 7.87 (s, 4 H), 7.77 (dd,  $J=8.53, 1.74$  Hz, 2 H), 7.60 (t,  $J=8.60$  Hz, 4 H), 7.52 (td,  $J=7.50, 1.00$  Hz, 2 H), 7.42 (dd,  $J=3.48, 1.10$  Hz, 2 H), 7.39 (t,  $J=6.97$  Hz, 2 H), 7.32 (dd,  $J=5.04, 1.01$  Hz, 2 H), 7.16 (dd,  $J=5.14, 3.48$  Hz, 2 H);  $^{13}C$  NMR (100 MHz,  $CDCl_3$ )  $\delta$  ppm 128.3, 128.1, 127.2, 126.5, 124.8, 124.1, 124.0, 123.5, 122.4, 120.6, 120.6, 118.0, 110.1, 109.9. HR-ESI-MS:  $m/z$  calcd for  $[M+H]^+ = C_{38}H_{24}N_2S_2$  573.1459; found 573.1484.

#### 5.4.7 Synthesis of compound **2.41 (P4)** (4,4'-bis(3,6-di(thiophen-2-yl)-9H-carbazol-9-yl)-1,1'-biphenyl)



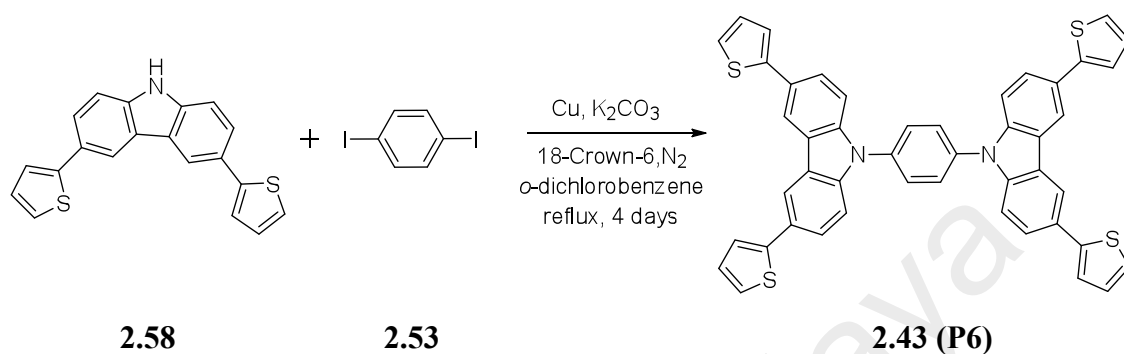
3,6-Dithiophene-2-yl)9H-carbazole **2.58** 2 eq (0.43 g, 1.30 mmol), 1 eq 4,4'-diiodobiphenyl **2.51** (0.25 g, 0.60 mmol), 1 eq  $K_2CO_3$  (0.20 g), 2 eq copper powder (0.25 g) and 20 mol % 18-crown-6 (0.05 g) were dissolved in *o*-dichlorobenzene (35 ml). The system was purged under nitrogen for 30 minutes and start reflux for 4 days. The solution was filtered and the solvent removed under vacuo. Recrystallization from absolute ethanol giving **2.41 (P4)** as pale yellow solid (1.0 g, 75 %).  $^1H$  NMR (600 MHz,  $CDCl_3$ )  $\delta$  ppm 8.44 (s, 4 H), 7.98 (d,  $J=8.44$  Hz, 3 H), 7.76 (d,  $J=8.07$  Hz, 8 H), 7.53 (d,  $J=8.44$  Hz, 4 H), 7.43 (dd,  $J=3.48, 1.10$  Hz, 4 H), 7.32 (dd,  $J=5.13, 0.92$  Hz, 4 H), 7.16 (dd,  $J=4.95, 3.48$  Hz, 5 H);  $^{13}C$  NMR (100 MHz,  $CDCl_3$ )  $\delta$  ppm 145.3, 140.8, 139.4, 137.0, 128.7, 128.1, 127.3, 127.3, 125.0, 124.0, 123.9, 122.5, 118.0, 110.4. Mp 268 °C. HR-APCI-MS:  $m/z$  calcd for  $[M+H]^+ = C_{52}H_{32}N_2S_4$  813.1526; found 813.1522.

#### 5.4.8 Synthesis of compound 2.42 (P5) (9,9'-(2,2'-dimethyl-[1,1'-biphenyl]-4,4'-diyl)bis(3,6-di(thiophen-2-yl)-9H-carbazole))



3,6-Dithiophene-2-yl)9H-carbazole **2.58** 2.2 eq (0.17 g, 0.05 mmol), 1 eq 4,4'-diiodo-2,2'-dimethyl-1,1'-biphenyl **2.52** (0.10 g, 0.02 mmol), 1 eq K<sub>2</sub>CO<sub>3</sub> (0.03 g), 2 eq copper powder (0.03 g) and 20 mol % 18-crown-6 (0.01 g) were dissolved in *o*-dichlorobenzene (10 ml). The system was purged under nitrogen for 30 minutes and start reflux for 4 days. The solution was filtered and the solvent removed under vacuo. Purified by column chromatography (silica, dichloromethane-hexane) to give **2.42 (P5)** as white solid (0.01 g, 60 %). <sup>1</sup>H NMR (400 MHz, CDCl<sub>3</sub>) δ ppm 8.45 (s, 4 H), 7.69 - 7.83 (m, 6 H), 7.49 - 7.63 (m, 6 H), 7.37 - 7.49 (m, 6 H), 7.29 - 7.35 (m, 4 H), 7.11 - 7.19 (m, 4 H), 1.28 (s, 6 H). <sup>13</sup>C NMR (100 MHz, CDCl<sub>3</sub>) δ ppm 145.6, 145.4, 142.1, 141.8, 140.9, 128.1, 124.9, 124.2, 124.0, 123.9, 123.6, 122.4, 122.3, 118.0, 111.4, 110.4, 20.2. HR-ESI-MS: m/z calcd for [M+H]<sup>+</sup> = C<sub>54</sub>H<sub>36</sub>N<sub>2</sub>S<sub>4</sub> 841.1841; found 841.1842.

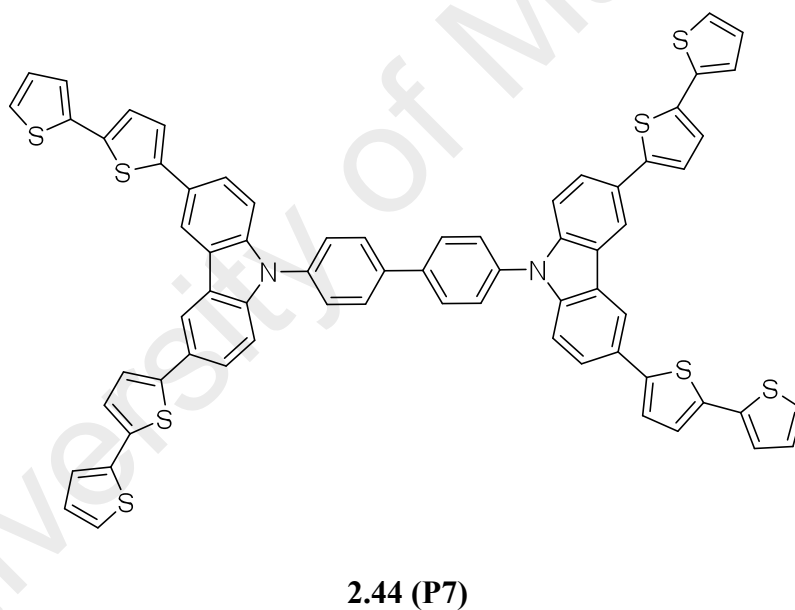
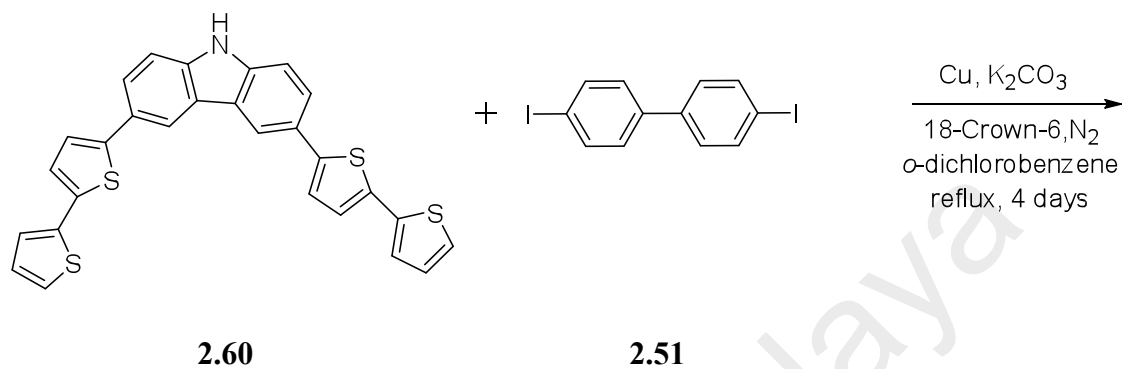
#### 5.4.9 Synthesis of compound 2.43 (P6) (1,4-bis(3,6-di(thiophen-2-yl)-9H-carbazol-9-yl)benzene)



3,6-Dithiophene-2-yl)9H-carbazole **2.58** 2 eq (0.21 g, 0.60 mmol), 1 eq 1,4-diiodobenzene **2.53** (0.10 g, 0.30 mmol), 1 eq  $K_2CO_3$  (0.10 g), 2 eq copper powder (0.04 g) and 20 mol % 18-crown-6 (0.002 g) were dissolved in o-dichlorobenzene (10 ml). The system was purged under nitrogen for 30 minutes and start reflux for 3 days. The solution was filtered and the solvent removed under vacuo. Purified by column chromatography (silica, chloroform-hexane) to give **2.43 (P6)** as pale yellow solid (0.1 g, 50 %).  $^1H$  NMR (400 MHz,  $CDCl_3$ )  $\delta$  ppm 8.46 (s, 4 H), 7.90 (s, 4 H), 7.79 (dd,  $J=8.50, 1.65$  Hz, 4 H), 7.60 (d,  $J=8.44$  Hz, 4 H), 7.44 (d,  $J=3.55$  Hz, 4 H), 7.33 (d,  $J=4.52$  Hz, 4 H), 7.17 (dd,  $J=4.95, 3.61$  Hz, 4 H).  $^{13}C$  NMR (100 MHz,  $CDCl_3$ )  $\delta$  ppm 145.2, 140.6, 129.5, 128.3, 128.1, 127.5, 125.1, 124.1, 124.0, 122.6, 118.1, 110.3. HR-ESI-MS:  $m/z$  calcd for  $[M+H]^+ = C_{46}H_{28}N_2S_4$  737.1213; found 737.1210.



**5.4.10 Synthesis of compound 2.44 (P7) (4,4'-bis(3,6-di([2,2'-bithiophen]-5-yl)-9H-carbazol-9-yl)-1,1'-biphenyl)**

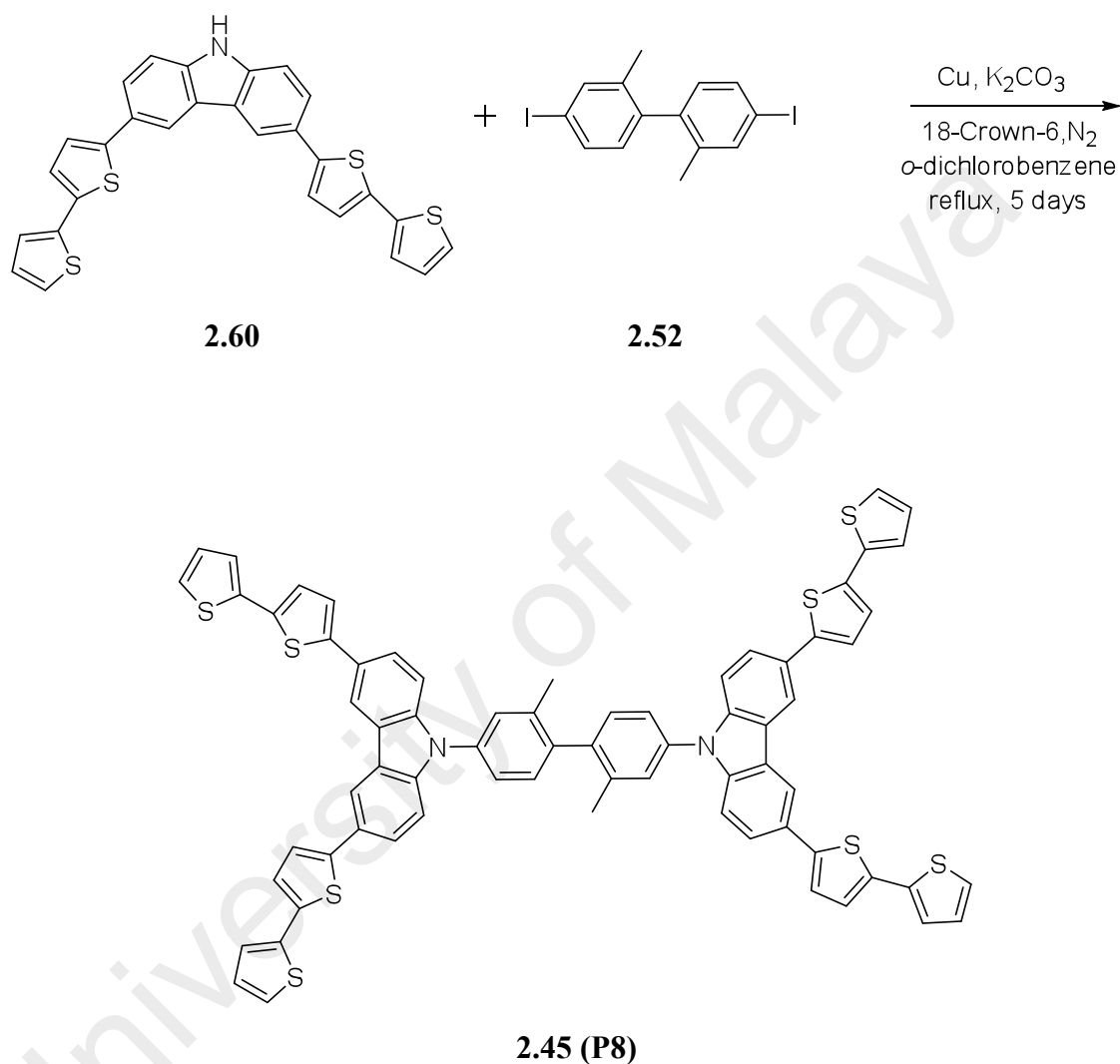


Compound **2.60** 2.1 eq (0.13 g, 0.03 mmol), 1 eq 4,4'-diiodobiphenyl **2.51** (0.05 g, 0.01 mmol), 1 eq  $\text{K}_2\text{CO}_3$  (0.02 g), 2 eq copper powder (0.02 g) and 20 mol % 18-crown-6 (0.01 g) were dissolved in o-dichlorobenzene (25 ml). The system was purged under nitrogen for 30 minutes and start reflux for 4 days. The solution was filtered and the solvent removed under vacuo. Purified by column chromatography (silica,

chloroform-hexane) giving **2.44 (P7)** as dark brown-yellow powder (0.01 g, 40 %).  $^1\text{H}$  NMR (400 MHz,  $\text{CDCl}_3$ )  $\delta$  ppm 8.42 (s, 4 H), 7.66 - 7.79 (m, 8 H), 7.54 - 7.58 (m, 4 H), 7.29 - 7.37 (m, 8 H), 7.18 - 7.27 (m, 12 H), 7.04 - 7.14 (m, 6 H).  $^{13}\text{C}$  NMR (100 MHz,  $\text{CDCl}_3$ )  $\delta$  ppm 145.4, 144.1, 140.9, 137.7, 135.9, 131.2, 130.7, 130.2, 128.2, 127.8, 126.9, 124.7, 124.1, 123.0, 123.3, 123.0, 117.7, 110.6. Maldi-Tof MS: m/z calcd for  $[\text{M}^+] = \text{C}_{68}\text{H}_{40}\text{N}_2\text{S}_8$  1140.096; found 1140.092.

University of Malaya

**5.4.11 Synthesis of compound 2.45 (P8) (9,9'-(2,2'-dimethyl-[1,1'-biphenyl]-4,4'-diyl)bis(3,6-di([2,2'-bithiophen]-5-yl)-9H-carbazole))**

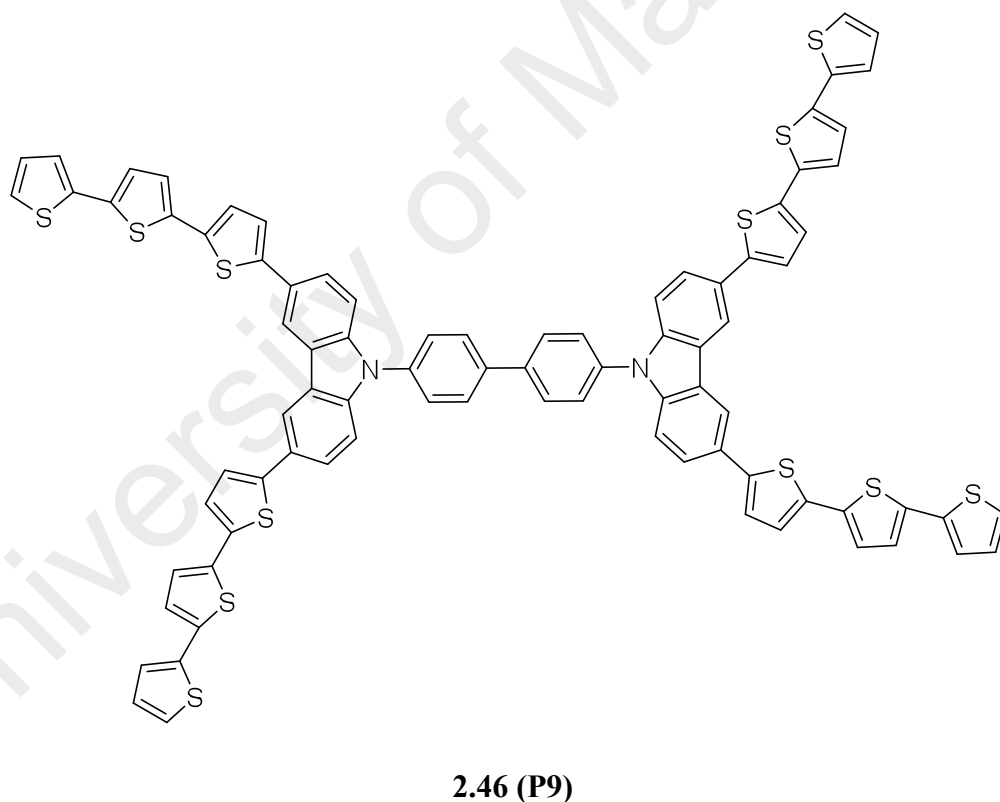
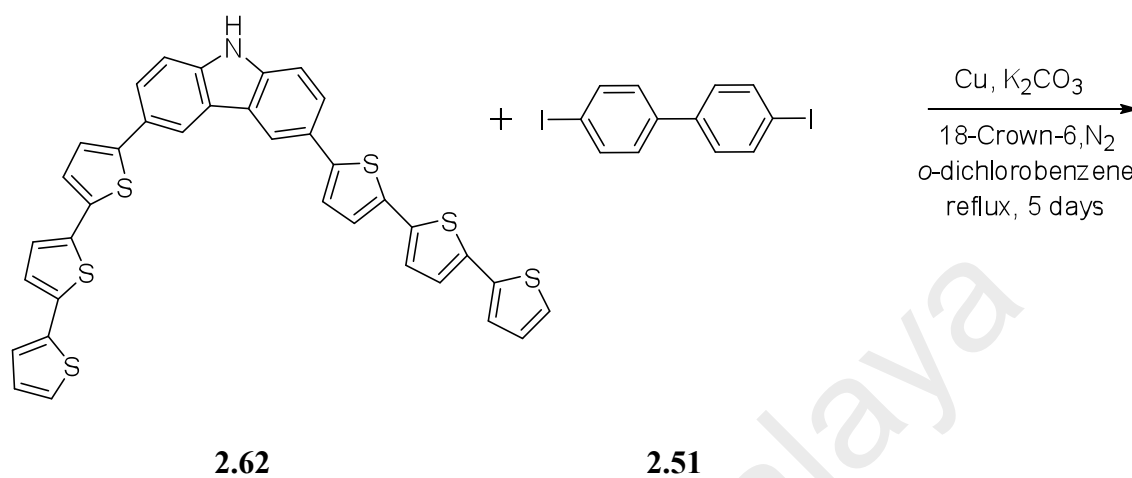


Compound **2.60** 2.1 eq (0.12 g, 0.03 mmol), 1 eq 4,4'-diiodo-2,2'-dimethyl-1,1'-biphenyl **2.52** (0.03 g, 0.01 mmol), 1 eq  $\text{K}_2\text{CO}_3$  (0.01 g), 2 eq copper powder (0.01 g) and 20 mol % 18-crown-6 (0.003 g) were dissolved in o-dichlorobenzene (15 ml). The system was purged under nitrogen for 30 minutes and start reflux for 5 days. The solution was filtered and the solvent removed under vacuo. Purified by column

chromatography (silica, chloroform-hexane) giving **2.45 (P8)** as yellow solid (0.01 g, 38 %).  $^1\text{H}$  NMR (400 MHz,  $\text{CDCl}_3$ )  $\delta$  ppm 8.42 (s, 4 H), 7.66 - 7.79 (m, 6 H), 7.54 - 7.58 (m, 4 H), 7.29 - 7.37 (m, 6 H), 7.18 - 7.27 (m, 12 H), 7.04 - 7.14 (m, 6 H), 1.45 (s, 6 H).  $^{13}\text{C}$  NMR (100 MHz,  $\text{CDCl}_3$ )  $\delta$  ppm 145.4, 144.1, 140.9, 137.7, 135.9, 131.6, 131.2, 130.7, 130.2, 128.2, 127.8, 126.9, 124.7, 124.6, 124.1, 123.7, 123.4, 122.9, 117.7, 110.6, 21.0. Maldi-Tof MS:  $m/z$  calcd for  $[\text{M}^+]$  =  $\text{C}_{70}\text{H}_{44}\text{N}_2\text{S}_8$  1168.127; found 1168.122.

University of Malaya

**5.4.12 Synthesis of compound 2.46 (P9) (4,4'-bis(3,6-di([2,2':5',2''-terthiophen]-5-yl)-9H-carbazol-9-yl)-1,1'-biphenyl)**

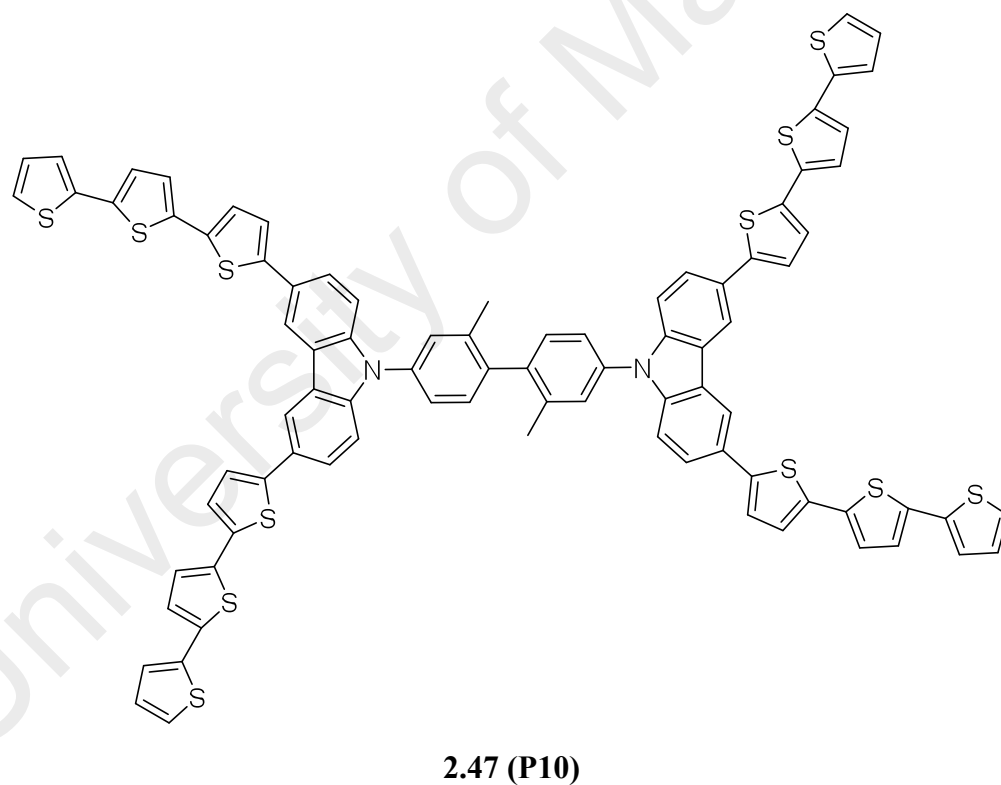
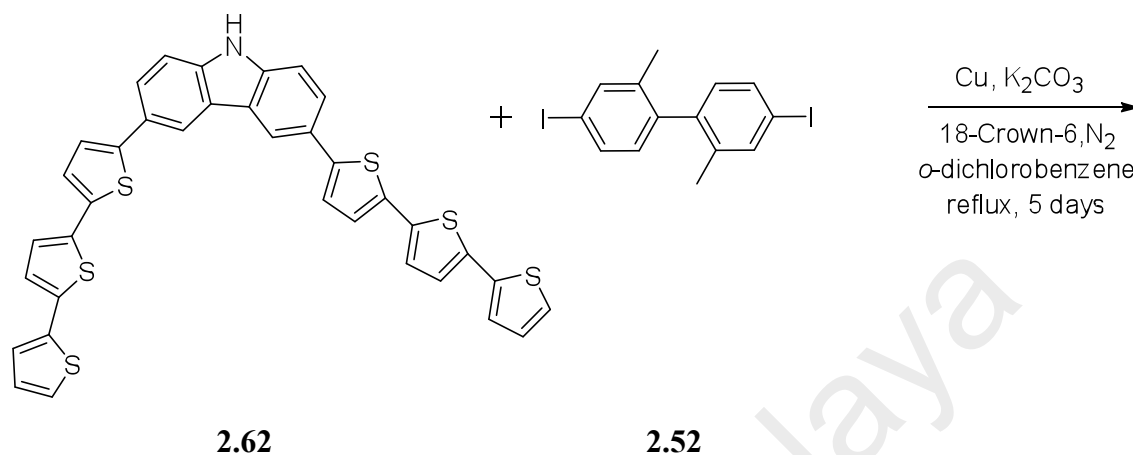


Compound **2.62** 2.1 eq (0.08 g, 0.01 mmol), 1 eq 4,4'-diiodobiphenyl **2.51** (0.02 g, 0.01 mmol), 1 eq  $\text{K}_2\text{CO}_3$  (0.01 g), 2 eq copper powder (0.01 g) and 20 mol % 18-crown-6 (0.003 g) were dissolved in o-dichlorobenzene (15 ml). The system was purged under nitrogen for 30 minutes and start reflux for 5 days. The solution was filtered and

the solvent removed under vacuo. Purified by column chromatography (silica, chloroform-hexane) giving **2.46 (P9)** as yellow solid (0.01 g, 40 %).  $^1\text{H}$  NMR (400 MHz,  $\text{CDCl}_3$ )  $\delta$  ppm 7.65 (s, 4 H), 7.47 (s, 4 H), 7.32 (dd,  $J=5.13, 1.10$  Hz, 6 H), 7.29 (s, 6 H), 7.27 (d,  $J=1.10$  Hz, 4 H), 7.24 (dd,  $J=3.55, 1.10$  Hz, 4 H), 7.20 (d,  $J=3.79$  Hz, 4 H), 7.17 (d,  $J=3.91$  Hz, 4 H), 7.14 (d,  $J=3.91$  Hz, 4 H), 7.08 (td,  $J=4.98, 3.61$  Hz, 8 H).  $^{13}\text{C}$  NMR (100 MHz,  $\text{CDCl}_3$ )  $\delta$  ppm 144.6, 140.4, 139.4, 137.7, 136.9, 134.2, 128.1, 128.0, 127.1, 127.1, 126.1, 125.7, 125.2, 124.7, 124.7, 124.5, 124.4, 120.7, 119.3, 111.1. Maldi-Tof MS:  $m/z$  calcd for  $[\text{M}^+] = \text{C}_{84}\text{H}_{48}\text{N}_2\text{S}_{12}$  1468.047; found 1468.042.

University of Malaysia

**5.4.13 Synthesis of compound 2.47 (P10) (9,9'-(2,2'-dimethyl-[1,1'-biphenyl]-4,4'-diyl)bis(3,6-di([2,2':5',2''-terthiophen]-5-yl)-9H-carbazole))**

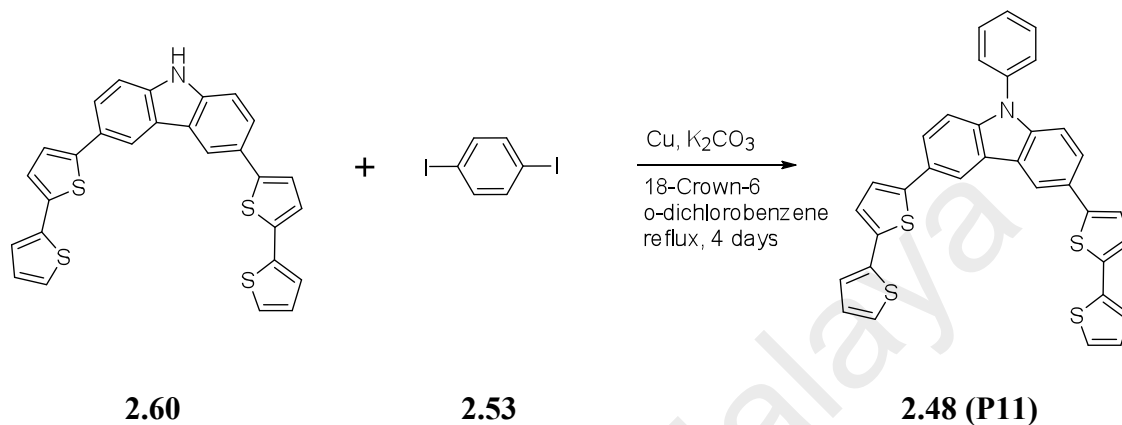


Compound **2.62** 2.1 eq (0.08 g, 0.01 mmol), 1 eq 4,4'-diiodo-2,2'-dimethyl-1,1'-biphenyl **2.52** (0.02 g, 0.01 mmol), 1 eq  $\text{K}_2\text{CO}_3$  (0.01 g), 2 eq copper powder (0.01 g) and 20 mol % 18-crown-6 (0.002 g) were dissolved in *o*-dichlorobenzene (20 ml). The system was purged under nitrogen for 30 minutes and start reflux for 5 days. The

solution was filtered and the solvent removed under vacuo. Purified by column chromatography (silica, chloroform-hexane) giving **2.47 (P10)** as orange solid (0.01 g, 36 %).  $^1\text{H}$  NMR (400 MHz,  $\text{CDCl}_3$ )  $\delta$  ppm 7.65 (s, 4 H), 7.47 (s, 4 H), 7.32 (dd,  $J=5.13$ , 1.10 Hz, 6 H), 7.29 (s, 4 H), 7.27 (d,  $J=1.10$  Hz, 4 H), 7.24 (dd,  $J=3.55$ , 1.10 Hz, 4 H), 7.20 (d,  $J=3.79$  Hz, 4 H), 7.17 (d,  $J=3.91$  Hz, 4 H), 7.14 (d,  $J=3.91$  Hz, 4 H), 7.08 (td,  $J=4.98$ , 3.61 Hz, 8 H), 1.45 (s, 6 H).  $^{13}\text{C}$  NMR (100 MHz,  $\text{CDCl}_3$ )  $\delta$  ppm 144.6, 140.4, 139.4, 137.7, 136.9, 136.7, 134.2, 128.1, 128.0, 127.1, 127.1, 126.1, 125.7, 125.2, 125.0, 124.7, 124.7, 124.5, 124.4, 120.7, 119.3, 111.1, 29.7. Maldi-Tof MS:  $m/z$  calcd for  $[\text{M}^+] = \text{C}_{86}\text{H}_{52}\text{N}_2\text{S}_{12}$  1496.078; found 1496.072.

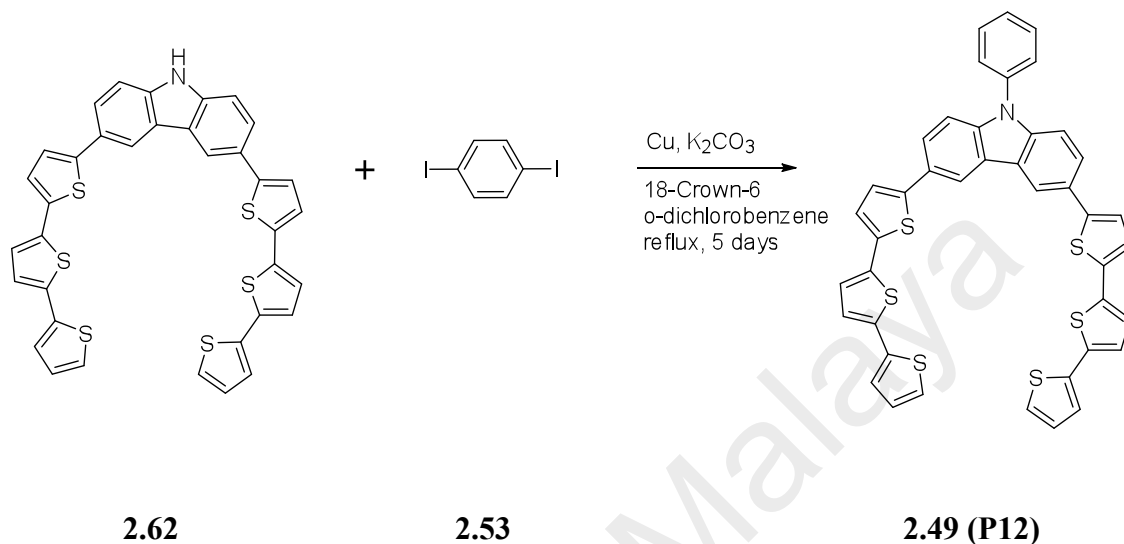


#### 5.4.14 Synthesis of compound **2.48 (P11)** (3,6-di([2,2'-bithiophen]-5-yl)-9-phenyl-9H-carbazole)



Compound **2.60** 2.1 eq (0.13 g, 0.03 mmol), 1 eq 1,4-diodobenzene **2.53** (0.03 g, 0.01 mmol), 1 eq  $K_2CO_3$  (0.01 g), 2 eq copper powder (0.02 g) and 20 mol % 18-crown-6 (0.01 g) were dissolved in *o*-dichlorobenzene (15 ml). The system was purged under nitrogen for 30 minutes and start reflux for 4 days. The solution was filtered and the solvent removed under vacuo. Purified by column chromatography (silica, chloroform-hexane) giving **2.48 (P11)** as brown-yellow solid (0.07 g, 40 %).  $^1H$  NMR (400 MHz,  $CDCl_3$ )  $\delta$  ppm 8.39 (s, 2 H), 7.98 (d,  $J=8.56$  Hz, 2 H), 7.70 (dd,  $J=8.56$ , 1.71 Hz, 2 H), 7.38 (dd,  $J=13.69$ , 8.56 Hz, 4 H), 7.31 (d,  $J=3.67$  Hz, 2 H), 7.25 (d,  $J=4.40$  Hz, 5 H), 7.21 (d,  $J=1.00$  Hz, 2 H), 7.07 (t,  $J=1.00$  Hz, 2 H).  $^{13}C$  NMR (100 MHz,  $CDCl_3$ )  $\delta$  ppm 143.9, 140.5, 139.3, 137.6, 137.0, 135.9, 128.7, 127.9, 127.1, 124.7, 124.2, 123.9, 123.4, 123.1, 123.0, 117.6, 110.2. Maldi-Tof MS:  $m/z$  calcd for  $[M^+]$  =  $C_{34}H_{21}NS_4$  571.056; found 571.050.

#### 5.4.15 Synthesis of compound **2.49 (P12)** (3,6-di([2,2':5',2''-terthiophen]-5-yl)-9-phenyl-9H-carbazole)



Compound **2.62** 2.1 eq (0.08 g, 0.01 mmol), 1 eq 1,4-diodobenzene **2.53** (0.02 g, 0.01 mmol), 1 eq  $K_2CO_3$  (0.01 g), 2 eq copper powder (0.01 g) and 20 mol % 18-crown-6 (0.003 g) were dissolved in o-dichlorobenzene (15 ml). The system was purged under nitrogen for 30 minutes and start reflux for 5 days. The solution was filtered and the solvent removed under vacuo. Purified by column chromatography (silica, chloroform-hexane) giving **2.49 (P12)** as yellow-orange solid (0.03 g, 40 %).  $^1H$  NMR (400 MHz,  $CDCl_3$ )  $\delta$  ppm 8.44 (d,  $J=1.59$  Hz, 2 H), 8.37 (d,  $J=1.00$  Hz, 4 H), 8.11 (d,  $J=1.83$  Hz, 2 H), 7.76 (dd,  $J=8.56, 1.71$  Hz, 2 H), 7.69 (td,  $J=1.00$  Hz, 5 H), 7.64 (d,  $J=8.44$  Hz, 2 H), 7.51 (dd,  $J=8.50, 2.02$  Hz, 2 H), 7.33 (d,  $J=8.56$  Hz, 2 H), 7.24 (d,  $J=8.56$  Hz, 2 H), 7.13 (d,  $J=8.56$  Hz, 2 H).  $^{13}C$  NMR (100 MHz,  $CDCl_3$ )  $\delta$  ppm 140.9, 139.3, 138.8, 138.5, 135.1, 134.9, 129.6, 129.4, 129.3, 128.9, 125.7, 125.4, 124.6, 124.2, 123.2, 119.5. Maldi-Tof MS:  $m/z$  calcd for  $[M^+]$  =  $C_{42}H_{25}NS_6$  735.031; found 735.040.

## CONCLUSIONS

In conclusion, we have designed, synthesized and characterized twelve new carbazole-thiophene derivatives of **1.4 (CBP)**, **2.36 (CDBP)** and **2.37 (BCP)** scaffold having two to twelve thiophenes as donor units in its molecular structures via Suzuki Miyaura and Ullmann coupling reactions. Photophysical and electrochemical properties have revealed significant red shift after the subsequent addition of thiophenes units on **1.4 (CBP)**, **2.36 (CDBP)** and **2.37 (BCP)** backbone at 3,6-position of carbazole. Compounds **1.4 (CBP)**, **2.36 (CDBP)** and **2.37 (BCP)** connecting with more thiophenes leads to more stabilization of HOMO and LUMO level energy where the band gap ( $\Delta E$ ) of all compounds is significantly reduced. Compared with **1.4 (CBP)**, **2.36 (CDBP)** and **2.37 (BCP)** unit, the molecules with oligothiophenes unit can greatly decrease the band gap of the compounds, and such unit can be introduced into the backbone of  $\pi$ -conjugated small molecules to develop new materials with low band gap that may have potential application in optoelectronic fields. It is well-known that compounds **1.4 (CBP)**, **2.36 (CDBP)** and **2.37 (BCP)** were promising host materials that are frequently used in WOLED and OLED applications, therefore by tuning the achitecture of these small compounds by designing new derivatives compounds could futher developed their application into optoelectronic field. Compounds **2.46 (P9)** and **2.47 (P10)** have the narrowest band gap among these ten new compounds, which expected to have great potential in photophysical properties. We believe that the present study provides valuable information for the optimization and synthesis of new carbazole-thiophene based on **1.4 (CBP)**, **2.36 (CDBP)** and **2.37 (BCP)** towards photovoltaic architecture.

## REFERENCES

- Acar, N., Kurzawa, J., Fritz, N., Stockmann, A., Roman, C., Schneider, S., & Clark, T. (2003). Phenothiazine-pyrene dyads: photoinduced charge separation and structural relaxation in the CT state. *The Journal of Physical Chemistry A*, 107(45), 9530-9541.
- Allard, S., Forster, M., Souharce, B., Thiem, H., & Scherf, U. (2008). Organic semiconductors for solution-processable field-effect transistors (OFETs). *Angewandte Chemie International Edition*, 47(22), 4070-4098.
- Ambrose, J. F., & Nelson, R. F. (1968). Anodic Oxidation Pathways of Carbazoles I. Carbazole and N-Substituted Derivatives. *Journal of the Electrochemical Society*, 115(11), 1159-1164.
- Anthony, J. E. (2008). The larger acenes: versatile organic semiconductors. *Angewandte Chemie International Edition*, 47(3), 452-483.
- Arcadi, A., Cerichelli, G., Chiarini, M., Correa, M., & Zorzan, D. (2003). A Mild and Versatile Method for Palladium-Catalyzed Cross-Coupling of Aryl Halides in Water and Surfactants. *European Journal of Organic Chemistry*, 2003(20), 4080-4086.
- Asil, D., Cihaner, A., Algi, F., & Önal, A. M. (2008). A novel conducting polymer based on terthienyl system bearing strong electron-withdrawing substituents and its electrochromic device application. *Journal of Electroanalytical Chemistry*, 618(1), 87-93.
- Beaujuge, P. M., & Fréchet, J. M. J. (2011). Molecular design and ordering effects in  $\pi$ -functional materials for transistor and solar cell applications. *Journal of the American Chemical Society*, 133(50), 20009-20029.
- Beaujuge, P. M., & Reynolds, J. R. (2010). Color control in  $\pi$ -conjugated organic polymers for use in electrochromic devices. *Chemical Reviews*, 110(1), 268-320.
- Beletskaya, I. P., & Cheprakov, A. V. (2004). Copper in cross-coupling reactions: the post-Ullmann chemistry. *Coordination Chemistry Reviews*, 248(21), 2337-2364.
- Belletête, M., Bédard, M., Leclerc, M., & Durocher, G. (2004). Ground and excited state properties of carbazole-based dyads: correlation with their respective absorption and fluorescence spectra. *Journal of Molecular Structure: THEOCHEM*, 679(1), 9-15.
- Berlman, I. B. (1970). Empirical correlation between nuclear conformation and certain fluorescence and absorption characteristics of aromatic compounds. *The Journal of Physical Chemistry*, 74(16), 3085-3093.
- Bernier, P., Bidan, G., & Lefrant, S. (1999). *Advances in synthetic metals: twenty years of progress in science and technology*. Switzerland: Elsevier.

- Blouin, N., Michaud, A., Gendron, D., Wakim, S., Blair, E., Neagu-Plesu, Rodika, B., Michel, D., Gilles, T., Tao, Y., & Leclerc, M. (2008). Toward a rational design of poly (2, 7-carbazole) derivatives for solar cells. *Journal of the American Chemical Society*, 130(2), 732-742.
- Boudreault, P.-L. T., Najari, A., & Leclerc, M. (2010). Processable low-bandgap polymers for photovoltaic applications. *Chemistry of Materials*, 23(3), 456-469.
- Bowman, W. R., Heaney, H., & Smith, P. H. G. (1984). Copper (I) catalysed aromatic nucleophilic substitution: A mechanistic and synthetic comparison with the S<sub>N</sub>1 reaction. *Tetrahedron Letters*, 25(50), 5821-5824.
- Boys, S. F. (1950). *Electronic wave functions. II. A calculation for the ground state of the beryllium atom*. Proceedings of the Royal Society of London A: Mathematical, Physical and Engineering Sciences.
- Brabec, C., Scherf, U., & Dyakonov, V. (2011). *Organic photovoltaics: materials, device physics, and manufacturing technologies*. Germany: John Wiley & Sons.
- Brédas, J. L., & Heeger, A. J. (1994). Influence of donor and acceptor substituents on the electronic characteristics of poly (paraphenylene vinylene) and poly (paraphenylene). *Chemical Physics Letters*, 217(5), 507-512.
- Briehn, C. A., Schiedel, M. S., Bensen, E. M., Schuhmann, W., & Bäuerle, P. (2001). Single-compound libraries of organic materials: from the combinatorial synthesis of conjugated oligomers to structure–property relationships. *Angewandte Chemie International Edition*, 40(24), 4680-4683.
- Brockmann, T. W., & Tour, J. M. (1994). Synthesis of low-bandgap zwitterionic and planar conjugated pyrrole-derived polymers. Reversible optical absorptions from the UV to the near-IR. *Journal of the American Chemical Society*, 116(16), 7435-7436.
- Brook, T. E., & Narayanaswamy, R. (1998). Polymeric films in optical gas sensors. *Sensors and Actuators B: Chemical*, 51(1), 77-83.
- Brownell, L. V., Robins, K. A., Jeong, Y., Lee, Y., & Lee, D.-C. (2013). Highly systematic and efficient HOMO–LUMO energy gap control of thiophene-pyrazine-acenes. *The Journal of Physical Chemistry C*, 117(48), 25236-25247.
- Bundgaard, E., & Krebs, F. C. (2007). Low band gap polymers for organic photovoltaics. *Solar Energy Materials and Solar Cells*, 91(11), 954-985.
- Burroughes, J. H., Bradley, D. D. C., Brown, A. R., Marks, R. N., Mackay, K., Friend, R. H., Burns, P.L., Holmes, A. B. (1990). Light-emitting diodes based on conjugated polymers. *Nature*, 347(6293), 539-541.

- Cabala, R., Meister, V., & Potje-Kamloth, K. (1997). Effect of competitive doping on sensing properties of polypyrrole. *Journal of Chemical Society, Faraday Trans.*, 93(1), 131-137.
- Cao, H., Ma, J., Zhang, G., & Jiang, Y. (2005). Borole/thiophene cooligomers and copolymers with quinoid structures and biradical characters. *Macromolecules*, 38(4), 1123-1130.
- Capasso, F. (1987). Band-gap engineering: from physics and materials to new semiconductor devices. *Science*, 235(4785), 172-176.
- Carboni, B., Pourbaix, C., Carreaux, F., Deleuze, H., & Maillard, B. (1999). Boronic ester as a linker system for solid phase synthesis. *Tetrahedron Letters*, 40(45), 7979-7983.
- Chandler, L. D. (2012). MIT News Office. *Clean energy could lead to scarce materials, Rising demand for wind turbines and electric vehicles could strain supplies of some rare earth metals.*
- Chang, D. W., Lee, H. J., Kim, J. H., Park, S. Y., Park, S.-M., Dai, L., & Baek, J.-B. (2011). Novel quinoxaline-based organic sensitizers for dye-sensitized solar cells. *Organic letters*, 13(15), 3880-3883.
- Chen, H.-Y., Hou, J., Zhang, S., Liang, Y., Yang, G., Yang, Y., Yu, L., Wu, Y., & Li, G. (2009). Polymer solar cells with enhanced open-circuit voltage and efficiency. *Nature Photonics*, 3(11), 649-653.
- Chen, J., Reed, M. A., Dirk, S. M., Price, D. W., Rawlett, A. M., Tour, J. M., Grubisha D. S., Bennett, D. W. (2003). *Molecular electronic devices molecular electronics: bio-sensors and bio-computers.* Netherlands: Springer.
- Cheng, Y.-J., Yang, S.-H., & Hsu, C.-S. (2009). Synthesis of conjugated polymers for organic solar cell applications. *Chemical Reviews*, 109(11), 5868-5923.
- Chi, C., & Wegner, G. (2005). Chain-length dependence of the electrochemical properties of conjugated oligofluorenes. *Macromolecular Rapid Communications*, 26(19), 1532-1537.
- Chu, H.-C., Sahu, D., Hsu, Y.-C., Padhy, H., Patra, D., Bhattacharya, D., Lu, K.-L., Wei, K.-H., & Lin, H.-C. (2012). Structural planarity and conjugation effects of novel symmetrical acceptor–donor–acceptor organic sensitizers on dye-sensitized solar cells. *Dyes and Pigments*, 93(1), 1488-1497.
- Chu, T.-Y., Alem, S., Tsang, S.-W., Tse, S.-C., Wakim, S., Lu, J., Dennler, G., Waller, D., Gaudiana, R., & Tao, Y. (2011). Morphology control in polycarbazole based bulk heterojunction solar cells and its impact on device performance. *Applied Physics Letters*, 98(25), 253301-253301-253303.

- Cohen, A. J., Mori-Sánchez, P., & Yang, W. (2008). Insights into current limitations of density functional theory. *Science*, 321(5890), 792-794.
- Coulson, C. A. (1948). Excited electronic levels in conjugated molecules: I. Long wavelength ultra-violet absorption of naphthalene, anthracene and homologs. *Proceedings of the Physical Society*, 60(3), 257.
- Daku, K. M. L., Newton, R. F., Pearce, S. P., Vile, J., & Williams, J. M. J. (2003). Suzuki cross-coupling reactions using reverse-phase glass beads in aqueous media. *Tetrahedron Letters*, 44(27), 5095-5098.
- Damit, E. F., Nordin, N., Ariffin, A., & Sulaiman, K. (2016). Synthesis of novel derivatives of carbazole-thiophene, their electronic properties, and computational studies. *Journal of Chemistry*, 14 pages.
- Deloux, L., Skrzypczak-Jankun, E., Cheesman, B. V., Srebnik, M., & Sabat, M. (1994). First example of stable 1, 1-bimetalloalkenes of boron and zirconium: Synthesis, reactivity, X-ray analysis, and NMR studies. *Journal of the American Chemical Society*, 116(22), 10302-10303.
- Dennler, G., Sariciftci, N. S., Brabec, C. J., Hadziioannou, G., & Malliaras, G. G. (2007). *Semiconducting polymers*. 2<sup>nd</sup> edn. Weinheim: Wiley-VCH.
- Desbene-Monvernay, A., Lacaze, P.-C., & Dubois, J.-E. (1981). Polarographic study of colored radical films formed by the electrochemical oxidation of carbazoles: Part I. Carbazole and N-ethyl, N-phenyl and N-carbazyl derivatives. *Journal of Electroanalytical Chemistry and Interfacial Electrochemistry*, 129(1), 229-241.
- DeVasher, R. B., Moore, L. R., & Shaughnessy, K. H. (2004). Aqueous-phase, palladium-catalyzed cross-coupling of aryl bromides under mild conditions, using water-soluble, sterically demanding alkylphosphines. *The Journal of Organic Chemistry*, 69(23), 7919-7927.
- Devlin, F. J., Finley, J. W., Stephens, P. J., & Frisch, M. J. (1995). Ab initio calculation of vibrational absorption and circular dichroism spectra using density functional force fields: a comparison of local, nonlocal, and hybrid density functionals. *The Journal of Physical Chemistry*, 99(46), 16883-16902.
- Dietrich-Buchecker, C., Jime, M. C., & Sauvage, J.-P. (1999). Selective and efficient synthesis of di-, tri- and tetrasubstituted 1, 10-phenanthrolines. *Tetrahedron Letters*, 40(17), 3395-3396.
- Dimitrakopoulos, C. D., & Malenfant, P. R. L. (2002). Organic thin film transistors for large area electronics. *Advanced Materials*, 14(2), 99.
- Dreizler, R. M., & Gross, E. K. U. (1990). *Density functional theory: an approach to the quantum many-body problem*. Berlin: Springer.

- Dupuis, C., Adiey, K., Charruault, L., Michelet, V., Savignac, M., & Genêt, J.-P. (2001). Suzuki cross-coupling of arylboronic acids mediated by a hydrosoluble Pd (0)/TPPTS catalyst. *Tetrahedron Letters*, 42(37), 6523-6526.
- Durmus, A., Gunbas, G. E., Camurlu, P., & Toppare, L. (2007). A neutral state green polymer with a superior transmissive light blue oxidized state. *Chemical Communications*(31), 3246-3248.
- Duvva, N., Kanaparthi, R. K., Kandhadi, J., Marotta, G., Salvatori, P., De Angelis, F., & Giribabu, L. (2015). Carbazole-based sensitizers for potential application to dye sensitized solar cells. *Journal of Chemical Sciences*, 127(3), 383-394.
- El-Azhary, A. A., & Suter, H. U. (1995). Correlated ab Initio Force Fields and Vibrational Analysis of the Spectra of Isoxazole and Isothiazole. *The Journal of Physical Chemistry*, 99(34), 12751-12758.
- European Photovoltaic Industry, A. (2010). Global market outlook for photovoltaics until 2014. See [http://www.epia.org/fileadmin/EPIA\\_docs/public/Global\\_Market\\_Outlook\\_for\\_Photovoltaics\\_until\\_2014.pdf](http://www.epia.org/fileadmin/EPIA_docs/public/Global_Market_Outlook_for_Photovoltaics_until_2014.pdf).
- Evano, G., Blanchard, N., & Toumi, M. (2008). Copper-mediated coupling reactions and their applications in natural products and designed biomolecules synthesis. *Chemical Reviews*, 108(8), 3054-3131.
- Facchetti, A., Yoon, M. H., Stern, C. L., Katz, H. E., & Marks, T. J. (2003). Building blocks for n-type organic electronics: regiochemically modulated inversion of majority carrier sign in perfluoroarene-modified polythiophene semiconductors. *Angewandte Chemie International Edition*, 42(33), 3900-3903.
- Ferraris, J. P., & Lambert, T. L. (1991). Narrow bandgap polymers: poly-4-dicyanomethylene-4H-cyclopenta [2, 1-b; 3, 4-b'] dithiophene (PCDM) *Journal of Chemical Society, Chemical Communication* (18), 1268-1270.
- Frankevich, E. L., Lymarev, A. A., Sokolik, I., Karasz, F. E., Blumstengel, S., Baughman, R. H., & Hörhold, H. H. (1992). Polaron-pair generation in poly (phenylene vinylenes). *Physical Review B*, 46(15), 9320.
- Friend, R. H., Denton, G. J., Halls, J. J. M., Harrison, N. T., Holmes, A. B., Köhler, A., Lux, A., Moratti, S. C., Pichler, K., Tessler, N. (1997). Electronic processes of conjugated polymers in semiconductor device structures. *Synthetic Metals*, 84(1), 463-470.
- Funahashi, M., Zhang, F., & Tamaoki, N. (2007). High Ambipolar Mobility in a Highly Ordered Smectic Phase of a Dialkylphenylterthiophene Derivative That Can Be Applied to Solution-Processed Organic Field-Effect Transistors. *Advanced Materials*, 19(3), 353-358.



- Gauthier, S., & Frechet, J. M. J. (1987). Phase-transfer catalysis in the Ullman synthesis of substituted triphenylamines. *Synthesis*(4), 383-385.
- Gene<sup>^</sup>t, J. P., Linquist, A., Blart, E., Mouries, V., Savignac, M., & Vaultier, M. (1995). Suzuki-type cross coupling reactions using palladium-water soluble catalyst. Synthesis of functionalized dienes. *Tetrahedron letters*, 36(9), 1443-1446.
- Greenham, N. C., Moratti, S. C., Bradley, D. D. C., Friend, R. H., & Holmes, A. B. (1993). Efficient light-emitting diodes based on polymers with high electron affinities. *Nature*, 365, 628-630.
- Guillier, F., Nivoliers, F., Godard, A., Marsais, F., & Quéguiner, G. (1994). An original one-pot synthesis of 5-(4-pyridyl)-benzo [c]-2, 7-naphthyridine as key intermediate in the synthesis of amphimedine by metalation connected with cross-coupling reaction. *Tetrahedron Letters*, 35(35), 6489-6492.
- Guo, Y., Du, C., Di, C.-a., Zheng, J., Sun, X., Wen, Y., Zhang, L., Wu, W., Yu, G., Liu, Y. (2009). Field dependent and high light sensitive organic phototransistors based on linear asymmetric organic semiconductor. *Applied Physics Letters*, 94(14), 143303-143303-143303.
- Haas, S., Takahashi, Y., Takimiya, K., & Hasegawa, T. (2009). High-performance dinaphtho-thieno-thiophene single crystal field-effect transistors. *Applied Physics Letters*, 95(2), 022111-022113.
- Hagberg, D. P., Edvinsson, T., Marinado, T., Boschloo, G., Hagfeldt, A., & Sun, L. (2006). A novel organic chromophore for dye-sensitized nanostructured solar cells. *Chemical Communications*(21), 2245-2247.
- Hagberg, D. P., Marinado, T., Karlsson, K. M., Nonomura, K., Qin, P., Boschloo, G., Brinck, T., Hagfeldt, A., & Sun, L. (2007). Tuning the HOMO and LUMO energy levels of organic chromophores for dye sensitized solar cells. *The Journal of Organic Chemistry*, 72(25), 9550-9556.
- Hara, K., Miyamoto, K., Abe, Y., & Yanagida, M. (2005). Electron transport in coumarin-dye-sensitized nanocrystalline TiO<sub>2</sub> electrodes. *The Journal of Physical Chemistry B*, 109(50), 23776-23778.
- Harris, D. C., & Bertolucci, M. D. (1978). *Symmetry and spectroscopy: an introduction to vibrational and electronic spectroscopy*. New York: Dover Publication Inc.
- Havinga, E. E., Ten Hoeve, W., & Wynberg, H. (1992). A new class of small band gap organic polymer conductors. *Polymer Bulletin*, 29(1-2), 119-126.
- Havinga, E. E., Ten Hoeve, W., & Wynberg, H. (1993). Alternate donor-acceptor small-band-gap semiconducting polymers; Polysquaraines and polycroconaines. *Synthetic Metals*, 55(1), 299-306.

- He, Y., Hong, W., & Li, Y. (2014). New building blocks for  $\pi$ -conjugated polymer semiconductors for organic thin film transistors and photovoltaics. *Journal of Materials Chemistry C*, 2(41), 8651-8661.
- Heliatek GmbH Press Release. (2010). *Heliatek GmbH Press Release*, <http://www.heliatek.com>.
- Hlel, A., Mabrouk, A., Chemek, M., Khalifa, I. B., & Alimi, K. (2015). A DFT study of charge-transfer and opto-electronic properties of some new materials involving carbazole units. *Computational Condensed Matter*, 3, 30-40.
- Hoffmann, S. T., Schrogel, P., Rothmann, M., Albuquerque, R. Q., Strohriegl, P., & Kohler, A. (2010). Triplet Excimer Emission in a Series of 4, 4'-Bis (N-carbazolyl)-2, 2'-biphenyl Derivatives. *The Journal of Physical Chemistry B*, 115(3), 414-421.
- Hohenberg, P., & Kohn, W.(1964). Inhomogeneous electron gas. *Physical Review*, 136(3B), 864.
- Kohn, W., Sham, L. J.(1965). Inhomogeneous electron gas. *Phys Rev*, 140, 1133.
- Hsieh, K. H., Ho, K. S., Wang, Y. Z., Ko, S. D., & Fu, S. C. (2001). Miscibility of poly (thiophene-3-acetic acid) and poly (ethylene oxide). *Synthetic Metals*, 123(2), 217-224.
- Huang, W.-S., & Pu, L. (2000). New and improved ligands for highly enantioselective catalytic diphenylzinc additions to aryl aldehydes. *Tetrahedron Letters*, 41(2), 145-149.
- Hwang, S.-W., & Chen, Y. (2001). Synthesis and electrochemical and optical properties of novel poly (aryl ether) s with isolated carbazole and p-quaterphenyl chromophores. *Macromolecules*, 34(9), 2981-2986.
- Ikeda, N., & Miyasaka, T. (2005). A solid-state dye-sensitized photovoltaic cell with a poly (N-vinyl-carbazole) hole transporter mediated by an alkali iodide. *Chemical Communications*(14), 1886-1888.
- Inganäs, O., Zhang, F., & Andersson, M. R. (2009). Alternating polyfluorenes collect solar light in polymer photovoltaics. *Accounts of Chemical Research*, 42(11), 1731-1739.
- Iraqi, A., & Wataru, I. (2004). Preparation and properties of 2, 7-linked N-alkyl-9 H-carbazole main-chain polymers. *Chemistry of Materials*, 16(3), 442-448.
- Izumi, T., Kobashi, S., Takimiya, K., Aso, Y., & Otsubo, T. (2003). Synthesis and spectroscopic properties of a series of  $\beta$ -blocked long oligothiophenes up to the 96-mer: reevaluation of effective conjugation length. *Journal of the American Chemical Society*, 125(18), 5286-5287.

- Johns, B. A., & Johnson, C. R. (1998). Scaffolded bis-azasugars: a dual warhead approach to glycosidase inhibition. *Tetrahedron Letters*, 39(8), 749-752.
- Johnson, B. G., Gill, P. M. W., & Pople, J. A. (1993). The performance of a family of density functional methods. *The Journal of Chemical Physics*, 98(7), 5612-5626.
- Kaafarani, B. R., Ala'a, O., Trattng, R., Fonari, A., Sax, S., Wex, B., Risko, C., Khnayzer, R. S., Barlow, S., & Patra, D. (2013). Bis (carbazolyl) derivatives of pyrene and tetrahydropyrene: synthesis, structures, optical properties, electrochemistry, and electroluminescence. *Journal of Materials Chemistry C*, 1(8), 1638-1650.
- Kamtekar, K. T., Monkman, A. P., & Bryce, M. R. (2010). Recent Advances in White Organic Light-Emitting Materials and Devices (WOLEDs). *Advanced Materials*, 22(5), 572-582.
- Kato, S.-i., Noguchi, H., Kobayashi, A., Yoshihara, T., Tobita, S., & Nakamura, Y. (2012). Bicarbazoles: systematic structure–property investigations on a series of conjugated carbazole dimers. *The Journal of Organic Chemistry*, 77(20), 9120-9133.
- Kato, S.-i., Shimizu, S., Kobayashi, A., Yoshihara, T., Tobita, S., & Nakamura, Y. (2014). Systematic structure–property investigations on a series of alternating carbazole–thiophene oligomers. *The Journal of Organic Chemistry*, 79(2), 618-629.
- Kato, S.-i., Shimizu, S., Taguchi, H., Kobayashi, A., Tobita, S., & Nakamura, Y. (2012). Synthesis and electronic, photophysical, and electrochemical properties of a series of thienylcarbazoles. *The Journal of Organic Chemistry*, 77(7), 3222-3232.
- Kelly, T. R., Garcia, A., Lang, F., Walsh, J. J., Bhaskar, K. V., Boyd, M. R., Götz, R., Keller P. A., Walter, R., & Bringmann, G. (1994). Convergent total synthesis of the michellamines. *Tetrahedron Letters*, 35(41), 7621-7624.
- Kim, D., Lee, J. K., Kang, S. O., & Ko, J. (2007). Molecular engineering of organic dyes containing N-aryl carbazole moiety for solar cell. *Tetrahedron*, 63(9), 1913-1922.
- Kim, S., Choi, H., Kim, D., Song, K., Kang, S. O., & Ko, J. (2007). Novel conjugated organic dyes containing bis-dimethylfluorenyl amino phenyl thiophene for efficient solar cell. *Tetrahedron*, 63(37), 9206-9212.
- Klapars, A., Huang, X., & Buchwald, S. L. (2002). A general and efficient copper catalyst for the amidation of aryl halides. *Journal of the American Chemical Society*, 124(25), 7421-7428.
- Klauk, H. (2006). *Organic electronics: materials, manufacturing, and application*. Germany: John Wiley & Sons.

- Kobayashi, K., Ahmed, M. S. M., & Mori, A. (2006). Introduction of ethynylene and thienylene spacers into 2, 5-diarylthiazole and 2, 5-diarylthiophene. *Tetrahedron*, 62(41), 9548-9553.
- Koene, B. E., Loy, D. E., & Thompson, M. E. (1998). Asymmetric triaryldiamines as thermally stable hole transporting layers for organic light-emitting devices. *Chemistry of materials*, 10(8), 2235-2250.
- Kohn, W., & Sham, L. J. (1965). Self-consistent equations including exchange and correlation effects. *Physical Review*, 140(4A), A1133.
- Kotha, S., Lahiri, K., & Kashinath, D. (2002). Recent applications of the Suzuki–Miyaura cross-coupling reaction in organic synthesis. *Tetrahedron*, 58(48), 9633-9695.
- Koumura, N., Wang, Z.-S., Mori, S., Miyashita, M., Suzuki, E., & Hara, K. (2006). Alkyl-functionalized organic dyes for efficient molecular photovoltaics. *Journal of American Chemical Society*, 128(44), 14256-14257.
- Koyuncu, F. B., Koyuncu, S., & Ozdemir, E. (2011). A new multi-electrochromic 2, 7 linked polycarbazole derivative: Effect of the nitro subunit. *Organic Electronics*, 12(10), 1701-1710.
- Kunz, K., Scholz, U., & Ganzer, D. (2003). Renaissance of Ullmann and Goldberg reactions: progress in copper catalyzed CN-, CO-and CS-coupling. *Synlett*, (15), 2428-2439.
- Kwong, F. Y., & Buchwald, S. L. (2003). Mild and efficient copper-catalyzed amination of aryl bromides with primary alkylamines. *Organic Letters*, 5(6), 793-796.
- Lam, P. Y. S., Vincent, G., Clark, C. G., Deudon, S., & Jadhav, P. K. (2001). Copper-catalyzed general C-N and C-O bond cross-coupling with arylboronic acid. *Tetrahedron Letters*, 42(20), 3415-3418.
- Langhoff, S. R. (1996). Theoretical infrared spectra for polycyclic aromatic hydrocarbon neutrals, cations, and anions. *The Journal of Physical Chemistry*, 100(8), 2819-2841.
- Leadbeater, N. E. (2005). Fast, easy, clean chemistry by using water as a solvent and microwave heating: the Suzuki coupling as an illustration. *Chemical Communications*, (23), 2881-2902.
- Lee, C., Yang, W., & Parr, R. G. (1988). Development of the colle-salvetti correlation-energy formula into a functional of the electron density. *Physical Review B*, 37(2), 785.

- Lei, T., Dou, J. H., & Pei, J. (2012). Influence of alkyl chain branching positions on the Hole mobilities of polymer thin-film transistors. *Advanced Materials*, 24(48), 6457-6461.
- Lei, Y., Niu, Q., Mi, H., Wang, Y., Nurulla, I., & Shi, W. (2013). Carbazole-based conjugated polymer with tethered acetylene groups: synthesis and characterization. *Dyes and Pigments*, 96(1), 138-147.
- Ley, S. V., & Thomas, A. W. (2003). Modern synthetic methods for copper-mediated C (aryl)- O, C (aryl)- N, and C (aryl)-S bond formation. *Angewandte Chemie International Edition*, 42(44), 5400-5449.
- Li, C.-J., & Chan, T.-H. (1997). *Comprehensive Organic reactions in aqueous media*: Canada: Wiley.
- Li, Y. (2012). Molecular design of photovoltaic materials for polymer solar cells: toward suitable electronic energy levels and broad absorption. *Accounts of Chemical Research*, 45(5), 723-733.
- Liang, Y., Feng, D., Wu, Y., Tsai, S.-T., Li, G., Ray, C., & Yu, L. (2009). Highly efficient solar cell polymers developed via fine-tuning of structural and electronic properties. *Journal of the American Chemical Society*, 131(22), 7792-7799.
- Lin, V. S., DiMugno, S. G., & Therien, M. J. (1994). Highly conjugated, acetylenyl bridged porphyrins: new models for light-harvesting antenna systems. *Science*, 264(5162), 1105-1111.
- Lindley, J. (1984). Copper assisted nucleophilic substitution of aryl halogen. *Tetrahedron*, 40(9), 1433-1456.
- Liu, J., Yang, X., Islam, A., Numata, Y., Zhang, S., Salim, N. T., Chen, H., & Han, L. (2013). Efficient metal-free sensitizers bearing circle chain embracing  $\pi$ -spacers for dye-sensitized solar cells. *Journal of Materials Chemistry A*, 1(36), 10889-10897.
- Liu, L., Zhang, Y., & Xin, B. (2006). Synthesis of biaryls and polyaryls by ligand-free Suzuki reaction in aqueous phase. *The Journal of Organic Chemistry*, 71(10), 3994-3997.
- Lo, C., Doucoure, B. I., Aaron, J.-J., Svoboda, J., Kozmik, V., Brochon, J.-C., Henry, E., Maurel, F., Capochichi, M. (2014). Synthesis and spectral properties of new fluorescent alkoxy-substituted thieno [3, 2-b] indole derivatives. *Spectrochimica Acta Part A: Molecular and Biomolecular Spectroscopy*, 120, 47-54.
- Lu, X., Fan, S., Wu, J., Jia, X., Wang, Z.-S., & Zhou, G. (2014). Controlling the charge transfer in D-A-D chromophores based on pyrazine derivatives. *The Journal of Organic Chemistry*, 79(14), 6480-6489.

- Mangione, M. I., & Spanevello, R. A. (2015). Synthesis of nitrogenated scaffolds derived from fluorene by a modified Ullmann type reaction. *Tetrahedron Letters*, 56(2), 465-467.
- Mas-Torrent, M., & Rovira, C. (2008). Novel small molecules for organic field-effect transistors: towards processability and high performance. *Chemical Society Reviews*, 37(4), 827-838.
- Masui, K., Ikegami, H., & Mori, A. (2004). Palladium-catalyzed CH homocoupling of thiophenes: facile construction of bithiophene structure. *Journal of the American Chemical Society*, 126(16), 5074-5075.
- Matsusue, N., Suzuki, Y., & Naito, H. (2005). Charge carrier transport in neat thin films of phosphorescent iridium complexes. *Japanese Journal of Applied Physics*, 44(6R), 3691.
- McCullough, R. D. (1998). The chemistry of conducting polythiophenes. *Advanced Materials*, 10(2), 93-116.
- McMurry, J. E. (1989). Carbonyl-coupling reactions using low-valent titanium. *Chemical Reviews*, 89(7), 1513-1524.
- McQuade, D. T., Pullen, A. E., & Swager, T. M. (2000). Conjugated polymer-based chemical sensors. *Chemical Reviews*, 100(7), 2537-2574.
- Mello, S. V., Dynarowicz-Łątka, P., Dhanabalan, A., Bianchi, R. F., Onmori, R., Janssen, R. A. J., & Oliveira, O. N. (2002). Langmuir and Langmuir-Blodgett films from the N-hexyl-pyrrole-thiophene (AB) semi-amphiphilic copolymer. *Colloids and Surfaces A: Physicochemical and Engineering Aspects*, 198, 45-51.
- Melucci, M., Favaretto, L., Bettini, C., Gazzano, M., Camaioni, N., Maccagnani, P., Ostoja, P., Monari, M., & Barbarella, G. (2007). Liquid-crystalline rigid-Core semiconductor oligothiophenes: influence of molecular structure on phase behaviour and thin-film properties. *Chemistry-A European Journal*, 13(36), 10046-10054.
- Mishra, A., Ma, C.-Q., & Bäuerle, P. (2009). Functional oligothiophenes: molecular design for multidimensional nanoarchitectures and their applications. *Chemical Reviews*, 109(3), 1141-1276.
- Miyaura, N., Satoh, Y., Hara, S., & Suzuki, A. (1986). Stereospecific synthesis of the fungal prohormone (.+.-)-trisporel B via the palladium-catalyzed cross-coupling reaction of 1-alkenylborane with 1-haloalkene. *Bulletin of the Chemical Society of Japan*, 59(6), 2029-2031.
- Miyaura, N., & Suzuki, A. (1995). Palladium-catalyzed cross-coupling reactions of organoboron compounds. *Chemical Reviews*, 95(7), 2457-2483.

- Miyaura, N., Yamada, K., Suginome, H., & Suzuki, A. (1985). Novel and convenient method for the stereo- and regiospecific synthesis of conjugated alkenes and alkyne-alkenes via the palladium-catalyzed cross-coupling reaction of 1-alkenylboranes with bromoalkenes and bromoalkynes. *Journal of the American Chemical Society*, 107(4), 972-980.
- Miyaura, N., Yamada, K., & Suzuki, A. (1979). A new stereospecific cross-coupling by the palladium-catalyzed reaction of 1-alkenylboranes with 1-alkenyl or 1-alkynyl halides. *Tetrahedron Letters*, 20(36), 3437-3440.
- Morvillo, P., & Bobeico, E. (2008). Tuning the LUMO level of the acceptor to increase the open-circuit voltage of polymer-fullerene solar cells: a quantum chemical study. *Solar Energy Materials and Solar Cells*, 92(10), 1192-1198.
- Murphy, A. R., & Fréchet, J. M. J. (2007). Organic semiconducting oligomers for use in thin film transistors. *Chemical Reviews*, 107(4), 1066-1096.
- Murphy, A. R., Liu, J., Luscombe, C., Kavulak, D., Fréchet, J. M. J., Kline, R. J., & McGehee, M. D. (2005). Synthesis, characterization, and field-effect transistor performance of carboxylate-functionalized polythiophenes with increased air stability. *Chemistry of Materials*, 17(20), 4892-4899.
- Negishi, E. i., Takahashi, T., Baba, S., Van Horn, D. E., & Okukado, N. (1987). Palladium- or nickel-catalyzed reactions of alkenylmetals with unsaturated organic halides as a selective route to arylated alkenes and conjugated dienes: Scope, limitations, and mechanism. *Journal of the American Chemical Society*, 109(8), 2393-2401.
- Nelson, J., Kwiatkowski, J. J., Kirkpatrick, J., & Frost, J. M. (2009). Modeling charge transport in organic photovoltaic materials. *Accounts of Chemical Research*, 42(11), 1768-1778.
- Newman, C. R., Frisbie, C. D., da Silva Filho, D. A., Brédas, J.-L., Ewbank, P. C., & Mann, K. R. (2004). Introduction to organic thin film transistors and design of n-channel organic semiconductors. *Chemistry of Materials*, 16(23), 4436-4451.
- Nguyen, V. C., & Potje-Kamloth, K. (1999). Electrical and chemical sensing properties of doped polypyrrole/gold Schottky barrier diodes. *Thin Solid Films*, 338(1), 142-148.
- Noma, N., Tsuzuki, T., & Shirota, Y. (1995a).  $\alpha$ -Thiophene octamer as a new class of photo-active material for photoelectrical conversion. *Advanced Materials*, 7(7), 647-648.
- Noma, N., Tsuzuki, T., & Shirota, Y. (1995b).  $\alpha$ -Thiophene octamer as a new class of photo-active material for photoelectrical conversion. *Advanced Materials*, 7(7), 647-648.

- Okamoto, T., Jiang, Y., Qu, F., Mayer, A. C., Parmer, J. E., McGehee, M. D., & Bao, Z. (2008). Synthesis and characterization of pentacene- and anthradithiophene-fluorene conjugated copolymers synthesized by Suzuki reactions. *Macromolecules*, *41*(19), 6977-6980.
- Okano, K., Tokuyama, H., & Fukuyama, T. (2003). Synthesis of secondary arylamines through copper-mediated intermolecular aryl amination. *Organic Letters*, *5*(26), 4987-4990.
- Ooyama, Y., Yamaguchi, N., Imae, I., Komaguchi, K., Ohshita, J., & Harima, Y. (2013). Dye-sensitized solar cells based on D- $\pi$ -A fluorescent dyes with two pyridyl groups as an electron-withdrawing-injecting anchoring group. *Chemical Communications*, *49*(25), 2548-2550.
- Paine, A. J. (1987). Mechanisms and models for copper mediated nucleophilic aromatic substitution. 2. Single catalytic species from three different oxidation states of copper in an Ullmann synthesis of triaryl amines. *Journal of the American Chemical Society*, *109*(5), 1496-1502.
- Parr, R. G., & Yang, W. (1989). *Density-functional theory of atoms and molecules* (Vol. 16): Oxford university press.
- Perepichka, I. F., & Perepichka, D. F. (2009). *Handbook of thiophene-based materials: applications in organic electronics and photonics*: Wiley Online Library.
- Pomerantz, M., Yang, H., & Cheng, Y. (1995). Poly (alkyl thiophene-3-carboxylates). Synthesis and characterization of polythiophenes with a carbonyl group directly attached to the ring. *Macromolecules*, *28*(17), 5706-5708.
- Pommerehne, J., Vestweber, H., Guss, W., Mahrt, R. F., Bässler, H., Porsch, M., & Daub, J. (1995). Efficient two layer leds on a polymer blend basis. *Advanced Materials*, *7*(6), 551-554.
- Punji, B., Ganesamoorthy, C., & Balakrishna, M. S. (2006). Suzuki cross-coupling reactions catalyzed by palladium complex of an inexpensive phosphinite, 2-diphenylphosphinoxynaphthyl. *Journal of Molecular Catalysis A: Chemical*, *259*(1), 78-83.
- Radke, K. R., Ogawa, K., & Rasmussen, S. C. (2005). Highly fluorescent oligothiophenes through the incorporation of central dithieno [3, 2-b: 2', 3'-d] pyrrole units. *Organic Letters*, *7*(23), 5253-5256.
- Rasmussen, S. C., Schwiderski, R. L., & Mulholland, M. E. (2011). Thieno [3, 4-b] pyrazines and their applications to low band gap organic materials. *Chemical Communications*, *47*(41), 11394-11410.
- Rauhut, G., & Pulay, P. (1995). Transferable scaling factors for density functional derived vibrational force fields. *The Journal of Physical Chemistry*, *99*(10), 3093-3100.



- Rauscher, U., Bässler, H., Bradley, D. D. C., & Hennecke, M. (1990). Exciton versus band description of the absorption and luminescence spectra in poly (p-phenylenevinylene). *Physical Review B*, 42(16), 9830.
- Rocca, P., Marsais, F., Godard, A., & Quéguiner, G. (1993). A new approach to the synthesis of lavendamycin analogues. *Tetrahedron Letters*, 34(18), 2937-2940.
- Romero, D. B., Schaer, M., Leclerc, M., Ades, D., Siove, A., & Zuppiroli, L. (1996). The role of carbazole in organic light-emitting devices. *Synthetic Metals*, 80(3), 271-277.
- Romero-Gázquez, P., Pastorelli, F., Mantilla-Páez, P., Mariano, M., Martínez-Otero, A., Elias, X., Betancur, R., Martorell, J. (2015). Semi-transparent polymer solar cells. *Journal of Photonics for Energy*, 5(1), 057212-057212.
- Roncali, J. (1997). Synthetic principles for bandgap control in linear  $\pi$ -conjugated systems. *Chemical Reviews*, 97(1), 173-206.
- Roncali, J. (2007). Molecular engineering of the band gap of  $\pi$ -conjugated systems: facing technological applications. *Macromolecular Rapid Communications*, 28(17), 1761-1775.
- Rossi, R. A., & de Rossi, R. H. (1983). Aromatic Substitution by the Swl Mechanism, ACS Monograph 178: American Chemical Society: Washington, DC.
- Rothberg, L. J., Yan, M., Papadimitrakopoulos, F., Galvin, M. E., Kwock, E. W., & Miller, T. M. (1996). Photophysics of phenylenevinylene polymers. *Synthetic Metals*, 80(1), 41-58.
- Rothberg, L. J., Yan, M., Son, S., Galvin, M. E., Kwock, E. W., Miller, T. M., Katz, H. E., Haddon, R. C., & Papadimitrakopoulos, F. (1996). Intrinsic and extrinsic constraints on phenylenevinylene polymer electroluminescence. *Synthetic Metals*, 78(3), 231-236.
- Sanda, F., Nakai, T., Kobayashi, N., & Masuda, T. (2004). Synthesis of polyacetylenes having pendant carbazole groups and their photo-and electroluminescence properties. *Macromolecules*, 37(8), 2703-2708.
- Satoh, T., & Miura, M. (2007). Catalytic direct arylation of heteroaromatic compounds. *Chemistry Letters*, 36(2), 200-205.
- Schrögel, P., Tomkevičienė, A., Strohriegl, P., Hoffmann, S. T., Köhler, A., & Lennartz, C. (2011). A series of CBP-derivatives as host materials for blue phosphorescent organic light-emitting diodes. *Journal of Materials Chemistry*, 21(7), 2266-2273.
- Schultz, D. M., & Yoon, T. P. (2014). Solar synthesis: prospects in visible light photocatalysis. *Science*, 343(6174), 1239176.

- Schwendeman, I., Hickman, R., Sönmez, G., Schottland, P., Zong, K., Welsh, D. M., & Reynolds, J. R. (2002). Enhanced contrast dual polymer electrochromic devices. *Chemistry of Materials*, 14(7), 3118-3122.
- Scuseria, G. E. (1999). Linear scaling density functional calculations with Gaussian orbitals. *The Journal of Physical Chemistry A*, 103(25), 4782-4790.
- Selampinar, F., Toppare, L., Akbulut, U., Yalçin, T., & Süzer, Ş. (1995). A conducting composite of polypyrrole II. As a gas sensor. *Synthetic metals*, 68(2), 109-116.
- Service, R. F. (2011). Outlook brightens for plastic solar cells. *Science*, 332, 293.
- Sessler, J. L., & Hoehner, M. C. (1994). An efficient, high-yield preparation of substituted 2, 2'-bipyrroles. *Synlett*, (3), 211-212.
- Shaughnessy, K. H., & Booth, R. S. (2001). Sterically demanding, water-soluble alkylphosphines as ligands for high activity Suzuki coupling of aryl bromides in aqueous solvents. *Organic Letters*, 3(17), 2757-2759.
- Sheats, J. R. (2004). Manufacturing and commercialization issues in organic electronics. *Journal Material Research*, 19(07), 1974-1989.
- Shinamura, S., Miyazaki, E., & Takimiya, K. (2010). Synthesis, properties, crystal structures, and semiconductor characteristics of naphtho [1, 2-b: 5, 6-b'] dithiophene and-diselenophene derivatives. *The Journal of Organic Chemistry*, 75(4), 1228-1234.
- Shreve, O. D. (1952). Infrared, Ultraviolet, and Raman Spectroscopy. *Analytical Chemistry*, 24(11), 1692-1699.
- Sista, P., Nguyen, H., Murphy, J. W., Hao, J., Dei, D. K., Palaniappan, K., Servello, J., Kularatne, R. S., Gnade, B. E., & Xue, B. (2010). Synthesis and electronic properties of semiconducting polymers containing benzodithiophene with alkyl phenylethynyl substituents. *Macromolecules*, 43(19), 8063-8070.
- Skoog, D. A., Holler, F. J., & Crouch, S. R. (2007) *Principles of Instrumental Analysis 6th Edition*. Belmont: Thomson Brooks.
- Skotheim, T. A., Elsenbaumer, R. L., & Reynolds, J. R. (1997). *Handbook of conducting polymers*. New York: Marcel Dekker.
- Smith, G. B., Dezeny, G. C., Hughes, D. L., King, A. O., & Verhoeven, T. R. (1994). Mechanistic studies of the suzuki cross-coupling reaction. *The Journal of Organic Chemistry*, 59(26), 8151-8156.
- Sonmez, G., Sonmez, H. B., Shen, C. K. F., Jost, R. W., Rubin, Y., & Wudl, F. (2005). A processable green polymeric electrochromic. *Macromolecules*, 38(3), 669-675.

- Spanggaard, H., & Krebs, F. C. (2004). A brief history of the development of organic and polymeric photovoltaics. *Solar Energy Materials and Solar Cells*, 83(2), 125-146.
- Starks, C. M., Liotta, C., & Starks, C. (1978). *Phase transfer catalysis: principles and techniques*. New York: Academic Press London.
- Starks, C. M., & Owens, R. M. (1973). Phase-transfer catalysis. II. Kinetic details of cyanide displacement on 1-haloocanes. *Journal of the American Chemical Society*, 95(11), 3613-3617.
- Steeman, R., Yong, J., Mjøs, Ø., & Song, A. (2012). Integrating the value chain: the impact of silicon quality on cell performance. *Energy Procedia*, 15, 20-29.
- Stephens, P. J., Devlin, F. J., Chabalowski, C. F., & Frisch, M. J. (1994). Ab initio calculation of vibrational absorption and circular dichroism spectra using density functional force fields. *The Journal of Physical Chemistry*, 98(45), 11623-11627.
- Stille, J. K. (1986). The palladium-catalyzed cross-coupling reactions of organotin reagents with organic electrophiles [new synthetic methods (58)]. *Angewandte Chemie International Edition in English*, 25(6), 508-524.
- Sugie, A., Kobayashi, K., Suzaki, Y., Osakada, K., & Mori, A. (2006). Observation of sequential electrophilic substitution of bromothiophene and immediate reductive elimination of arylpalladium complexes. *Chemistry Letters*, 35(10), 1100-1101.
- Suzuki, A. (1999). Recent advances in the cross-coupling reactions of organoboron derivatives with organic electrophiles, 1995–1998. *Journal of Organometallic Chemistry*, 576(1), 147-168.
- Suzuki, A., & Brown, H. C. (2003). *Organic Syntheses Via Boranes, Vol. 3, Suzuki Coupling*. Aldrich. Milwaukee: Wisconsin.
- Suzuki, H., Enya, T., & Hisamatsu, Y. (1997). Synthesis and characterization of some nitrobenzanthrones: Suspected new mutagens in atmospheric environment. *Synthesis*(11), 1273-1276.
- Swager, T. M. (1998). The molecular wire approach to sensory signal amplification. *Accounts of Chemical Research*, 31(5), 201-207.
- Takahashi, M., Masui, K., Sekiguchi, H., Kobayashi, N., Mori, A., Funahashi, M., & Tamaoki, N. (2006). Palladium-catalyzed CH homocoupling of bromothiophene derivatives and synthetic application to well-defined oligothiophenes. *Journal of the American Chemical Society*, 128(33), 10930-10933.
- Tan, L.-L., Xie, L.-J., Shen, Y., Liu, J.-M., Xiao, L.-M., Kuang, D.-B., & Su, C.-Y. (2014). Novel organic dyes incorporating a carbazole or dendritic 3, 6-

- diiodocarbazole unit for efficient dye-sensitized solar cells. *Dyes and Pigments*, 100, 269-277.
- Tanaka, I., Tabata, Y., & Tokito, S. (2004). Energy-transfer and light-emission mechanism of blue phosphorescent molecules in guest-host systems. *Chemical Physics Letters*, 400(1), 86-89.
- Thomas, S. W., Joly, G. D., & Swager, T. M. (2007). Chemical sensors based on amplifying fluorescent conjugated polymers. *Chemical Reviews*, 107(4), 1339-1386.
- Thompson, B. C., & Fréchet, J. M. J. (2008). Polymer–fullerene composite solar cells. *Angewandte Chemie International Edition*, 47(1), 58-77.
- Tirado-Rives, J., & Jorgensen, W. L. (2008). Performance of B3LYP density functional methods for a large set of organic molecules. *Journal of Chemical Theory and Computation*, 4(2), 297-306.
- Tour, J. M. (1996). Conjugated macromolecules of precise length and constitution. Organic synthesis for the construction of nanoarchitectures. *Chemical Reviews*, 96(1), 537-554.
- Toussaint, J. M., & Brédas, J. L. (1993). Novel low bandgap polymers: polydicyanomethylene-cyclopentadithiophene and-dipyrrole. *Synthetic metals*, 61(1), 103-106.
- Treboux, G., Mizukami, J., Yabe, M., & Nakamura, S. (2008). Blue phosphorescent iridium (III) complex. Aromaticity of the triplet potential energy surface. *Journal of Photopolymer Science and Technology*, 21(3), 347-348.
- Tretiak, S., & Mukamel, S. (2002). Density matrix analysis and simulation of electronic excitations in conjugated and aggregated molecules. *Chemical Reviews*, 102(9), 3171-3212.
- Tsuda, A., & Osuka, A. (2001). Fully conjugated porphyrin tapes with electronic absorption bands that reach into infrared. *Science*, 293(5527), 79-82.
- Tucker, S. H. (1926). Iodination in the carbazole series. *J Chem Soc*, 1, 548-553.
- Ullmann, F. (1903). Ueber eine neue Bildungsweise von Diphenylaminderivaten. *Berichte der deutschen chemischen Gesellschaft*, 36(2), 2382-2384.
- Uozumi, Y., & Nakai, Y. (2002). An amphiphilic resin-supported palladium catalyst for high-throughput cross-coupling in water. *Organic Letters*, 4(17), 2997-3000.
- Van Mullekom, H. A. M., Vekemans, J., Havinga, E. E., & Meijer, E. W. (2001). Developments in the chemistry and band gap engineering of donor–acceptor

- substituted conjugated polymers. *Materials Science and Engineering*, 32(1), 1-40.
- Wang, H. M., Hsiao, S. H., Liou, G. S., & Sun, C. H. (2010). Synthesis, photoluminescence, and electrochromism of polyamides containing (3, 6-di-tert-butylcarbazol-9-yl) triphenylamine units. *Journal of Polymer Science Part A: Polymer Chemistry*, 48(21), 4775-4789.
- Wang, Z.-S., Koumura, N., Cui, Y., Takahashi, M., Sekiguchi, H., Mori, A., Kubo, T., Furebe, A., & Hara, K. (2008). Hexylthiophene-functionalized carbazole dyes for efficient molecular photovoltaics: tuning of solar-cell performance by structural modification. *Chemistry of Materials*, 20(12), 3993-4003.
- Watanabe, T., Miyaura, N., & Suzuki, A. (1992). Synthesis of sterically hindered biaryls via the palladium-catalyzed cross-coupling reaction of arylboronic acids or their esters with haloarenes. *Synlett*, 3, 207-210.
- Welch, G. C., Perez, L. A., Hoven, C. V., Zhang, Y., Dang, X.-D., Sharenko, A., Toney, M. F., Kramer E. J., Nguyen, T.-Q., & Bazan, G. C. (2011). A modular molecular framework for utility in small-molecule solution-processed organic photovoltaic devices. *Journal of Materials Chemistry*, 21(34), 12700-12709.
- Wellinchoff, S. T., Deng, Z., Kedrowski, T. J., Dick, S. A., Jenekhe, S. A., & Ishida, H. (1984). Electronic conduction mechanism in polycarbazole iodine complexes. *Molecular Crystals and Liquid Crystals*, 106(3-4), 289-304.
- Wheless, C. J. M., Zhou, X., & Liu, R. (1995). Density functional theory study of vibrational spectra. 2. Assignment of fundamental vibrational frequencies of fulvene. *The Journal of Physical Chemistry*, 99(33), 12488-12492.
- Wipf, P., & Lynch, S. M. (2003). Synthesis of highly oxygenated dinaphthyl ethers via SNAr reactions promoted by barton's base. *Organic Letters*, 5(7), 1155-1158.
- Wu, Y., Guo, H., James, T. D., & Zhao, J. (2011). Enantioselective Recognition of Mandelic Acid by a 3, 6-Dithiophen-2-yl-9 H-carbazole-Based Chiral Fluorescent Bisboronic Acid Sensor. *The Journal of organic chemistry*, 76(14), 5685-5695.
- Yamashiro, T., Aso, Y., Otsubo, T., Tang, H., Harima, Y., & Yamashita, K. (1999). Intramolecular energy transfer of (60) fullerene-linked oligothiophenes. *Chemistry Letters*(5), 443-444.
- Yamashita, Y. (2009). Organic semiconductors for organic field-effect transistors. *Science and Technology of Advanced Materials*, 10(2), 024313.
- Yang, L., Feng, J.-K., Ren, A.-M., & Sun, J.-Z. (2006). The electronic structure and optical properties of carbazole-based conjugated oligomers and polymers: a theoretical investigation. *Polymer*, 47(4), 1397-1404.

- Yasuda, S., Yoshida, S., Sasaki, J., Okutsu, Y., Nakamura, T., Taninaka, A., Takeuchi, O., & Shigekawa, H. (2006). Bond fluctuation of S/Se anchoring observed in single-molecule conductance measurements using the point contact method with scanning tunneling microscopy. *Journal of the American Chemical Society*, *128*(24), 7746-7747.
- Yokooji, A., Satoh, T., Miura, M., & Nomura, M. (2004). Synthesis of 5, 5'-diarylated 2, 2'-bithiophenes via palladium-catalyzed arylation reactions. *Tetrahedron*, *60*(32), 6757-6763.
- Zhan, X., Liu, Y., Zhu, D., Jiang, X., & Jen, A. K. Y. (2001). Synthesis and characterization of processible electroluminescent poly [(2, 7-diethynyl-9, 9-di-2-ethylhexylfluorene)-alt-co-(2, 5-thienylene)]. *Synthetic Metals*, *124*(2), 323-327.
- Zhang, F., & Bäuerle, P. (2007). A controlled approach to well-defined oligothiophenes via oxidatively induced reductive elimination of stable Pt (II) oligothiophenyl complexes. *Journal of the American Chemical Society*, *129*(11), 3090-3091.
- Zhang, F., Wu, D., Xu, Y., & Feng, X. (2011). Thiophene-based conjugated oligomers for organic solar cells. *Journal of Materials Chemistry*, *21*(44), 17590-17600.
- Zhang, L., Tan, L., Wang, Z., Hu, W., & Zhu, D. (2009). High-performance, stable organic field-effect transistors based on trans-1, 2-(dithieno [2, 3-b: 3', 2'-d] thiophene) ethene. *Chemistry of Materials*, *21*(9), 1993-1999.
- Zhang, X.-H., Cui, Y., Katoh, R., Koumura, N., & Hara, K. (2010). Organic dyes containing thieno [3, 2-b] indole donor for efficient dye-sensitized solar cells. *The Journal of Physical Chemistry C*, *114*(42), 18283-18290.
- Zhang, Y., Wada, T., Wang, L., Aoyama, T., & Sasabe, H. (1996). Photorefractive polymers containing a single multifunctional chromophore. *Chemical Communications*, (20), 2325-2326.
- Zhang, Y., Wada, T., Wang, L., & Sasabe, H. (1997). Amorphous conjugated carbazole trimers for photorefractive materials. *Chemistry of Materials*, *9*(12), 2798-2804.
- Zhou, H., Yang, L., & You, W. (2012). Rational design of high performance conjugated polymers for organic solar cells. *Macromolecules*, *45*(2), 607-632.
- Ziehlke, H., Fitzner, R., Koerner, C., Gresser, R., Reinold, E., Bäuerle, P., Leo, K., & Riede, M. K. (2011). Side Chain Variations on a Series of Dicyanovinyl-Terthiophenes: A Photoinduced Absorption Study. *The Journal of Physical Chemistry A*, *115*(30), 8437-8446.
- Zotti, G., Schiavon, G., Zecchin, S., & Groenendaal, L. (1999). Conductive and magnetic properties of poly (3, 6-bis (2-(3, 4-ethylenedioxy) thienyl)-N-dodecylcarbazole). A polyconjugated polymer with a high spin density polaron state. *Chemistry of Materials*, *11*(12), 3624-3628.

Zotti, G., Schiavon, G., Zecchin, S., Morin, J.-F., & Leclerc, M. (2002). Electrochemical, conductive, and magnetic properties of 2, 7-carbazole-based conjugated polymers. *Macromolecules*, 35(6), 2122-2128.

University of Malaya

## LIST OF PUBLICATIONS AND PAPERS PRESENTED

1. E.F. Damit, N. Nordin, A. Ariffin and K. Sulaiman; Synthesis of Novel Derivatives of Carbazole-Thiophene, Their Electronic Properties, and Computational Studies, Journal of Chemistry, **2016**, vol. 2016, 14 pages. DOI: 10.1155/2016/9360230.
2. E.F. Damit, N. Nordin, A. Ariffin and K. Sulaiman, Synthesis, Characterization and Systematic Structure-Property Investigations On A Series of Carbazole-Thiophene Derivatives, Russian Journal of General Chemistry, **2016**, vol. 86 or 87. Registry no. g16-046.
3. Synthesis of Novel Derivatives of Carbazole-Thiophene, Their Electronic Properties, and Computational Studies. 18<sup>th</sup> Malaysian International Chemical Congress (MICC), 2014, Putra World Trade Centre, Kuala Lumpur, Malaysia.
4. Structure-Property Investigation on 3,6-Position Substituted Carbazole-Thiophene Materials. International Symposium of Chemical Engineering ISChE 2014, Putra World Trade Centre, Kuala Lumpur, Malaysia.